Synthesis and characterisation of zincobalamin

the zinc analogue of vitamin B_{12}

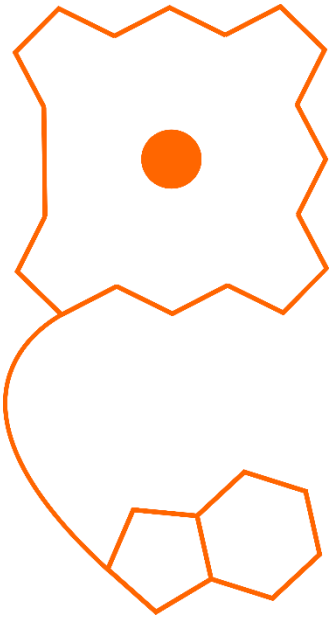

Joseph Aubry Baker

March 2018

Declaration

No part of this thesis has been submitted in support of any application for a qualification at the University of Kent Canterbury or any other institute of learning.

Joseph Aubry Baker

March 2018

Aknowledgements

I would like to thank the entire Warren Lab for help and support throughout the course of my PhD project. In particular I would like to thank Dr Evelyne Deery and Dr Emi Nemoto Smith for providing some of the plasmids used in this work.

I would like to thank Professor Martin Warren for giving me the opportunity to undertake a PhD research project in the group, it's been a fantastic experience. I would like to thank Professor Bernhard Kräutler for hosting me at the University of Innsbruck, Christoph Keininger for making me feel welcome in an organic chemistry lab and for assisting me in "driving" the NMR.

Matt and Rokas thank you for the useful or not so useful discussions we've had over the past few years.

I would also like to thank my parents and grandparents for all the help and support over the years. Without the encouragement and belief provided by you all this thesis would probably have never been finished.

Abstract

Cobalamin or vitamin B_{12} is one of the most complex small molecules produced by prokaryotic organisms. B_{12} is a member of the metabolically diverse group of compounds called tetrapyrroles, whose members include haem, chlorophyll, sirohaem and co-enzyme F_{430}. The metabolic activity of B_{12} is dependent upon the cobalt ion located at the centre of a contracted corrin macrocycle. Replacement of this central cobalt ion with an alternative metal ion results in the formation of a compound that structurally resembles B_{12} but shares none of its vitamin function. Zincobalamin (Zbl), the zinc analogue of B_{12}, was synthesised from an intermediate of B_{12} biosynthesis, hydrogenobyrinic acid *a, c* diamide (HBAd). This intermediate is the last metal-free intermediate of B_{12} biosynthesis. The synthesis of Zbl from HBAd involves a combination of chemical synthesis and biochemical modification of the starting material. Regiospecific amidation of 4 out the 5 carboxylic acid sidechains decorating the macrocycle of HBAd is required in order to produce Zbl. During B_{12} biosynthesis these amidations are catalysed by a single enzyme CobQ. Previously characterised CobQs are highly specific for a cobalt containing intermediate of B_{12} biosynthesis. A CobQ capable of acting "out of turn" with respect to the normal order of B_{12} biosynthesis was identified within the genome of *Allochromatium vinosum.* This enzyme was used to good effect in the conversion of HBAd into hexa-amidated compound called hydrogenobyric acid (Hby), the metal free analogue of a late intermediate of B_{12} biosynthesis cobyric acid. A structural reason as to why *A. vinousm* CobQ is able to recognise HBAd as a substrate was investigated through sequence alignment and structural prediction. The remaining steps towards Zbl synthesis were completed chemically through the abiotic insertion of zinc into the macrocycle of Hby and the attachment of the pre-fabricated lower nucleotide loop. As both Hby and its zinc containing counterpart have not been previously described in the literature all three compounds including Zbl were subject to biochemical characterisation by UV-visible, NMR and mass spectroscopy. The influence of these analogues on the growth of a strain of *Salmonella enterica* dependent on exogenous B_{12} for growth, was investigated.

Contents

Chapter 1: Introduction

1:1:1 Introduction to B_{12}

Modified tetrapyrroles are a group of molecules found across all kingdoms of life. Members of this family include the light harvesting pigment chlorophyll, the oxygen binding and redox active haems, the methanogenic pigment coenzyme F_{430} and the cobalamins (Battersby 2000, Scott 1993, Blanche et al 1995). As the most chemically complex member of the modified tetrapyrroles, cobalamins are comprised of a 19 membered corrin ring contrasting the 20 membered rings of haem, chlorophyll and coenzyme F_{430} (Figure 1:1:1). Structurally, cobalamins extend into three dimensions by way of a lower nucleotide loop attached directly to the propionate sidechain *f* and an upper ligand attached directly to a central cobalt ion. The term cobalamin describes a number of different compounds, the uniting factor for this class of molecule is an identical 19 membered corrin ring with a centrally chelated cobalt ion. Variations within the cobalamins exist regarding the identity of the lower nucleotide loop as well as the upper axial ligand (Helliwell et al 2016, Krautler et al 1987, Stupperich et al 1988).

Cobalamins found in nature can harbour a number of different ligands attached to the upper β face of the central cobalt ion. The best studied of these B_{12} variants are adenosyl and methyl cobalamin (Ado-Cbl and Me-Cbl), where the upper β ligand is either an adenosine or a methyl group. Significantly these groups are attached directly to the central cobalt ion by way of an organometallic carbon cobalt bond (Kräutler 2005). Without biological intervention the upper ligand of cobalamins can also be comprised of a number of different groups from halogenated derivatives to a hydroxyl group as in hydroxocobalamin (OH-Cbl) or cyanide as is the case for vitamin B_{12}. The latter is a by-product of the industrial process used to extract B_{12}. Technically vitamin B_{12} refers only to cyano-cobalamin but the term B_{12} is often used more loosely to refer to cobalamins in general.

A shared trait of the naturally occurring tetrapyrroles is the presence of a metal ion at the centre of the macrocycle. Chlorophylls contain magnesium within a chlorin ring, haems have an iron at the centre of a porphyrin ring and F_{430} has a nickel ion entrapped within an isobacteriochlorin ring. Cobalamin is no exception to this containing a cobalt ion at the centre of a corrin ring. It is thought that by

entrapping metals in a tetrapyrrolic ring the reactivity of the metal ion can be modulated and made more compatible with the predominantly protein based chemistry essential to life (Eschenmoser 1988). In the case of chlorophylls the central magnesium ion plays more of a structural role maintaining a planar conformation of the chlorin ring (Fiedor et al 2008). In cyanobacteria the central magnesium ion plays an additional role in the supramolecular organisation of chlorophylls in chlorosomes (Tamiaki 1996, Olsen 1998).

The different ring types found within the tetrapyrrole family probably represent nature's tuning of the reactivity of each metal centre, this is probably the evolutionary driving force behind the production of these compounds. The organic scaffolds provided by B_{12}, haem, chlorophyll and F_{430} allow access to the chemistry of these metal ions that may have otherwise been unavailable to biology (Eschenmoser 1988).

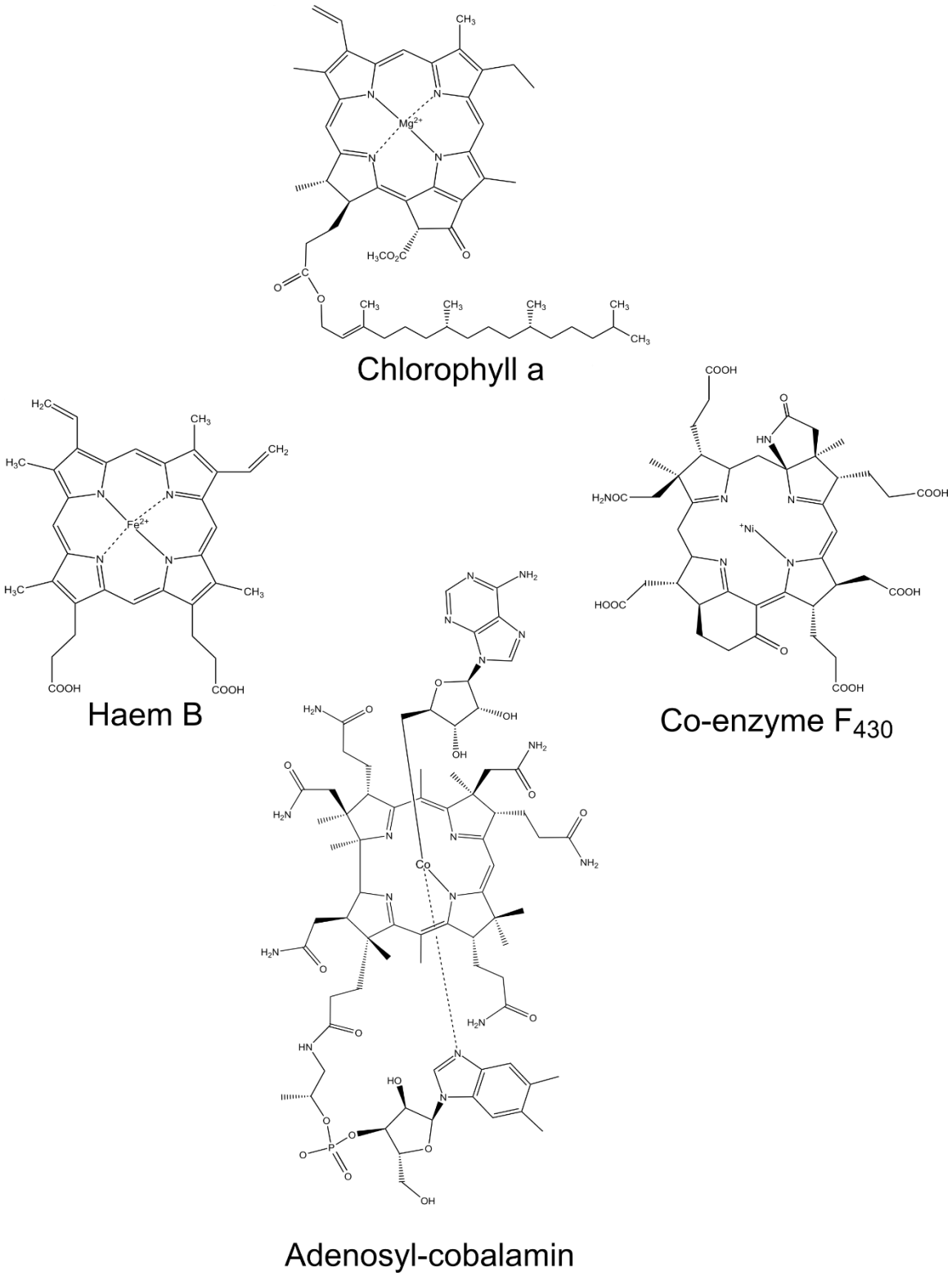

Figure 1:1:1: Naturally occurring tetrapyrroles. Clockwise from top, Chlorophyll a magnesium containing modified chlorin. Coenzyme F_{430} a nickel containing modified isobacteriochlorin. Cobalamin a highly modifed corrin and Haem B a modified iron containing porhyrin.

1:1:2 Biological role of B_{12}

B_{12} and other cobalt containing corrins are essential cofactors in numerous biological processes required by both eukaryotic and prokaryotic organisms. The biological activity of the various cobalamins implicated in biological process is dependent upon the cobalt ion found at the centre of these compounds (Eschenmoser 2011). In particular it is the ability of the central cobalt ion to form stable organo-metallic bonds as well as the high nucleophilicity of the Co^{1+} species it is possible to form (Banerjee 2003, Marsh et al 2001).

The forms of cobalamin most relevant for human health, and consequently the best studied, are Me-Cbl and Ado-Cbl (Banerjee et al 2003). These co-factors harbour a unique organo-metallic bond between the central cobalt ion and the organic upper β ligand. The cellular functions of both Me-Cbl and Ado-Cbl rely upon the properties of these carbon cobalt bonds (Banerjee et al 2003, Matthews et al 2011).

The properties of the C-Co bond in Ado-Cbl is such that homolytic cleavage of this bond can occur with relative ease resulting in the formation of an adenosyl radical (Marsh et al 2010). This radical is utilised for a variety of carbon skeleton rearrangements, the C-C bond reorganisations catalysed by Ado-Cbl requiring enzymes play a vital role in the metabolism of a range of organisms (Reitzer et al 1999, Masuda et al 2000, Mancia et al 1996). From a human health perspective this radical chemistry is required for the interconversion of methylmalonyl-CoA and succinyl-CoA as part of the catabolism of odd chain fatty acids and branched amino acids. The conversion of methylmalonyl-CoA to its isomer succinyl-CoA is catalysed by methylmalonyl-CoA mutase (Mancia et al 1998). A deficiency in this enzyme results in the build-up of methylmalonylic acid leading to the condition methylmalonate acidemia and in extreme cases can lead to neurological damage (Allen et al 1993). The same enzyme is a feature of bacterial metabolism where methylmalonyl CoA mutase plays an important role in the production of propionate in *Propionibacterium,* here the reverse reaction is favoured and succinate is converted to methylmalonylic acid *en route* to propionic acid (Allen et al 1964).

The carbon-cobalt bond found in Ado-Cbl is unstable under conditions of illumination. Light induced cleavage of this bond occurs homolytically resulting in the formation of an adenosyl radical and a pentacoordinate Co^{2+} species in both oxygenic and anoxic environments (Schwartz et al 2007, Walker et al 1998). Unless the adenosyl radical is otherwise directed it is possible to reform Ado-Cbl through reaction with the central cobalt of the parent molecule. However, the main pathway by which the adenosyl radical is lost when Ado-Cbl is illuminated is through reaction with molecular oxygen forming adenosyl 5' aldehyde (Finke and Hay 1984). Under anoxic conditions 5' 8' cycloadenosine is formed instead (Law et al 1973, Hogenkamp 1963). The sensitivity of Ado-Cbl to a broad spectrum of light underpins its function as a light sensing pigment in some photosynthetic bacteria (Cheng et al 2014, Guerrero et al 2011).

One such light sensor CarH has been described in detail. CarH controls the expression of genes associated with carotenoid biosynthesis under conditions of illumination (Guerrero et al 2011). Carotenoids are produced by a number of photosynthetic organisms to protect against light induced oxidative damage (Armstrong et al 1997). The biosynthesis of these often complex small molecules is therefore limited to conditions where photo-oxidative damage is likely. CarH acts as a light inducible transcription factor supressing the transcription of the carotenoid biosynthetic operon in *Myxococcus xanthus* in the absence of light (Perez-Marin et al 2007). The mechanism of this suppression is based upon the oligomeric state of the protein and consequently the DNA binding capability of CarH. In the absence of light with an intact Ado-Cbl bound this protein exists as a homo-tetramer with Ado-Cbl bound to each monomer, the stability of the tetramer being dependent upon the presence of Ado-Cbl. Photolysis of the carbon cobalt bond of Ado-Cbl results in the formation of an adenosyl radical, which due to proximity to the genomic DNA of the organism is directed to form 4', 5' – anhydroxyadeonsine before it can induce DNA damage (Jost et al 2015). Loss of the adenosyl group from Ado-Cbl causes dissociation of the CarH tetramer allowing transcription of the carotenoid biosynthetic operon.

Ado-Cbl plays a role in the synthesis of deoxyribonucleotides from the corresponding ribonucleotide and is the co-factor required for a family of enzymes termed ribonucleotide reductases (Tauer and Brenner 1997). Three distinct families of ribonucleotide reductase exist all involved in the synthesis of deoxyribonucleotides from ribonucleotides (Norlund and Reichard 2006). All ribonucleotide reductases rely on a radical mechanism to produce deoxyribonucleotides from the corresponding ribonucleotide, they differ only in how this adenosyl radical is generated. Class II ribonucleotide reductases are Ado-Cbl dependent and found solely in prokaryotes they rely on the generation of an adenosyl radical to reduce the 2' carbon of a ribonucleotide in order to produce the corresponding deoxyribonucleotide (Norlund and Reichard 2006). Interestingly class III ribonucleotide reductases uses an adenosyl radical generated from *S*-adenosyl methionine to perform the same reaction (Fontecave et al 2002). The fact that SAM can be coaxed into forming an adenosyl radical under certain conditions as well as sharing many of the same cellular functions as Ado-Cbl and Me-Cbl in terms of adenosyl radical formation and methyl transferase activity has led to SAM being described as a "poor man's cobalamin" (Frey 2001). The apparent redundancy of these two cofactors is reconciled somewhat in B_{12} dependent radical SAM methylases and isomerases. Theses dual cofactor enzymes bind both SAM and methyl or hydroxyl cobalamin and catalyse a number of challenging methylations of un-activated carbon and phosphorous centres (Bauerle et al 2015, Broderick et al 2014). This class of enzyme is leveraged by a large number of bacteria for the production of secondary metabolites, particularly a number of compounds with anti-microbial properties (Bridwell et al 2017, Zhou et al 2016). The enzyme BchE involved in the anaerobic biosynthesis of bacteriochlorophylls has been shown to be a dual cofactor SAM, Ado-B12 dependent radical isomerase. Studies conducted with *R. capsulatus* demonstrated that BchE requires B_{12} in order to catalyse the cyclisation of ring E (Gough et al 2000). In higher plants ring E cyclisation is achieved by the action of a haem dependent monooxygenase (Heys and Hunter 2009).

The second organometallic cobalamin derivative, Me-Cbl, is required for methionine biosynthesis in both humans and bacteria (Banerjee et al 1990, Drennan et al 1994). In humans, methionine synthase activity is linked intimately with folate metabolism, specifically the recycling of methyl-tetrahydrofolate though transfer of the methyl group from methyl tetrahydrofolate to cobalamin forming Me-Cbl and tetrahydrofolate. This same methyl group is then transferred from Me-Cbl to homocysteine forming methionine and freeing the Cbl cofactor for another round of catalysis. In bacteria this methionine synthase is encoded by the *metH* gene and allows for the synthesis of methionine under anaerobic conditions (Banerjee et al 1990). Mechanistically the methyl group of methyl tetrahydrofolate is transferred to a Co^{1+} B_{12} species to form methyl-cobalamin before this same methyl group is transferred to homocysteine to form methionine. This folate recycling system is leveraged by acetogenic bacteria for the fixation of CO_2 via the Wood Ljungdahl pathway (Ragsdale 2008). In both these cases it is due to the unique properties of Me-Cbl, particularly the ability of the central cobalt ion to be reduced to a "supernucleophilic" Co^{1+} species that allows for the efficient transfer of the methyl group from methyl-tetrahydrofolate (Liptak et al 2006).

The cobalt ion at the centre of B_{12} has been implicated as the catalytic centre in a number of dehalogenase enzymes. These reductive dehalogenases are found in a variety of bacteria, where halogenated organic molecules can be used as part of anaerobic respiration. The dehalogenation activity of B_{12} has important implications for the environmental breakdown of halogenated pesticides and bioremediation of contaminated soils and waterways (Collins et al 2015).

1:1:3 Discovery of cobalamin and elucidation of its biosynthetic pathway

B_{12} was first discovered through efforts to treat patients suffering from a condition known as pernicious anaemia. The cause of this disease, while unknown at the time, was later found to be due to a deficiency in B_{12} uptake and therefore levels of B_{12} that are too low for normal metabolic function. Modern management of pernicious anaemia involves periodic subcutaneous injections of a B_{12} solution, prior to discovery of this treatment pernicious anaemia was a fatal condition. Early work towards an effective treatment for pernicious anaemia and the subsequent isolation of B_{12} began when physician George Whipple first noticed the curative effects of raw liver in patients suffering from this condition. Through fractionation of large quantities of raw liver more concentrated isolates with greater curative properties could be generated. Continuing on from this work George Minot and William Murphy would eventually isolate a bright red compound from these liver fractions that was sufficient to reverse the symptoms of pernicious anaemia. For this work all three would receive the 1934 Nobel Prize in physiology and medicine (Minot and Murphy 1926).

While treatment of pernicious anaemia with these liver isolates was a vast improvement over the initial treatment of the consumption of 100 g of liver a day, the curative factor contained within these fractions (B_{12}) would not be isolated until 1948. Initially a bioassay method was implemented for screening various fractions from beef liver for B_{12} (Shorb 1947). This method was based on the requirement of *Lactobacillis lactis* for B_{12} under certain growth conditions and was developed by Mary Shaw Shorb. This relatively high throughput method would greatly aid in the eventual isolation of B_{12}. The isolation of B_{12}, however, was achieved in parallel in an industrial setting when chromatographic separation techniques were used to isolate B_{12} from fractions of liver. The groups of Karl Folkers at Merck and Lester Smith at Glaxo were able to isolate small quantities of the red water soluble B_{12} for the first time (Rickes et al 1948, Smith 1948).

The isolation of B_{12} led to studies designed to deduce the structure of this vitamin. Early structural studies using traditional degradative methods were undertaken by Karl Folkers at Merck and Alexander Todd at Cambridge. This approach led to

the conclusion that B_{12} was possibly a tetrapyrrole containing cobalt with a nucleotide attached in some fashion (Bonnett 1963). These degradative experiments led to the conclusion that cobalamin was structurally more complex than either haem or chlorophyll and as such a different methodology would be required to determine the structure. The structures of both haem and chlorophyll were well known at this time having been determined by degradative means by Richard Willstatter and Hans Fischer in the 1920's and 1930's respectively (Fischer 1930).

X-ray crystallography would prove to be the technique by which the structure of B_{12} was revealed. However, B_{12} was not the first corrin to have its structure solved by X-ray crystallography. While investigating the alkaline hydrolysis of the peripheral amides of B_{12} a member of Alexander Todd's group inadvertently produced crystals of cobyrinic acid *c* lactam (Figure 1:1:2). The quality of these crystals was sufficient to be analysed by X-ray crystallography (Hodgkin et al 1955).

Dorothy Crowfoot Hodgkin, one of the early pioneers of X-ray crystallography as a structural technique, eventually solved the structure of cobyric acid *c* lactam. She revealed for the first time the asymmetric corrin ring complete with central cobalt ion. Microbiological work revealed that the cyanide ligand present in the original crystals was an artefact of the extraction from liver using charcoal and that the biologically active form of cobalamin had an adenosyl group somehow associated with the molecule. The later crystal structure of adenosyl-cobalamin revealed that the adenosyl group is attached directly to the cobalt via a cobalt carbon bond. This was the first time that an organometallic bond had been observed in a natural product (Hodgkin et al 1956).

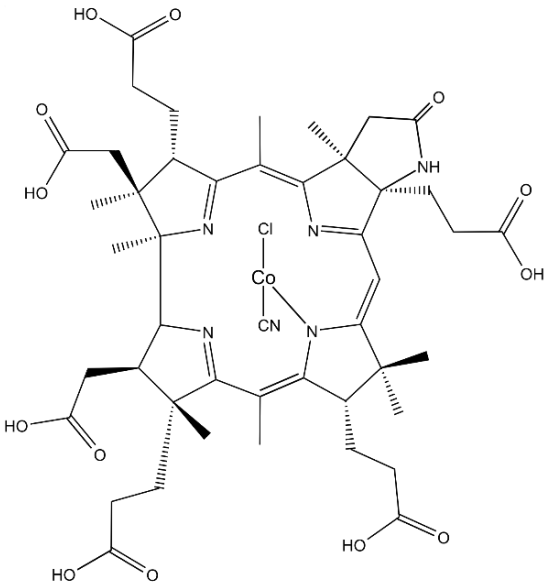

α cyano, β chloro
cobyrininc acid *c* lactam

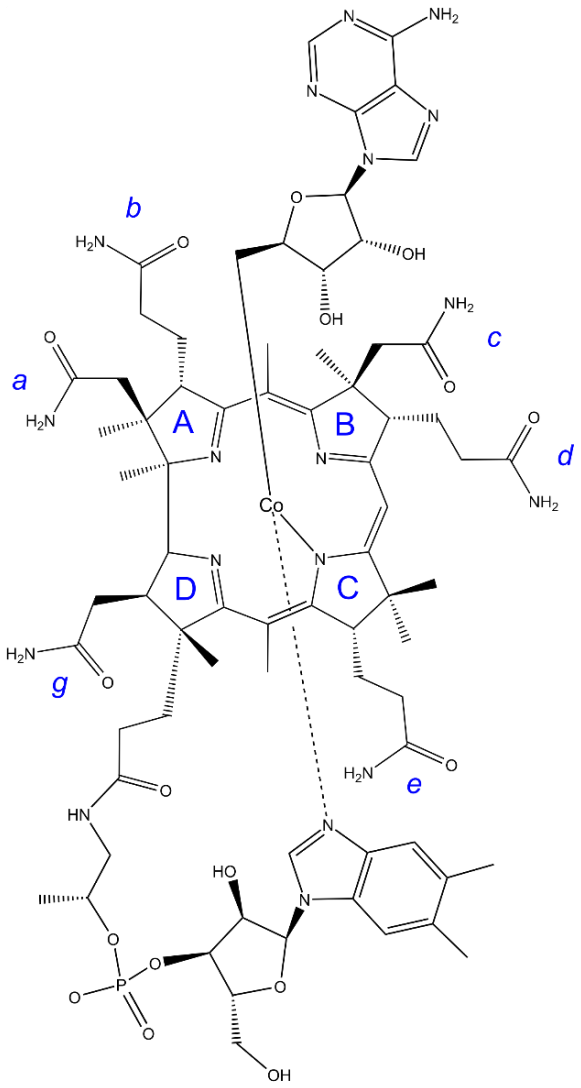

Adenosylcobalamin

Figure 1:1:2: The structure of the first deriviative of B_{12} solved as depicted on the left. Right the full structure of adenosylcobalamin. The pyrrole rings of adenosyl cobalamin are labelled A to D clockwise and the peripheral sidechains are labelled a-g.

1:1:4 Early steps of tetrapyrrole biosynthesis

The biosynthesis of all tetrapyrroles begins from δ-aminolevulinic acid (ALA). Two distinct pathways for the biosynthesis of ALA are present in nature. The first of these pathways produces ALA via the condensation of glycine and succinyl-CoA. This pathway is known as the Shemin pathway and is present in humans and other higher eukaryotes; excluding plants and some bacteria, specifically α-proteobacteria (Shemin and Rittenberg 1945). The second route, whereby ALA is synthesised from glutamate via a glutamyl-tRNA intermediate, is found in plants and most prokaryotes and is referred to as the C5 pathway (Beale 1970, Granick 1950). Interestingly, the synthesis of ALA from glutamate is one of the few cellular process requiring a glutamyl-tRNA that is not related to translation.

The condensation of two molecules of ALA gives the first pyrrole intermediate of tetrapyrrole biosynthesis, porphobilinogen (PBG). Through the asymmetric condensation of two molecules of ALA PBG is synthesised by the enzyme ALA dehydratase. Physiologically, ALA dehydratase exists in an equilibrium between an active octomeric form and a less active hexameric form (Van Hyningen and Shemin 1971).

The first tetrapyrrolic intermediate is formed when 4 molecules of PBG are linked head to tail generating a linear tetrapyrrole, which is called hydroxymethylbilane (HMB). The synthesis of HMB proceeds via deamination of PBG and is catalysed by the enzyme PBG deaminase. Early work concerning the mechanism of PBG deaminase revealed that this enzyme produces its own dipyrromethane cofactor through the deamination and subsequent linkage of two molecules of PBG. This cofactor is bound covalently to a cysteine residue within the active site of PBG deaminase. Four molecules of PBG are linked sequentially to the dipyrromethane cofactor with the subsequent loss of ammonia for each PBG unit that is attached. The linear bilane is released from the active site of PBG deaminase, after hydrolysis of the linkage between dipyrromethane and the tetrapyrrole. Hydroxymethylbilane can cyclise spontaneously to form uroporphyrinogen I, without biological intervention (Figure 1:1:4). However, all tetrapyrroles derived from natural sources are ultimately derived from a different isomer of

uroporphyrinogen, uroporphyrinogen III (uro'gen III). The different isomers of uroporphyrinogen are defined by the pattern of acetate and propionate sidechains attached to each pyrrole unit. Each of the pyrrole units that form all tetrapyrroles are labelled A to D, with A being the first PBG unit added to PBG deaminase and D being the final PBG unit added before release of HMB. In order to form uro'gen III from HMB ring D must be inverted with respect to the other pyrrole units of hydroxymethylbilane to give the proper patterning of acetate and propionate sidechains in the final product (Figure 1:1:4).

The cyclisation of HMB to give uro'gen III is an enzyme driven process catalysed by uro'gen III synthase. This monomeric protein catalyses the cyclisation of HMB and inversion of ring D resulting in the formation of uro'gen III the final common precursor to all tetrapyrroles as the branch of tetrapyrrole biosynthesis resulting in the formation of haem and chlorophyll begins with decarboxylation of the acetate sidechains of uro'gen III (Heinmann et al 2008, Tanaka and Tanaka 2006).

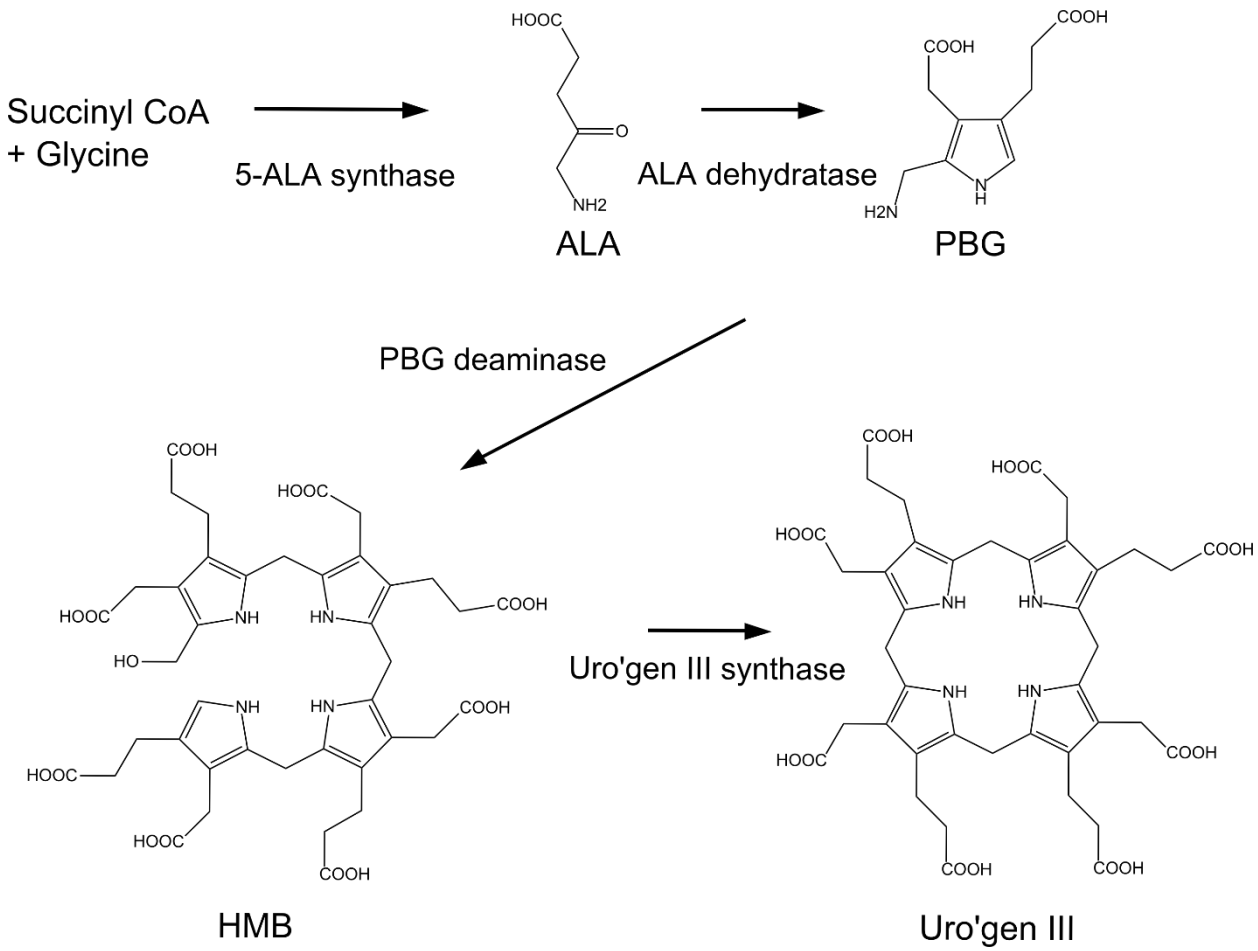

Figure 1:1:3: the early steps in the biosynthesis of all tetrapyrroles. ALA can be synthesied by two routes either from glycine and succinyl CoA or via glutamic acid. 4 units are porphobilogen (PBG) are linked together to form the linear tetrapyrrole hydroxymethyl bilane. Of the 16 possible isomers of HMB that can be formed the final product of PBG deaminase has ring D inverted relative to the positons of the other three pyrrole units. HMB is cyclised by uroporphyrinogen III synthase. Uroporphyrinogen III is the precursor to all tetrapyrroles found in nature.

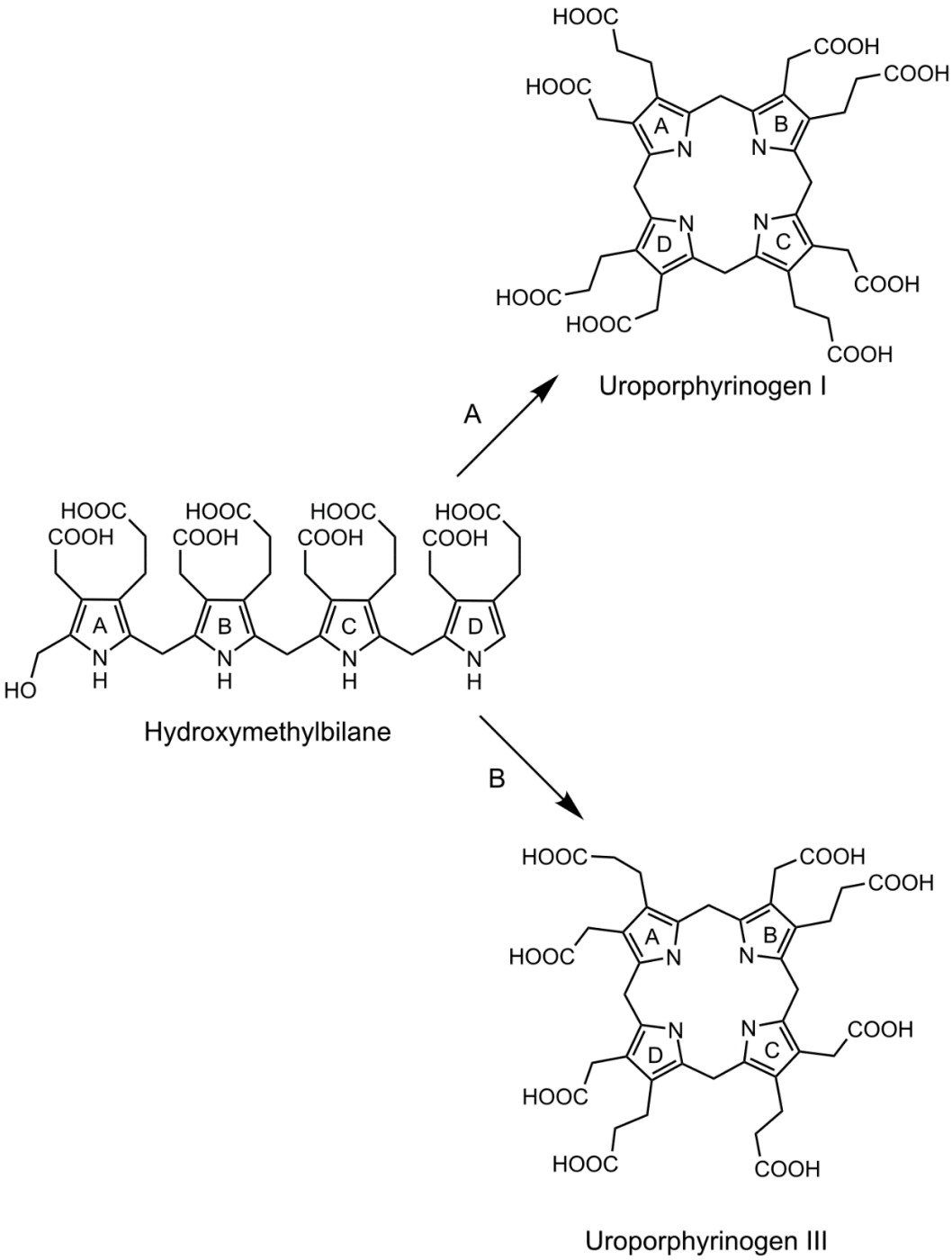

Figure 1:1:4: Cyclisation of hydroxymethylbilane. Route A is the uncatalysed cyclisation of HMB to uro'gen I while route B shows the cyclisation of HMB as catalysed by uro'gen III synthase. The resulting type III isomer shows the same pattern of acetate and propionate sidechains as all modified tetrapyrroles found in nature.

1:1:5 Determination of the intermediates of B_{12} biosynthesis

Uroporphyrinogen III is the first macrocyclic intermediate for the biosynthesis of all modified tetrapyrroles and also represents the first branch point in the pathway as decarboxylation of the acetate sidechains decorating uro'gen III sets this compound down the path for haem and chlorophyll biosynthesis (Heinmann et al 2008, Tanaka and Tanaka 2007). For B_{12} biosynthesis the first modification to uro'gen III is the attachment of two *S*-adenosyl methionine derived methyl groups to carbons C2 and C7 of the macrocycle, a modification that generates precorrin-2. This intermediate also represents a branch as it is an intermediate for sirohaem biosynthesis and may be referred to in the context of sirohaem biosynthesis as dihydro-sirohydrochlorin (Raux et al 1997). Intermediates of B_{12} biosynthesis are designated "precorrins" with the proceeding number indicating how many methyl groups have been added to the macrocycle of the molecule (Battersby 2000, Blanche et al 1995).

Addition of the first two methyl groups to uro'gen III is catalysed by the uro'gen III methyl transferase, an enzyme that has a remarkably slow turnover rate of approximately 38 h^{-1}. This enzyme, CobA, is subject to inhibition by one of its products, *S*-adenosyl homocysteine as well as by the tetrapyrrolic substrate uro'gen III at concentrations above 2 µM (Blanche et al 1989). It is thought that the combination of slow turnover rate and both product and substrate inhibition serves to limit flux of uro'gen III towards B_{12} biosynthesis as this compound is required in significantly lower levels than both haem, chlorophyll. The synthesis of coenzyme F_{430} also occurs via the oxidised form of precorrin-2, sirohydrochlorin (Moore et al 2017). As coenzyme F_{430} is required in large amounts for methanogenic prokaryotes the same product inhibition is not present in the CobA like protein required for addition of methyl groups to C2 and C6 of uro'gen III (Blanche et al 1991[3]).

The pathways for haem and chlorophyll biosynthesis diverge at uro'gen III via decarboxylation of the 4 acetic acid sidechains to form coproporphyrinogen III. Some organisms are able to make haem via a different route starting with sirohaem, which begins its biosynthesis with the oxidised form of precorrin-2

sirohydrochlorin (Bali et al 2014). However, to direct precorrin-2 towards B_{12} biosynthesis a third methyl group is added to the C20 positon of precorrin-2. CobI catalyses the addition of this third SAM derived methyl group to the C20 positon of precorrin-2 to form precorrin-3a. This methyl carbon will later be extruded and lost as acetate during the ring contraction process that yields the 19 membered corrin ring of B_{12} (Crouzet et al 1990).

The trimethylated intermediate precorrin-3a is a substrate for the next enzyme of the B_{12} biosynthetic pathway, CobG. This enzyme is a monooxygenase that attaches an oxygen atom derived from molecular oxygen to C20 of precorrin-3a to form a tertiary alcohol, this modification aids in the later extrusion of C20 (Scott et al 1993). In addition to hydroxylation of C20 CobG also mediates the formation of a γ lactone between the carboxylate group of sidechain *α* and C1 of precorrin-3b. The result of these modifications is a compound that is primed for contraction of the macrocycle by extrusion of C20 as an acyl group and direct bonding of C1 and C19 of the corrin ring (Spencer et al 1993).

While formation of the tertiary alcohol at C20 of precorrin-3 primes this molecule for ring contraction the actual ring contraction step is mediated by the next enzyme in the pathway CobJ. Extrusion of C20 to form an acyl group attached to C1 occurs concurrently with methylation of precorrin-3b at C17 to form the first 19 membered intermediate of B_{12} biosynthesis, precorrin-4. Thus, both the methylation and ring contraction steps are catalysed by CobJ (Scott et al 1993).

Precorrin-4 is methylated at the C11 positon by CobM (Schubert et al 1998). The structure of B_{12} shows that in the final product no methyl group is present at C11 and instead two methyl groups are present at C12. Isotopic labelling studies have shown that the methyl group attached to C11 by CobM ultimately ends up at C12. The second α facing methyl group at C12 is derived for the later decarboxylation of the acetate sidechain at this positon. It has been postulated that methylation at the C12 positon would block this decarboxylation providing the chemical logic for the addition of a methyl group at C11 and its subsequent migration to C12 (Thibaut et al 1992).

CobF catalyses the deacetylation of C1 and its subsequent replacement with a SAM derived methyl group (Min et al 1993). The chemical environment of this acyl group makes it highly labile. These carbon atoms are lost as acetic acid with the second oxygen atom required for acetic acid formation being derived from the solvent (Scott et al 1993). Following these modifications the macrocyclic oxidation level of precorrin-6a is higher than that of the final product (Blanche et al 1995). The next step of the biosynthesis addresses this disparity and a double bond of the dihydrocorrin macrocycle is reduced. Reduction of the double bond between C18 and C19 is performed by CobK and is NADPH dependent (Blanche et al 1992[2]). Reduction of the dihydrocorrin by one NADPH derived hydrogen and one solvent derived hydrogen atom brings the oxidation state of the macrocyclic ring back to that of a corrin (Battersby 1993). The resulting compound precorrin-6b is the substrate for the next enzyme in the pathway CobL which adds the final two methyl groups to C5 and C15 of precorrin-6b (Blanche et al 1992[1]). This enzyme, CobL also facilitates the decarboxylation of the acetate sidechain attached to C12. The methyl transferase activity for C5 and C15 can be separated and assigned to the N and C portions of CobL. Additionally the order of methylation has been shown to occur at C15 before methylation at C5. The decarboxylation and methyl transferase activities of the C terminus of CobL have not been separated. However, it has been proposed, that mechanistically, methylation is likely to precede decarboxylation as the two occur in a concerted process (Deerey et al 2013). The methylation of C5 is catalysed by the N-terminus of CobL, overall, these steps result in the synthesis of precorrin-8.

The subsequent step in the pathway involves an enzyme designated CobH which catalyses the suprafacial rearrangement of the methyl group from C11 to C12, in doing so precorrin-8 is converted to HBA. As a result of this methyl migration the conjugated π system extends from C4 to C16 of the corrin macrocycle of HBA as it is no longer blocked by the presence of a tertiary carbon atom at C11 (Deery et al 2013, Thibaut et al 1992). Extension of this network of delocalised electrons results in a drastic change to the UV visible spectrum of HBA relative to precorrin-8 reflective of the newly formed chromophore (Figure 1:1:4).

The synthesis of HBA from ALA represents the core of the cobalamin biosynthetic pathway. HBA has a corrin ring at the same oxidation level as the final product and the stereo chemistry of the peripheral sidechains is locked in by the presence of 8 methyl groups. The next steps in B_{12} biosynthesis concern the attachment of peripheral amide groups, insertion of cobalt and attachment of the upper and lower ligands of the cobalt ion (Figure 1:1:5).

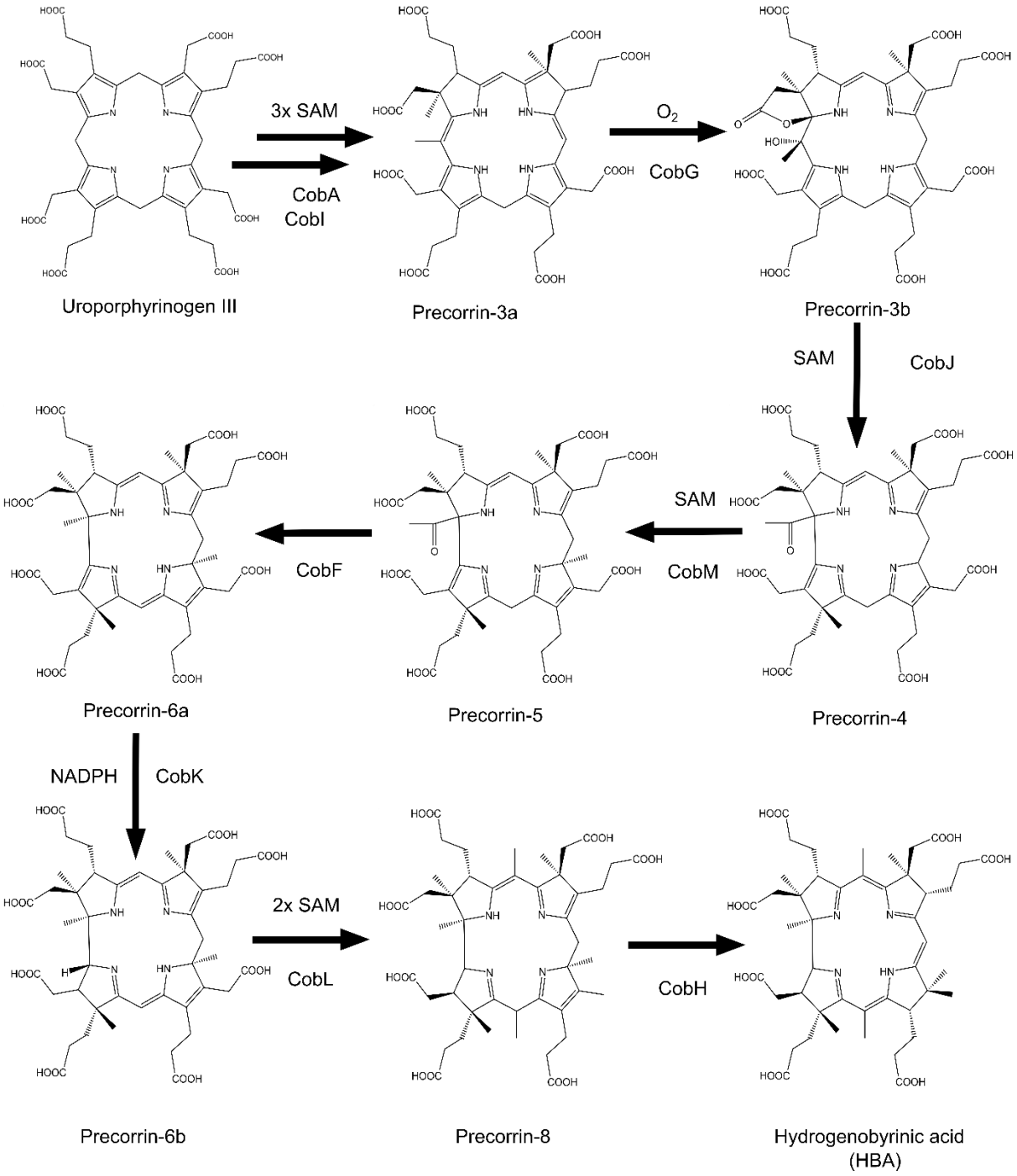

Figure 1:1:5: Section of the aerobic B_{12} biosynthetic pathway from uroporphyrinogen III to hydrogenobyrinic acid.

The peripheral sidechains of B_{12} are comprised of 3 propionamide and 3 acetamide groups. The conversion of the carboxylic acid sidechains of HBA to their amide counterparts begins with the amidation of the two β facing acetate sidechains *a* and *c*. These groups are amidated by the glutamine dependent amidotransferase CobB. The amidation of these groups proceeds in an ordered fashion with sidechain *c* amidation occurring before amidation of sidechain *a* (Debussche et al 1990). The resulting compound hydrogenobyrinic acid *a,c* diamide (HBAd), is the substrate for cobalt insertion.

The process of cobalt insertion is catalysed by the multi-component CobN, CobS and CobT chelation complex (Debussche et al 1992). CobNST shows sequence and structural homology to the magnesium chelatase complex involved in the synthesis of bacteriochlorophyll (Brindley et al 2003). The largest component of the cobaltochelatase complex is CobN. This 115 kDa protein is responsible for the binding of both cobalt and HBAd. CobS and CobT form a AAA ring-like complex and hydrolyses ATP in order to drive the process of Co^{2+} insertion into the corrin macrocycle of HBAd (Debussche et al 1992).

Initially many of the cobalt containing intermediates from the aerobic pathway were generally isolated as their cyano derivatives. *In vivo* the cobalt containing intermediates of B_{12} biosynthesis harbour an adenosyl group on the upper β face of the cobalt ion. Adenosylation, therefore, occurs relatively soon after insertion of cobalt, by a process that is catalysed by CobO (Debussche et al 1991). A number of adenosyl transferases exist that are able to transfer an adenosyl group to the β position of B_{12} as part of co-factor recycling pathways (Escalante-Semerena 2007). CobO, however, shows greater activity towards cobyrinic-acid *a,c* diamide than towards Cbl (Debussche et al 1991). As a prerequisite to adenosylation the cobalt ion must first be reduced to the supernucleophilic Co^{1+} species. Co(II)yrinic-acid *a,c* diamide is reduced in an NADPH dependant fashion by CobR (Lawrence et al 2008). The activity of CobO is inhibited by HBAd, which possibly represents some kind of regulation of B_{12} biosynthesis (Debussche et al 1991).

The product of CobO, adenosyl-cobyrinic acid *a,c* diamide is the substrate for the second glutamine dependent amidotransferase involved in B_{12} biosynthesis. CobQ catalyses the amidation of sidechains *b,d,e,g* and *f* (Blanche et al 1991[1]). The order of amidation has been determined for the CobQ equivalent from *Salmonella enterica* CbiP and found to proceed in the order *e, d, b* and *g* (Fresquet et al 2007).

The final steps in the synthesis of cobalamin involve the synthesis and attachment of the lower nucleotide loop. The lower loop is comprised of two components synthesised separately from the main pathway (Roth et al 1993). The first of these components to be attached is the aminopropanol linker that separates the corrin macrocycle of B_{12} from the dimethylbenzimidazole (DMB) nucleotide that co-ordinates the central cobalt ion. Aminopropanol is synthesised from threonine where the first step involves phosphorylation catalysed by PduX or the isofunctional enzyme BluF (Blanche et al 2000, Fan and Bobik 2008). This is followed by decarboxylation of threonine phosphate by CobC resulting in the formation of aminopropanol-*O*-2 phosphate. This linker is then attached to adenosyl-cobyric acid by the action of a CobD (Escalante-Semerena 2008). Both CobD and CobC form a high molecular weight complex *in-vitro* (Blanche et al 1995).

The second component of the lower nucleotide loop is a ribose containing nucleotide. In the case of the Cbl this nucleotide is DMB. Other variants of B_{12} exist in which this nucleotide is substituted for another group (Hazra et al 2013, Stuppperich et al 1988). In the absence of DMB a number of bacteria produce pseudocobalamin, here the nucleotide component of the lower loop is adenine in place of DMB. Interestingly when these organisms are supplemented with DMB they will incorporate this in preference to adenine to produce Cbl (Helliwell et al 2016). Naturally occurring analogues of B_{12} exist in nature differentiated by the identity of the nucleotide loop attached to sidechain *f*, these groups include phenyl, benzimidazole and nucleotide substituents (Stupperich et al 1988). Different organisms display preferences for certain B_{12} analogues and will alter

the attached nucleotide to suit their biochemical preferences, most B_{12} utilising organisms display a preference for DMB containing cobalamins.

DMB can be synthesised via one of two routes, an anaerobic route and better characterised aerobic route (Hazra et al 2015, Taga et al 2007). The starting point for the aerobic synthesis of DMB is Flavin mononucleotide, DMB is synthesised in a single O_2 dependent step by BluB (Gray et al 2007). The next step in lower nucleotide loop biosynthesis concerns the attachment of DMB to a phosphoribosyl sugar derived from nicotinate mononucleotide, this is catalysed by CobU and results in the formation of a DMB containing nucleotide called α-ribazole (Cameron et al 1991).

Before the attachment of the lower nucleotide loop a guanylyl group is added to the terminal phosphate of Adeosyl-cobinamide phosphate by the guanylyltransferase CobP, this enzyme has two functions as it acts as both a kinase and a guanylyltransferase (Blanche et al 1991[2]). CobP is responsible for phosphorylation of adenosylcobinamide as well as the attachment of GMP to the phosphorylated aminopropanol linker to form adenosyl-GDP cobinamide.

The final step in B_{12} biosynthesis brings together GDP-cobinamide and α-ribazole the attachment of these two components with the subsequent loss of GDP is catalysed by CobV (Figure 1:1:6).

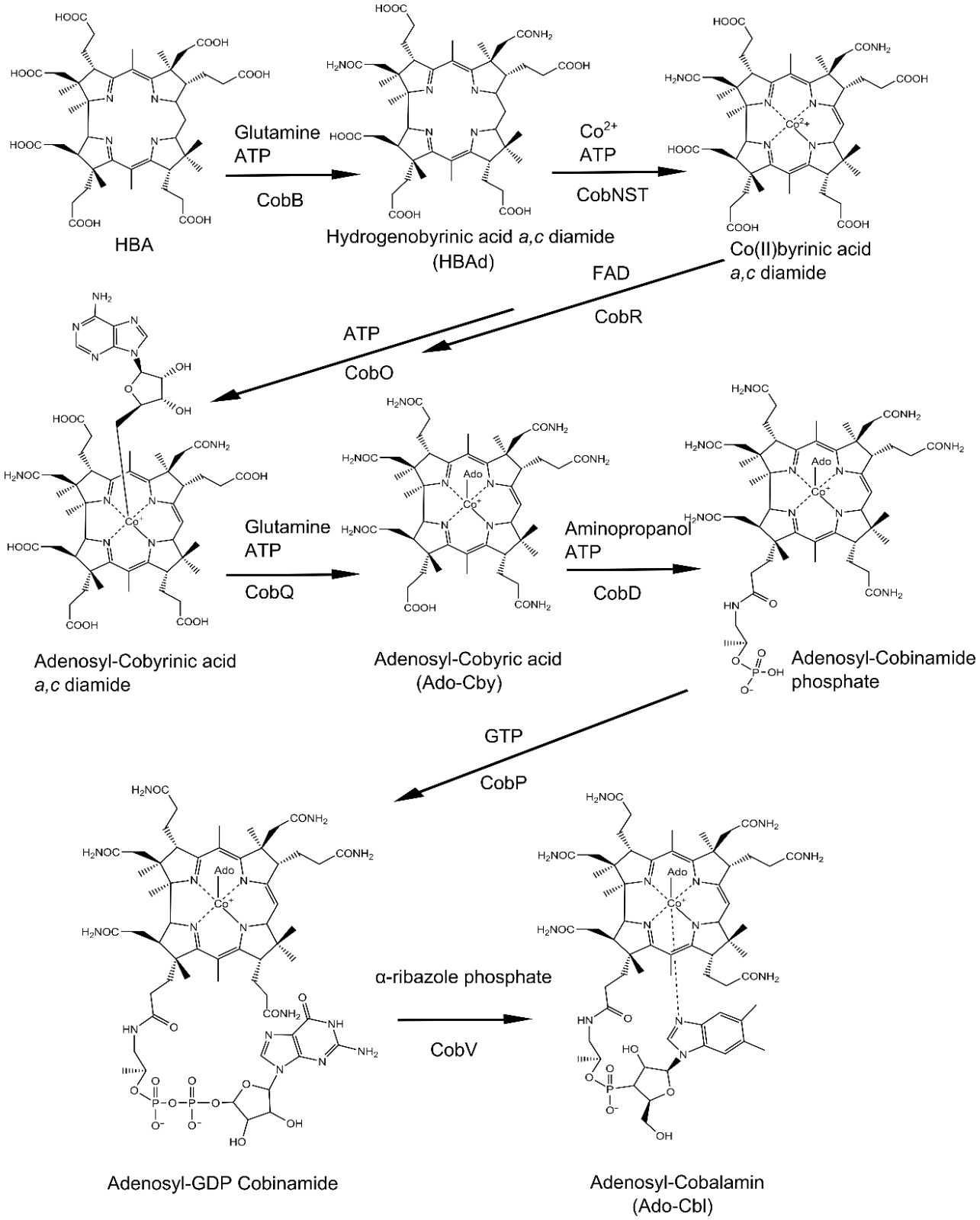

Figure 1:1:6: The terminal steps of cobalamin biosynthesis from cobalt chelation through to attachment of the lower nucleotide loop.

1:1:6 Anaerobic B_{12} biosynthesis

A second pathway for B_{12} biosynthesis exists in nature that, in contrast to the previously described aerobic pathway, has no requirement for O_2 (Santander et al 1997). Biosynthesis of B_{12} via the anaerobic or oxygen independent route proceeds via cobalt insertion into the macrocycle of sirohydrochlorin by one of two cobalt chelatases, CbiK or CbiX (Brindley et al 2003, Schubert et al 1999). Despite catalysing the same reaction both CbiK and CbiX show little homology to one another and are highly dissimilar to the relatively complex CobNST chelatase utilised during aerobic B_{12} biosynthesis (Mendel et al 2007).

Once cobalt is inserted into precorrin-2 the anaerobic biosynthesis of B_{12} broadly follows that of the aerobic pathway. The first step is highly similar to aerobic B_{12} biosynthesis, CbiL catalyses the addition of a SAM derived methyl group to C20 in a reaction analogous to that catalysed by CobI in the aerobic pathway (Frank et al 2007). Methylation at this position primes cobalt precorrin-3 for ring contraction through extrusion of C20 and the attached methyl group.

Ring contraction in the anaerobic pathway relies on a different mechanism to its aerobic counterpart. Aerobically the mechanism of ring contraction proceeds via direct incorporation of oxygen at C20 to form a tertiary alcohol followed by rearrangement of the corrin ring to extrude C20 as an acyl group. Anaerobically extrusion of C20 is achieved via formation of a δ lactone formed between sidechain *a* and C20. This allows for the direct bonding of C1 and C19. Ring contraction is catalysed by CbiH. Sidechain *a* of cobalt precorrin-3 forms a δ-lactone with C20 of the corrin ring leading to its extrusion. CbiH also catalyses the addition of a SAM derived methyl group to C17 of the corrin macrocycle. Completion of these two steps yields cobalt precorrin-4 (Santander et al 1997, Moore et al 2013).

CbiF, another SAM dependent methyltransferase, is responsible for the methylation of C11. As with the analogous methylation that occurs as part of the aerobic biosynthesis of B_{12}, methylation at this position seems counter intuitive

as the final product has no methyl group at C11 (Schubert et al 1998, Kajiwara et al 2006).

Excision of the carbon atom that began as C20 of the macrocycle of precorrin-2 is completed by CbiG through its removal as acetaldehyde (Kajiwara et al 2006). During aerobic biosynthesis these carbons are lost as acetic acid. The resulting intermediate, pecorrin-5b is methylated at position C1 by CbiD to form cobalt precorrin-6a (Moore et al 2013). As with the aerobic pathway cobalt precorrin-6a is more oxidised than the final product. This difference in oxidation level is rectified by the action of CbiJ an NADPH dependent reductase that catalyses the reduction of the double bond between C17 and C18 (Rossner and Scott 2006).

During aerobic B_{12} biosynthesis methylation of C5 and C15 as well as the decarboxylation of the acetate sidechain at C12 is catalysed by a single protein called CobL (Blanche et al 1992[1]). This same set of activities are encoded by two separate proteins in some cases when biosynthesis proceeds via the anaerobic route. CbiT, which shows homology to the C terminal portion of CobL catalyses methylation of C15 as well as the decarboxylation of C12 to produce an intermediate that has 7 methyl groups. An eighth SAM derived methyl group is attached to C5 of cobalt-precorrin-7 forming cobalt precorrin-8 catalysed by CbiE (Rossner et al 2006).

The final steps before the identity of the intermediates of both B_{12} biosynthetic pathways converge are highly similar. First CbiC is responsible for the migration of the C11 attached methyl group to C12 catalysing a reaction analogous to that catalysed by CobH (Shipman et al 2001). Migration of the methyl group attached at C11 to C12 forms cobyrinic acid. Cobyrinic acid is then the substrate for the first glutamine dependent amidotransferase of the anaerobic pathway CbiA (Fresquet et al 2004). CbiA is analogous to CobB of the aerobic pathway and catalyses the amidation of sidechains *a* and *c*. Once cobyrinic acid *a,c* diamide is formed the remaining biosynthetic steps are identical (Moore et al 2013).

1:1:7 Metal free corrins and metal analogues of cobalamin

Apart from the differences in some of the earlier intermediates from the aerobic and anaerobic pathways the identities of the intermediates of B_{12} biosynthesis remain fixed especially the core synthesis of the corrin ring (Blanche et al 1995, Moore et al 2013). Some variation however, exists regarding the nature of the lower nucleotide loop as some organisms' display a preference for lower nucleotide loops comprised of nucleotides other than DMB (Stupperich et al 1988, Watanabe et al 1999).

B_{12} is metabolically a costly molecule to produce, it is therefore more energetically favourable for organisms that require B_{12} to acquire the full compound or later intermediates of B_{12} biosynthesis from the environment. As B_{12} is present at such low concentrations high affinity transporters have evolved to bring B_{12} into cells. Intermediates of B_{12} biosynthesis are not generally found outside of cells owing to the metabolic cost of producing them. Additionally a mechanism by which B_{12} or intermediates of B_{12} biosynthesis are exported from the organism that produce them has not be described to date. However, a number of metal free corrins had been isolated from the growth media of cultures of *Allochromatium vinosum, Rhodospirillium rubrum* and *Rhodobacter capsulatus.* Isolation of these compounds preceded the full elucidation of the aerobic pathway of B_{12} biosynthesis (Toohey et al 1965). A majority of the extracellular-corrins isolated from cultures of these organisms were identified as HBAd, HBA and HBA *c* monoamide (Dresow et al 1980, Fukuzaki et al 1989). Of particular note was that cultures of *A. vinosum* produced an extracellular corrin chemically similar to B_{12} but containing no cobalt (Toohey et al 1965). The identity of this cobalt free corrin was deduced through degradative experiments as well as by reaction with cobalt to produce a molecule spectrally and chromatographically identical to B_{12}. The similarity of this metal free corrin to B_{12} resulted in it being designated hydrogenobalamin (Hbl), following the naming convention for its cobalt containing counterpart (Thomson 1969, Toohey et al 1965, Dresow et al 1980).

Shortly after the isolation of Hbl various transition metal analogues of cobalamin were synthesised in a single step using Hbl as the starting material. From 1970 to

1980 reports regarding the synthesis of the zinc, copper, and rhodium analogues of cobalamin along with a brief communication describing the iron analogue of the B_{12} and various patents relating to the production of Co^{57} B_{12} from Hbl had been published (Bieganowski et al 1979, Charlton and Hamilton 1979, Koppenhagen et al 1970, Koppenhagen et al 1973). The paucity of starting material resulted in only small quantities of these compounds being synthesised. This coupled with the available analytical techniques of the time prevented a more rigorous characterisation of Hbl as well as the metal analogues synthesised from this compound. In particular little data was generated on the effects of these compounds with regards to biological activity.

Due to the chemical similarity of these metal analogues to B_{12} they are predicted to interact with the uptake machinery responsible for B_{12} import into cells (Carmel et al 1977, Kräutler 2015). More recently, uptake of rhodibalamin has been demonstrated using a *Salmonella enterica* bioassay system along with a bactericidal effect at high concentrations (Widner et al 2016). It would be of interest to produce analogues of B_{12} that vary the central metal ion as other metal analogues of Cbl should also act as antagonists to B_{12} dependent processes and could therefore be considered anti-vitamins. The increased B_{12} requirement of many bacteria or of cancerous cells during proliferation relative to normal mammalian cells may lead to clinical application for such metal analogues of Cbl (Russell-Jones et al 2004). These B_{12} analogues may also find uses as aids to probing B_{12} dependent systems *in vivo* as uptake and binding of these compounds can be separated from the metabolic functions of B_{12}. The differing chemical properties associated with various transition metal ions may also provide a greater understanding of the evolution of these compounds, particularly why nature selected cobalt as the core of B_{12}.

While historically Hbl was used as the starting material for the synthesis of these compounds the low amounts produced by cultures of *A. vinosum*, 1 mg of Hbl being isolated from 100g of cell paste (Toohey et al 1965). An alternative approach utilising a more abundant starting material would allow for the

production and characterisation of metal analogues of B_{12} using more modern analytical techniques.

The synthesis of adenosylrhodibalamin, the rhodium analogue of adenosyl-cobalamin was completed starting from the metal-free intermediate of B_{12} biosynthesis, HBAd (Widner et al 2016). While rhodibalamin had been synthesised previously from Hbl (Koppenhagen et al 1970), the characterisation of this molecule was somewhat limited due to the small amounts of the compound it was possible to synthesise. The more recent synthesis of adenosylrhodibalamin enabled the characterisation of this molecule by X-ray crystallography and NMR spectroscopy along with a comparison of the data for the rhodium compound to that of its cobalt containing counterpart (Widner et al 2016).

The synthesis of rhodibalamin from HBAd presents a way to more efficiently generate metal analogues of Cbl as HBAd can be produced at the mg scale from a plasmid based expression system (Deery et al 2013). The relative ease with which HBAd can be produced on the mg scale offsets the greater number of synthetic steps required to reach the final product. The synthetic scheme outlined by Widner et al, while an effective method for the synthesis of rhodibalamin cannot be adapted for the synthesis of analogues that cannot be stably adenosylated due to the specificity of the amidase used as part of the chemi-bio synthesis of adenosylrhodibalamin. In order to mimic the structure of B_{12} as closely as possible any analogues produced must harbour amide groups at positions *a, b, c, d, e* and *g* (Figure 1:1:2). The biosynthetic intermediate HBAd has 2 of the 6 required amide groups at positions *a* and *c* (Figure 1:1:6) necessitating the specific amidation of sidechains *b, d, e* and *g*, leaving *f* as a carboxylic acid.

Following the B_{12} biosynthetic pathway Widner et al inserted rhodium into the macrocycle of HBAd to produce its rhodium analogue before this compound was then adenosylated and the remaining amides added by the action of *Rhodobacter capsulatus* CobQ resulting in the formation of adenoyslrhodybyric acid. The specificity of *R. capsulatus* CobQ prevents the synthesis of additional metal analogues due to the requirement of this CobQ for adenosylated substrates

(Blanche et al 1991[1]). Therefore, in order to produce a wider variety of metal analogues of B_{12}, particularly those that cannot be adenosylated an alternative synthetic scheme for the production of B_{12} analogues needs to be developed.

The most important obstacle that needs to be overcome is to identify a means by which non-adenosylated metal analogues of HBAd can be specifically amidated at positons *b, d, e* and *g.* It is critical that sidechain *f* be differentiated from the other peripheral sidechains due to the need for nucleotide loop attachment at this position.

1:2:1 Project aims

The aim of this project is to develop a synthetic scheme by which non-adenosylated metal analogues of cobalamin can be produced. In doing so this reaction scheme could potentially be adapted to produce a number of metal analogues of B_{12} from HBAd. The main barrier to the development of such a synthetic scheme is a method by which sidechains *b, d, e* and *g* can be amidated while retaining sidechain *f* as a carboxylic acid group. Identification of a method that allows either metal containing non-adenosylated intermediates or metal free intermediates will broaden the scope of metal analogues that can be produced.

As a proof of concept the zinc analogue of B_{12} was to be produced from HBAd. By undertaking this synthesis some of the intermediates produced *en-route* were characterised by NMR and their effect on bacterial metabolism investigated.

Chapter 2: Materials and methods

2:1 Materials

2:1:1 Chemicals

Name	Grade	Supplier
(2-Amino-1-methylethyl)-3‟-(α-ribazole)-diphosphate, C17H26N3O7P	N/A	Prof B. Kräutler
Acetonitrile	HPLC reagent grade	Fisher Scientific
Acrylamide	30% Acrylamide/Bis Solution, 29:1	Bio-Rad
Agar bacteriological	N/A	Oxoid
Agarose	N/A	Alpha Laboratories
Ammonium acetate	ReagentPlus ≥99.5 %	Sigma-Aldrich
Ammonium chloride	ReagentPlus ≥99.5 %	Sigma-Aldrich
Ampicillin Sodium Salt	N/A	Melford
ATP	≥99 %	Sigma-Aldrich
Broad range protein marker	N/A	NEB
Calcium chloride dihydrate	ReagentPlus ≥99 %	Sigma-Aldrich
Chelating Sepharose Fast Flow	N/A	GE Healthcare
Chloramphenicol	≥98 %	Sigma-Aldrich
Deuterium oxide	99%	
Dimethyl sulfoxide (DMSO)	99%	NEB
2-(Diethylamino)ethyl spehacel	N/A	GE Healthcare
DNA Ligase (T4)	1–3u/µL	Promega
DNA loading buffer (5x)	N/A	Bioline
DNA Polymerase (FastStart Taq)	5 U/µl	Roche
dNTP’s	100mM	Sigma-Aldrich
Ethanol	99.8+% analysis grade	Fisher Scientific
Ethidium bromide	General purpose grade	Fisher Scientific
L-glutamine	ReagentPlus ≥99 %	Sigma-Aldrich

D-glucose, anhydrous	Analytical reagent grade	Fisher Scientific
Glycerol	99.0+% 1.257-1.261g/mL	Fisher Scientific
HEPES sodium salt	Buffer grade ≥99 %	Fisher Scientific
Hydrochloric acid	31.5-33.0%	Fisher Scientific
Hyper Ladder 1 kb DNA marker	N/A	Bioline
Imidazole	ACS reagent, ≥99%	Sigma-Aldrich
IPTG	N/A	Melford
Lichroprep RP-18 20-40µM particle size	N/A	Merck
Methanol	Analytical grade	Fisher Scientific
MgCl2	Analytical reagent grade	Fisher Scientific
NaCl	99.9+% for analysis	Fisher Scientific
Nickel(II) sulphate hexahydrate	99% analysis grade	Acros Organics
Potassium phosphate dibasic	ACS reagent grade	Sigma-Aldrich
Potassium phosphate monobasic	ACS reagent grade	Sigma-Aldrich
Potassium sulphate	≥99 %	BDH Laboratory Supplies
Restriction enzymes	Variable	NEB / Promega
Sodium acetate	Reagent grade 99%	Sigma-Aldrich
Sodium dodecyl sulphate	99+%	Fisher Scientific
Sodium hydroxide	Reagent grade ≥99 %	Sigma-Aldrich
Sodium phosphate dibasic	ReagentPlus ≥99 %	Sigma-Aldrich
Trifluoroacetic acid	ReagentPlus ≥99 %	Sigma-Aldrich
Tris(hydroxymethyl) methylamine	Tris buffer 99.8+%	Fisher Scientific
Tris-Acetate-EDTA	50X	Fisher Scientific
Tryptone	N/A	Oxoid
Yeast extract	N/A	Oxoid

Zinc acetate dihydrate	≥99 %	Sigma-Aldrich

Table 2.1 Chemicals used in this study

2:1:2 Protein crystallography screens

All screens were purchased from molecular dimensions Cambridge. Structure screen 1 was used for initial screening (Wooh et al 2003). Additional screens were conducted using Molecular dimensions Midas screen (Grimm et al 2010)

2:1:3 *Escherichia coli* strains

Strain	Genotype	Source
JM109	endA1, recA1, gyrA96, thi, hsdR17 (rk–, mk+), relA1, supE44, Δ(lac-proAB), [F', traD36, proAB, laqIqZΔM15]	Promega
BL21 (DE3)	F– ompT hsdSB (rB– mB–) gal dcm (DE3)	Novagen
BL21 (DE3) pLysS	F- ompT hsdSB(rB- mB-) gal dcm (DE3) pLysS (CamR)	Novagen

Table 2.2 E. coli strains used in this study

2:1:4 Plasmids

Plasmids used in this project.

Plasmid name	Genotype	Description
pET-AvCobQ	pET14b-AvCobQ	Protein overexpression vector containing N-terminal polyhistidine-tag Allochromatium vinosum CobQ
pET14b-RcCobQ	pET14b-RcCobQ	Overexpression vector containing N-terminal polyhistidine-tag Rhodobacter capsulatus CobQ (Dr Evelyne Deerey)
pET14b-CobB	pET14b-CobB	Overexpression vector containing N-terminal polyhistidine-tag Rhodobacter capsulatus CobB (Dr Evelyne Deerey)
pET14b-BtuF	pET14b-BtuF	Overexpression vector containing N-terminal polyhistidine tagged Escherichia coli BtuF
pET3a-HBAd	pET14b-HBAd	Overexpression vector containing the cobalamin biosynthetic genes AIGJFMKLHB kindly donated by Dr Evelyne Deerey
pET3a-Hby	pET3a-Hby	Overexpression vector containing the cobalamin biosynthetic genes AIGJFMKLHBQ kindly donated by Dr Emi Nemoto-Smith
pLysS	PlysS	Overexpression vector

2:1:5 Primers

Name	Sequence
pET14b-Av_CobQ_FW	CGGCATATGACCGATTCAGCCCCCACCATC
pET14ba-Av_CobQ_RV	GCCACTAGTTCAGCGTGGCCAGTTCGAGCAG

Table 2.4 Primers used in this study

2:1:6 Equipment

Glassware was purchased from SCHOTT and Fisher.

Micro-centrifuge tubes were purchased from Eppendorf.

50ml falcon tubes were purchased from SARSTEDT

Millipore water was dispensed from a Simplicity 185 device with a Simpak 1 cartridge.

Solutions and equipment were autoclaved using a Priorclave 40 benchtop autoclave. 121 °C at 1 bar pressure for 15 minutes

Centrifugations were performed with the following centrifuges and rotors:

Beckman Coulter Avanti J-30I

-JLA_9.100

-JA_25.50

ALC, Multispeed refrigerated centrifuge

-T527

Thermo Scientific, Megafuge 16R

-TX-400

Eppendorf, MiniSpin Plus

-F45-12-11

Polymerase chain reactions were carried out in an Eppendorf Mastercycler 5341 thermal cycler.

DNA Electrophoresis was performed with a PerfectBlue Gel System Mini M (Peqlab) and a Bio-Rad PowerPak 300. DNA was visualised with a UVIsave HD5 device from UVItec.

Sonications were performed with a Sonics vibracell sonicator equipped with a Jencons solid titanium alloy probe.

Buffer exchange of proteins was performed with PD-10 size exclusion columns from GE Healthcare.

Protein electrophoresis was performed with an Atta Mini Power Electrophoresis Power Supply, SJ-1082.

All UV-vis measurements were performed using an Agilent Cary 60 UV/ Vis with semi micro UV cuvettes from Brand or quartz crystal cuvettes, 1.5-3 ml path length 1 cm.

NMR spectra were collected using 600 MHz: Bruker Ultrashield spectrometer or a 500 MHz: Varian Unity Inova 500. Spectra were collected at 298K referenced against HDO δ = 4.79 ppm for both D2O and 10% D2O 90% H_2O solvent systems.
1D-1H spectra for Hby, Zby and Zbl recorded in D_2O used a presat pulse program. 2D-1H homonuclear COSY and ROESY spectra for Zby and Zbl were recorded using a gCOSY and ROSEYAD pulse programs respectively. 2D-1H, 13C heteronuclear HSQC experiments for Zby and Zbl were recorded using a gHSQC pulse program. These experiments were recorded using a 500 MHz Varian Unity Inova 500.
The 1D-1H spectrum of Hby recorded in 90% H_2O 10% D_2O was produced using a Watergate-zgesgp pulse program for solvent suppression. A 2D-1H ROESY homonuclear run in 90% H_2O 10% D_2O was recorded using a ROESYesgpph pulse program for suppression of the water peak. A 2D-1H 13C heteronuclear HSQC recorded in 90% H_2O 10% D_2O was produced using a HSQCetfpgpsi2 pulse program for suppression of the water peak. These spectra were recorded on a Bruker Ultrashield 600 MHz spectrometer.

Fast protein liquid chromatography (FPLC) was conducted using an Äkta FPLC system; P-920 pump, UPC-900 monitor for UV detection at 280 nm. Analyses were performed using a Superdex G200 size exclusion column able of separating protein complexes between 10 KDa and 600 KDa.

High performance liquid chromatography (HPLC) was performed using an Agilent 1100 HPLC system with diode array detector. Analyses were conducted using an

ACE chromatography 5AQ column 150 mm x 2.1 mm 5 µM particle size. Additional chromatography was performed using a Hitachi HPLC system, L-2130 pump with online degasser and diode array detector (Phenomenex hyperclone C18, 250 mm x 4.6 mm).

Mass spectra were collected using a Finigan MAT 95s LCQ classic electrospray mass spectrometer. Additional spectra were collected using a Bruker micro Qtof II with electrospray ionisation.

Growth curves were collected using a FLUOstar omega microplate reader by BMG labtech.

2:1:7 Solutions for molecular biology work

Molecular weight marker

Hyper Ladder 1 kb DNA Marker:

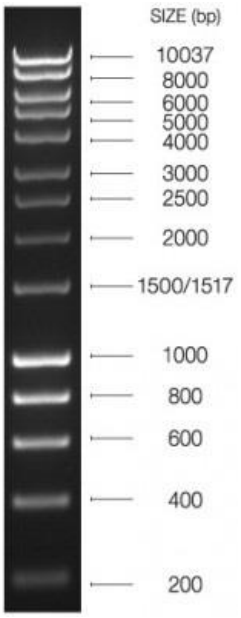

Figure 2.1.1 Hyper Ladder 1 kb DNA Marker run on a 1% agarose gel (Bioline, MA)

Ligation buffer.

60 mM Tris pH7.8

20 mM $MgCl_2$

20 mM DTT

2 mM ATP

10% w/v PEG 8K

2:1:8 Media and solutions for microbiological work

Lysogeny broth (LB)

NaCl	86.2 mM
Yeast extract	5 g/L
Tryptone	10 g/L

Diluted in dH_2O before autoclaving (121 °C 3 bar pressure for 15 minutes)

2YT + Ammonium acetate

Ammonium acetate	13 mM
NaCl	86.2 mM
Yeast extract	10 g/L
Tryptone	16 g/L

Diluted in dH_2O before autoclaving (121 °C 3 bar pressure for 15 minutes)

Lysogeny broth agar (LB agar)

Add 15 g of bacteriological agar to 1 L of LB

10X M9 salts

Na2HPO4	478 mM
KH2PO4	222 mM
NH4Cl	187 mM
NaCl	86.2 mM

Diluted in dH_2O before autoclaving (121 °C 3 bar pressure for 15 minutes)

0.1M CaCl2

Made up with milliQ filtered water and filter sterilised, 0.2 µm filter.

1M MgSO4

Made up with milliQ filtered water and filter sterilised, 0.2 µm filter.

20% w/v D-glucose

Made up with H_2O and sterilised by autoclave

L-cysteine 5mg/ml

Made up with milliQ filtered water and filter sterilised, 0.2 µm filter.

L-methionine 5mg/ml

Made up with milliQ filtered water and filter sterilised, 0.2 µm filter.

M9 minimal media

Minimal media was made up as follows in a container sterilised by autoclave. 100 ml of 10X M9 salts, 20 ml 20% w/v glucose 2ml of MgSO4 1ml of CaCl2 10 ml of 5 mg/ml cysteine the solution was made up to 1 L with H_2O sterilised by autoclave.

Minimal media agar supplemented with methionine and cysteine

100 ml of 10X M9 salts, 20 ml 20% w/v glucose 2ml of MgSO4 1ml of CaCl2 10 ml of 5 mg/ml cysteine and 10 ml 5 mg/ml methionine the solution was made up to 1 L with 900 ml H_2O containing 15 g of agar at 45^{o} C

Salmonella bioassay plates

Minimal media Agar was made up using 100 ml 10X M9 salts, 20 ml 20% w/v glucose 2ml of MgSO4 1ml of CaCl2 10 ml of 5 mg/ml cysteine. The Final volume was adjusted to 1 L with 900 ml H_2O containing 15 g agar at 40°C. A lawn of *Salmonella enterica* (AR2680 *cysG, cbiB*) was scraped from minimal media plates containing both cysteine 0.05 mg/L and methionine 0.05 mg/L. Salmonella was washed in 0.9% w/v NaCl before being added to the bioassay agar at 40°C. Plates were allowed to cool and stored at 4°C.

Antibiotics:

Ampicillin

Stock concentration: 100 mg/ ml in H_2O. Filter sterilised 0.2µm filter, working concentration 100 µg/ ml

Chloramphenicol

Stock concentration: 34 mg/ ml in ethanol, working concentration: 34 µg/ ml

Antibiotics were stored at -20 °C until use.

Calcium chloride (0.1 M) + 10% glycerol

CaCl2.2H2O + 10% glycerol made up with H_2O and filter sterilised (0.2 µm)

Isopropyl β-D-1-thiogalactopyranoside (IPTG) (1 M)

IPTG dissolved in H_2O and filter sterilised (0.2 µm) stored at -20 °C until use

2:1:9 Solutions for biochemical work

NaCl solution (5 M) made up with H_2O

Tris-HCl solution (1 M) made up with H_2O and adjusted to pH 8.0 with concentrated HCl

Imidazole solution (1 M) made up with H_2O

Nickel sulphate (100 mM) made up with H_2O

4-(2-Hydroxyethyl)piperazine-1-ethanesulfonic acid (HEPES) solution (100 mM) made up with dH_2O

Ammonium acetate (10mM) made up with H_2O

Running buffer for SDS-PAGE:

25 mM Tris-HCl

192 mM glycine

0.1% SDS

In H_2O

Prestained Protein Marker, Broad Range (7-175 kDa)

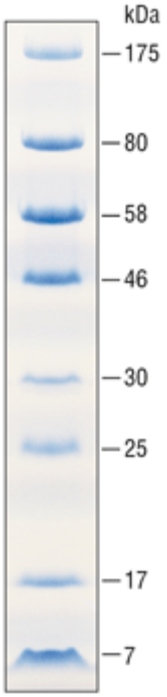

Figure 2.1.2 Prestained Protein Marker, Broad Range (7-175 kDa) run on a 10-20% Tris-glycine SDS-PAGE gel (New England Biolabs, MA)

2X Laemmli sample buffer:

0.125 M Tris-HCl pH 6.8

20% v/v Glycerol

4% w/v SDS

10% v/v β-mercaptoethanol:

0.004% w/v Bromophenol blue

Coomassie blue stain:

250 ml Trichloroacetic acid (TCA) (100%)

0.73 mM Coomassie brilliant blue

0.35 mM SDS

2 mM Tris

2 mM Glycine

Solutions for immobilised metal ion affinity chromatography (IMAC)

Binding buffer:

20 mM Tris-HCl, pH 8.0

500 mM NaCl

5 mM Imidazole

Wash buffer 1:

20 mM Tris-HCl, pH 8.0

500 mM NaCl

50 mM Imidazole

Wash buffer 2:

20 mM Tris-HCl, pH 8.0

500 mM NaCl

100 mM Imidazole

Elution buffer:

20 mM Tris-HCl, pH 8.0

500 mM NaCl

400 mM Imidazole

FPLC running buffer:

20 mM Tris-HCl, pH 8.0

200 mM NaCl

2:2 Molecular biology methods

2:2:1 PCR amplification of genes

Amplification of *A. vinosum* CobQ by PCR. A sterile PCR tube was set up with the following reagents:

PCR-A	Stock concentration	Volume (µl)
PCR reaction buffer with 20mM MgCl2	10X	5
Template DNA	N/A	1
FW primer	10 µM	2
Rev Primer	10 µM	2
FastStart Taq DNA Polymerase	5 U/µl	0.5
dNTP's	5 mM	2
DMSO	N/A	1
Autoclaved H_2O	N/A	37.5

Table 2.5 PCR reaction mixture

The PCR reaction was run in a thermocycler using the following program:

Step	Time	Temperature	Cycles
1	60 sec	94 °C	1-3 repeat 20 times
2	60 sec	50 °C	
3	1 min 30 sec	72 °C	
4	1 min	94 °C	1
5	10 min	72 °C	1
6	Hold	4°C	-

Table 2.7 PCR reaction cycles for PCR1-A and PCR1-B

PCR products were run on a 1% agarose gel, bands were cut out and gel extracted using the a gel extraction kit (Qiagen)

2:2:2 Analysis of DNA by gel electrophoresis

DNA fragments were separated in a 1% agarose gel run in 1X TAE buffer, DNA was visualised with ethidium bromide at a final concentration of 0.5 µg/ml. Prior to loading DNA was mixed with 5X loading buffer.

2:2:3 Gel extraction of DNA

DNA was extracted from agarose gels and from PCR clean-up reactions using a QIAquick Gel Extraction Kit (Qiagen), according to the handbook

2:2:4 Restriction digests

DNA was digested in a total reaction volume of 10 µl in a sterile 1.5 ml Eppendorf with appropriate enzymes and reaction buffers. Reactions were incubated at 37 °C for 2 hours.

Typical restriction digest protocol:

Plasmid DNA, 5 µl

Restriction enzyme 1, 0.5 µl

Restriction enzyme 2, 0.5 µl

10X Buffer, 1 µl

H_2O, 3 µl

2:2:5 DNA Ligations

DNA fragments were ligated in 10 µl reactions in sterile 1.5 ml Eppendorf tubes.

Typical ligation protocol:

Vector, 1.5 µl

Insert, 2.5 µl

2 X ligation buffer, 5 µl

T4 DNA ligase, 1 µl

2:2:6 Purification of plasmid DNA

Plasmid DNA was purified using a QIAprep Spin Miniprep Kit (Qiagen) according to the handbook

2:3 Microbiological methods

2:3:1 LB Agar plates

Bacteria were applied to LB agar plates with appropriate antibiotics. Agar plates were incubated overnight at 37 °C.

2:3:2 LB Liquid cultures

Liquid cultures were inoculated 1:100 from overnight starter cultures, with appropriate antibiotics and grown at 37 °C with shaking (160 rpm).

2:3:3 Cultures for production of HBAd and Hby

BL21(DE3) expressing pET3a-Hby or pET3a-HBAd were used to inoculate 1 l of 2YT with 1 g/l ammonium acetate. Cells were grown in 2 l borosilicate baffled flasks at 28°C for 36 hours with shaking at 120 RPM.

2:3:4 Competent cells

50 ml of LB was inoculated with 5 colonies; cells were grown at 37 °C with shaking to an OD600 of ~ 0.7. Cells were cooled on ice for 10 minutes then centrifuged at 2,700 x g for 10 minutes at 4°C. Pelleted cells were resuspended in 10 ml 0.1 M CaCl2 + 10% glycerol and stored on ice for 15 minutes. Following centrifugation at 2,700 x g for 10 minutes at 4 °C the supernatant was removed and the cells were resuspended in 1 ml 0.1 M CaCl2 + 10% glycerol. Cells were then aliquoted into 30 µl aliquots in sterile 1.5 ml Eppendorf tubes and stored at -80 °C.

2:3:5 Transformations

3 µl of plasmid DNA was added to 30 µl of competent cells for single transformations, for double transformations 1.5 µl of each plasmid was used. The cells were incubated on ice for 15 minutes, they were then heat shocked at 42 °C for 1 minute then incubated on ice for a further 2 minutes. 200 µl of LB was then added, cells were incubated at 37 °C for 20 – 60 minutes. Cells were subsequently plated on LB agar plates with appropriate antibiotics and incubated overnight at 37 °C.

2:3:6 Overexpression of recombinant protein

BL21 (DE3) pLysS competent cells were transformed with a plasmid containing the gene(s) of interest and plated on LB agar plates and incubated overnight at 37 °C. 10 ml of LB was inoculated with colonies from the transformation plate and appropriate antibiotics. 1 l LB in baffled flasks was inoculated with the overnight starter culture with appropriate antibiotics. The cultures were grown at 37 °C with shaking for 7 hours; protein production was induced by the addition of IPTG to a final concentration of 400 mM. The cultures were then incubated overnight at 19 °C with shaking. Cells were harvested by centrifugation at 3320 x g for 15 minutes at 4 °C, pellets were resuspended in binding buffer.

2:3:7 Production of HBAd and Hby in E.coli

BL21 (DE3) pLysS competent cells were transformed with a plasmid containing either the cobalamin biosynthetic genes AIGJFMKLHB (pET3a-HBAd) or AIGJFMKLHBQ (pET3a-Hby) and plated on LB agar plates containing 0.5% w/v glucose and incubated overnight at 28 °C. 10 ml of LB was inoculated with colonies from the transformation plate and appropriate antibiotics. 1 l 2YT supplemented with 1 g/l ammonium acetate in baffled flasks was inoculated with the overnight starter culture with appropriate antibiotics. The cultures were grown at 28 °C with shaking for 24 hours. Cells were harvested by centrifugation at 4000 x g for 20 minutes at 4 °C, pellets were resuspended in H_2O.

2:3:8 Salmonella bioassay plates

Salmonella typherium ΔCbiB ΔCysG was grown initially as a lawn on M9 minimal media plates supplemented with 0.05 mg/l L-cysteine and L-methionine. *Salmonella* was scraped from the surface of a 92mm diameter agar plate using a sterile loop. *Salmonella* was resuspended in 0.9% NaCl and pelleted by centrifugation at 2500 x g for 2 minutes this process was repeated 3 times. *Salmonella* was added to M9 minimal media agar without methionine at 40 °C, *Salmonella* was distributed throughout the agar by swirling before plates were poured and left to set. In order to test the biological activity of hydrogenobyrinic and zincobyric acid 5 µl of these compounds at various concentrations was dropped onto the surface of the plates and allowed to adsorb into the agar before the plate was incubated at 37°C for 15 hours.

2:3:9 Plate reader recorded growth of Salmonella ΔCbiB ΔCysG

Salmonella typherium ΔCbiB ΔCysG was grown initially as a lawn on M9 minimal media plates supplemented with 0.05 mg/l L-cysteine and L-methionine. *Salmonella* was scraped from the surface of a 92 mm diameter agar plate using a sterile loop. Salmonella collected in this way was used to inoculate 100ml M9 minimal media giving a final OD of 0.1. 1 ml of inoculated media was transferred to one of 24 wells containing various concentrations of Hby and B_{12}. The cultures were incubated with shaking in a Fluostar omega plate reader at 37°C OD 600 measurements were recorded at 600 nm every 10 minutes. Each growth condition was recorded in triplicate.

2:4 Cell lysis

Cells were lysed by one of two methods outlined below:

2:4:1 Sonication

Cell pellets resuspended in binding buffer were sonicated for 5 minutes with a 30 second pulse at an amplitude of 65%. Followed by 30 seconds with no pulse. sonications were performed on ice.

2:4:2 Boiling water bath

Cell pellets expressing plasmids pET3a-HBAd and pET3a-Hby resuspended in H_2O were immersed in water at 90 °C for 15 minutes.

2:5 Biochemical methods

2:5:1 Immobilised metal ion affinity chromatography (IMAC)

Preparation of nickel ion affinity column

Add a filter to an empty column and load with 5 ml of Chelating Sepharose Fast Flow, wash column with dH_2O.The column was charged with 10 ml of 100 mM $NiSO_4$ and equilibrated with 20 ml binding buffer.

Immobilised nickel ion affinity chromatography

Following cell lysis, cell debris was removed by centrifugation at 39,191 x g for 20 minutes at 4 °C. The supernatant was applied to the column and then column was then washed with 20 ml of binding buffer, followed by 10 ml of wash buffer 1. The column was then washed with 10 ml of wash buffer 2. Proteins of interest were eluted with 15 ml of elution buffer and 1 ml elution fractions were collected.

2:5:2 Buffer exchange

Following IMAC 625 µl of the four strongest elution fractions (determined by Bradford assay) were loaded onto a PD-10 desalting column equilibrated in exchange buffer and allowed to flow through. The protein of interest was eluted by addition of 3.5 ml of exchange buffer.

2:5:3 Fast protein liquid chromatography (FPLC)

The protein solution, depending on the size of the protein, was loaded onto a pre-packed, high resolution Superdex 10/300 G200 column, equilibrated with 1.5 - 2 column volumes of FPLC buffer. The protein was eluted at 0.5 ml/min into 1 ml fractions with buffer on an Äkta FPLC chromatography system with in line UV light source and UV detector set at 280 nm.

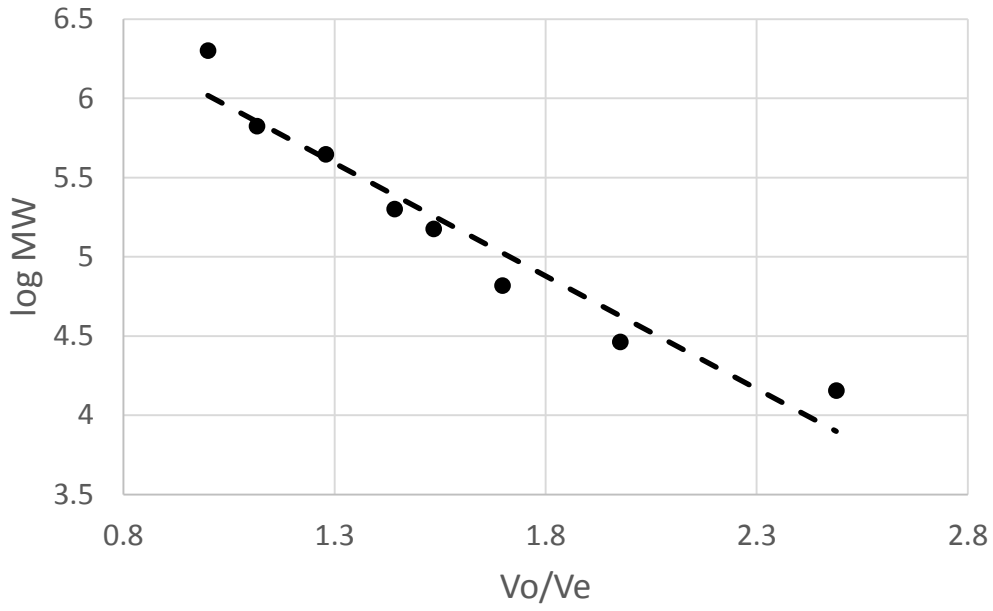

*Figure 2:5:1: Calibration curve for Superdex G200. A number of proteins of known molcuelar weight were applied to the colmn and the retention times recored the void volume of the column (8.6) was determined by the addition of blue dextran (MW 2000000 KDa). The log MW of the standard proteins were plotted against their elution volume (Vo) divided by the void volume of the column (Ve). A linear fit for this data gave the equation log MW = (Vo/Ve) * -1.42 +7.44.*

2:5:4 Determination of protein concentration

Protein concentrations were determined by measuring absorbance at 280 nm in cuvette with a path length of 1 cm. A blank is set using 1 ml of exchange buffer. The molar extinction coefficient (ε) was calculated using the EXPASY protparam bioinformatics tool (Gasteiger et al 2005). Protein concentrations were calculated using the Beer Lambert law A = εCL, where A is absorbance, C is the molar concentration and L is the path length.

2:5:4 In-vitro synthesis of Hby

HBAd was incubated with N-terminal polyhistidine tagged *A. vinosum* CobQ (0.64 µM), purified by nickel affinity chromatography. Was mixed with a solution of HBAd (27.3 µM), 20 mM Tris pH 8.0, 200 mM NaCl 1 mM ATP and 3mM glutamine. The reaction mixture was protected from light and incubated at 28°C for 15 hours.

2:5:5 Analysis of recombinant proteins by gel electrophoresis

Protein samples were collected mixed with 2X Laemmli sample buffer and boiled for 10 minutes.

Polyacrylamide gels were set up as outlined below:

Resolving gel	12.5%	Stacking gel	5%
H_2O (ml)	3.4	H_2O (ml)	3.4
30% Acrylamide (ml)	6.3	30% Acrylamide (ml)	1.5
1.5M Tris-HCl pH 8.8 (ml)	3.8	0.5M Tris-HCl pH 6.8 (ml)	1.9
10% SDS (ml)	1.5	10% SDS (ml)	0.75
10% APS (ml)	0.15	10% APS (ml)	0.075
TEMED (ml)	0.01	TEMED (ml)	0.01

Table 2.9 Composition of SDS-PAGE gels

Gels were run in running buffer at 200 volts for 1 hour and stained with coomassie blue stain. Gels were de-stained overnight in H2O under gentle agitation.

2:5:6 Protein crystallography

A. vinosum CobQ was concentrated to 8 mg/ml and used to generate protein crystals by hanging drop diffusion. 1 µL CobQ solution (8 mg/ml CobQ 20 mM tris pH 8.0 200 mM NaCl) was mixed with 1 µL of each of the precipitants on a siliconized glass cover slip the resulting drop was inverted over 1 ml of the precipitant condition and the experiment was allowed to stand for 3 days at 20 °C. The experimental set up is shown schematically in figure 2:5:1

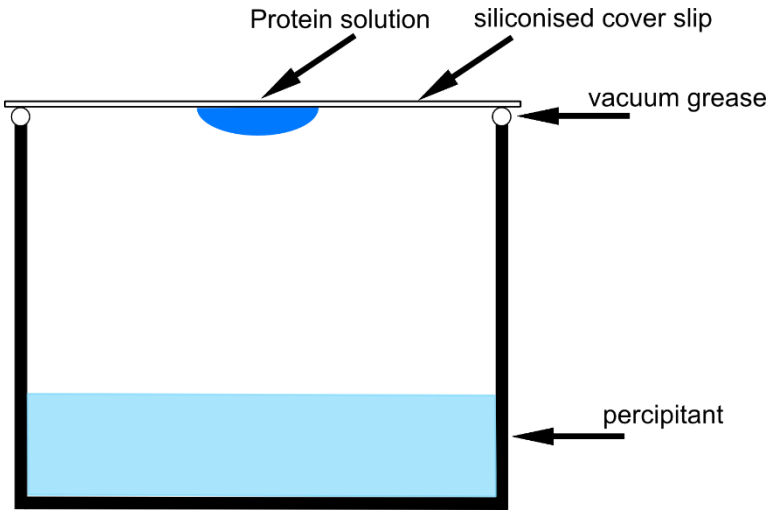

Figure 2:5:2: Schematic representation of hanging drop vapour diffusion experiment by which crystals of CobQ were generated. 1 µl of CobQ at a concentration of 8 mg/ml was mixed with 1 µl precipitant. This drop was inverted over 1 ml of the precipitant solution and incubated for 3 days at 20 ^{o}C

2:6 Chromatographic methods

2:6:1 Weak anion exchange chromatography of HBAd

Extraction of HBAd from cells expressing pET3a-HBAd cell pellets were lysed by boiling water bath. Precipitated protein was removed by centrifugation at 32,000xg for 15 minutes the supernatant was retained and the pellet resuspended in 25 ml 10 mM ammonium acetate before centrifugation at 36,000xg. The supernatant was combined with the supernatant from the previous step and applied to DEAE resin equilibrated in 10mM ammonium acetate. Once bound the resin was washed with 2 column volumes of 10 mM ammonium acetate. Additional washes consisted of 1 column volume each of 10 mM ammonium 100 mM NaCl and 10 mM ammonium acetate 150 mM NaCl. HBAd was eluted with 10 mM ammonium acetate 250 mM NaCl.

2:6:2 Reverse Phase chromatographic separation of Hby

Hby was purified by reverse phase chromatography either from cells expressing pET3a-Hby lysed by boiling water bath and precipitated protein removed by centrifugation at 36,000 x g for 20 minutes. Alternatively from Hby produced in-vitro from HBAd and recombinantly produced *A. vinosum* CobQ the reaction mixture was clarified by centrifugation at 36,000 x g for 20 minutes. The supernatant was applied to Lichroprep RP-18 resin equilibrated in 10 mM ammonium acetate. The resin was washed with 2 column volumes of 10 mM ammonium acetate. The resin was washed with 1 column volume each of 10 mM ammonium acetate 10 % v/v methanol and 10mM ammonium acetate 20 % v/v methanol. Hby was eluted in 10 mM ammonium acetate 30 % v/v methanol.

2:6:3 HPLC analysis of Hby

HPLC analysis of Hby using an Agilent 1100 HPLC system using an ACE chromatography 5 AQ C18 column samples were analysed using 0.1% v/v TFA in H_2O and acetonitrile as the organic phase. Samples were analysed using a 0 - 100% acetonitrile gradient over 40 minutes.

Additional HPLC analysis of Hby was performed on a Hitachi L-2130 pump system using a Phenomenex hyperclone 250 reverse phase C18 column. Analyses were performed with 10mM ammonium acetate as the aqueous phase and acetonitrile as the organic phase. The following gradient was used to separate Hby 0-5 minutes up to 5% acetonitrile 5-40 minutes up to 20% acetonitrile 40-45 minutes up to 5% acetonitrile.

2:6:4 HPLC analysis of Zby, Zbl and Hbl

Zincobyric acid was analysed by HPLC using a Hitachi L-2130 pump system using a Phenomenex hyperclone 250 reverse phase C18 column. Analysis were conducted using a 10mM ammonium acetate in H_2O as the aqueous phase and acetonitrile as the organic phase. The following gradient was used 0-5 minutes up to 10% acetonitrile 5-40 minutes up to 16% acetonitrile. UV chromatograms were collected using the in line diode array detector.

2:6:5 HPLC standards

HBA monoamide, HBAd and Hby retention times for these compounds when analysed using Agilent 1100 HPLC system and an ACE chromatography 5AQ C18 column and a 0.1 % TFA, acetonitrile gradient were determined by mass spectroscopy on account of a Bruker Qtof II electrospray mass spectrometer in line.

Retention times for Hby, Zby, Hbl and Zbl when analysed using a Hitachi L-2130 pump system and phenomenez hyperclone 250 C18 column using a 10 mM ammonium acetate, acetonitrile gradient were determined by comparsion to standard solutions of these compounds. Retention times are as follows, Hby 30.8 minutes, Zby 31.4 minutes, Hbl 37.5 minutes and Zbl 39 minutes.

2:7:1 Chemical synthesis

2:7:2 Synthesis of zincobyric acid

6.93 mg of hydrogenobyric acid is mixed with 34 mg (20 equivalents) of zinc acetate and 2.6 mg (4 equivalents) of sodium acetate the mixture is dissolved in 10 mL of H_2O degassed with argon. The mixture was heated to 50 °C for 1 hour 30 minutes before the reaction was stopped by binding the material to a Se-Pak column (1 g, C18 Waters) equilibrated in water and desalted by washing with 40 mL of H_2O the zincobyric acid was eluted in methanol and dried by rotary evaporation (30 °C at 120 mbar pressure). Zby produced in this was further purified by reverse phase chromatography on the bench. The material was bound to lichroprep RP-18 resin equilibrated in 10mM ammonium acetate buffer at pH 7.0, the material was bound to the resin in the same buffer before being washed with 10% methanol in 10 mM ammonium acetate buffer pH 7.0. The column as further washed with 3 column volumes of 15% v/v methanol in 10 mM ammonium acetate buffer. Zby was eluted with 20% methanol in 10 mM ammonium acetate buffer pH 7.0. Zby was dried by rotary evaporation to remove methanol and desalted over Se-Pak. Zby was dried by rotary evaporation before precipitation of the material using water acetone. Zby was dissolved in 500 µl H_2O and acetone added to a total volume of 10 ml the mixture was incubated at 4 °C for 2 hours before the acetone was removed the precipitate was washed with fresh acetone at 0 °C before the precipitate was dried *in-vacuo* overnight. 7.02 mg of zincobyric acid was synthesised in this way giving a yield of 95%.

2:7:3 Synthesis of Zbl

4.71 mg of zincobyric acid was mixed with 2.21 mg (1.2 equivalents) of lower nucleotide loop along with 2.3 mg (2 equivalents) of hydroxybenzotriazol. Reactants were dissolved in 2.5 ml H_2O and stirred at room temperature under an argon atmosphere. 9.3 mg (9.4 equivalents) of 1-ethyl-3-(3-dimethylaminopropyl)carbodiimide hydrochloride (EDC*HCl) was dissolved in 500 µl H_2O. The two solutions were mixed under an argon atmosphere and stirred

at room temperature for 4 hours. Previous syntheses began stirring at 0 °C for two hours before stirring for 4 hours at room temperature. The reaction was stopped by binding the material to Lichroprep RP-18 resin equilibrated in 10 mM ammonium acetate the resin is washed with 10 % acetonitrile followed by 15 % acetonitrile in 10mM ammonium acetate buffer at pH 7.0. Zbl was eluted in 30 % acetonitrile. Acetonitrile was removed by rotary evaporation and the Zbl was desalted by Se-pak and eluted in methanol and dried by rotary evaporation. 6.62 mg of zincobalamin was produced in this way giving a yield of approximately 96%.

Chapter 3: Isolation and characterisation of *Allochromatium vinosum* CobQ

3:1 Introduction

One of the more challenging aspects regarding the synthesis of metal analogues of B_{12} from HBAd is the specific amidation of the peripheral sidechains. As part of the biosynthesis of B_{12} the carboxylic acid sidechains decorating the corrin ring are converted to amides aside from sidechain *f,* which is retained as a carboxylic acid until nucleotide loop attachment (Blanche et al 1995, Warren et al 2002).

While it is possible to amidate these groups by chemical means the need to retain sidechain *f* as a carboxylic acid requires a more specific method. The synthesis of adenosylrhodibalamin reported by Widner and co-workers used the enzyme responsible for the amidation of these sidechains *in-vivo* to produce rhodibalamin. The recombinantly produced CobQ used in the study by Widner et al was a *R. capsulatus* derived enzyme and is specific for substrates that harbour an upper adenosyl group (Blanche et al 1991[1], Widner et al 2016). This methodology is therefore unsuitable for the synthesis of an expanded range of metal analogues due to the requirement for adenosylated substrates.

A second route by which metal analogues of B_{12} have been synthesised is the direct incorporation of a metal ion into the corrin ring of Hbl (Bieganowski et al 1979, Koppenhagen et al 1970, Koppenhagen et al 1975). This red metal-free corrin was shown to be produced by cultures of *A. vinosum* when grown in cobalt deficient media (Toohey et al 1965). Later experiments in which cultures of *A. vinousm* were supplemented with the nucleotide dimethylbenzimidazole (DMB) resulted in the formation of a compound that was shown to be identical to that of B_{12} but contained no cobalt (Koppenhagen and Pfiffner 1971). Determination of the structure of hydrogenobalamin was achieved through degradative experiments and comparison of the fragments with those of B_{12} treated in the same way. The structures of HBA, HBAd and Hbl are shown alongside the structure of B_{12} and its metal free counterpart, hydrogenoabalamin in Figure 3:1:1.

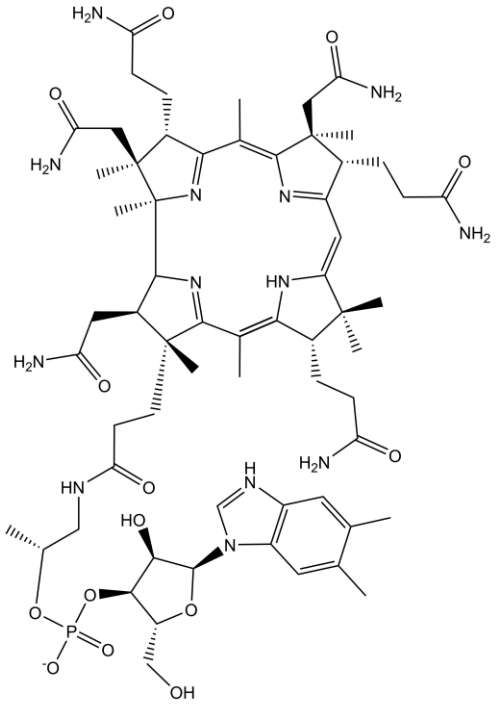

Hydrogenobalamin

(Hbl)

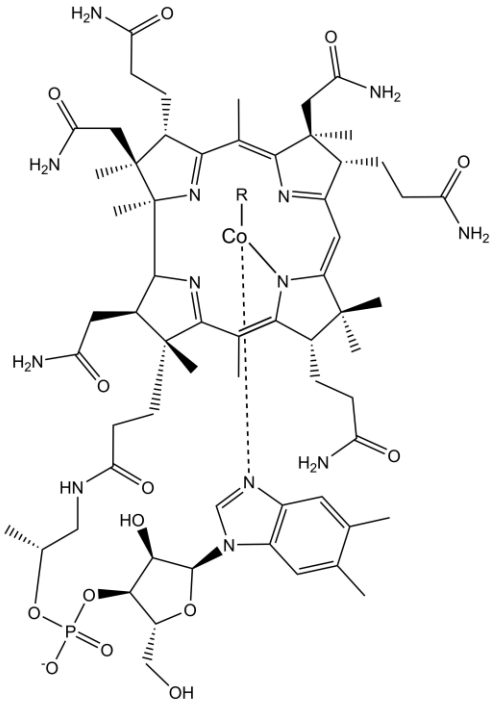

Cobalamin

(Cbl)

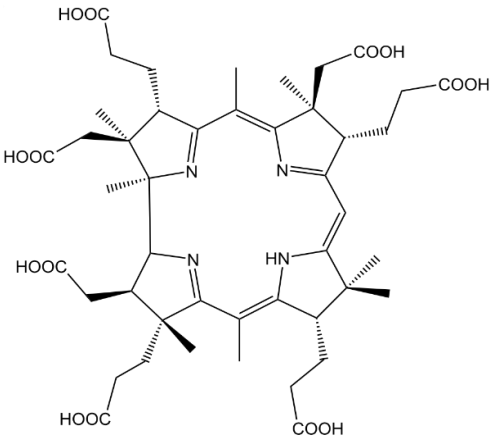

Hydrogenobyrinic acid

(Hby)

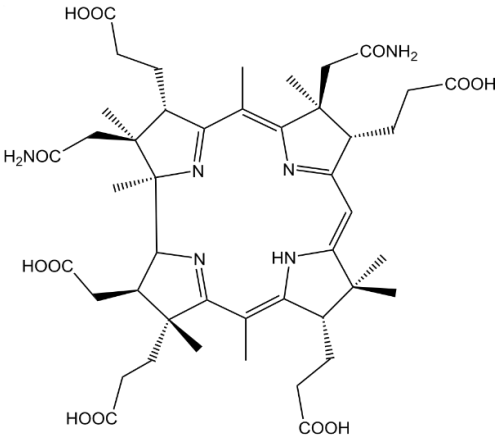

Hydrogenobyrinic acid *a,c* diamide

(HBAd)

Figure 3:1:1 Structures of hydrogenobalamin (Hbl), cobalamin, hydrogenobyrinic acid (Hby) and hydrogenobyrinic acid a, c diamide (HBAd).

The isolation of Hbl led to the synthesis of various analogues of B_{12} that varied the central metal ion. These analogues were produced from Hbl through the insertion of zinc, copper and rhodium (Koppenhagen et al 1971, Koppenhagen et al 1970). A brief report describing the synthesis of an iron analogue of B_{12} was published later (Bieganowski et al 1979). Hbl represents an appealing starting point for the synthesis of metal analogues as it allows for the synthesis of the desired analogue in a single step. However, hydrogenobalamin is produced only in small quantities from wild type bacteria such as *A. vinosum, Rhodospirillum rubrum* and *Rhodobacter spheroides* (Toohey 1974). Hence, alternative methods need to be developed for production of larger amounts of these analogues.

The driving force behind the isolation of Hbl was the ability for this compound to be easily transformed into a number of metal analogues of B_{12} by chemical metal insertion. Access to a number of different B_{12} analogues that have none of the associated metabolic functions of B_{12} would allow these compounds to be used as tools to probe the mechanism of a number of B_{12} dependent enzymes. More recently the synthesis of the rhodium analogue of B_{12} was achieved starting from the aerobic biosynthetic intermediate HBAd (Widner et al 2016).

The two methods described in the literature relating to the synthesis of metal analogues are limited either by the availability of suitable starting material, as is the case for methods using hydrogenoabalamin, or by the specificity of CobQ in the case of the synthesis of rhodibalamin from HBAd. Therefore, in order to expand the range of metal analogues of B_{12} that can be produced from HBAd a CobQ that amidates HBAd rather than adenosylcobyrinic acid *a, c* diamide needs to be identified. A good starting point for the isolation of such an enzyme is the γ proteobacterium *A. vinosum,* which has been reported in the literature as producing the metal free analogue of B_{12} (Toohey et al 1965). It follows that as hydrogenobalamin has the same pattern of amides as cobalamin the enzyme responsible for adding these groups, CobQ will recognise metal free substrates. *A. vinosum* CobQ is therefore a promising candidate for an amidase that has the ability to recognise substrates that contain no central metal ion or upper adenosyl

group. Isolation of such an amidase will allow for the production of a wider range of B_{12} analogues.

The work presented in this chapter concerns the identification of a CobQ that is able to amidate a metal free intermediate of B_{12} biosynthesis, HBAd. In identifying such a CobQ the most challenging aspect of B_{12} analogue synthesis could be overcome.

3:2:1 cloning and expression of *A. vinosum CobQ*

The genome of *A. vinosum* has been fully sequenced and the genomic data deposited into a number of databases (Weissgerber et al 2011). Annotation of the genome of *A. vinosum* shows this organism has a single gene annotated as *cobQ* within the genome. Primers were designed flanking the entirety of this gene, introducing an NdeI and SpeI restriction site upstream and downstream of the gene respectively. PCR was used in order to amplify this gene (Method 2:2:1). The fragment generated was ligated into a pET14b plasmid to form the plasmid pET14b-AvQ. This vector provides an expression platform that allows the gene product to be produced with an N-terminal hexahistidine tag. This plasmid was transformed into *E. coli* BL21-DE3 containing an additional pLysS plasmid, encoding lysozyme and maintained by a chloramphenicol resistance gene (Method 2:3:6). The expression strain was used to produce N-terminally hexahistidine tagged CobQ, allowing the protein to be purified initially by nickel affinity chromatography (Method 2:5:1). SDS page analysis of the fractions produced as a result of nickel affinity chromatography was performed and the corresponding gel shown in Figure 3:2:1.

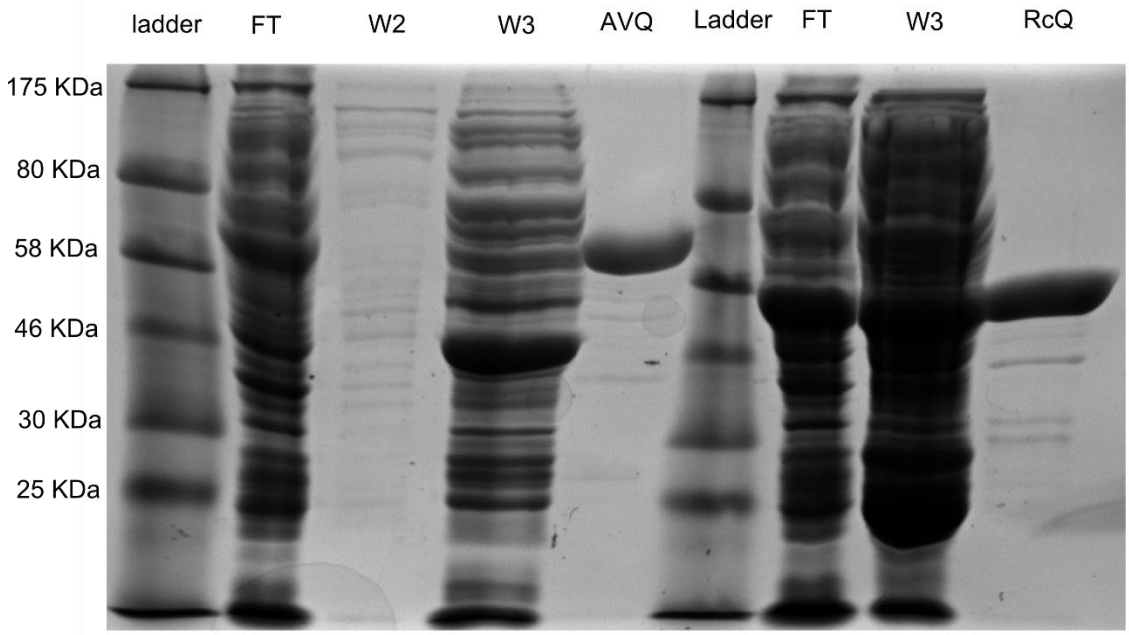

Figure 3:2:1: Analysis of fractions from the nickel affinity chromatography of A. vinosum CobQ predicted mass 56 kDa and R. capsulatus CobQ predicted mass 50 kDa. As analysed by denaturing polyacrylamide electrophoresis. FT corresponds to material not bound to the column upon application of supernatant. W2 and W3 correspond to washing the column with 20 mM Tris pH 8.0 containing 500 mM NaCl and 50 mM imidazole (W2) or 100 mM imidazole (W3). Eluted A. vinosum CobQ is shown in AvQ, R. capuslatus CobQ is shown as RcQ.

Analysis of the fractions collected from nickel affinity chromatography shows that *A. vinosum* CobQ can be produced recombinantly and isolated to a reasonable degree of purity. Further analysis of isolated *A. vinosum* CobQ was conducted by size exclusion chromatography, the elution profile from this experiment is show in Figure 3:2:2.

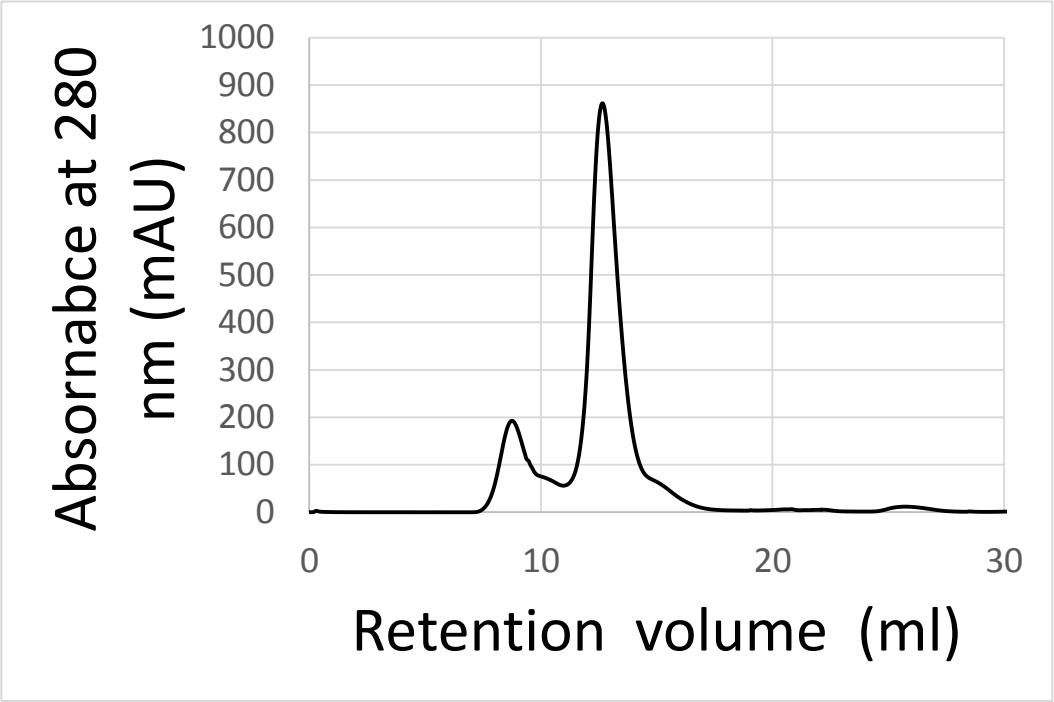

Figure 3:2:2 Size exclusion chromatogram of A.vinosum CobQ as initially purified by nickel affinity chromatography. The first elution peak corresponds to CobQ aggregate with a molecular mass of approximately 877 kDa. The large peak with a molecular mass of approximately 214 kDa corresponds to a tetramer of CobQ. The monomer having an approximate mass of 55 kDa.

3:2:3 Reaction of CobQ with HBAd

CobQ is an amidase and is responsible for the amidation of sidechains *b, d, e* and *g* of adenosylcobyrinic acid *a, c* diamide in organisms that operate the aerobic biosynthetic pathway for production of cobalamin. The synthesis of hydrogenobalamin by *A. vinosum* indicates that it has a CobQ capable of recognising metal free substrates. To validate *A. vinosum* CobQ as a suitable tool for the production of metal analogues of B_{12} the activity of this enzyme with the last metal free intermediate of B_{12} biosynthesis, HBAd was investigated. The activity of recombinantly produced *A. vinosum* CobQ (Alvin_2223) was compared to that of *R. capsulatus* CobQ (RCAP_rcc02051) prepared in the same way with HBAd as the substrate. Previously Widner et al have demonstrated that CobQ from *R. capsulatus* can amidate sidechains *b, d, e* and *g* of adenosyl-rhodibyrinic acid *a, c* diamide to form adenosyl-rhodibyric acid. It has been previously demonstrated that *R. capsulatus* CobQ shows a strong specificity for substrates that harbour an upper adenosyl group (Widner et al 2016). *A. vinosum* CobQ should not share this specificity for adenosylated substrates and be able to convert HBAd to hydrogenobyrinic acid *a, b, c, d, e, g* hexamide (Hby).

Purified CobQ from both *A. vinosum* and *R. capsulatus* were incubated separately in a solution containing a mixture of HBAd and as a result of incomplete purification of HBAd, HBA *c* monoamide along with ATP, Mg^{2+} and L-glutamine. The reaction mixture was buffered with 20 mM Tris buffer at pH 8.0 and incubated overnight at 30 °C (Method 2:5:4). Protein was removed by heating the reaction mixture to 100 °C for 5 minutes before removal of the precipitant by centrifugation at 36000 xg for 15 minutes. The sample was then analysed by HPLC (Method 2:6:3). The HPLC chromatogram of the reaction mixture is shown in Figure 3:2:3.

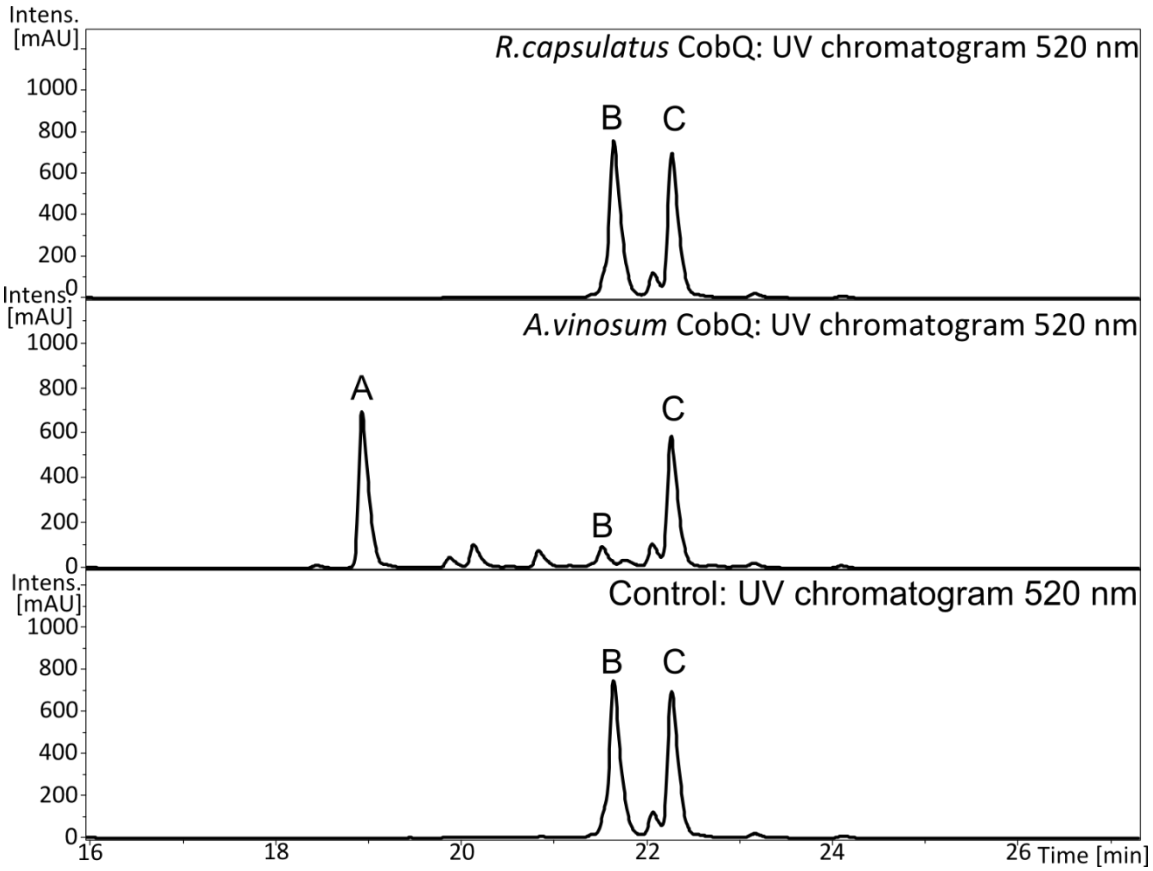

Figure 3:2:3: HPLC chromatogram of a mixture of HBA mono and diamide incubated with either R. capsulatus CobQ (Top,) A. vinosum CobQ (middle) or no protein (bottom). Peak C corresponds to HBA monoamide. Peak B corresponds to HBA diamide and Peak A corresponds to hydrogenobyrinic acid a, b, c, d, e, g hexamide (Hby). Peak identity was determined by the method outlined in Method 2.6.5.

As shown in Figure 3:2:3 incubation of *R. capsualtus* CobQ with a mixture of HBA mono and diamide results in no change to the retention times of either compound when compared to an enzyme-free control. In contrast when the reaction mixture contains *A. vinosum* CobQ the peak corresponding to HBAd is reduced compared to the control and *R. capsulatus* samples. In addition to the disappearance of HBAd a new peak appears (Peak A) with a similar intensity to that of the peak corresponding to HBAd (Peak B) but with a reduced retention time (19 minutes peak A 22 minutes peak B). Between peaks A and B 3 minor peaks with retention times of 20 minutes, 20.8 minutes and 21 minutes are present in the sample. The reduced retention time of peak A compared to peak B indicates that at pH 2.0 this new species is more polar than HBAd. This change in polarity at low pH is consistent with the replacement of a carboxylic acid group with an amide.

Interestingly, the peak corresponding to HBA *c* monoamide (Peak C) remains unchanged when incubated with either *R. capsulatus* or *A. vinosum* CobQs. This indicates that it is not recognised as a substrate by *A. vinosum* CobQ despite the high degree of similarity between HBAd and HBA *c* monoamide.

3:2:1 Genomic and phylogenic analysis of CobQ

A. vinosum is a purple sulphur bacterium belonging to the class of γ-proteobacteria. These motile bacteria are highly metabolically versatile and are capable of photoautotrophic growth in anoxic conditions using sulphite and sulphide as electron donors. Chemotrophic growth is possible under microanoxic conditions utilising a number of organic molecules (Weissgerber et al 2011). The B_{12} requirements of *A. vinosum* are at present unclear. Deutsche Sammlung von Mikroorganismen und Zellkulturen (DSMZ) media recommendations suggest that B_{12} is added to the growth media whereas *A. vinosum* is described as producing intermediates of B_{12} biosynthesis (Pfennig and Trüper 1981, Toohey et al 1965). As with other organisms it is possible that B_{12} is only required and/or synthesised under certain growth conditions (Bobik et al 1992, Zappa et al 2010). Interestingly the closely related organism *Allochromatium warmingii* is auxotrophic for B_{12} (Bregey's manual of systematic bacteriology 2nd edition 2005).

The genome of *A. vinosum* has been sequenced and annotated (Weissgerber et al 2011). Figure 3.2.4 shows a schematic view of the B_{12} biosynthetic genes identified in *A. vinosum*, the majority of the gene annotations are based on the Kyoto encyclopaedia of genes and genomes (Kegg) data base (Kanehisa and Goto 2000).

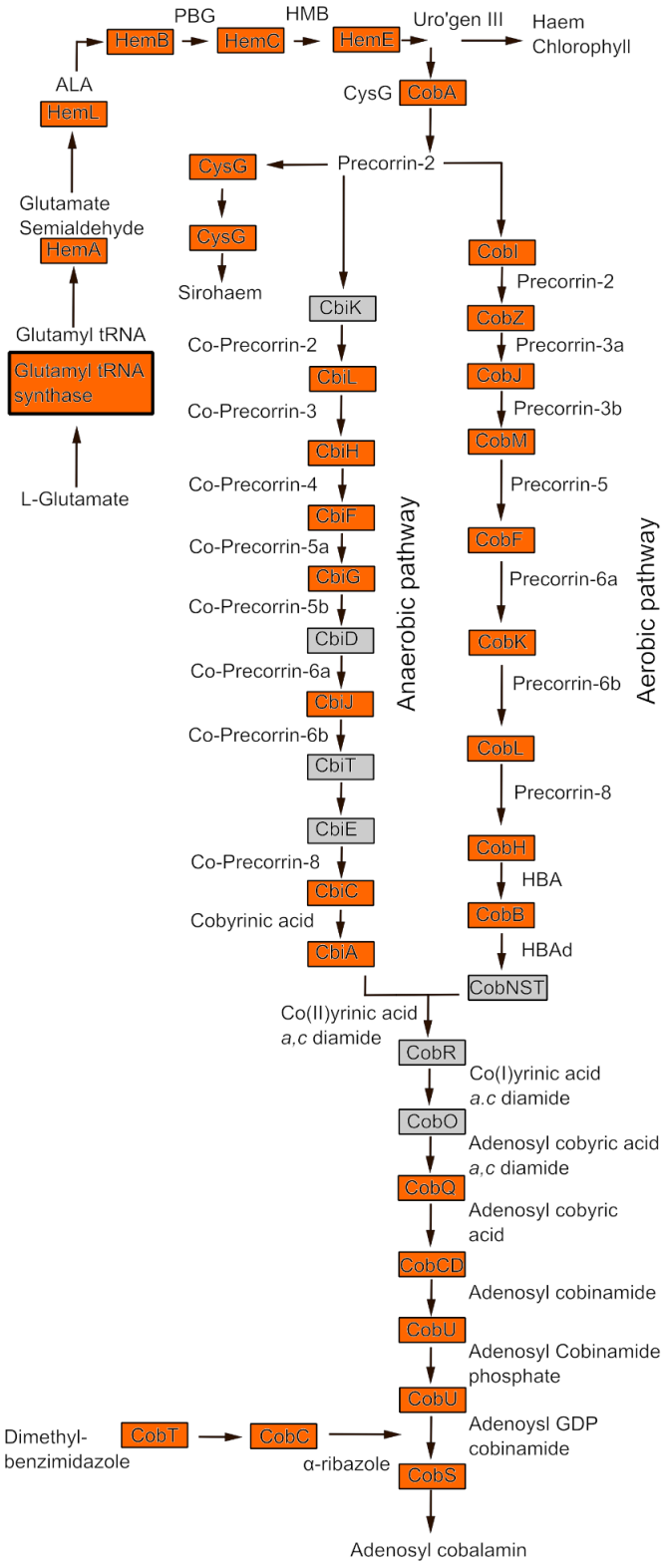

Figure 3:2:4: Tetrapyrrole biosynthetic genes annotated from the genome of A. vinosum. Genes present are coloured orange whereas genes that are not present within the genome are coloured grey.

Analysis of the *A. vinousm* genome shows that a vast majority of the genes associated with aerobic B_{12} biosynthesis are present. The most striking omission is the lack of the genes encoding both the large subunit of the cobalt chelatase *cobN* as well as one of the smaller subunits *cobT*, *cobS* is present yet all 3 components are required to form a functional cobalt chelatase (Debussche et al 1992). *A. vinosum* is also lacking the anaerobic cobaltochelatases *cbiK* and its homologue *cbiX*. However the genome does contain a copy of c*ysG,* the ferrochelatase involved in the biosynthesis of sirohaem. It has been demonstrated that CysG can insert cobalt into precorrin-2 in the anaerobic B_{12} pathway. However, this activity was demonstrated under artificially high concentrations of cobalt so may not be relevant *in-vivo* (Spencer et al 1993). The lack of a suitable cobalt chelatase is unexpected considering that the genes associated with aerobic B_{12} biosynthesis are otherwise complete barring any of the known cobalt reductases (*cobR, btuR*) and the adenosyl transferases *(cobO, pduO*). In addition to an almost complete set of aerobic B_{12} biosynthetic genes *A. vinosum* has a number of the genes that comprise the anaerobic B_{12} biosynthetic pathway. It lacks only the methyl transferases c*biD, cbiE* and c*biT* from the anaerobic route. Potentially the aerobic counterparts' c*obF* and c*obL* can substitute for these missing genes.

The purpose of the B_{12} biosynthetic genes within the genome of *A. vinosum* is unclear as this organism seems to be unable to produce cobalt containing corrins (Toohey et al 1965). Interestingly a single B_{12} dependent enzyme annotated within the *A. vinosum* genome involved in bacteriochlorophyll biosynthesis implies that B_{12} is essential for this organism. The annotated gene b*chE* encodes a B_{12} dependent radical SAM enzyme involved in the formation of ring E of bacteriochlorophyll under anaerobic conditions. The equivalent gene from *R. capsulatus* has been shown to be dependent upon adenosylcobalamin for activity (Gough et al 2000).

Regardless of the B_{12} metabolism of this organism the ability of *A. vinosum* to produce Hbl would indicate that the CobQ from this organism is distinct from previously described CobQ sequences as it is able to recognise non-adenosylated compounds as substrates. In order to gain a better understanding of how the sequence of *A. vinosum* CobQ compares to that of other B_{12} producing organisms it was compared to the equivalent amino acid sequences from a range of bacteria. The results of this alignment are arranged in a phylogenetic tree shown in Figure 3:2:1. A number of bacteria belonging to the order *Rhodobacteraceae* have multiple amino acid sequences within their genomes annotated as c*obQ*. The longer CobQ sequences are typically around 520 amino acids in length whereas the shorter proteins that are around 480 amino acids in length. The shorter CobQ sequences are the most common amongst the bacteria sampled.

Within the sampled group, bacteria belonging to the order *Rhodobacteraceae* are the only organisms to have both short and long CobQ proteins. *A. vinosum* is unique as it has a single long *cobQ* sequence with no annotated short *cobQ* sequence. Previously characterised CobQ sequences from *P. denitrificans* and *R. capsulatus* describe short sequences containing approximately 480 amino acids each (Crouzet et al 1991). The CobQ from both *R. capsulatus* and *P. denitfrificans* have strict substrate specificities accepting only substrates that harbour a β adenosyl group attached to a central cobalt ion (Blanche et al 1991[1], Widner et al 2016). The documented production of Hbl by *A. vinosum* as well as the conversion of HBAd to Hby shows that this same specificity is not present.

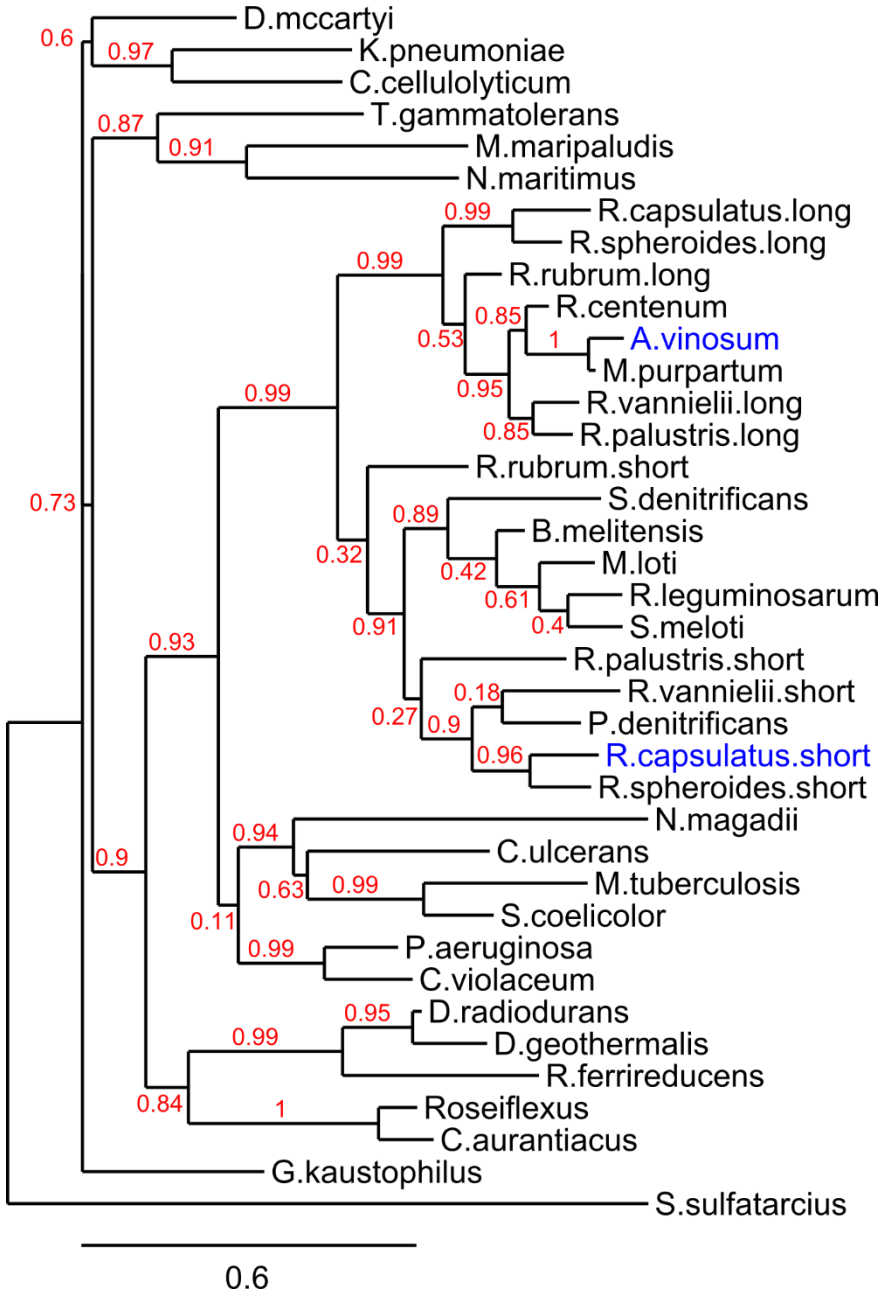

Figure 3:2:5: Phylogenetic analysis of cobyric acid synthases from a range of organisms across the main bacterial phyla. The sequences of A. vinosum and R. capsulatus are highlighted in blue. The sequence from A. vinosum clusters with a number of long CobQ sequences. The short R. capsulatus sequence clusters with the short sequences from a number of organisms reported to synthesise B_{12}.

Broadly, the aligned sequences shown in Figure 3:2:5 fall into three main groups. The first group within the tree is comprised of sequences belonging to a number of archaea and the bacteria including *Dehalocoides mccartyi* and *Kleibsiella pneumonieae*. The largest central portion of the tree contains sequences of many *proteobacteria* from among this group *R. capsulatus, Brucella melitensis, Pseudomonas denitrificans, Mesorhizobium loti* and *Sinorhizobium meloti* are known B_{12} producers operating an aerobic B_{12} biosynthetic pathway (Warren et al 2002). The final lower section of the phylogenic tree is comprised of numerous archaea and extremeophilic bacteria.

Within the central branch of the phylogenetic tree two sub-groups exist, a set of sequences that align more closely with *A. vinosum* CobQ and a second group comprised of sequences more similar to *R. capsulatus* short CobQ. The sequences that align with short CobQ from *R. capsulatus* are from bacteria that are known to produce B_{12} via the aerobic pathway. The longer CobQ sequences cluster with *A. vinosum* CobQ and are from organisms reported to produce hydrogenobalamin under cobalt limited conditions specifically *R.capsulatus*, *R. rubrum, R. palustris* and *R. spheroides* (Toohey 1974).

To understand better the differences between long and short CobQ sequences a selection of CobQ sequences were chosen from the central portion of the phylogenic tree shown in Figure 3:2:5. Alignment of these sequences was achieved using a progressive pairwise alignment technique, Clustal Omega (Sievers et al 2011). The alignment of these sequences is shown in Figure 3:2:6.

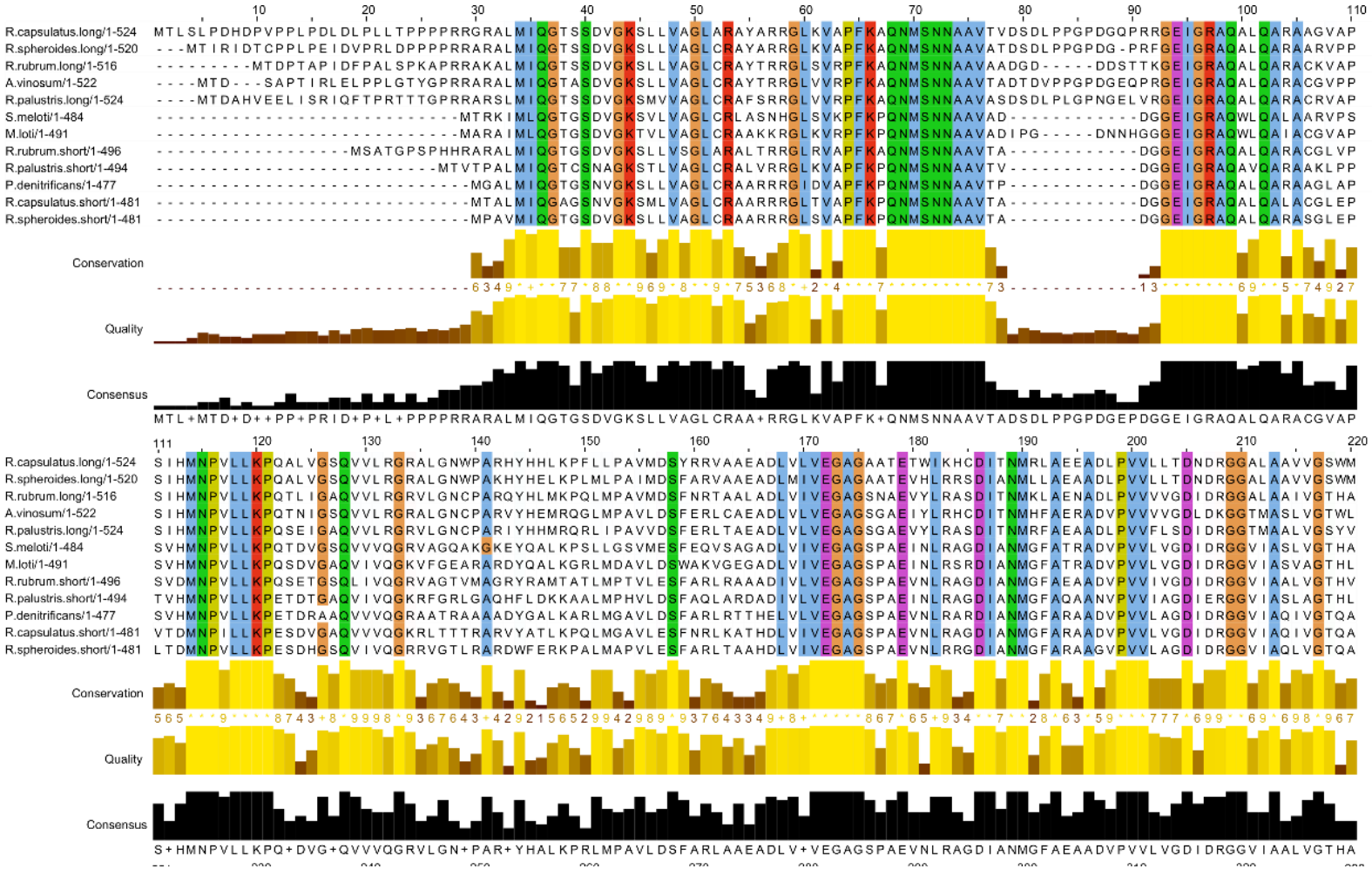

Figure 3:2:6: sequence alignment of CobQ sequences from bacteria known to produce B_{12} via the aerobic pathway and bacteria reported to produce hydrogenobalamin conserved residues are highlighted.

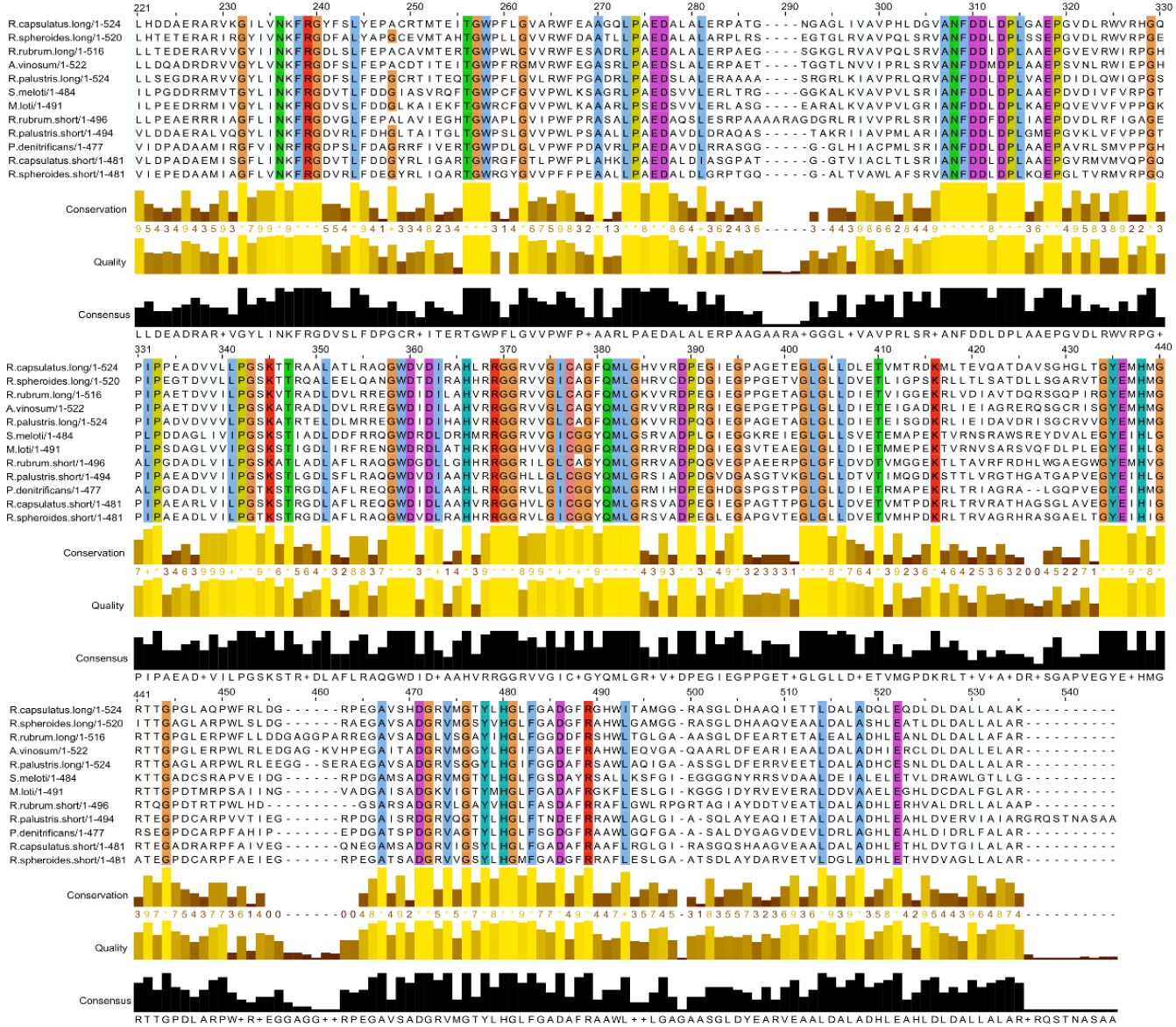
R.capsulatus.long/1-524
R.spheroides.long/1-520
R.rubrum.long/1-516
A.vinosum/1-522
R.palustris.long/1-524
S.meloti/1-484
M.loti/1-491
R.rubrum.short/1-496
R.palustris.short/1-494
P.denitrificans/1-477
R.capsulatus.short/1-481
R.spheroides.short/1-481
Conservation
Quality
Consensus

Alignment of short and long CobQ sequences from a number of B_{12} producing organisms reveals that the main difference between short and long sequences are the presence of an N-terminal extension of between 29 – 20 amino acids in length and an insert of 12 amino acids from position 88. A third insert from positon 456 of 5-6 amino acids is present in the long sequence from *R. rubrum* and *A. vinosum* that is not present in either the long or short sequence from *R. capsulatus* (Figure 3:2:6).

To date no structural data is available for any of the amidases involved in B_{12} biosynthesis. However, a number of other glutamine dependent amidotransferases have been better characterised and the general properties of this class of enzyme described (Massiere et al 1998). Generally, glutamine dependent amidotransferases have separate domains for the deamination of glutamine and the attachment of the ammonia yielded by this first reaction to the substrate. These domains are separate and the ammonia liberated form aminolysis of glutamine is channelled through the protein to a synthetase domain. Correspondingly a catalytic cysteine residue is found within the glutaminase domain of all glutamine dependent amidotransferases, a single cysteine residue is conserved at positon 384 across all the CobQ sequences aligned in Figure 3:2:3. It is therefore highly likely that this cysteine residue is essential for the glutaminase activity of CobQ and that the C-terminal of CobQ is responsible for the deamination of glutamine. The N-terminal region is then most likely to be involved in the binding of HBAd in the case of *A. vinosum* CobQ. The insert at position 88 is therefore likely to be in the synthetase domain of CobQ and may be involved in tetrapyrrole binding or substrate recognition.

3:2:5 Predicted structure

Both of the amidases involved in B_{12} biosynthesis, CobB and CobQ have been characterised biochemically as part of the effort to determine the sequence of biosynthetic steps required for B_{12} synthesis (Blanche et al 1991[1], Debussche et al 1992). The anaerobic equivalent of CobB (CbiA) and of CobQ (CbiP) have been characterised best in terms of mechanistic detail and substrate recognition (Fresquet et al 2004, Williams et al 2007). These studies were limited to the mutation of a few key residues predicted to be involved in substrate recognition and did not extend to any data concerning the wider architectural organisation of CbiP. While detailed structural data has yet to be generated for any of the amidases involved in B_{12} biosynthesis, structures are available for other glutamine dependent amidases. Members of this class of enzyme share many features particularly the separation of glutaminase and amidase activities (Massière et al 1998).

As described earlier glutamine dependent amidotransferses consist of two disparate domains, a glutamine deaminase (GAT) domain responsible for the deamination of glutamine to yield ammonia and glutamate. Ammonia is then channelled through to an ATP hydrolysing synthetase domain where it is attached to a phosphorylated carboxyl group of the substrate that is to be amidated (Massière et al 1998). CobQ is no exception to this two domain architecture having a C-terminal GAT domain and an N-terminal synthetase domain as determined by sequence alignment with other glutamine dependent amidotransferases (Galperin and Grishin 2000).

Due to the wide variety of substrates that are accepted by various glutamine dependent amidotransferases, the synthetase domains of this class of enzyme show little homology aside from motifs involved in ATP binding. While the synthetase domains show little homology to one another, the GAT domains of this class of enzyme fall broadly into two groups based on sequence similarity (Massière et al 1998). Class I GAT domains show greater similarity to anthranilate synthetase and are also known as triad amidotransferases due to a conserved set

of three residues (cysteine, histidine and glutamic acid) within the active site of the GAT domain. Class II glutamine dependent amidotransferases show greater homology to glutamine-phosphoribosylpyrophosphate amidotransferase involved in the *de novo* synthesis of purine bases (Muchmore et al 1998).

For this reason the N and C termini of both R. capsulatus and A. vinousm CobQ were modelled separately and compared to one another. In doing so a greater insight into differences concerning the synthetase domains may become apparent. Additionally CobB and CobQ have not been classified as either class I or class II glutamine dependent amidotransferases.

The N- and C-terminal portions of both *A. vinosum* and *R. capsulatus* CobQ were modelled separately using Phyre 2 structure prediction server (Kelley et al 2015). Here, the submitted sequences were compared to sequences of proteins with published structures, using this comparative data likely structures are modelled for the query sequence.

Figure 3:2:7 shows the predicted structure of the C-terminal GAT domain of both *A. vinosum* and *R. capsulatus* CobQ. The super imposed predicted structures are shown as cartoons with residues thought to be involved in glutamine deamination represented in stick form.

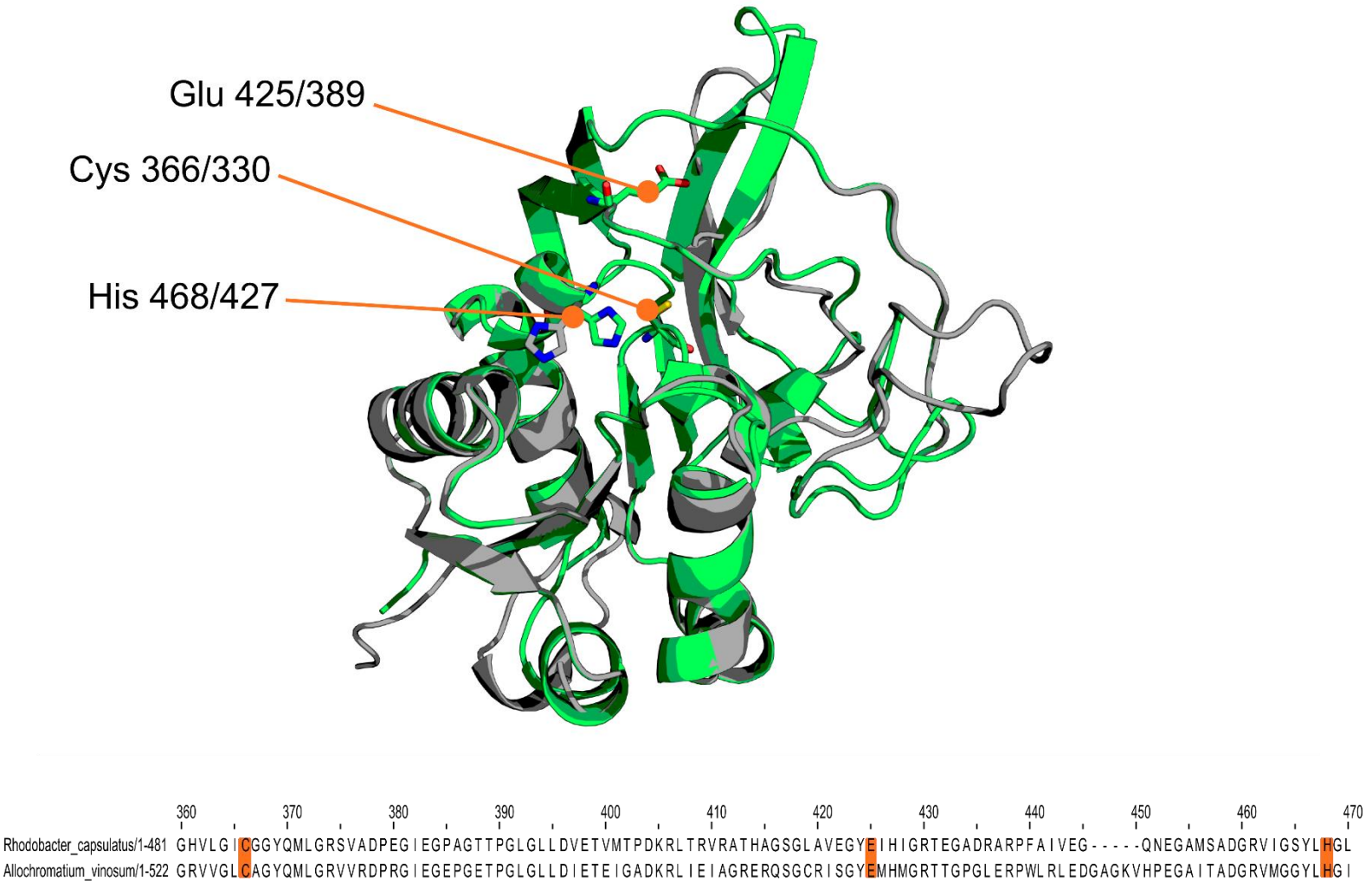

Figure 3:2:7 Phyre 2 predicted structure of the C terminal GAT domain of A. vinosum CobQ (green) and R. capsulatus CobQ (grey).

Figure 3:2:7 shows a superimposition of the predicted structures of the C terminal GAT domains of *R. capsulatus* and *A. vinosum* CobQ. Glutamine dependent amidotransferases are broadly divided into two groups, Class I and Class II based upon the similarity of the glutaminase domain to two of the earliest described examples (Massier et al 1998).

The CobQs from *R. capsulatus* and *A. vinosum* show greater homology to the structures of class I glutamine dependent amidotransferases due to the presence of a likely catalytic triad comprised of histidine, glutamine and cysteine. This triad is a hallmark of class I amidotransferases. The predicted structure shown in Figure 3:2:4 shows the likely arrangement of these residues in space, the predicted structure of *R. capsulatus* CobQ has these three residues arranged in such a way that they are spatially close enough to act as a site for glutamine deamination. The Predicted structure of *A. vinosum* CobQ shows that His 468 is angled away from the active site, this would suggest a non-functional protein. However, biochemical data (Figure 3:2:3) suggests that *A. vinosum* CobQ is functional and that the predicted orientation of His 468 in figure 3:2:7 is incorrect. A likely mechanism for the glutaminase domain of *A. vinosum* CobQ is presented in figure 3:2:8

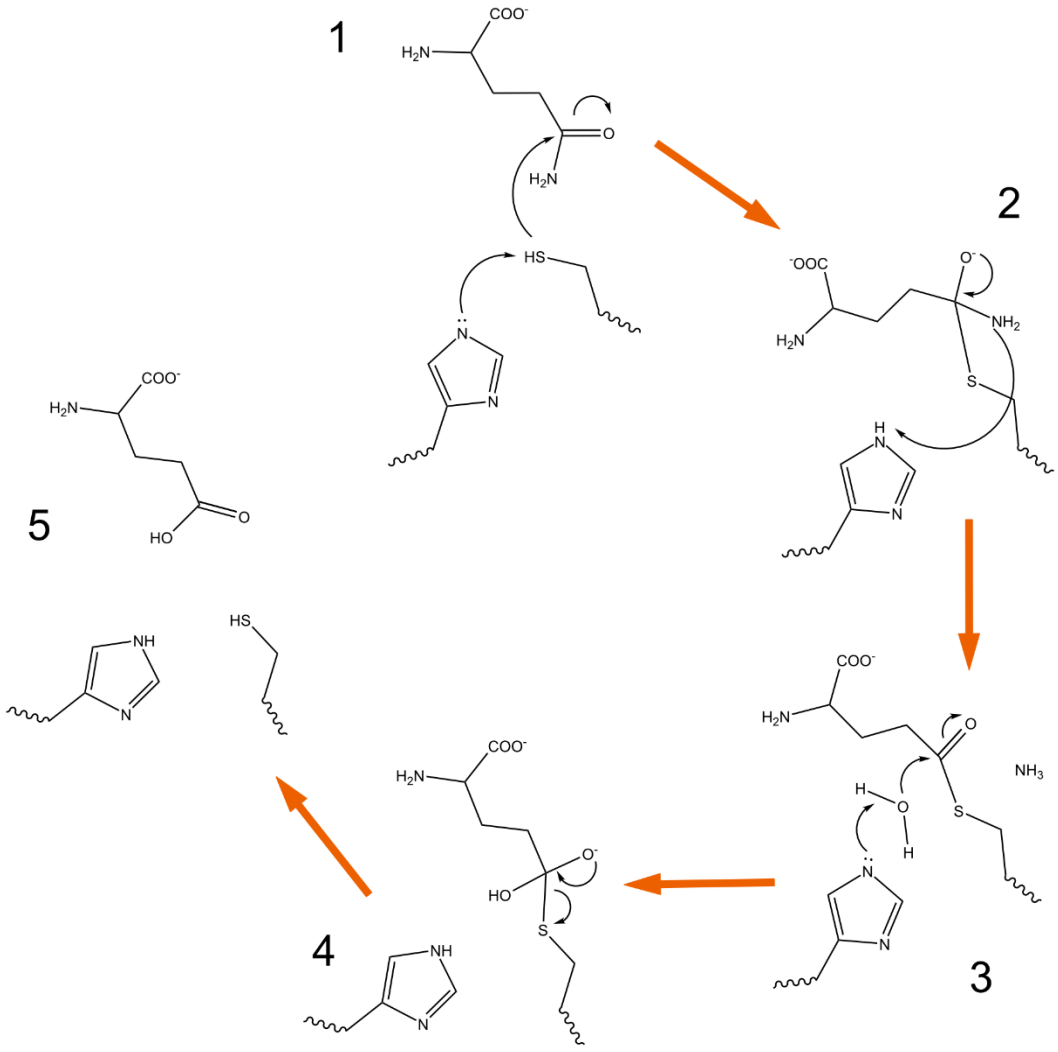

Figure 3:2:8. Proposed catalytic mecahmism of the glutaminase domain of A. vinosum CobQ. Deamination of glutamine is initated by deprotonation of a catalytic cysteine (1-2). Resulting in the formation of a thioester and liberation of ammonia (3). Ammonia is channelled through the protein to a synthetase domain. The catalytic cysteine is reactivated by hydrolysis of the thioester liberating glutamic acid (4-5).

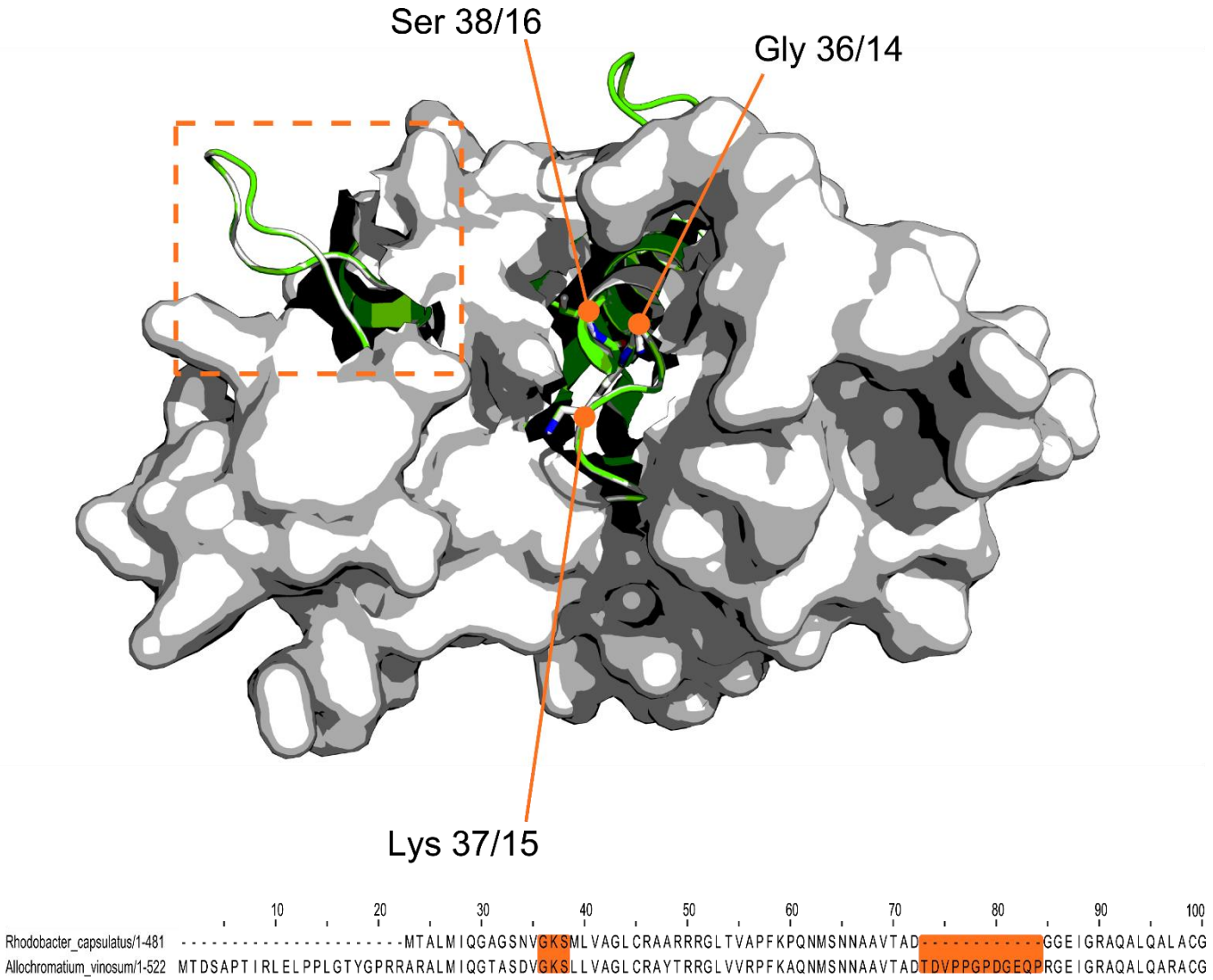

Figure 3:2:9 Phyre 2 predicted structure of the N- terminal synthetase domain of A. vinosum CobQ (green) and R. capsulatus (grey)

The sequence alignment shown in Figure 3:2:6 highlights a number of conserved residues within the N terminus of both *A. vinosum* (G30, G36, K37 and S8) and *R. capsulatus* (G8, G14, K15, S16) CobQ. These residues are conserved among all of the aligned CobQ sequences shown in Figure (3:2:6). The spatial organisation of these amino acids is such that they are close enough to be involved in ATP hydrolysis. The modelled N termini shown in Figure 3:2:9 shows that the Walker-A motif sits within a cleft. This cleft may be the binding site for the tetrapyrollic substrate of CobQ as most glutamine dependent amidotransferases rely on ATP dependent phosphorylation of the substrate before amidation occurs.

A. vinosum cobQ has an insert of 12 amino acids within the N-terminal region of the protein. This same insert is lacking in *R. capsulatus* CobQ. The amino acid sequence of this insert is proline rich as well as containing a number of negatively charged residues. It is therefore likely that this region is intrinsically disordered. As this insert is predicted to sit opposite the site of ATP hydrolysis its flexibility may play a role in the ability of *A. vinosum* CobQ to recognise and correctly amidate metal free substrates.

3:2:4 X-ray crystallography

In order to gain a greater understanding as to the substrate specificity of *A. vinosum* CobQ, attempts were made to generate the 3-dimensional structure through X-ray crystallography. To produce crystals of *A. vinosum* CobQ hanging drop vapour diffusion experiments were conducted. Initial screens for potential crystallisation conditions used the pre formulated mixtures of salts and precipitants from Molecular Dimensions Cambridge (Jancarik and Kim 1991). *A. vinosum* CobQ was purified initially by nickel affinity chromatography before further purification by size exclusion chromatography, as described in (Method 2:5:3). The fractions corresponding to the tetrameric form of CobQ were concentrated to 8 mg/mL and screened by hanging drop vapour diffusion (Method 2:5:6).

Initial screens used the pre-formulated structure screens 1 and 2 from Molecular Dimensions, however, no crystals of diffractable quality were obtained using this system. Additional screening was conducted using the Midas screen also from Molecular Dimensions (Grimm et al 2010). Small crystals of *A. vinosum* CobQ were obtained using a precipitation condition from this screen (Midas box 2, condition 22, 28% v/v polyethylenimine 0.1 M Tris pH 8.0).

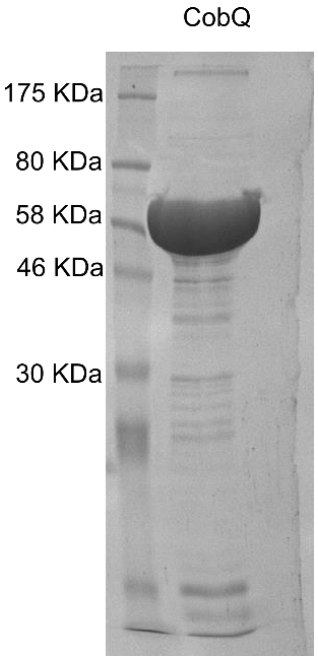

Figure 3:2:9: SDS PAGE analysis of A. vinosum CobQ, initially purified by nickle affinity chromatography before further purification by size exlusion chromatography. The FPLC purification of CobQ was perfomed using a G200 sephadex column. Fractions corresponding to the CobQ tetramer were pooled and analysed by SDS PAGE.

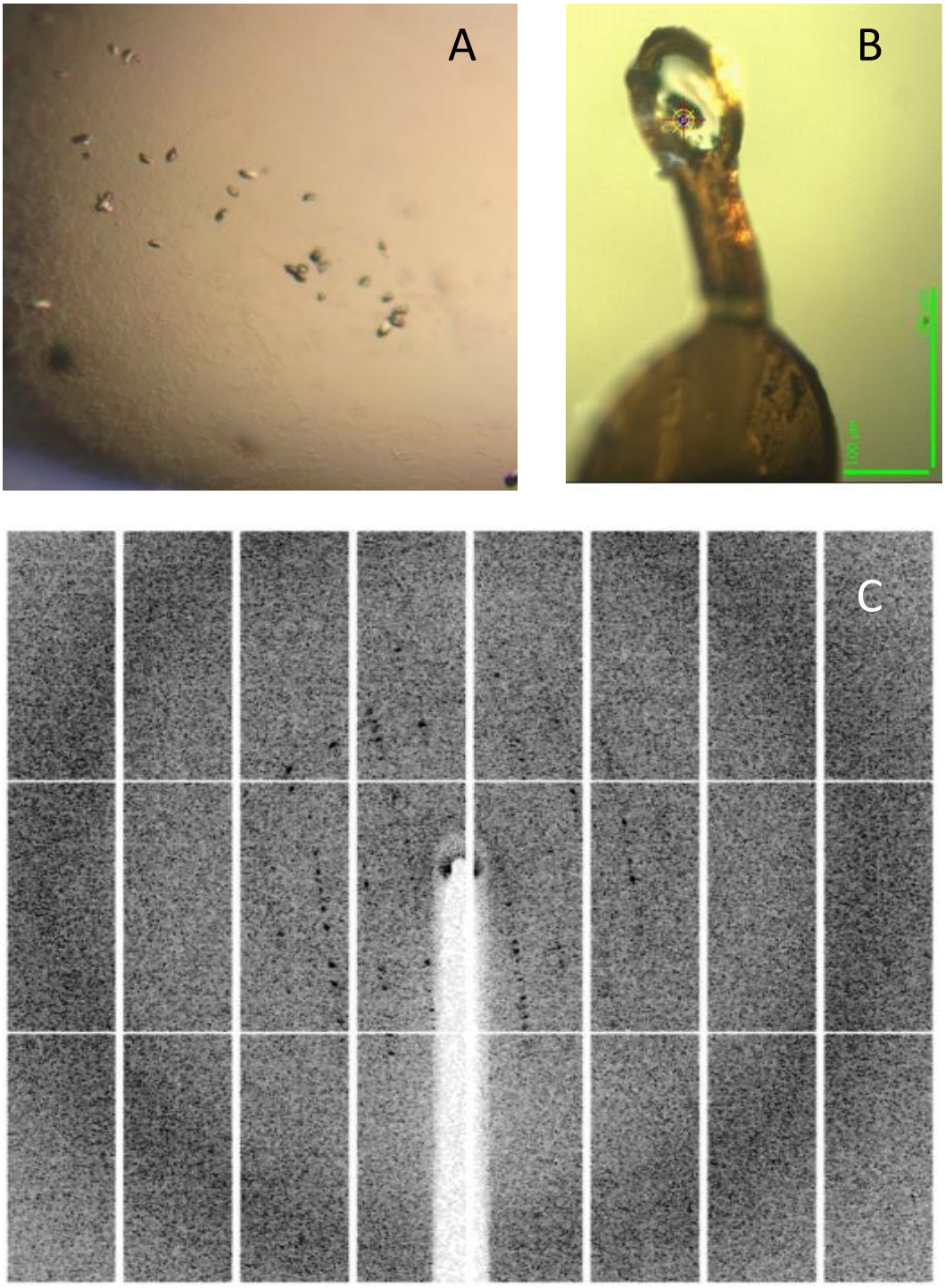

Figure 3:2:10: Crystals of A. vinosum CobQ produced by hanging drop vapour diffusion, A. B shows the CobQ crystals mounted in a polyamide loop after freezing in liquid nitrogen, no cryo-protectant was added due to the high proportion of polyethyenemine (28% v/v) present in the condtion. C, the diffraction pattern of CobQ crystals, crystals diffracted to a resolution of 6-8 Å making this data set unsuitable for determination of a structure.

While it was possible to generate small crystals of *A. vinosum* CobQ the quality could not be improved sufficiently through screening around the initial hit. Re-screening in the presence of HBAd and glutamine did not yield crystals diffracting to a higher resolution.

3:3:1 Discussion cloning and purification of *A. vinosum* CobQ

A. vinosum cobQ was successfully cloned into a pET14b vector allowing it to be expressed recombinantly in *E. coli* with an N-terminal hexahistidine tag. The soluble protein produced in this way was shown to have a mass of approximately 55 kDa when analysed by denaturing gel electrophoresis, consistent with the mass predicted from its amino acid sequence. Further analysis by size exclusion chromatography shows that in solution *A. vinosum* CobQ primarily exists as a tetramer. It has been shown that other glutamine dependent amidotransferases have activity that is dependent upon the oligomeric state of the protein (Lauritsen et al 2011). The best characterised example of this kind of regulation is exhibited by cytidine triphosphate synthetase where at low concentration the enzyme exists as a monomer but in the presence of additional enzyme and substrate CTP synthetase forms an active tetramer.

A. vinosum has been described as producing Hbl when grown in media containing no cobalt (Koppenhagen et al 1971). The structure of Hbl proposed by Koppenhagen et al depicts this compound as being chemically identical to cobalamin but containing no central cobalt ion. The CobQ from *A. vinosum* is able to recognise HABd as a substrate and amidate it accordingly (Figure 3:2:3). Incubation of the last metal free intermediate of B_{12} biosynthesis (HBAd) with purified *A. vinosum* CobQ, ATP and glutamine. As a consequence of an incomplete purification of HBAd some HBA monoamide was present in the reaction mixture. Interestingly *A. vinosum* only recognises HBAd and not HBA monoamide as substrate. HBA monoamide remained unchanged when incubated with ATP and glutamine in the presence of *A. vinosum* CobQ. HBAd in contrast was converted to a new compound as reflected in a reduced retention time (Figure 3:2:3).

Within the chromatogram shown in Figure 3:2:3 minor peaks are present with retention times between that of HBAd and Hby. These peaks are most likely to correspond to compounds with 3, 4 and 5 amide groups. The formation of these 3, 4 and 5 amidated compounds suggests that CobQ amidates HBAd in a processive manner with amide groups being added to defined positions around the ring. Amidation at random positions around the ring would result in the

formation of compounds with differing retention times and therefore multiple peaks between HBAd and Hby (Williams et al 2007). Previous work concerning the homologue to CobQ from the anaerobic pathway (CbiP) proposes that CbiP operates using a mechanism by which the substrate molecule is released and rebound in a different orientation for the addition of each amide group, this results in each amide group being added to a defined position (Williams et al 2007).

Annotation of the *A. vinosum* genome (Figure 3:2:4) shows that this organism has most but not all of the genes associated with B_{12} biosynthesis. Notable omissions include any of the known cobalt chelatases (CbiK, CbiX and CobNST). Also missing are the genes associated with cobalt reduction (CobR) and adenosyltransfer (CobO). The B_{12} requirement of *A. vinosum* is also unclear as it has no annotated sequences for B_{12} dependent enzymes apart from a copy of BchE (Alv_2224). This enzyme is involved in the anaerobic biosynthesis of bacteriochlorophyll and is responsible for the formation of ring E. *In vitro* studies in *R. capsulatus* suggest that this process is dependent on a B_{12} co-factor and may represent the major use of B_{12} in this organism (Gough et al 2000).

While *A. vinosum* CobQ recognises HABd and amidates it accordingly to form hydrogenobyric acid, the same is not true for *R. capsulatus* CobQ, which failed to alter HBAd in any way under the same conditions. Previous reports have demonstrated the specificity of *R. capsulatus* CobQ for adenosylated substrates (Widner et al 2016). Sequence alignment of a number of CobQ sequences from various organisms shows that, relative to *R. capsulatus* CobQ, *A. vinosum* CobQ has an N terminal extension and an insert of around 12 amino acids in the N-terminal portion of the protein (Figure 3:2:8). Comparison of the predicted structures of the N-terminal synthetase domains of *A. vinosum* and *R. capsulatus* CobQ shows that this insert sits opposite a motif associated with ATP hydrolysis and a cleft in the protein that may be the site of tetrapyrrole binding. This proline rich insert may therefore play a role in substrate recognition.

In order to determine a structural reason as to why *A. vinosum* CobQ is able to amidate HBAd attempts were made to crystallise this protein. Small crystals could be generated but the X-ray diffraction pattern gave data to only around 7 Å resolution, which is insufficient for any structural determination.

3:4:1 Conclusion

The CobQ from *A. vinosum* recognises the metal free B_{12} biosynthetic intermediate HBAd as a substrate. HBAd is amidated at positons *b, d, e* and *g* by *A. vinosum* CobQ to form hydrogenobyric acid (Hby). This molecule is the metal free analogue of cobyric acid. The sequence alignment of *A. vinosum* CobQ with other CobQ sequences reveals a number of conserved residues. Mapping these residues onto the predicted structure of *A. vinosum* identifies a number of residues as potentially being important for the catalytic function of CobQ.

Chapter 4: Production, isolation and characterisation of hydrogenobyric acid

4:1 introduction

The final metal free intermediate of the aerobic B_{12} biosynthetic pathway is hydrogenobyrinic acid *a,c* diamide (HBAd). HBAd has been described previously in the literature as the substrate for cobalt insertion during the biosynthesis of B_{12} (Debussche et al 1992). This cobalt free corrin has also been used as the starting material for the synthesis of the rhodium analogue of B_{12} (Widner et al 2016). HBAd is the product of CobB, a glutamine dependent amidotransferase responsible for the addition of amide groups to positions *a* and *c* of hydrogenobyrinic acid (Debussche et al 1990). After the addition of these amide groups the next steps in the biosynthesis of B_{12} involve insertion, reduction and adenosylation of the central cobalt ion followed by further amidation of the peripheral sidechains *b,d,e* and *g.* These final 4 amide groups are added by cobyric acid synthase (CobQ) to generate adenosyl cobyric acid (Blanche et al 1991[1]).

The first CobQ to be described in the literature was isolated from *P. denitfrificans* as part of the effort to characterise the aerobic B_{12} biosynthetic pathway (Blanche et al 1991[1]). More recently, CobQ from *R. capsulatus* was employed to help in the chemi-bio synthesis of rhodibalamin (Widner et al 2016). Both of these CobQs display a preference for adenosylated substrates and will not recognise non-adenosylated or cobalt-free substrates (Blanche et al 1991[1], Widner et al 2016). From a synthetic perspective the substrate specificity of these CobQ enzymes therefore limits the type of metal analogues of cobalamin that can be synthesised to those that can adenosylated.

While it is theoretically possible to amidate the remaining sidechains of HBAd by chemical means, the lack of specificity would result in the generation of a compound bearing 7 amide groups. This then presents a problem as nucleotide loop attachment must occur at sidechain *f* in order to mimic B_{12} as closely as possible. It is for this reason that the regiospecific amidation of the sidechains by CobQ is really the only option that can be considered, as the product of this amidotransferase reaction retains a carboxylic acid group at positon *f* (Blanche et al 1991[1]).

The previous synthesis of rhodibalamin by Widner and co-workers utilised the CobQ from *R. capsulatus* to amidate the *b,d,e* and *g* sidechains of adenosyl rhodibyric acid *a,c* diamide before attachment of the lower nucleotide loop (Widner et al 2016). By alternating between enzyme catalysed and chemical reactions as outlined in the synthesis of rhodibalamin the efficiency of the overall process is reduced due to the need to separate the products after each step. It would therefore be a simpler process if the amidation of sidechains *b,d,e* and *g* could be achieved before the insertion of the chosen metal ion.

Significantly, the isolation of CobQ from *A. vinosum* in Chapter 3 demonstrates that this enzyme will allow the direct conversion of HBAd to Hby. The ability to isolate large quantities of Hby would be very significant in helping generate a key building block for the construction of a range of different metal analogues of B_{12} through the reaction scheme outlined in Figure 4:1:1. However, before that can be accomplished the identity of Hby as the product of the reaction between *A. vinosum* CobQ, HBAd, ATP and glutamine needs to be confirmed. In this chapter details of the isolation of Hby are given along with detailed characterisation of some of the properties of this compound.

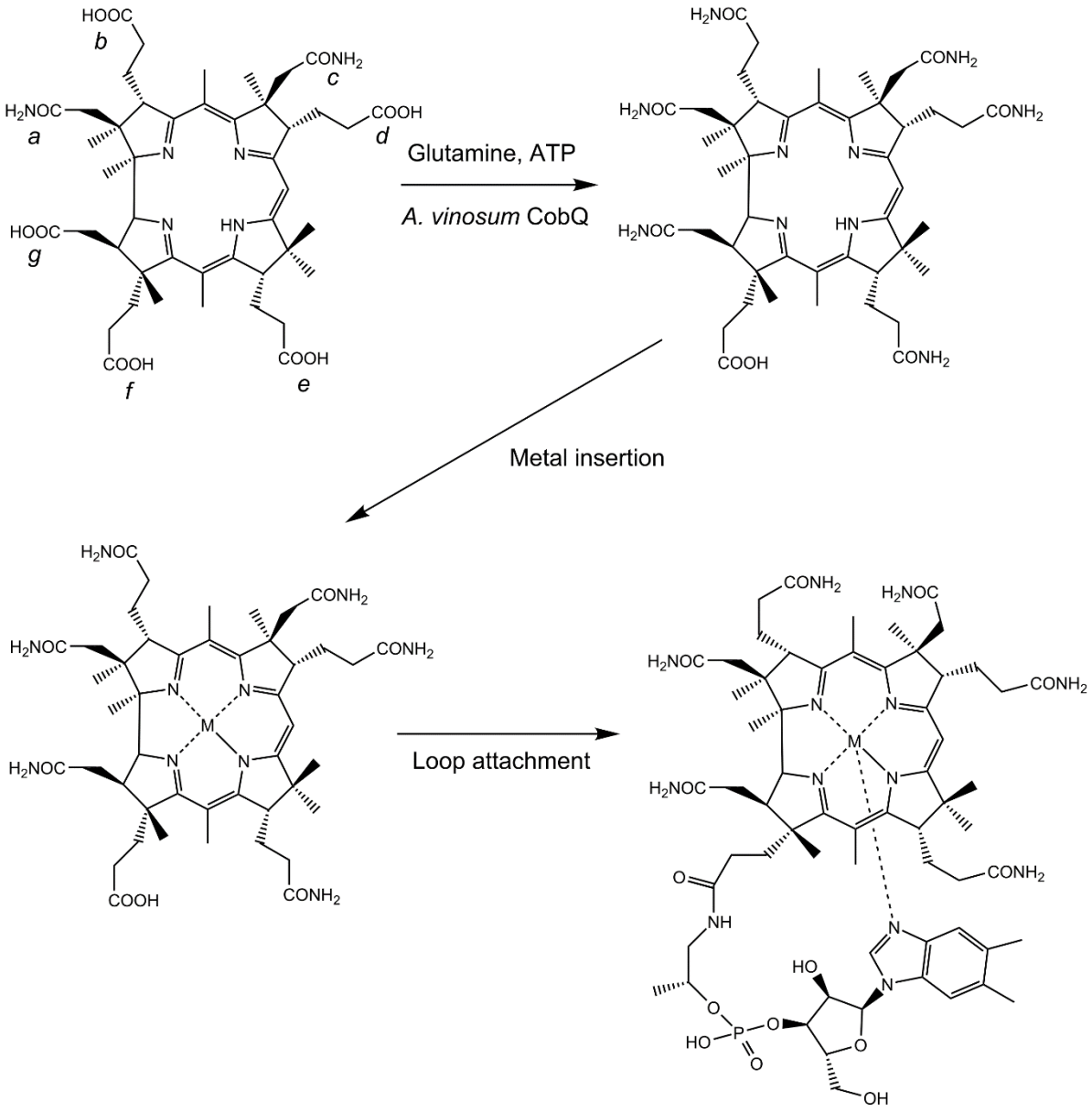

Figure 4:1:1: General synthetic scheme by which analogues of B_{12} can be synthesised from HBAd. The peripheral sidechains of HBAd are labelled clockwise from C1 a,b,c,d,e,f and g.

4:2:1 Purification of HBAd

Chapter 3 demonstrated the action of *A. vinosum* CobQ on the metal free B_{12} biosynthetic intermediate HBAd. By using *A. vinosum* CobQ amide groups can be added to HBAd to form the metal free analogue of cobyric acid, hydrogenobyric acid (Hby). Crucially amidating HBAd enzymatically to form Hby should result in the amidation of all the carboxylic acid sidechains except for *f*. Differentiation of sidechain *f* is important for the specific attachment of the lower nucleotide loop to this position.

Importantly, Hby has not previously been synthesised or isolated from natural sources and hence the material needs to be characterised in detail to ensure that its structure is correct. This, in turn requires a larger amount of the compound so that it can be subject to NMR analysis. To this end a pET3a plasmid containing the cobalamin biosynthetic genes *cobA-I-G-J-M-F-K-L-H-B* was transformed into *E. coli* BL21 DE3 cells. The plasmid, named pET3a-HBAd, is shown diagrammatically in Figure 4:2:1. The genes on this plasmid, cloned largely from the *R. capsulatus* aerobic cobalamin biosynthetic pathway, encode the enzymes that are sufficient for the production of HBAd when produced in *E. coli* (Deery et al 2012).

Cultures (1 L) of *E. coli* expressing pET3a-HBAd were grown for 36 hours at 28 °C in 2YT media. Cells were harvested by centrifugation at 4000 x g for 20 minutes. The cell pellet from each 1 L culture was re-suspended in 30 mL of 10 mM ammonium acetate buffer (pH 7.0). Cells were lysed by heating to 90 °C for 15 minutes. Precipitated protein was removed by centrifugation at 4500 x g and the supernatant was further clarified by centrifugation at 36000 x g. HBAd was isolated from the supernatant using weak anion exchange chromatography. Diethyl-amino-ethyl spehacel (DEAE resin) was equilibrated in 10 mM ammonium acetate buffer (pH 7.0) and the supernatant from the previous centrifugation step was applied to the column. Under these conditions HBAd binds to the resin and impurities are removed with buffers containing increasing concentrations of NaCl (100 mM, 150 mM). A mixture of hydrogenobyrinic acid, hydrogenobyrinic acid mono-amide and HBAd was washed form the column upon addition of a buffer

containing 300 mM NaCl. Figure 4:2:2 shows the clarified lysate bound to DEAE resin. The UV-vis spectra of band B is shown in figure 4:2:3.

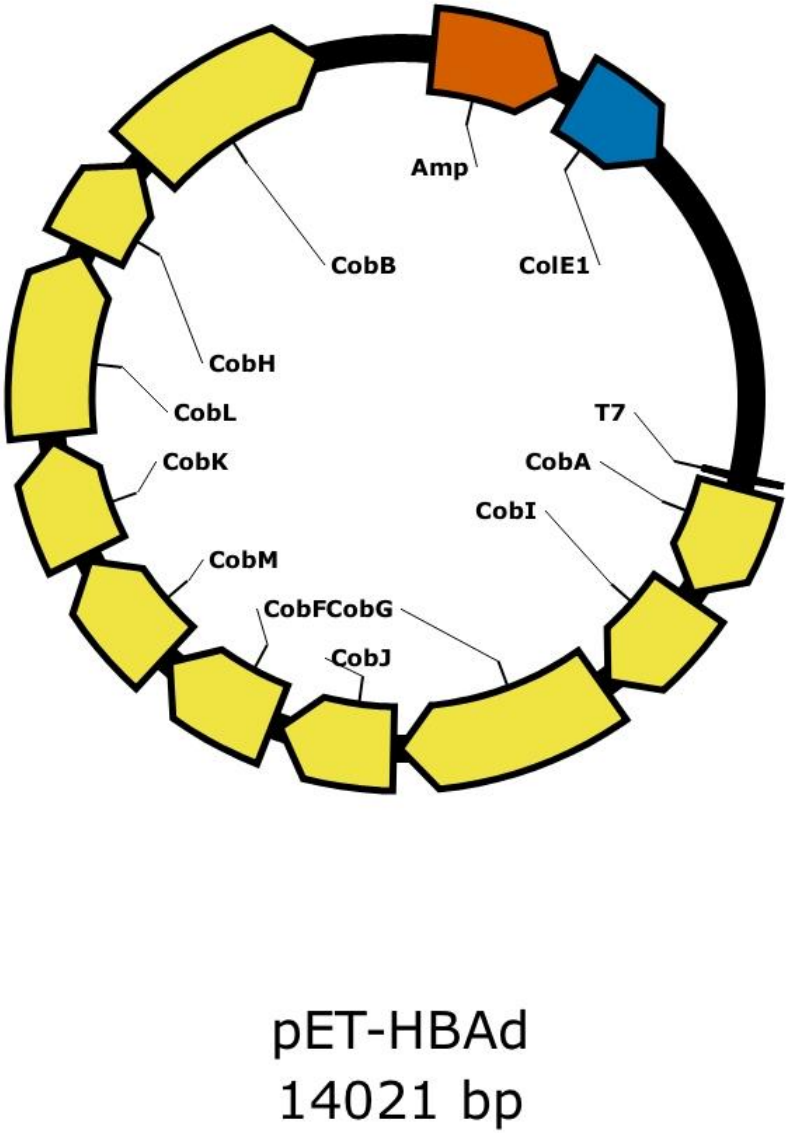

Figure 4:2:1: Schematic representation of pet3a-AIGJFMKLHB this plasmid has the genes necessary to produce HBAd when expressed in E.coli. Cobalamin biosynthetic genes are shown in orange. The origin of replication is shown in blue.

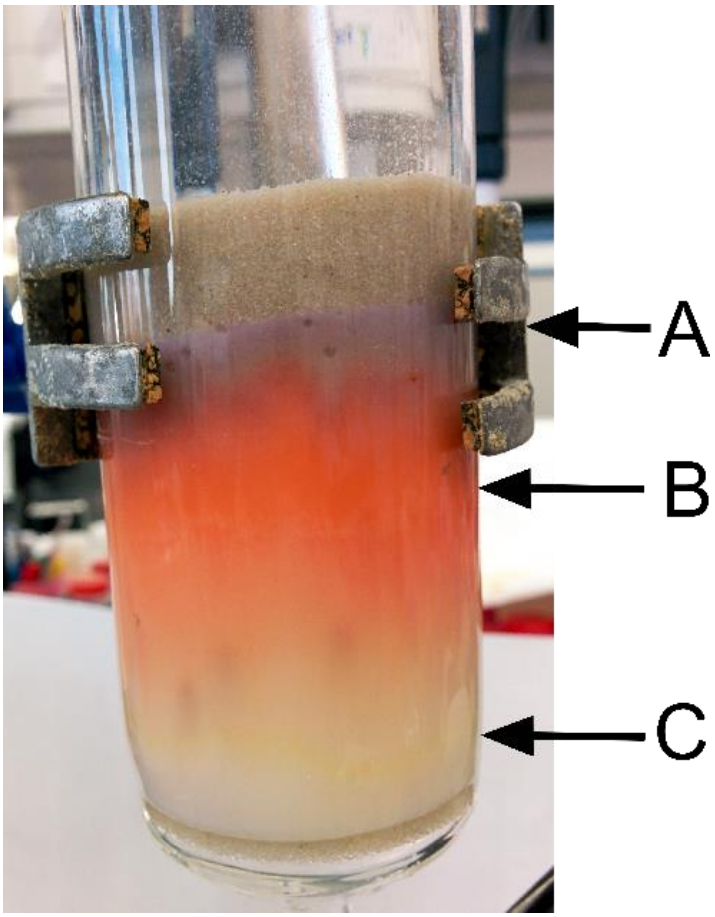

Figure 4:2:2: weak anion exchange chromatography (DEAE) of E.coli expressing pet3a-HBAd. Protein was precipitated by heat and removed by centrifugation. Bands A and C correspond to impurities band B contains HBAd and HBA monoamide.

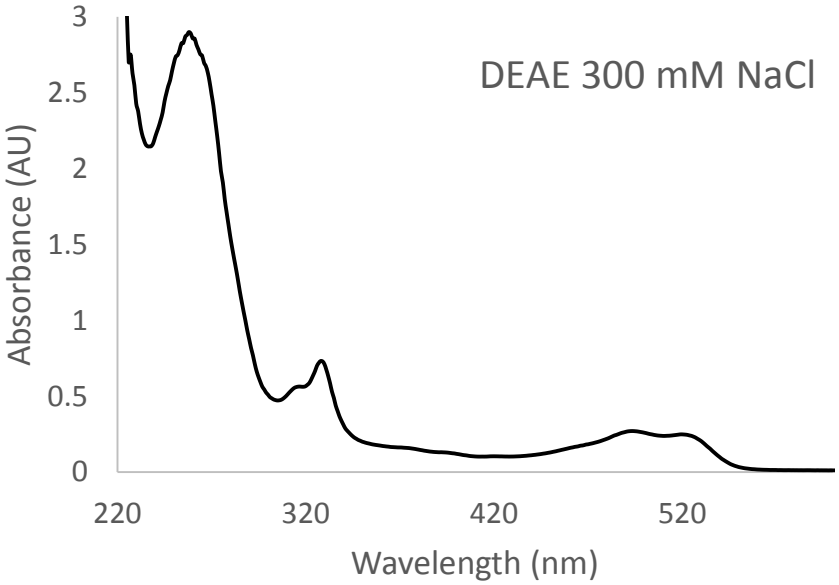

Figure 4:2:3: UV-vis spectrum of the corrinoid material separated by DEAE (300mM NaCl). The spectrum was recorded from 200-800 nm in a disposable plastic UV cuvette.

Analysis of the HBAd mixture (Figure 4:2:2 band B) that was isolated from the DEAE column by UV-vis spectroscopy (Figure 4:2:3) gave a spectrum broadly similar to that of purified HBAd (Figure 4:2:5). Most notable is the strong absorption from 240-300 nm indicating that large amounts of protein and nucleotide impurities are still present in the mixture. The spectrum however, has features that match the previously published spectra of HBA (Deery et al 2012). The αβ bands at 520 nm and 490 nm are visible as is the γ band at 320 nm. The material purified on the DEAE column was then analysed by HPLC m/s as shown in Figure 4:2:4.

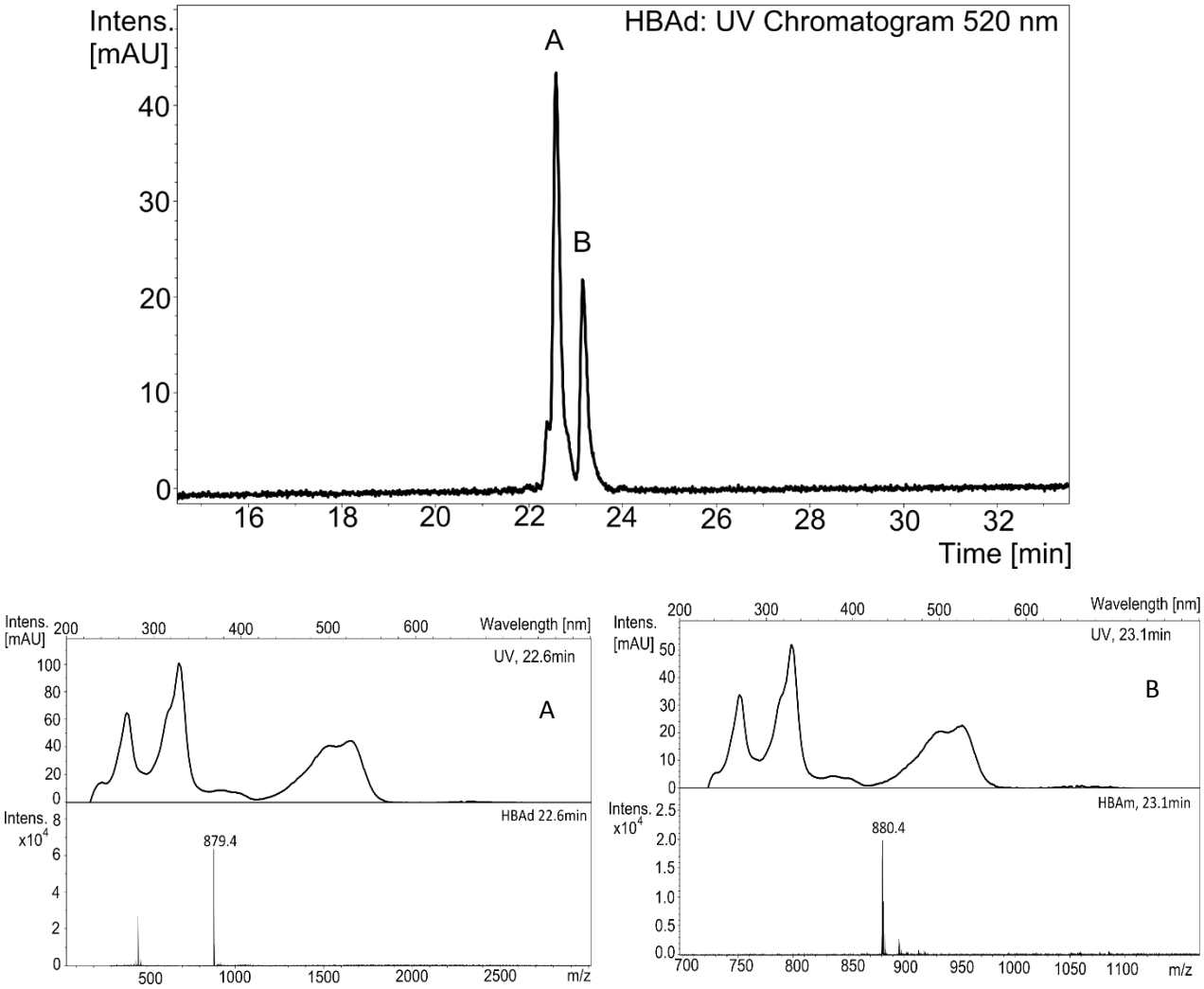

Figure 4:2:4: Top HPLC chromatogram at 520 nm of HBAd purified over DEAE resin. Bottom left UV-vis spectrum of Peak A and corresponding mass spectrum. Bottom right UV-vis spectrum of peak B and corresponding mass spectrum. The data are consistent with HBAd = A and HBA monoamide = B. The expected mass of HBAd as calculated from the chemical formula ($C_{45}H_{62}N_6O_{12}$) is 879 Da. The expected mass for HBA monoamide ($C_{45}H_{61}N_5O_{13}$) is 880 Da. Peak identities were determined as per method 2.6.5.

HPLC analysis of band B (figure 4:2:2) as purified by DEAE shows a mixture of both HBA mono and di-amide (Figure 4:2:4). Section 3:2:3 shows that HBA mono-amide cannot be converted to Hby by the action of CobQ. HBA mono-amide therefore first needs to be converted HBAd in order to be recognised as a substrate for *A. vinosum* CobQ. To achieve this the mixture of HBA mono and di-amide was incubated with recombinantly produced *R. capsulatus* CobB in a reaction containing glutamine and ATP in order to enhance the level of HBAd in the sample. Figure 4:2:5 shows the HPLC chromatogram of HBAd with an estimated purity of > 95%

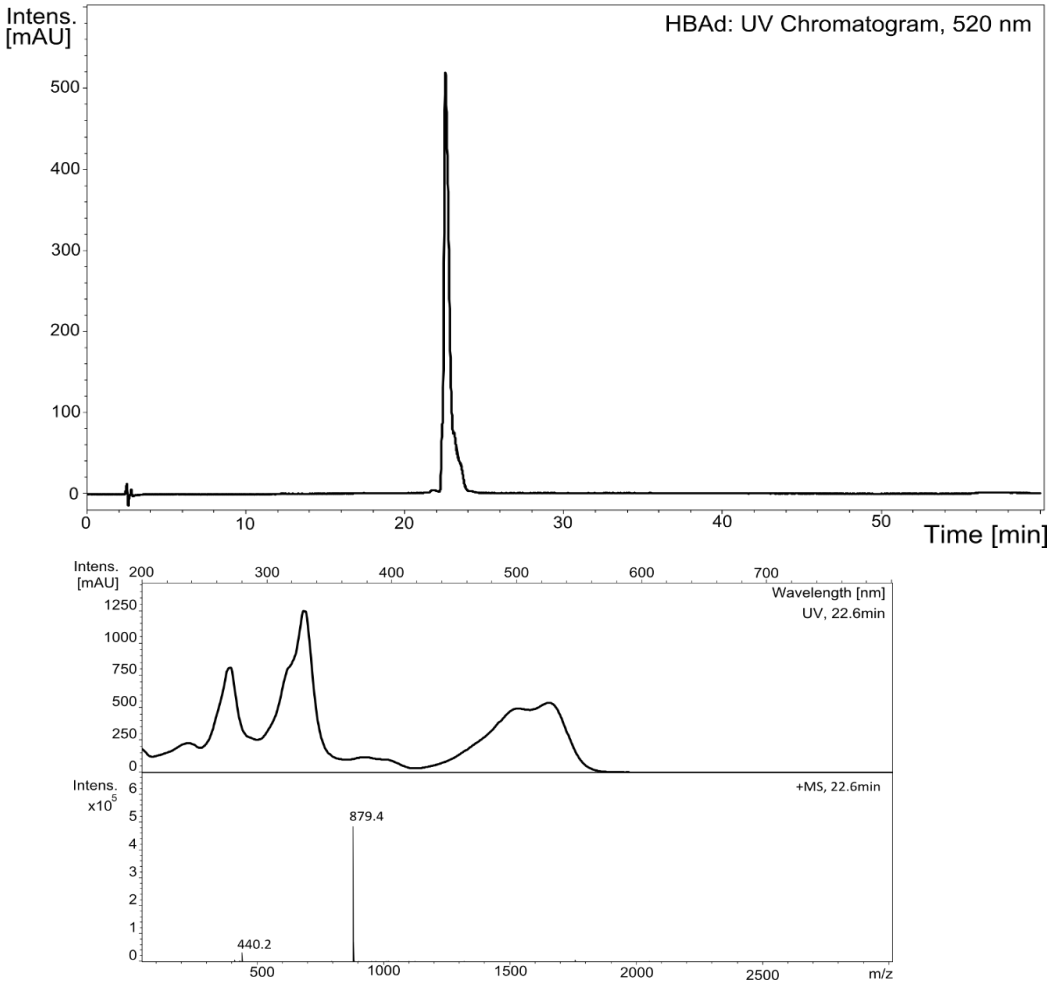

Figure 4:2:5: Above HPLC chromatogram at 520 nm showing HBAd produced by the action of R. capsulatus CobB on a mixture of HBA mono and di amide. Below UV-vis spectra and corresponding mass spectrum of HBAd as separated by HPLC. Data is consistent with the major peak being HBAd. The expected mass of HBAd as calculated from the chemical formula ($C_{45}H_{62}N_6O_{12}$) is 879 Da.

4:2:2 In-vitro production of Hby from HBAd

A. vinosum CobQ was expressed recombinantly with an N-terminal hexahistidine tag and purified by nickel affinity chromatography (method ref). The purified CobQ was incubated in 10 mM Tris, buffer pH 8.0, containing 100 µM HBAd, 1 mM ATP, 10 mM glutamine and 2 mM Mg^{2+}. The reaction was incubated at 28 °C for 15 hours protected from light. The protein was denatured by heating the incubation mixture to 80 °C and removed by centrifugation at 36000 x g. The reaction mixture was analysed by HPLC as shown in Figure 4:2:6.

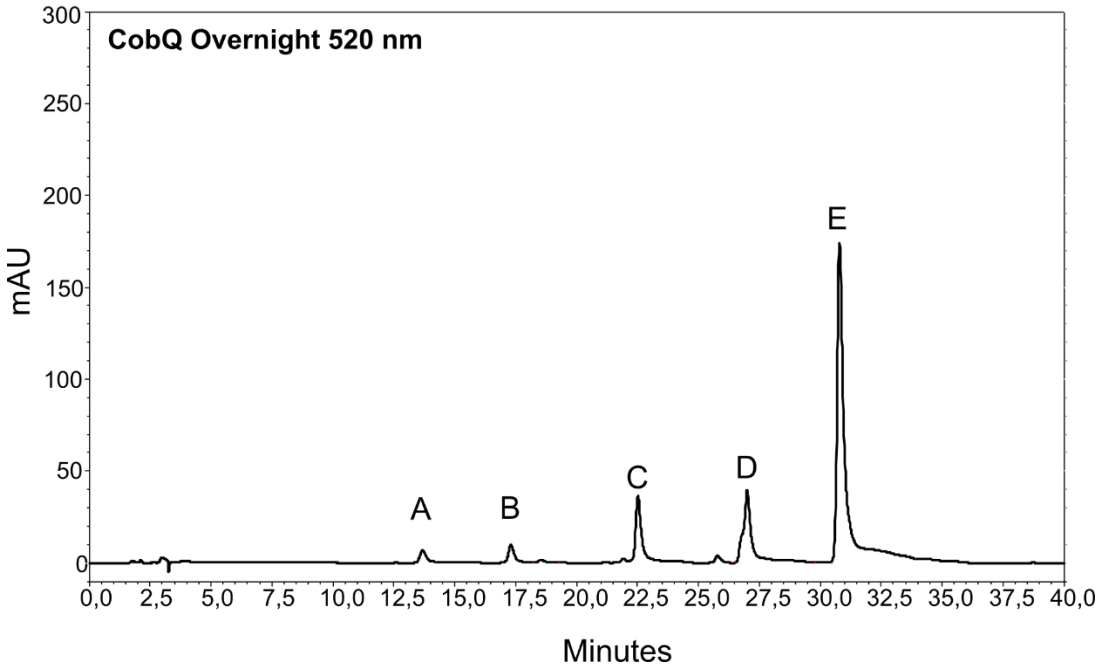

Figure 4:2:6: Reverse phase HPLC analysis of the reaction mixture used to convert HBAd to Hby by the action of A. vinosum CobQ. Peak A corresponds to the starting material HBAd, peak B is the triamide of HBA, peak C the quad amide, peak D the pent amide and peak E is Hby. HPLC analysis was conducted at pH 7.0 with 10mM ammonium acetate as the aqueous phase. Acetonitrile was used as the organic phase. Material was analysed using the following gradient 0-5 minutes up to 5% v/v acetonitrile 5-40 minutes up to 20% v/v acetonitrile. Peak Identity was determined as per method 2.6.5.

The incubation of HBAd with *A. vinosum* CobQ produces Hby as well as a number of lesser amides of HBA. HPLC analysis of this mixture was conducted at pH 7.0, as at this pH it is expected that the amide groups would be protonated. From the chromatographic behaviour of the observed peaks (Figure 4:2:6) it is likely that they correspond to molecules with 3, 4 and 5 amide groups. The reduction in polarity of the molecules at pH 7.0 as a result of the replacement of a carboxylic acid with an amide resulting in progressively longer retention times for each species. The peak with the longest retention time (Peak E) corresponds to Hby with the penta-amide (Peak D), quad-amide (Peak C), tri amide (Peak B) and residual di-amide (Peak A) exhibiting reduced retention times consistent with the number of carboxylic acid moieties each molecule retains. Hby (Peak E) represents around 70 % of the corrinoid material in the analysed sample.

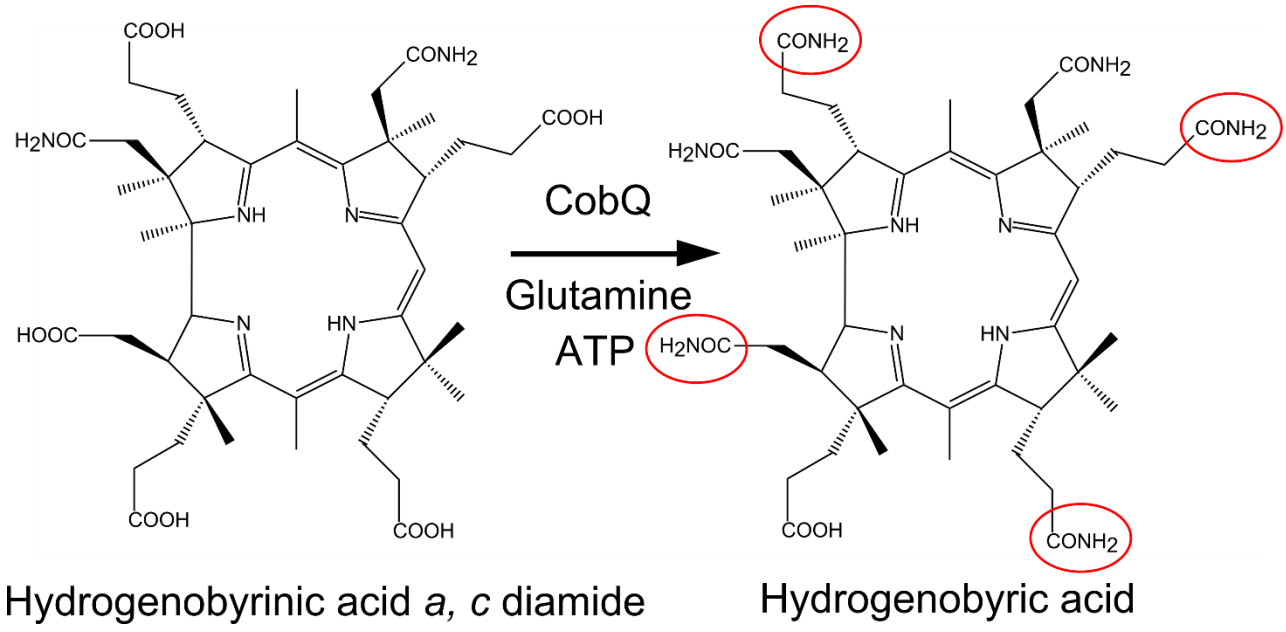

Figure 4:2:7: The reaction catalysed by A. vinosum CobQ HBAd left is converted to hydrogenobyric acid (Hby). Sidechains are labelled clockwise a to g. Amidated groups are highlighted in red.

4:2:3 Chromatographic separation of Hby

Hby was also isolated from other products of the reaction between CobQ, glutamine and ATP by reverse phase chromatography on the bench (Method 2:6:2). C-18 modified silica resin (particle size 25-40 µM) was equilibrated in 10 mM ammonium acetate buffer, pH 7.0. The Hby mixture was applied to the column and washed with increasing concentrations of methanol in the same ammonium acetate buffer at pH 7.0 (method). Using this reverse phase methodology it was possible to separate Hby from the less amidated products. Figure 4:2:8 shows the separation of Hby by RP-18 chromatography. Purified Hby was then analysed by HPLC (Figure 4:2:9)

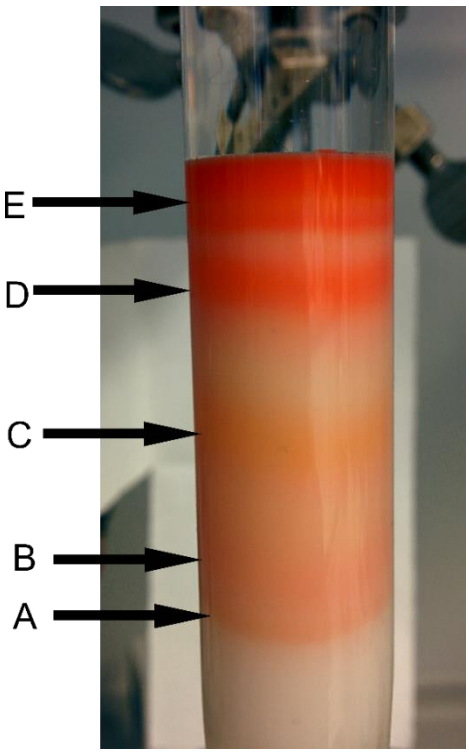

Figure 4:2:8: Benchtop reverse phase separation of Hby from other amides of HBA on the bench. Band A corresponds to the diamide, band B the tri amide, band C is an additional impurity band D contains both the quad and penta amides while band E corresponds to Hby. Hby could be isolated with good purity using this method.

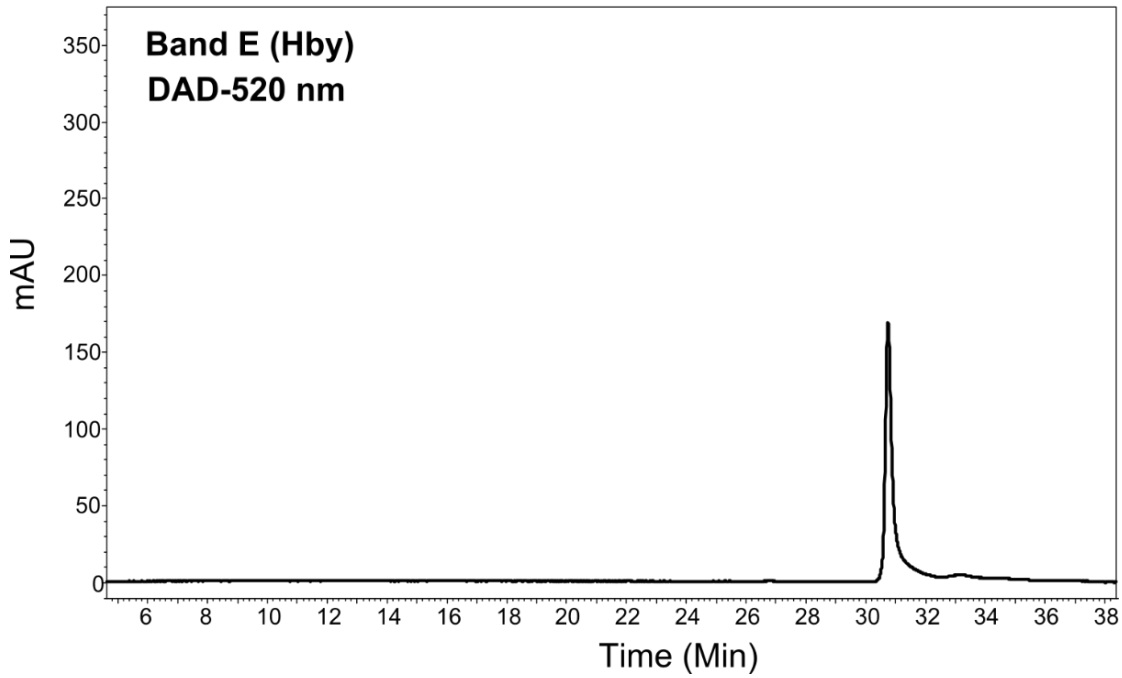

Figure 4:2:9: HPLC chromatogram of Hby as purified by reverse phase chromatography. Material was analysed using the following gradient 0-5 minutes up to 5% v/v acetonitrile 5-40 minutes up to 20% v/v acetonitrile the aqueous phase was 10 mM ammonium acetate pH 7.0.

HPLC analysis of purified Hby shows a single peak when analysed at 520 nm. The retention time of this single band is identical to the retention time of band E as shown in Figure 4:2:9. It was possible to separate Hby from the contaminating di, tri, tetra and penta-amide species.

4:2:4 In-vivo synthesis of Hby

An alternative route towards the production of Hby was explored, here all of the genes required for Hby biosynthesis were expressed on a single plasmid. The plasmid (pET3a-Hby) contains the cobalamin biosynthetic genes *cobA-I-G-J-L-M-F-K-L-H-B* in addition to *A. vinosum cobQ* (figure 4:2:10).

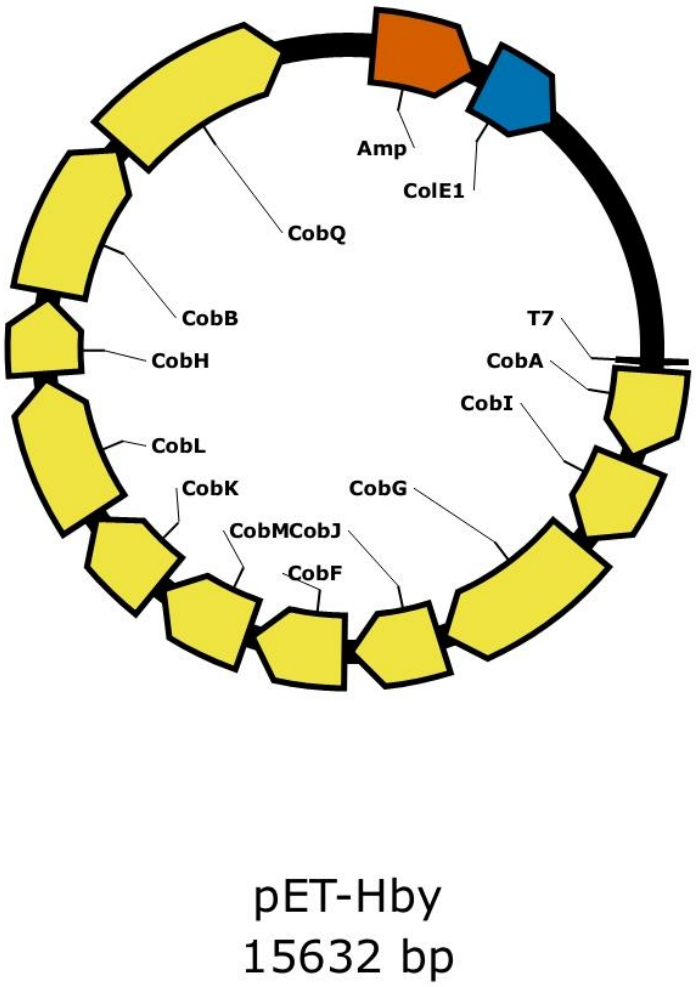

Figure 4:2:10: *Schematic representation of pET3a-AIGJFMKLHBQ this plasmid has the genes necessary to produce Hby when expressed in E. coli. Cobalamin biosynthetic genes are shown in orange, the origin of replication is shown in blue.*

The pET3a-Hby plasmid was transformed into *E. coli*. The resulting strain harbouring the pET3a-Hby plasmid was cultured in 1 L of 2YT growth medium at 28 °C for 36 hours (Method 2:3:7). Cells were harvested by centrifugation at 4000 x g and lysed by immersion in a water bath at 90 °C for 15 minutes. Precipitated protein was removed by centrifugation at 4000 x g and the supernatant clarified further by centrifugation at 36000 x g. The supernatant was applied to a C-18 modified silica resin that had previously equilibrated in 10 mM ammonium acetate buffer, pH 7.0 (Figure 4:2:11). Bound Hby was washed with increasing concentrations of methanol in the same ammonium acetate buffer, pH 7.0 (method 2:6:2).

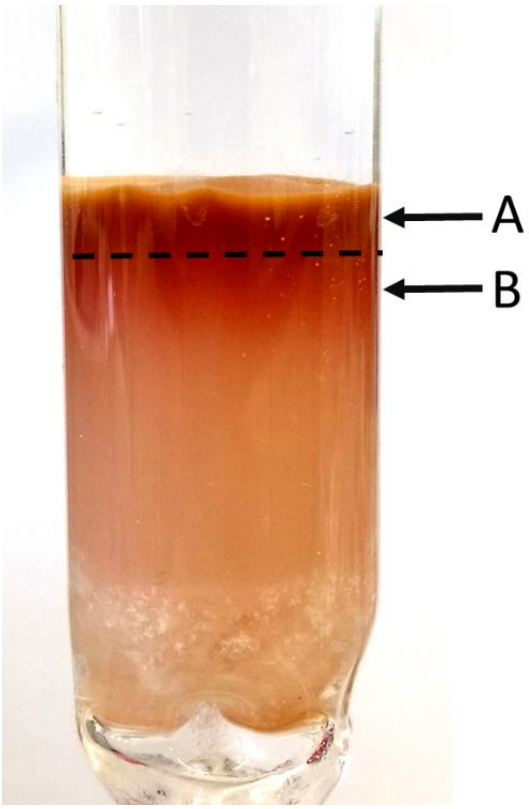

Figure 4:2:11: Reverse phase chromatography on the bench separating Hby from other contaminants derived from E. coli. Band A corresponds to contaminants derived from the E. coli strain used to produce Hby. The lower band designated B corresponds to Hby.

The HPLC analysis of band B (Figure 4:2:11) is shown in Figure 4:2:12. Band B was expected to contain Hby as isolated by bench top reverse phase chromatography shown in Figure 4:2:11.

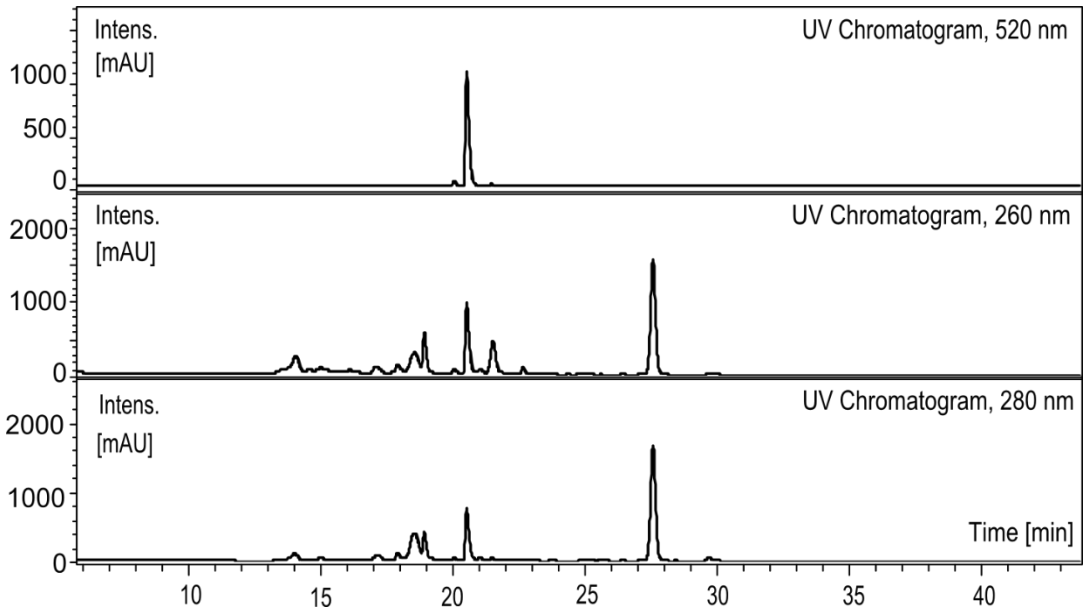

Figure 4:2:12: HPLC chromatogram of band B. The top chromatogram recorded at 520 nm corrpesponds to the α band of the UV vis spectrum of Hby. Contaminating material was identified by absorbance at 260 nm and 280 nm as shown in the middle (260 nm) and bottom chromatograms (280 nm). Peak identity was determined using the methodology outlined in method 2.6.5.

In total 0.5 mg of Hby was isolated from the cell pellet of each litre of bacterial culture grown. The supernatant from the initial cell harvesting step was significantly darker in colour than the equivalent cultures when *E. coli* was expressing pET3a-HBAd. The coloured media and low amount of Hby isolated from the pellet suggested that perhaps Hby was able to leave the cell and could accumulate in the growth media.

To determine whether Hby was indeed accumulating outside of the cell a sample of growth media was taken from *E. coli* expressing pET3a-Hby. After 36 hours of growth cells expressing pET3a-Hby were pelleted by centrifugation and the supernatant heated to 90 °C for 15 minutes to precipitate any proteins. The growth media was then centrifuged at 36000 x g to remove the precipitate and analysed by HPLC, the chromatogram is shown in Figure 4:2:13.

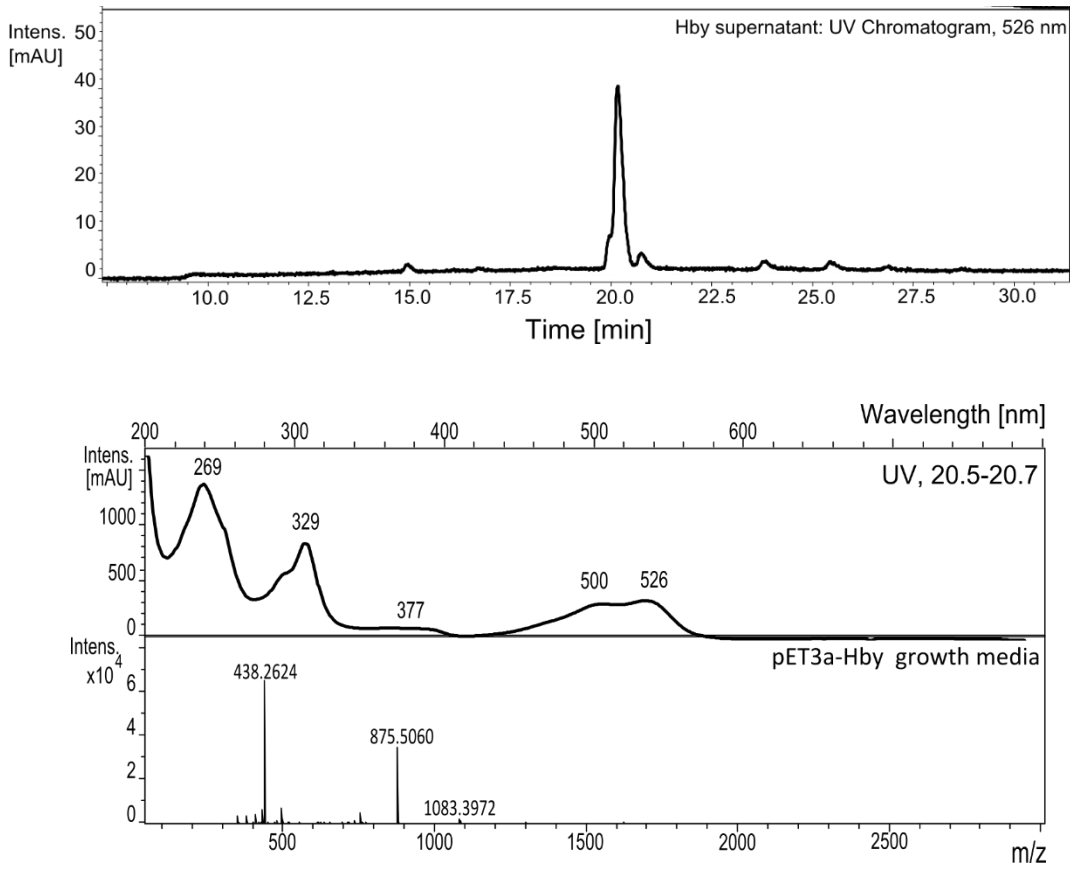

Figure 4:2:13 The top shows the HPLC chromatogram recorded at 526 nm of the growth media of E. coli expressing pET3a-Hby. The UV vis and m/s spectra correspond to the peak at 20 minutes. Both the UV-vis spectrum and observed mass are consistent with Hby. The expected mass of Hby ($C_{45}H_{66}N_{10}O_8$) is 874.51 Da.

Analysis of the growth media by HPLC indicated that Hby is indeed present as indicated by a peak with a UV visible spectrum and mass identical to that of Hby.

4:2:4 Extraction of Hby from growth media

The majority of the Hby produced by cells expressing the plasmid pET3a-Hby was found to accumulate in the growth media. As Hby appears to be the only corrinoid material found in the growth media of these cells a method of extracting it could prove to be the most efficient way to obtain large quantities of Hby as the material is partly purified by excretion. Initially, reverse phase chromatography was employed to isolate Hby from the growth media. However, the large amount of contaminating material coupled with the volume of media (1 l) and slow flow rate of the reverse phase resin perturbed attempts to isolate Hby in this way. A more selective approach was required to extract Hby from such a complex mixture.

B_{12} and other cobalamins are metabolically expensive molecules for prokaryotes to synthesise, due to the large number of biosynthetic enzymes required to synthesise cobalamin as well as the large amounts of ATP, SAM and glutamine required throughout the biosynthetic pathway. It is therefore more energy efficient to obtain B_{12} or B_{12} intermediates from the environment even if an organism is capable of *de novo* B_{12} synthesis. To this end highly specific transport systems have evolved in order to scavenge B_{12} from the environment, the low concentration of exogenous cobalamins has resulted in these systems showing remarkable affinity for B_{12} with Kd values in the nano molar range (Cadieux et al 2002). One such uptake pathway is the BtuCD system found in *E. coli* and other gram negative bacteria.

This system is formed of three components; an outer membrane transporter (BtuC), a globular periplasmic binding protein (BtuF) and a tonB dependent inner membrane transporter (BtuD) (Borths et al 2005). The crystal structure of BtuF (PDB 1N4A) shows the protein in complex with B_{12} (Karpowich et al 2003). Recognition of B_{12} seems to be due in part to numerous negatively charged aspartate residues lining the binding pocket and interacting with the amide groups at the periphery of B_{12}. Hby shares the same pattern of amides as B_{12} as deduced from NMR experiments described in this chapter (Figure 4:2:22), Hby should therefore be recognised and bound by BtuF.

In order to employ *E. coli* BtuF as a means of extracting Hby from the growth media of cells expressing the plasmid pET3a-Hby BtuF was expressed as an N-terminally hexahistidine-tagged protein from a pET14b plasmid (Method 2:3:6). Cells expressing pET14b-BtuF were lysed by sonication and the lysate clarified by centrifugation and loaded onto a nickel affinity column. Growth media from cells expressing pET14b-Hby was then loaded onto the column containing the immobilised BtuF. The resin was then washed with 20 mM Tris buffer, pH 8.0, containing 100 mM NaCl. The column appeared bright orange indicating Hby was bound to BtuF (Figure 2:2:14).

Figure 2:2:14: Isolation of Hby from the media of cells expressing pET3a-Hby. N-terminally his tagged BtuF was immobilised on a nickel affinity chromatography column and media from cells expressing pET3a-Hby was added to the column prior to washing with 20 mM Tris buffer pH 8.0 containing 100 mM NaCl. The orange/pink colour of the column after washing indicates that Hby is bound to the immobilised BtuF.

In order to extract the bound Hby, BtuF was unfolded by the application of an 8 M urea solution. BtuF could then be refolded by equilibrating the column in a buffer containing no urea. Upon refolding, however, the binding efficiency of the column was reduced resulting in less Hby being bound with each cycle of denaturing and refolding. For every 1 L of media processed in this way 1 L of *E. coli* expressing BtuF needed to be produced. Approximately 2 mg of Hby could be extracted from the growth media of cells expressing pET3a-Hby.

4:2:4 UV-vis and mass spectroscopy analysis of Hby

The proposed structure of Hby is presented along with the chemical formula and calculated mass (Figure 4:2:15). In order to confirm the structure of the isolated material as Hby it was subject to a range of spectroscopic techniques including UV-vis, mass spectroscopy and NMR. UV-vis spectra were recorded in H_2O in a quartz cuvette with a path length of 1 cm (Figure 4:2:16). The mass spectrum of Hby was recorded using electrospray ionisation of purified Hby dissolved in methanol. The spectrum was recorded in positive mode (Figure 4:2:17).

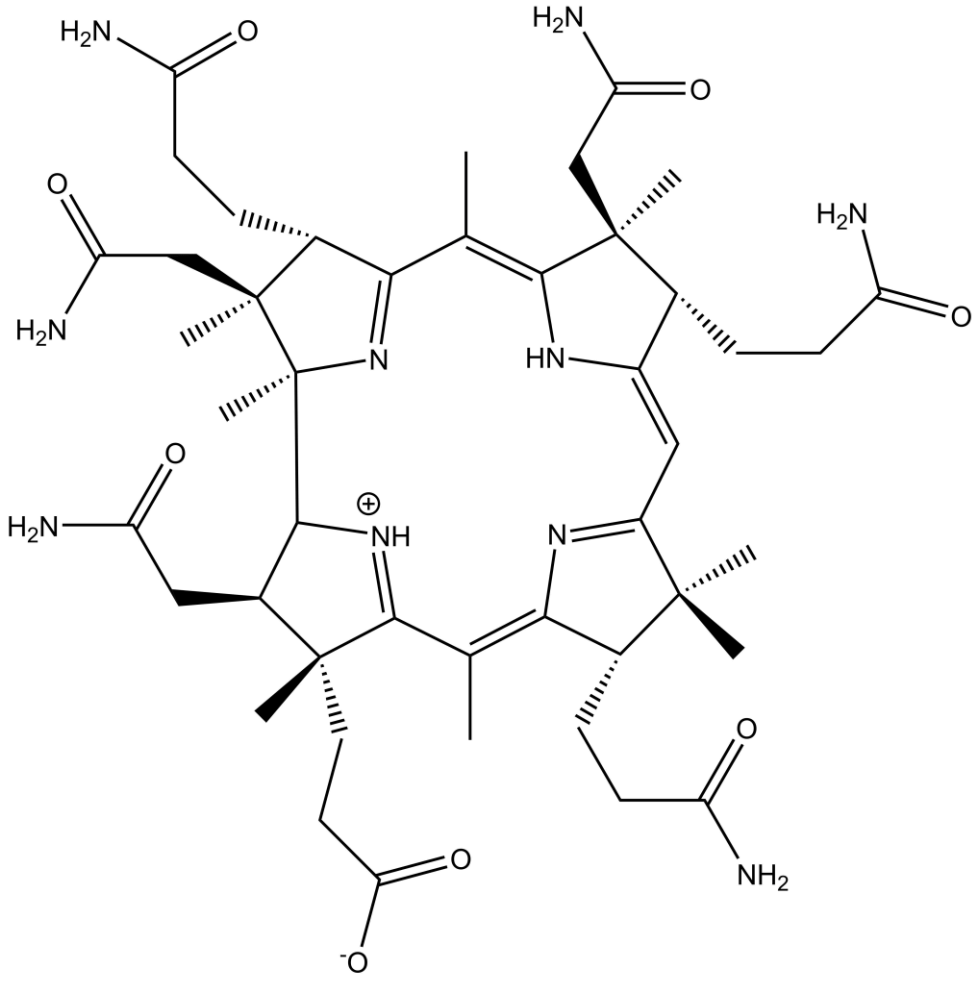

Chemical Formula: $C_{45}H_{66}N_{10}O_8$
Exact Mass: 874.51

Figure 4:2:15: Proposed structure of hydrogenobyric acid along with the molecular formula and mass.

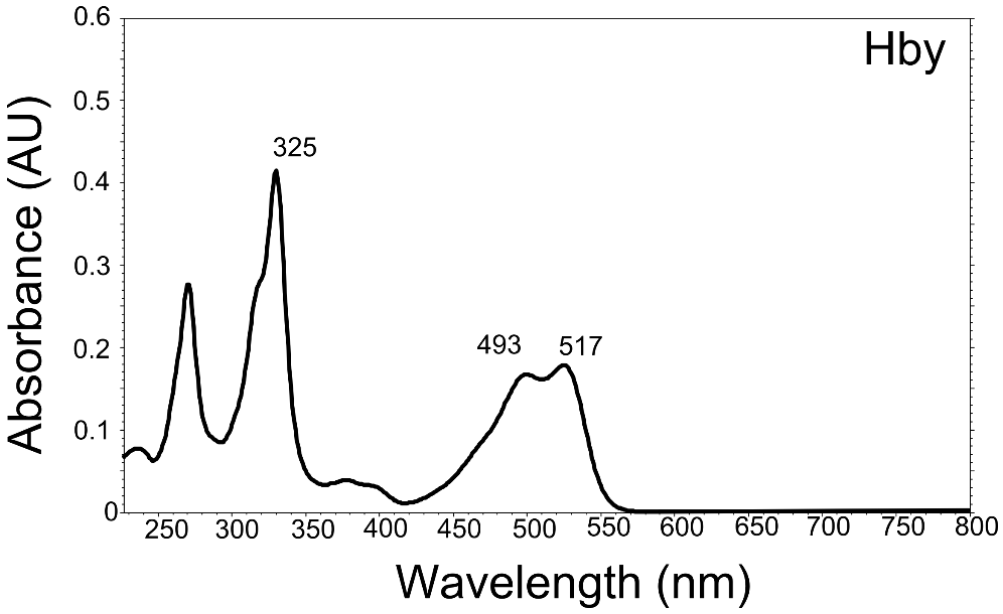

Figure 4:2:16: UV visible spectrum of hydrogenobyric acid in H_2O 220 nm-800 nm

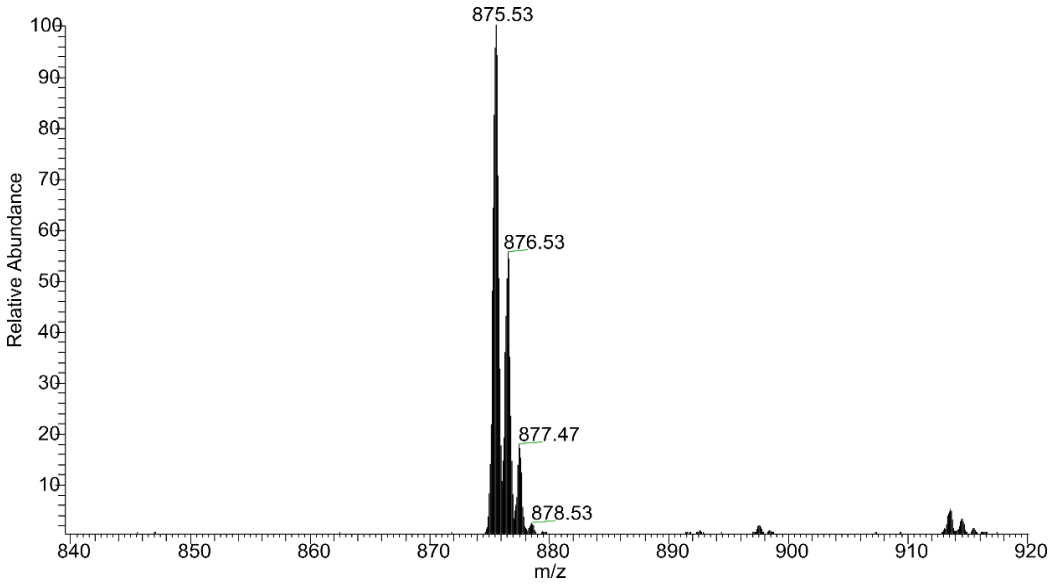

Figure 4:2:17: ESI mass spectrum of hydrogenobyric acid. Sample dissolved in methanol prior to ionisation by electrospray. The spectrum was recorded in positive mode. The mass is consistent with a formula $C_{45}H_{66}N_{10}O_8$ giving an expected mass of 874.51 Da

The UV-vis spectrum (Figure 4:2:16) matches exactly the spectrum observed with the red metal-free corrins as reported previously (Koppenhagen et al 1970) and more recently the UV-vis spectrum of hydrogenobyrinic acid (Deery et al 2012, Debussche et al 1992). The spectrum of Hby has two major absorption peaks with the λ max at 335 nm. This peak is designated the γ band. A second large absorption peak at 297 nm can be seen. The smaller maxima in the visible wavelengths are designated the α band at 517 nm and β band at 493 nm. Two smaller bands are present at 397 nm and 375 nm.

An analysis of Hby by electrospray ionisation mass spectroscopy, shows a compound with a *m/z* that is in agreement with the chemical formula $C_{45}H_{67}N_{10}O_8$ (Figure 4:2:15) with a single pseudo-molecular ion with a *m/z* of 875.53. The isotopic patterning is in agreement with the natural abundance of ^{13}C and ^{15}N isotopes for the chemical formula presented in Figure 4:2:15.

4:2:5 NMR analysis of Hby

A number of 1D and 2D NMR experiments were conducted in order to determine the structure of Hby. Initially Hby was subject to NMR experiments in D_2O. This ^1H 1D spectrum of Hby can be seen in Figure 4:2:18. The 1D spectrum shows signals for each of the non-solvent exchangeable protons in Hby. Due to the relative complexity of Hby 2D homo-nuclear experiments were also conducted. These experiments allowed for the positon of each ^1H atom to be determined relative to one another. Correlation spectroscopy (COSY) shows protons that are within the same J-coupled network allowing ^1H atoms on adjacent carbon atoms to one another to be identified. Rotating frame Overhauser spectroscopy (ROESY) identifies protons that are spatially close to one another. Using these spectra each ^1H atom of Hby could be assigned a chemical shift as shown in Figure 4:2:23. A hetero nuclear coherence spectroscopy (HSQC) experiment was conducted in order to determine the chemical shifts for all ^{13}C atoms with an attached ^1H atom (Figure 4:2:21). These experiments were only sufficient to assign the chemical shifts of non-solvent exchangeable ^1H atoms and hence additional NMR experiments were required to determine the chemical shifts of the solvent exchangeable ^1H atoms of Hby.

The relative positions of ^1H atoms exchangeable with the solvent were determined by conducting the same set of 1D and 2D experiments with Hby dissolved in 90% H_2O / 10% D_2O. Water suppression pulse programs were used in order to supress the signals from ^1H atoms in water and allow the spectra of Hby to be visualised Figure 4:2:19.

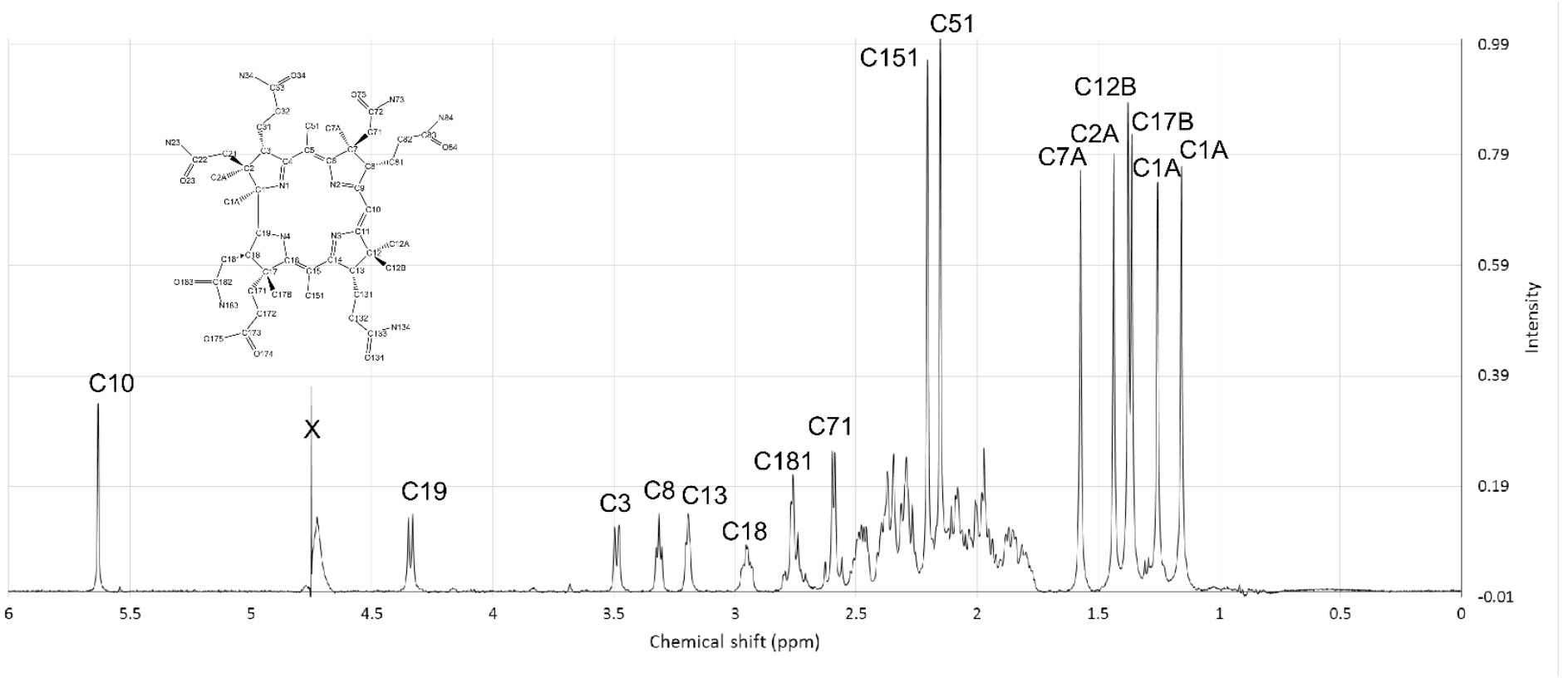

Figure 4:2:18 : 1D ^{1}H NMR spectra of hydrogenobyric acid in D_2O. The chemical shift corresponding to HDO is indicated with an X.

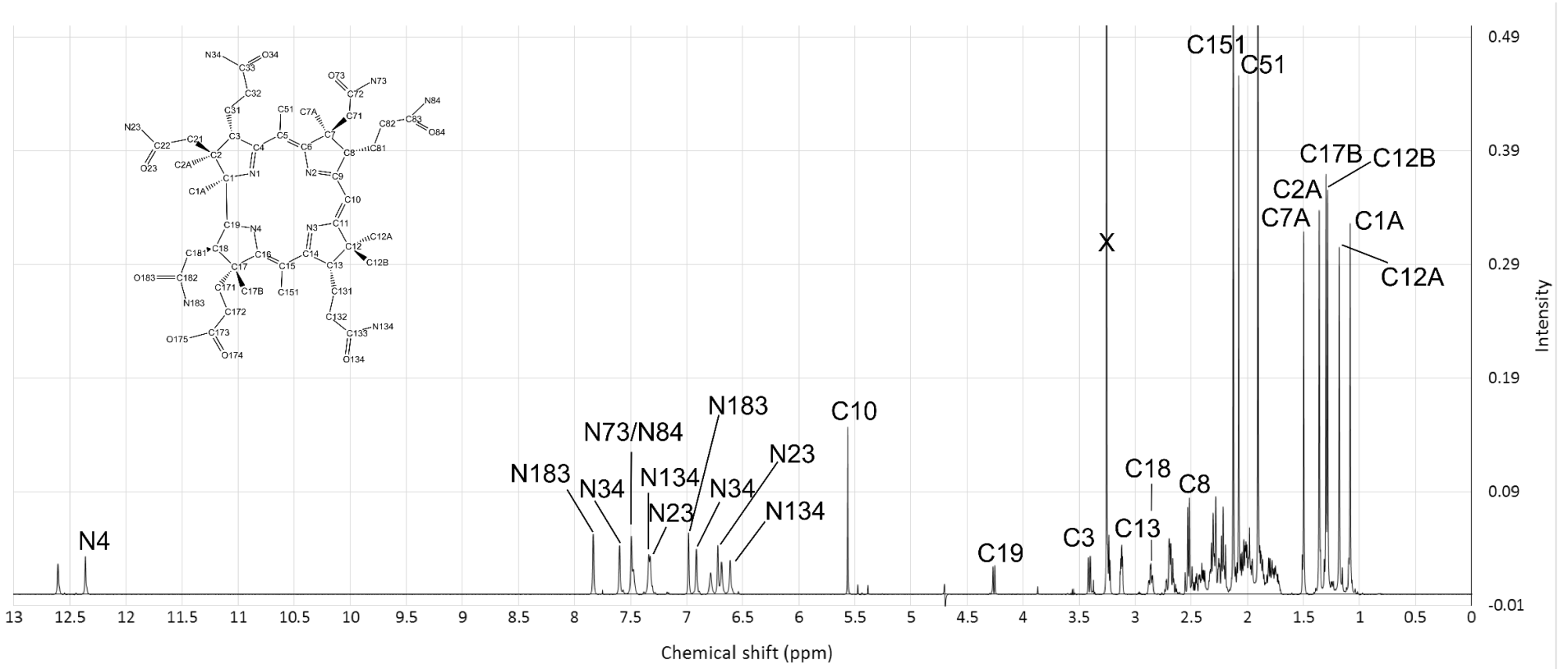

Figure 4:2:19: 1D ^{1}H NMR spectrum of hydrogenobyric acid in H_2O exchangeable amide protons can be seen between 6.0 and 8ppm. Two signals probably corresponding to protons attached to the pyrrole nitrogen atomsa can be seen at 13-13 ppm. Residual methanol from isolation of Hby is indicated with an X

The 1D NMR spectrum of Hby recorded in D_2O shown in Figure 4:2:18 and gives information on the chemical environment for each of the non-solvent exchangeable ^1H atom of Hby. The strongest signals in the spectrum correspond to the ^1H atoms of the methyl groups decorating the macrocycle (1.15 – 2.21 ppm). The central portion of the spectrum (2.25 - 3.55 ppm) is comprised of the CH_2 groups of the peripheral sidechains and methine ^1H atoms of the macrocycle. The low field signal at 5.2 ppm is characteristic of B_{12} NMR spectra and corresponds to the single ^1H atom at C10 (Widner et al 2017, Summers et al 1986).

The 1D ^1H NMR spectrum of Hby recorded in 90 % H_2O / 10 % D_2O (Figure 4:2:17) gives the same signals for non-solvent exchangeable ^1H atoms as the spectrum recorded in D_2O. In addition to the peaks corresponding to non-solvent exchangeable ^1H atoms additional peaks corresponding to ^1H atoms of the peripheral amide groups (6.6-7.9 ppm) and pyrrole nitrogen atoms can be seen (12.42 – 12.65 ppm).

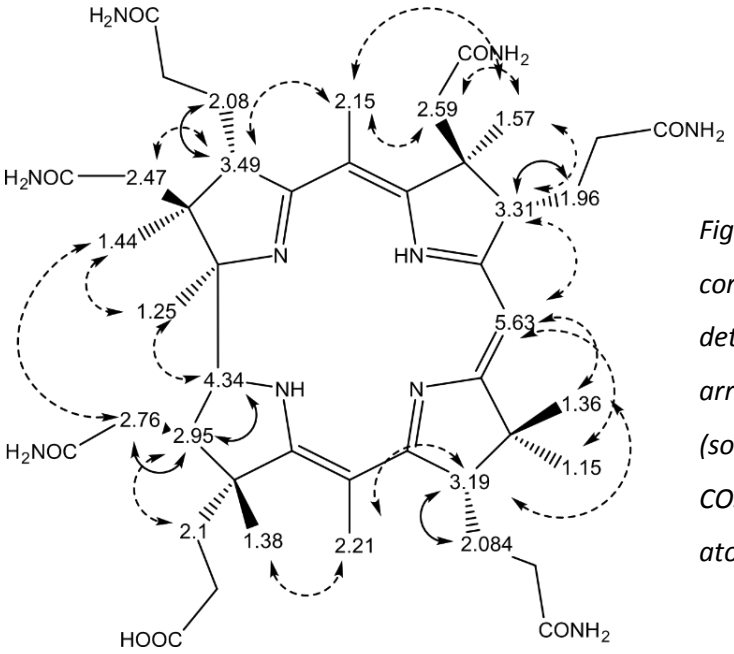

Figure 4:2:20: Through space correlations for Hby as determined by ROESY (dashed arrows) J-coupled networks (solid arrows) as determined by COSY. Chemical shifts for ^1H atoms are expressed in ppm.

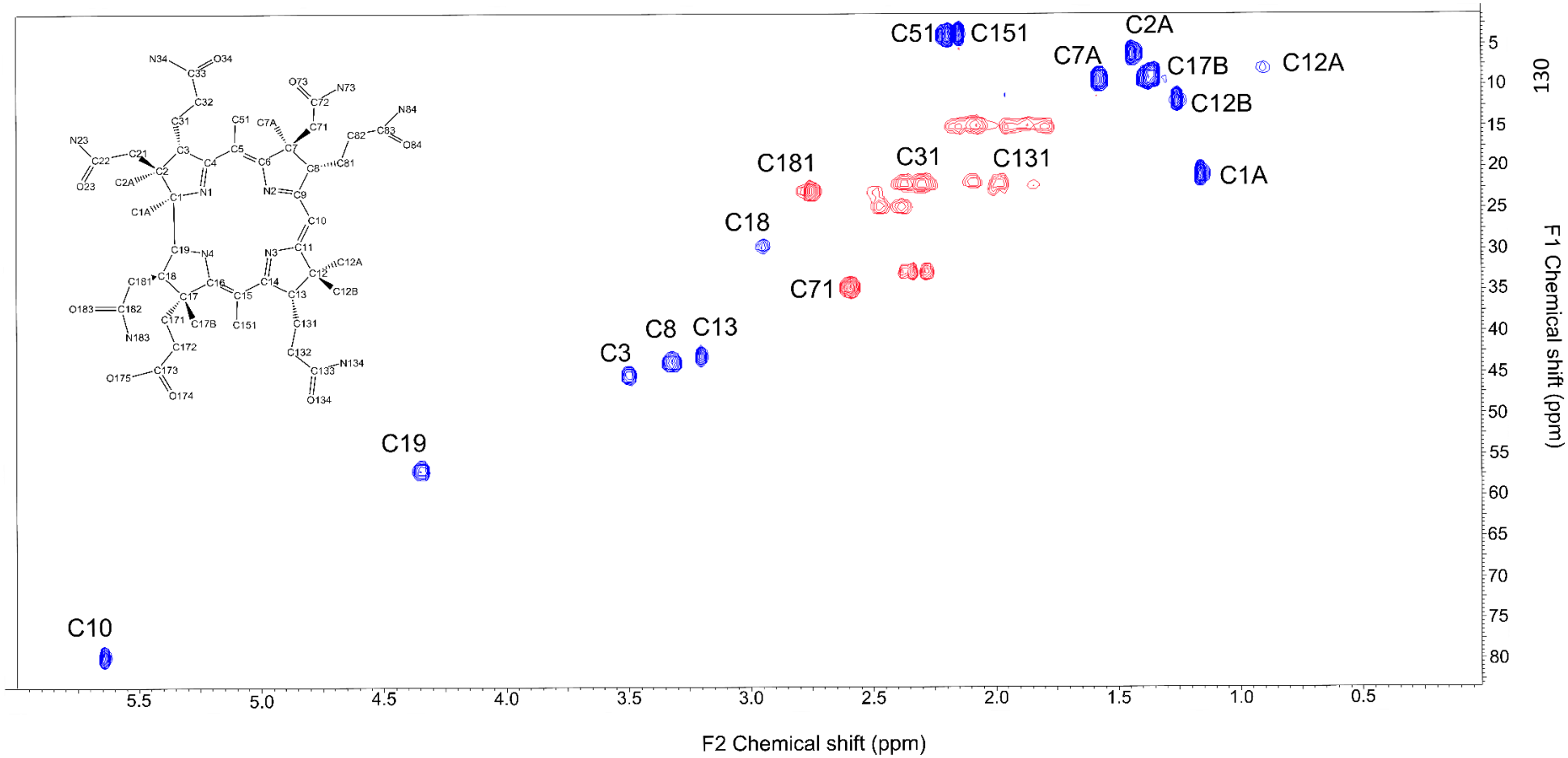

Figure 4:2:21: HSQC spectrum of Hby in D_2O positive signals (blue) correspond to carbon atoms with odd numbers of protons. Negative signals (red) correspond to carbon atoms with an even number of attached protons

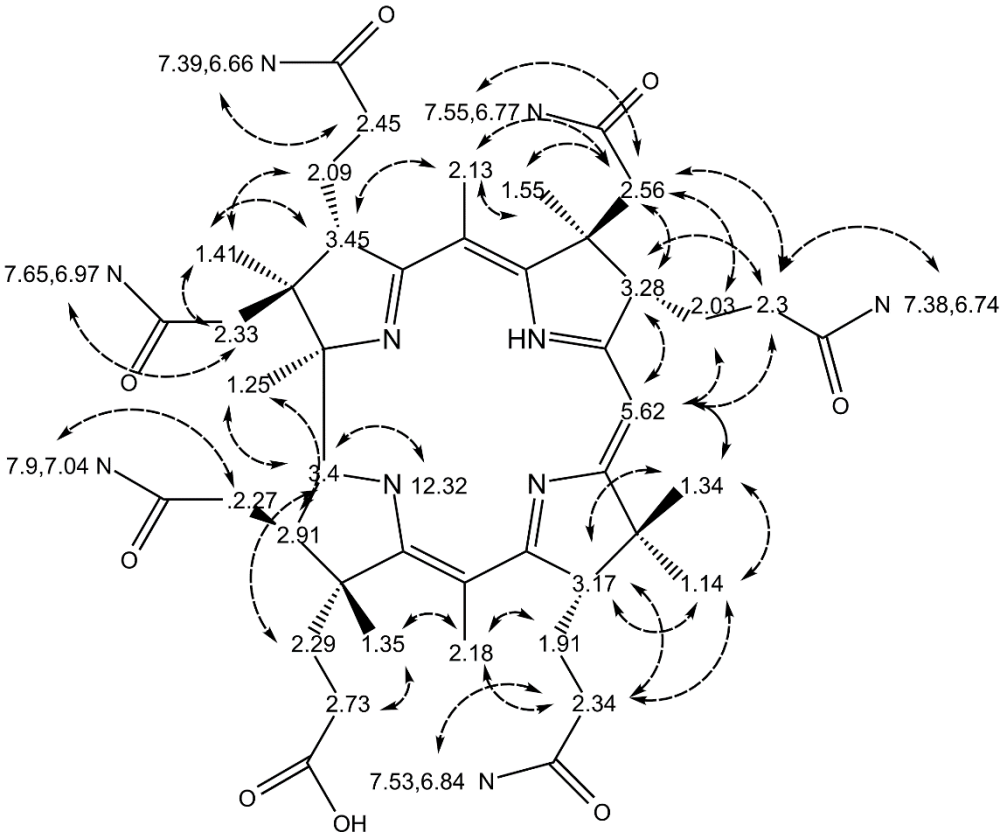

Figure 4:2:22: through space correlations for Hby in H_2O. Amide protons were assigned by correlations to each other in order to determine the pairs and back to CH_2 groups of the acetamide and propionamide sidechains in order to determine positions. The ROE signals were collected on a 600 MHz Bruker spectrometer. Chemical shifts for ^1H atoms are expressed in ppm.

2D rotating overhauser spectroscopy (ROESY) and correlation overhauser spectroscopy (COSY) were used in order to determine the positons of each ^1H atom relative to one another. The chemical shifts and through space correlations for Hby are shown in Figure 4:2:22. The positons of the amide protons were determined by the through space correlations to the CH_2 groups of the sidechains (Figure 4:2:22). Unfortunately the COSY data showing J coupled protons was of insufficent quality for any correlations to be determiend. As such the chemical shifts of the amide protons were determined using the through space correlations generated by the ROESY pulse sequence.

4:2:6 Biological activity of hydrogenobyric acid

The biosynthesis of cobalamin is energetically a costly undertaking with numerous biosynthetic enzymes required to produce and maintain (Martens et al 2002, Warren et al 2002). Moreover, the biosynthesis involves many high energy cofactors such as SAM and the hydrolysis of large quantities ATP for the cobalt chelation process. It is for this reason that many organisms instead scavenge B_{12} from the environment, even if they are capable of its *de novo* biosynthesis (Escalante-Semerena 2007). The production of B_{12} by certain bacteria and archaea can be investigated through the use of microbial bioassay (Taranto et al 2003, Roper et al 2000). Here the ability of a reporter strain to grow in the presence of exogenous corrin analogues is monitored. The reporter strain must be dependent on B_{12} for growth and hence must be capable of salvaging exogenously added B_{12} or late intermediates of B_{12} biosynthesis such as cobyric acid and cobinamide.

In this case the microbial assay used to investigate Hby was based on a strain of *Salmonella enterica.* The strain is deficient in the B_{12} independent methionine synthase (MetE) and is reliant on an alternative B_{12} dependent methionine synthase (MetH) when grown in the absence of methionine on minimal media. A second gene deletion in *cysG* prevents the *S. enterica* from synthesising B_{12}. The earliest exogenous intermediate that can be taken up and used to fulfil the B_{12} requirement of *S. enterica* is cobyric acid. The result of these deletions produces a strain of *S. enterica* that requires either the addition of exogenous $B_{12,}$ an intermediate between cobyric acid and B_{12} or methionine to sustain growth on minimal media (Raux et al 1996).

Application of a solution of Hby to *S. enterica* embedded in agar (Method 3:3:8) does not stimulate the growth of this organism (Figure 4:2:23). Additionally when a solution of Hby is dropped adjacent to a solution of B_{12} the stimulatory effect of B_{12} is no longer present at the interface of the solutions (Figure 4:2:23). This zone of inhibition is concentration dependent with higher concentrations of Hby showing a greater inhibitory effect.

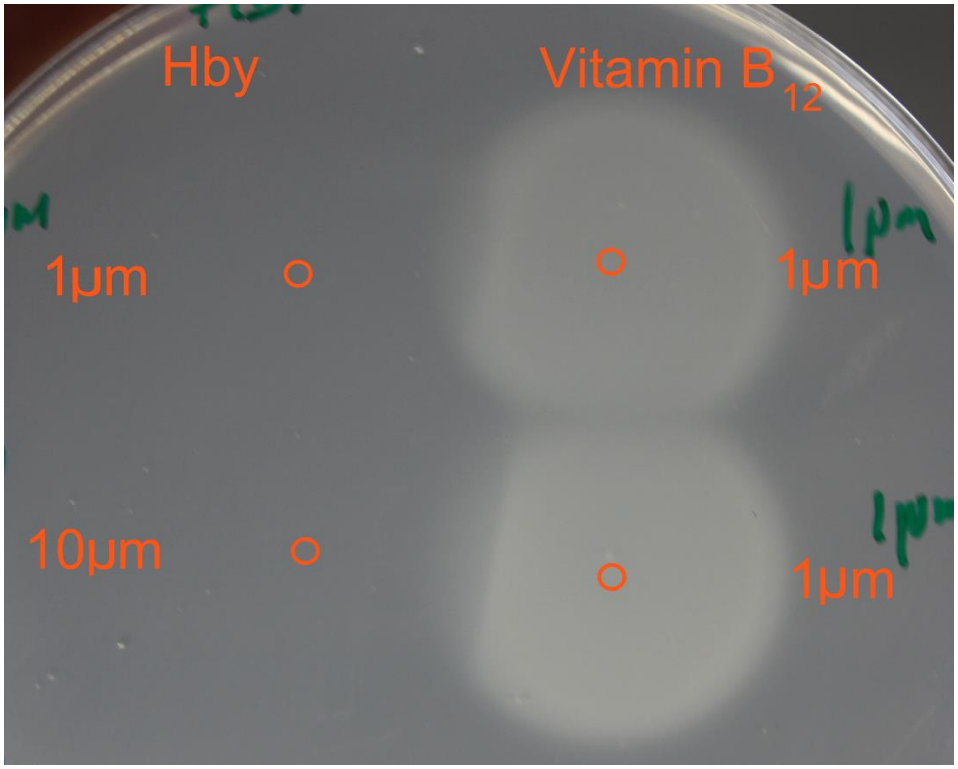

Figure 4:2:23: Salmonella bioassay plate. Vitamin B_{12} (1 µmole in 5µL H_2O) was dropped onto M9 minimal media agar containing Salmonella. 1 µmole Hby in 5µL H_2O and 10 µmoles was dropped next to vitamin B_{12} the point at which the drops were placed is marked with a circle.

To investigate this inhibitory effect further the same strain of *S. enterica* was grown in liquid culture. To stimulate the growth of *S. enterica* B_{12} was added at a concentration of either 10 nm (Figure 4:2:24) or 1 nm (Figure 4:2:25). In addition to this Hby was added at various concentrations and the cells allowed to grow at 37 °C (Method 2:3:9).

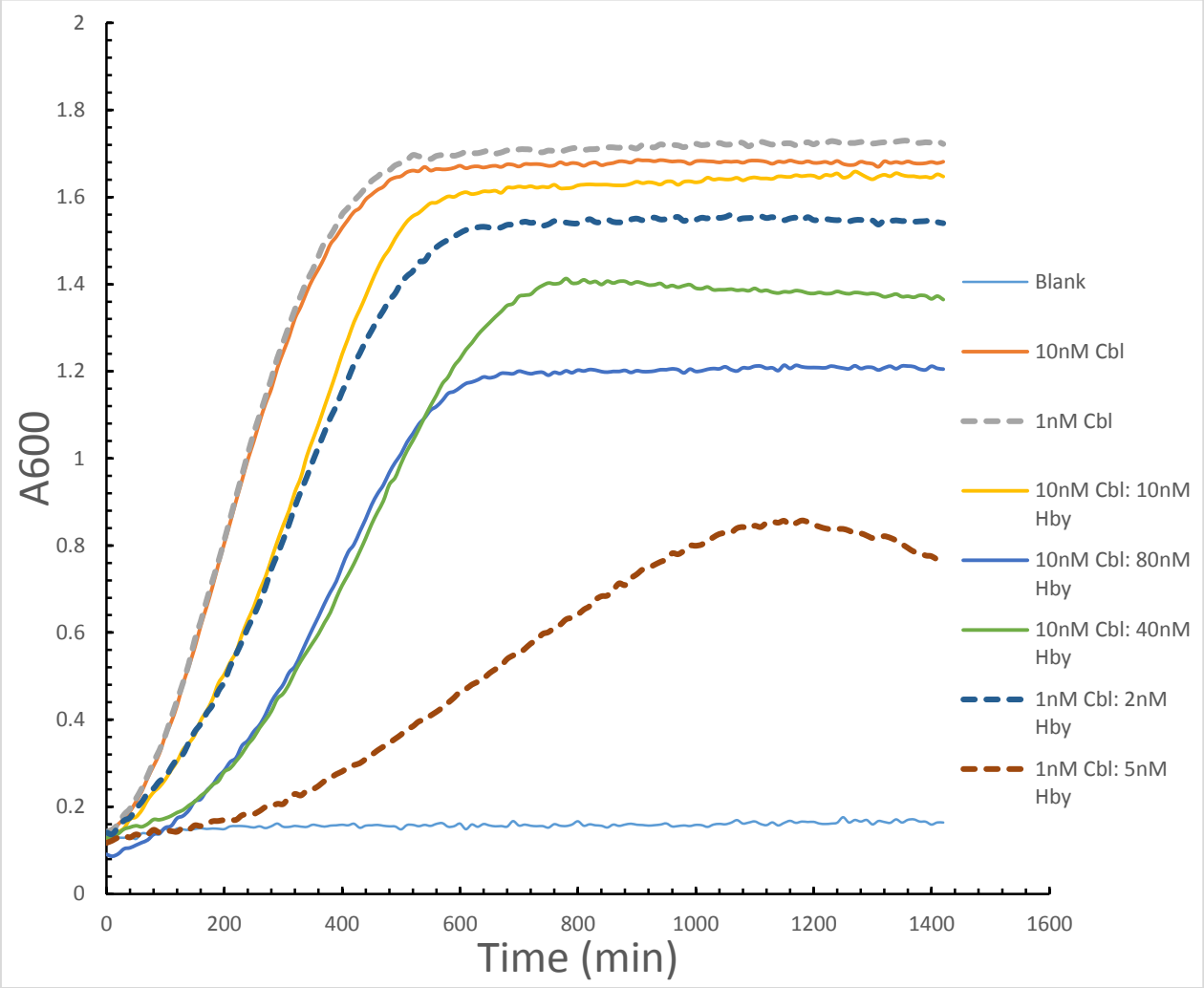

Figure 4:2:24: growth curve of Salmonella enterica ΔMetE ΔCbiB grown in M9 minimal media the presence of vitamin B_{12} at a concentration of 10 nM. Hby was added at a concentration of 10nM, 40 nM and 80 nM. The OD 600 was recorded every 10 minutes for 24 hours. Salmonella was grown in 1ml M9 in a 24 well plate at 37°C with shaking. Data was recorded in triplicate the curves shown are the mean average.

The degree of inhibition exhibited by Hby is concentration dependent with higher concentrations of Hby reducing the overall growth of *S. enterica* to a greater extent than lower concentrations (Figure 4:2:24). This is also true when B_{12} is more limiting (Figure 4:2:25), however, the highest concentration of Hby coupled with the lowest concentration of B_{12} Hby appears to exert a bactericidal effect after 13 hours.

4:3:1 Discussion: Production isolation and characterisation of Hby

The structure of Hby was confirmed by NMR spectroscopy, using a combination of experiments conducted in both D_2O and H_2O. NMR experiments conducted in D_2O gave information about the chemical environment of each of the ^1H atoms that are unable to exchange with the solvent. The positons of each ^1H atom relative to one another was determined by COSY and ROSY experiments. Initial 2D homonuclear experiments conducted in D_2O gave the expected positions for each of the non-solvent exchangeable ^1H atoms. Experiments conducted in D_2O were unable to provide any information about the exchangeable amide ^1H atoms.

In order to determine the positons of each of the amide ^1H atoms relative to other ^1H atoms in Hby a new set of NMR experiments were conducted in H_2O. This allowed for the relative positions of the exchangeable amide ^1H atoms to be determined and confirms that Hby shares the same pattern of amide groups as B_{12}. Interestingly signals were also observed that corresponded to the ^1H atoms attached to the pyrrole nitrogen atoms at the centre of the Hby macrocycle. Of these two atoms it was only possible to assign the position of one of them using the available data from a ROESY experiment (Figure 4:2:22).

The mass of Hby is also consistent with the mass of the predicted structure for Hby (Figure 4:2:15). Finally the UV-vis spectrum of Hby is identical to the previously reported spectrum of HBA (Deery et al 2012) and hydrogenobalamin (Toohey 1965) this indicates that the chromophore of each molecule is identical. The combination of NMR, UV-visible and mass spectra are sufficient to confirm that the proposed structure of Hby is correct.

The structure of Hby shows that it is the metal free analogue of the B_{12} biosynthetic intermediate cobyric acid. Many B_{12} requiring organisms are capable of importing exogenous B_{12} or intermediates of B_{12} biosynthesis. The earliest intermediate imported in this way is cobyric acid. These molecules are then converted to a functional form of B_{12} and used to fulfil the B_{12} requirement of the organism. Supplementing *S. enterica* with Hby results in no stimulatory effect in

the same way as supplementation with B_{12} and indicates that Hby is not converted to B_{12} by *S. enterica* under the conditions assayed.

Extraction of Hby from the growth medium of cells expressing pET3a-Hby using the *E. coli* periplasmic B_{12} binding protein BtuF demonstrated that Hby is recognised and bound by at least this component of the B_{12} import machinery of *E. coli*. Recognition of Hby by BtuF is due to multiple aspartate and glutamate residues lining the binding pocket of BtuF (PDB: 1N4A) and these negatively charged residues interact with the amide sidechains of B_{12} in the crystal structure of *E. coli* BtuF (Karpowich et al 2003). NMR analysis of Hby shows that it shares the same pattern of amides as B_{12} (Figure 4:2:22). The antagonistic effect of Hby on the growth of *S. enterica* when combined with B_{12} in solid culture (Figure 4:2:23) and liquid culture (Figure 4:2:24) is possibly due to competition between Hby and B_{12} for uptake via the BtuBCDF transport system.

The majority of the Hby produced by cells expressing pET3a-Hby accumulated in the growth media. This is in contrast to HBAd, which remains in the cells expressing the plasmid pET3a-HBAd. Structurally HBAd and Hby are highly similar and the only difference between the two molecules is the pattern of amides attached to the peripheral sidechains. As Hby is the only corrinoid that can be detected in the growth media of cells expressing pET3a-Hby this implies that Hby is specifically transported out of the cell and into the growth media. To date no B_{12} export system has been identified. It is, however, possible that Hby is exported via the BtuCD B_{12} import system. The role of this transport complex in Hby excretion could be investigated by knocking out either the BtuC or D component of this system.

Paradoxically the excretion of Hby into the growth media complicated the extraction and purification of this molecule. Large amounts of contaminating excreta present in the growing medium coupled with the large volumes (1 l) precluded the use of reverse phase chromatography for the isolation of Hby. The charge of the amide sidechains prevented the use of faster flowing anion exchange chromatography used as part of the purification of HBAd. It is possible

that cation exchange chromatography would be suitable for the extraction of Hby from this mixture. As a result of difficulties encountered isolating Hby from the growth media of cells expressing pET3a-Hby the most efficient way to produce sufficient Hby to allow for its spectroscopic characterisation and the synthesis of metal analogues was to begin from HBAd.

As HBAd remains in the cell, the lower volumes involved greatly aided the extraction process as 2.5 mg of HBAd was concentrated in approximately 30 mL of cell lysate as opposed to 2 mg of Hby in 1 l of growth media. Even with the additional step of using *A. vinosum* CobQ to convert HBAd to Hby. *In vitro* production of Hby from HBAd proved the most efficient way to produce the required amounts of Hby. In order to have sufficient material for the spectroscopic characterisation of Hby and the synthesis of a zinc analogue of cobalamin around 100 mg of Hby was produced in total.

HPLC analysis of the reaction mixture containing HBAd and *A. vinosum* CobQ gives single sharp peaks corresponding to the di, tri, tetra, penta and hexa-amide of HBA. This chromatographic behaviour indicates that the position of each amide group is fixed. Previous work has shown that CbiP, the CobQ homologue from the anaerobic pathway, amidates its substrate adenosyl cobyrinic acid *a,c* diamide in a sequential fashion (Williams et al 2007). The similarities between CobQ and CbiP in terms of sequence and function point towards CobQ adopting a similar reaction mechanism in which HBAd is bound amidated and released from the active site before rebinding for the addition of the next amide group.

4:4:1 Conclusions

Of the two routes explored for the synthesis of Hby the most efficient method of producing Hby was to synthesise this molecule *in vitro* from HBAd using recombinantly produced *A. vinosum* CobQ to catalyse the amidation reaction. Efforts to produce Hby *in vivo* were frustrated by the excretion of this molecule into the growth media.

Spectroscopic analysis of Hby confirmed the structure of this molecule, showing it to be the metal free analogue of cobyric acid.

Hby was shown to be unable to stimulate the growth of a strain of *S. enterica* dependent on exogenous B_{12} for growth. Hby did, however, bind to the periplasmic component of the BtuCDF uptake system. Binding of BtuF to Hby may explain the inhibitory effect Hby has on the growth of *S. enterica* as Hby can potentially compete with B_{12} for uptake.

Chapter 5: Synthesis and characterisation of zincobyric acid and zincobalamin

5:1:1 Introduction zinc analogues of cobyric acid and cobalamin

The zinc analogue of $B_{12,}$ zincobalamin (Zbl), has been synthesised previously from hydrogenobalamin (Hbl) (Koppenhagen et al 1971). The small amounts of compound synthesised meant that this molecule was analysed only by UV-vis spectroscopy and the structure was implied from the predicted structure of the starting material (Hbl). Further work would investigate the binding of Zbl to parts of the cobalamin uptake pathway in humans (Elshans et al 2008). Zbl specifically was shown to bind to human transcobalamin II, haptocorrin and intrinsic factor. These three proteins represent the main components of the cobalamin uptake pathway in humans.

The aim of the research described in this chapter was to synthesise zincobalamin from the more easily obtainable hydrogenobyric acid (Hby). Two synthetic steps need to be completed, including the insertion of a zinc ion into the metal free macrocycle and secondly the attachment of the lower nucleotide loop to sidechain *f*. Potentially the order of these steps is interchangeable as sidechain *f* is chemically distinct from the other 6 sidechains of Hby making lower loop attachment specific for this position. Likewise, metal insertion can proceed either pre- or post - loop attachment as the status of the sidechains should have no bearing on the metalation reaction of the ring. However, previous work has demonstrated that, thermodynamically, the most favourable site of attachment for the lower nucleotide loop is sidechain *f* if a metal ion is present in the centre of the macrocycle (Eschenmoser 1988). In order to take advantage of this intramolecular catalysis to enhance the covalent linkage of the complete lower nucleotide loop zinc was first inserted into the macrocycle of Hby to form zincobyric acid (Zby).

The lower nucleotide loop of cobalamin is formed of two parts. The first of these is the amino propanol linker that is attached directly to sidechain *f* forming an amide bond. The second is the phosphodiester bonded α-ribazole nucleotide; this group is attached to the aminopropanol group by the ribose sugar. There is some variation between the nucleotide selected by different organisms. In the case of

vitamin B_{12} this nucleotide is dimethylbenzimidazole (DMB) (Brink and Folkers 1949).

Carbodiimide coupling has been used previously to attach the lower nucleotide loop of B_{12} to the rhodium analogue of adenosylcobyric acid in order to produce rhodibalamin, the rhodium analogue of B_{12} (Widner et al 2016). Herein the same approach is applied to determine if the zinc analogue of cobalamin can be synthesised using this combined chemical and biological methodology.

5:2:1 Synthesis of zincobyric acid

The synthesis of zincobalamin has been described previously (Koppenhagen et al 1971). In this work Hbl was boiled with an excess of zinc acetate in aqueous solution in order to produce zincobalamin. As Hbl is not available as a starting material for the synthesis of Zbl the zinc analogue of cobyric acid, Zby was produced *en-route* to the final product Zbl. The predicted structure of this compound is shown in Figure 5:2:1

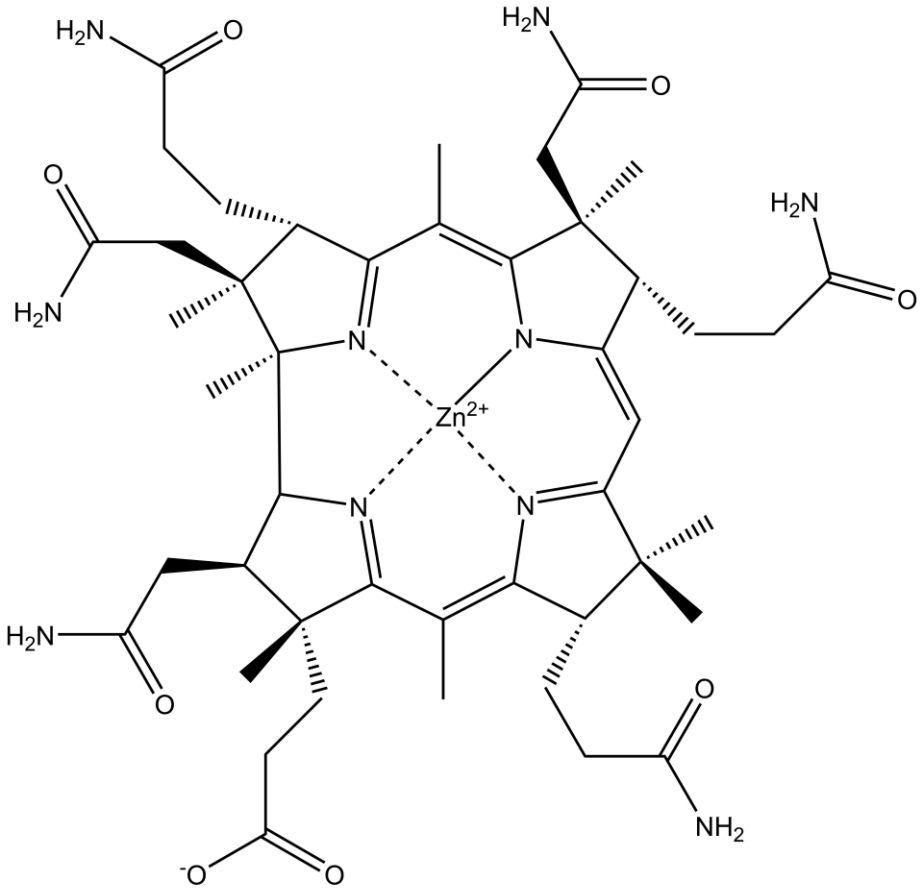

Chemical Formula: $C_{45}H_{64}N_{10}O_8Zn^+$
Exact Mass: 936.42

Figure 5:2:1: proposed structure of Zincobyric acid (Zby). The chemical formula for the structure is presented along with the exact and formula masses for this compound

To produce sufficient Zby for characterisation by NMR and to screen for activity as a potential anti-vitamin a large amount of this compound needed to be produced. Synthesis of Zby followed a very similar reaction scheme to the one outlined by Koppenhagen and co-workers when producing Zbl.

Hby (6.93 mg) along with 20 molar equivalents of zinc acetate (34 mg) and 4 equivalents of sodium acetate (2.6 mg) was dissolved in 10 ml of H_2O degassed under argon. The reaction mixture was incubated at 50 °C under an argon atmosphere for 90 minutes. The reaction scheme is shown in Figure 5:2:2. The reaction was stopped by binding of the reaction mixture to a C-18 modified silica resin and washing away residual salts with H_2O before the material was eluted from the column in methanol.

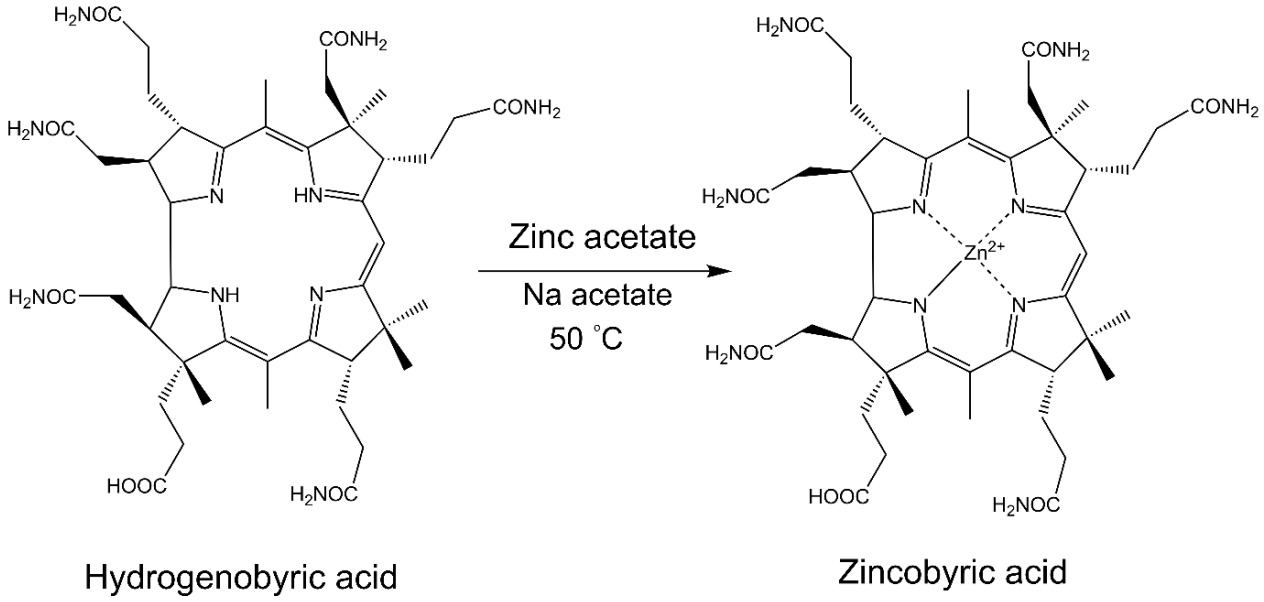

Figure 5:2:2: reactions scheme showing the synthesis of zincobyric acid (Zby) from Hydrogenobyric acid (Hby).

5:2:2 UV-vis mass spectroscopy zincobyric acid

Zincobyric acid synthesised and purified as described in Section 5:2:1 was analysed by UV-vis spectroscopy (Figure 5:2:2) and mass spectroscopy (Figure 5:2:3).

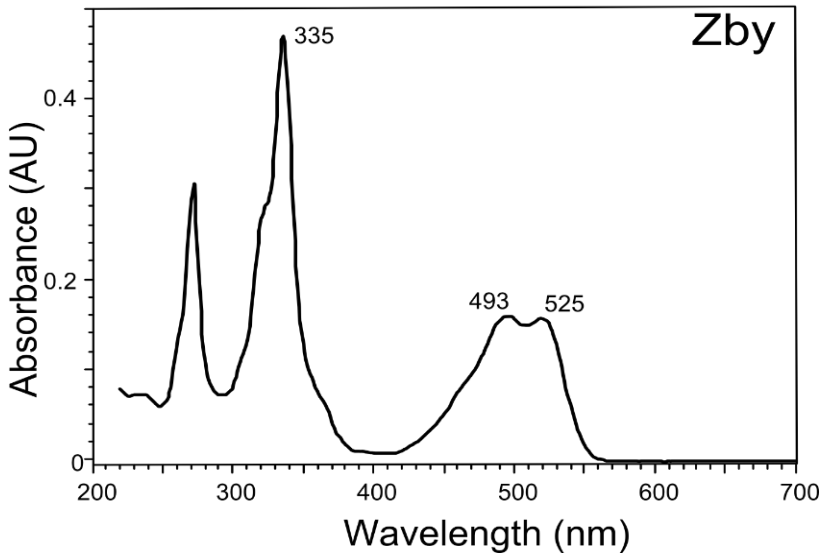

Figure 5:2:2: UV-vis spectrum of zincobyric acid recorded in H_2O in a quartz cuvette with a 1 cm path length. The spectrum was recorded between 220 nm and 700 nm.

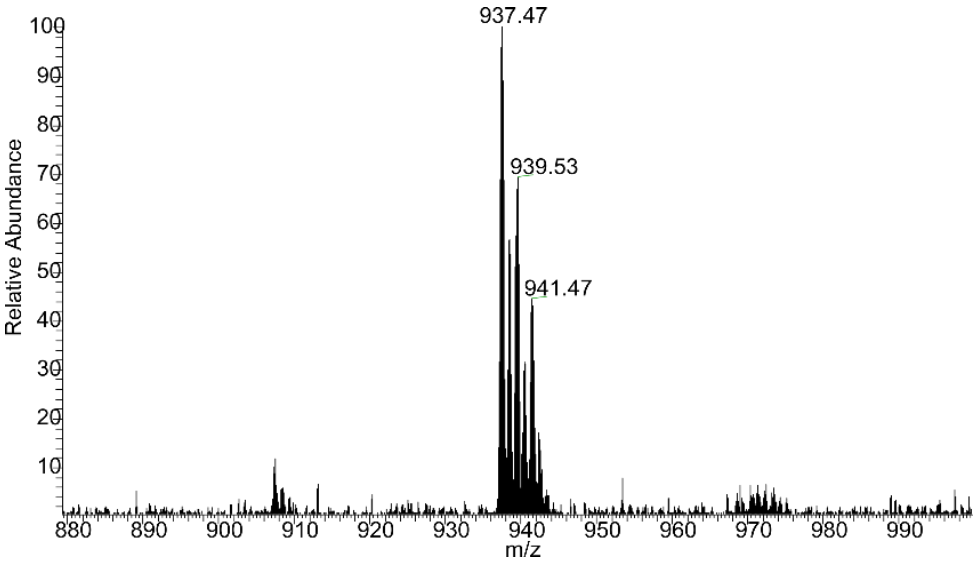

Figure 5:2:3: Mass spectrum of purified Zby dissolved in methanol and ionised by electrospray. Spectra were recorded in positive mode. The expected mass for Zby ($C_{45}H_{64}N_{10}O_8Zn$) is 936.42.

The UV visible absorption spectrum of Zby gives the same general features as the spectrum of Hby and the previously reported spectrum of HBA (Deery et al 2013). The same features are present across all three spectra although the presence of a zinc ion at the centre of the macrocycle shifts the maximum absorbance wavelength of the α, β and γ bands when compared to the spectrum of Hby.

band	Zby Wavelength (nm)	Hby Wavelength (nm)
α	525	520
β	493	496
γ	335	326

The largest change in comparing the spectrum of Zby to that of Hby is the absence of any absorbance maxima between the β and γ bands of the Zby spectrum. The absorbance spectrum of Hby shows two small maxima at 396 nm and 378 nm (Figure 4:2:16).

Analysis of Zby by mass spectroscopy gives a pseudomolecular ion with a m/z ratio of 937.47. The unusual isotopic pattern of the various ions is due to the isotopic distribution of zinc isotopes with ^{64}Zn being the most abundant isotope (50%) followed by ^{66}Zn (28%) and ^{68}Zn (18%) (Burgess and Prince 2006).

5:2:3 NMR analysis of Zby

Zby was analysed by NMR spectrosocpy. The 1D spectrum of of Zby recorded in D_2O is shown in Figure 5:2:4. To detemine the positions of ^1H atoms relative to one another nuclear overhauser spectroscopy was used, specifically ROESY and COSY experiments (Figure 5:2:5). A ROESY experiment was used in order to determine which ^1H atoms are spatially close to one another. A COSY spectrum was recoreded in order to determine which ^1H atoms are adjacent to one another. A heteronuclear HSQC spectrum was recorded in order to determine the ^{13}C chemical shifts of carbons with attached ^1H atoms (Figure 5:2:6).

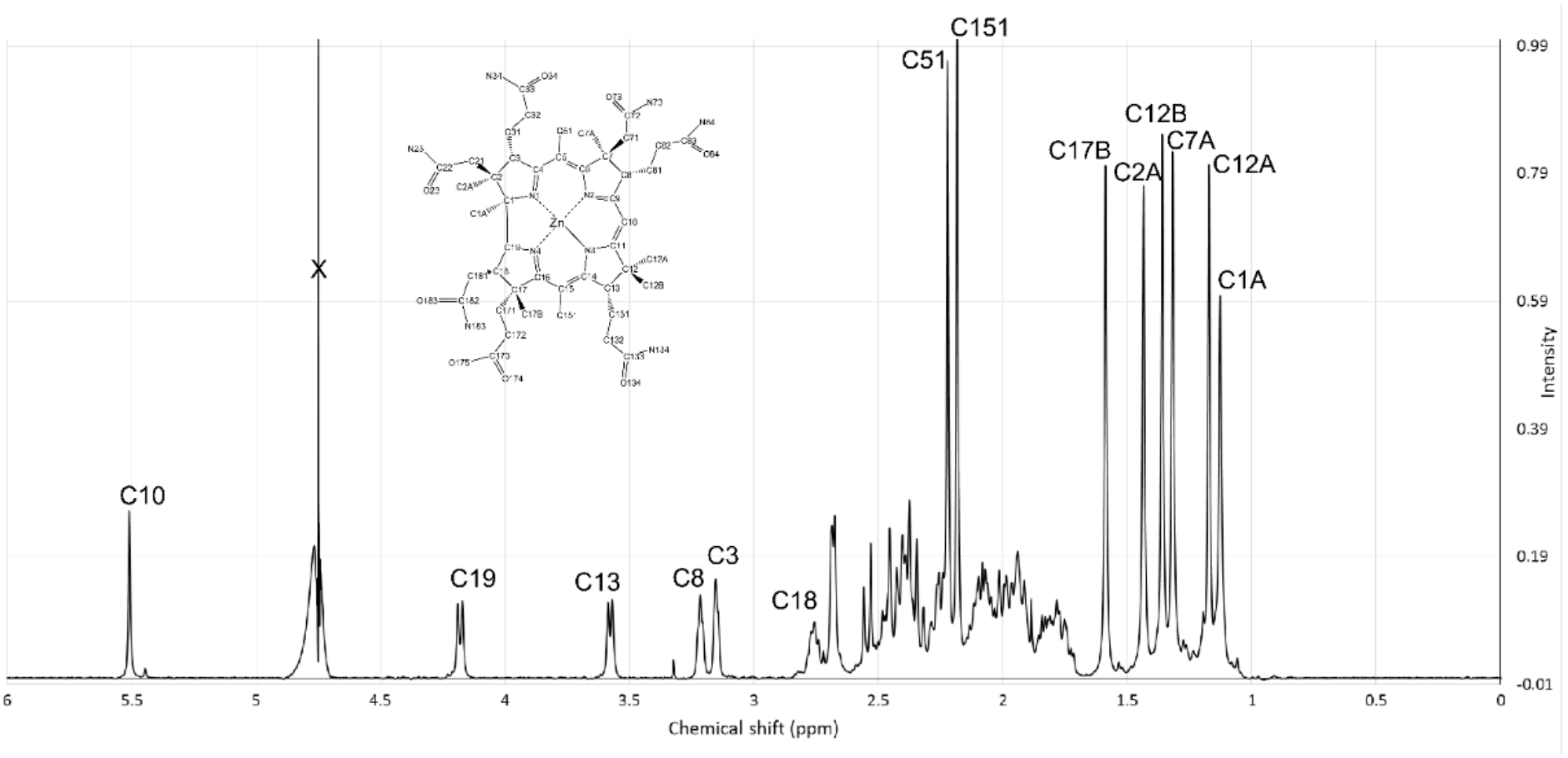

Figure 5:2:4: 1D ^{1}H spectrum of zincobyric acid in D_2O recorded on a Varian 500 MHz spectrometer chemical shifts are in PPM

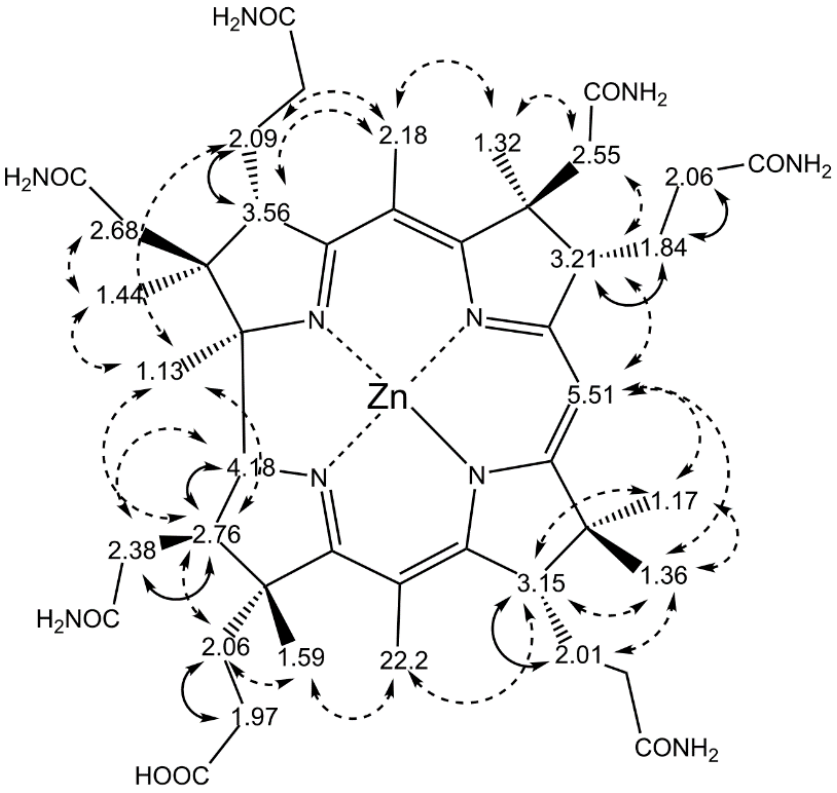

Figure 5:2:5: Through space correlations (dashed arrows) as determined by ROESY and J-coupled systems as determined by COSY (solid arrows). Chemical shifts for ^{1}H atoms are expressed in ppm.

The 1D NMR spectrum of Zby shows the expected features for this molecule. Signals for each of the methyl groups can be seen between 1.17 ppm to 2.22 ppm. The CH_2 groups give signals between 1.84 ppm to 2.68 ppm. The single ^{1}H atom at C10 gives a distinictive low field signal at 5.51 ppm. The postions of the ^{1}H atoms relative to one another were determined by a ROSY pulse sequence. ^{1}H atoms attached to adjacent carbon atoms were correlated via a COSY pulse sequence.

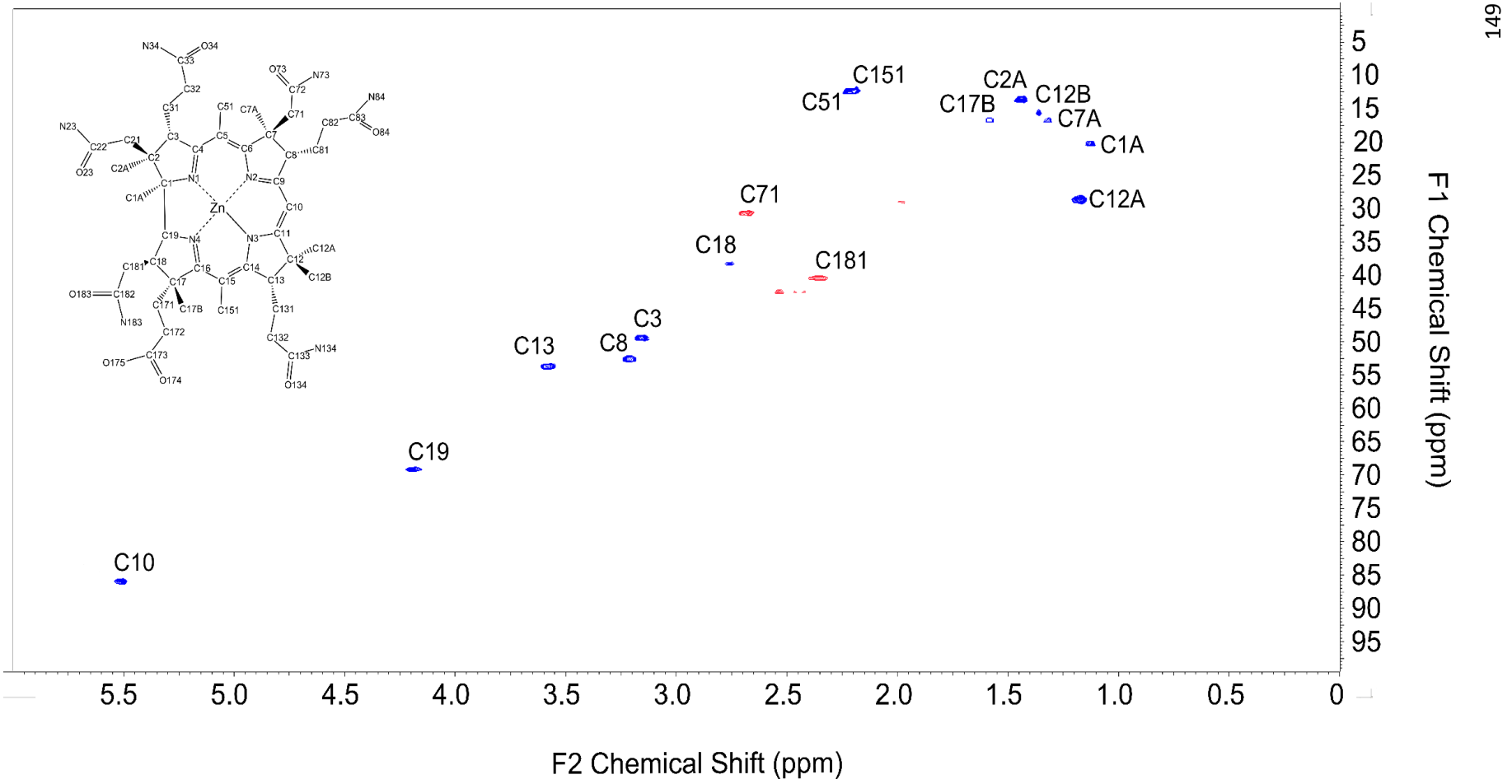

Figure 5:2:6 HSQC spectrum of Zby recorded in D_2O

5:2:4 Biological activity of Zincobyric acid

The biological activity of zincobyric acid was investigated using a *Salmonella* bioassay system (Method 3:3:8). A strain of *S. enterica* (AR2680; *metE*, *cysG*) dependent on exogenous cobalamins for growth was embedded in agar. Upon the addition of B_{12}, cobinamide or cobyric acid the growth of *S. enterica* is stimulated the size of the area of growth being roughly proportional to the amount of B_{12} added. Structurally Zby resembles the B_{12} biosynthetic intermediate cobyric acid and as such should be recognised and taken up by *S. enterica*. The central zinc ion of Zby should be unable to fulfil the same role as the cobalt ion in B_{12} and thus be unable to stimulate the growth of *S. enterica.*

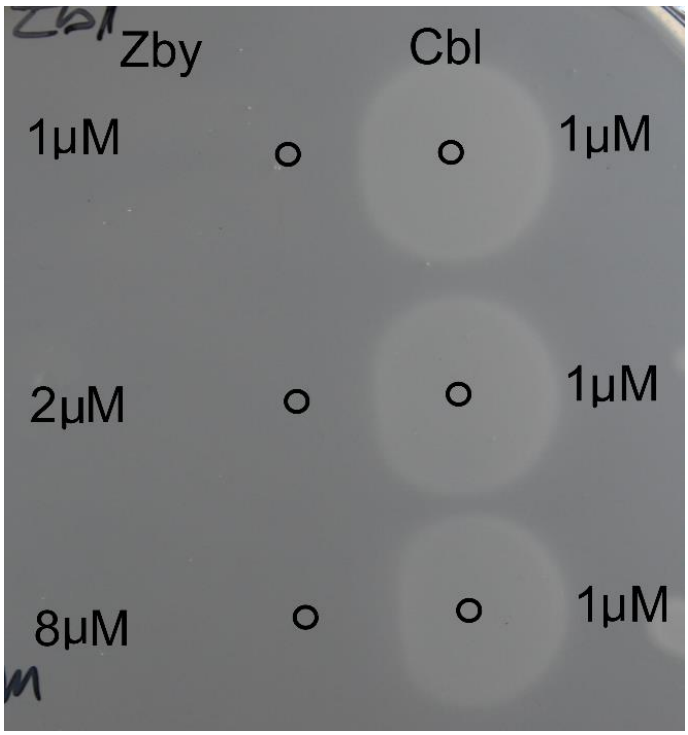

Figure 5:2:7: Bioassay plate with Zby and Cbl, 5 µL of Cbl at a concentration of 1 µM was dropped adjacent to 5 µL drops of Zby at a concentration of 1, 2 and 8 µM. The positon of the drops are indicated by black circles.

Addition of a solution containing Zby directly to agar containing *S. enterica* results in no stimulation of *S. enterica* growth (Figure 5:2:7). Additionally the experiment demonstrates that when Zby is dropped adjacent to a drop of Cbl, Zby exerts an inhibitory effect on the growth of *S. enterica.* Zby prevents the Cbl stimulated growth of the *S. enterica* at the interface of the two drops. This interface will be where the concentration of Zby is highest relative to the concentration of Cbl. Higher concentrations of Zby exaggerate this inhibition as seen by the larger zone of inhibition at the interface of the two drops.

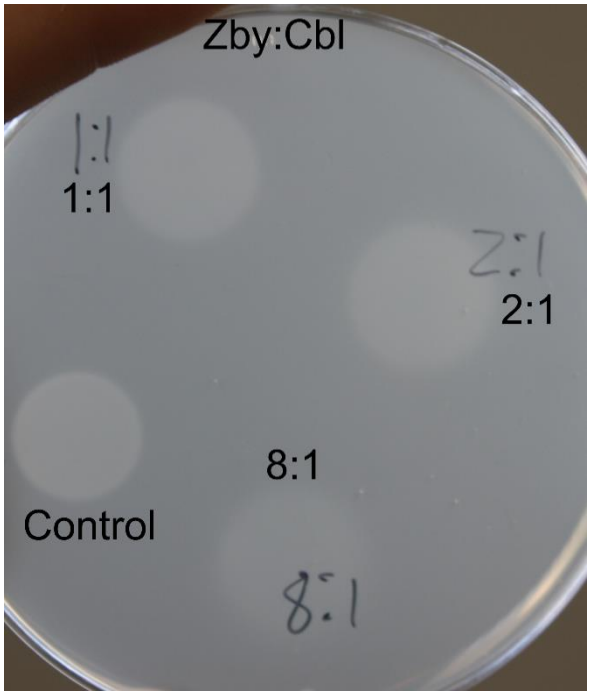

Figure5:2:8: Bioassay plate showing the effect of Zby on Salmonella AR2680 cysG, metE in competition with Cbl. 5 µL of Cbl at a concentration of 1µM was dropped onto a bioassay plate. 5 µL of Zby at a concentration of 1, 2, or 8 µM was dropped at the same position as the initial Cbl drop.

The inhibitory effect of Zby can also be seen on the bioassay plate when Zby is mixed directly with Cbl at various ratios (Figure 5:2:8). Although addition of a mixture of both Zby and Cbl still stimulates the growth of *S. enterica* the density of the growth circles is lower than that of the Cbl only control. Interestingly the diameter of the growth circles is roughly the same as that of the Cbl only control. The reduction in density of *S. enterica* growth is proportional to the concentration of Zby applied to the plate with higher concentrations exhibiting lower density growth rings.

5:2:5 Chemical stability of Zby

Zby is susceptible to degradation in the presence of oxygen and light, this was observed when handling solutions of Zby. Exposure of red fluorescent solutions of Zby become yellow within a few hours when left in direct light. Protecting Zby from light with aluminium foil extends the time it takes for solutions of Zby to become yellow. The same is true for solutions of Hby when exposed to direct light for prolonged periods of time, although the formation of yellow compounds in this case is slower.

The yellow products of Hbl and Zbl have been described previously in the literature (Toohey et al 1965; Koppenhagen et al 1970). It was found that Zbl degrades to form a yellow compound when exposed to light. No structures for the yellow compounds of Hbl or Zbl have been solved by either x-ray crystallography or by NMR spectroscopy. Structural data does exist for the yellow products of cobalt containing corrins as well as for HBAd (Dresow et al 1980; Grüning et al 1985). The data presented by Dresow et al suggest a structure for the yellow product of HBAd along with a UV-vis spectrum. The spectrum of the yellow product is identical to the observed UV-vis spectrum of yellow solutions of Zby (Figure 5:2:9). Changes to the chromophore as observed by UV-vis spectroscopy reflect changes in the arrangement of double bonds around the macrocycle of HBAd and Zby. The identical nature of the spectrum of the yellow product of Zby and the yellow product of HBAd are consistent with the formation of a lactam between sidechain *c* and C6 of the corrin ring (Figure 5:2:9).

.

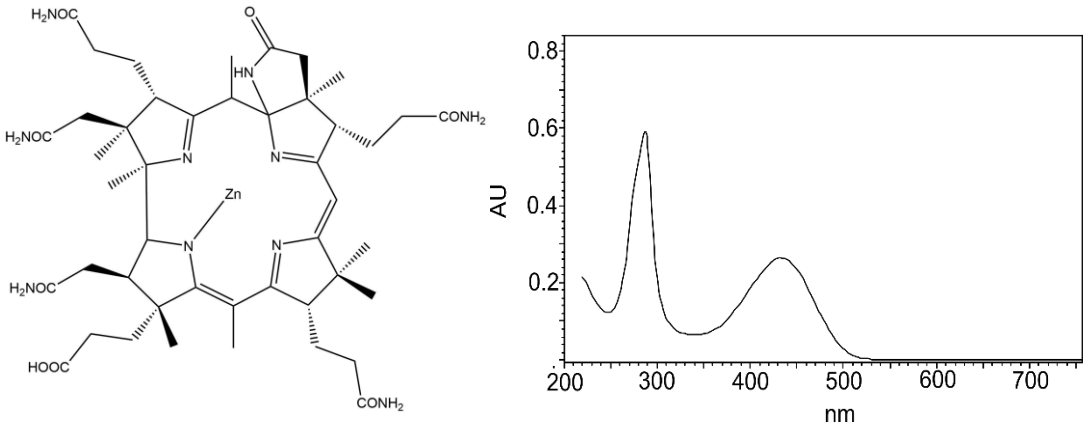

Figure 5:2:9: Proposed structure of the yellow product of zincobyric acid (left) alongside the UV-vis spectra of the compound in H_2O.

The UV-vis spectrum of the Zby derived yellow compound shows a broad maxima at 440 nm and a sharper maxima at 290 nm. The spectrum of the yellow product of Zby is very similar to that of the yellow product of zincobamide as reported by Koppenhagen et al 1971.

5:2:6 Co-ordination of Zby

The next step towards the synthesis of zincobalamin after zinc insertion to form Zby, is the attachment of the lower nucleotide loop. Previous work concerning the total synthesis of B_{12} gave some indication that the presence of a metal ion at the centre of the corrin ring allows the nucleotide loop to pre-coordinate in the correct orientation such that sidechain *f* is the most thermodynamically favourable site for attachment of the loop (Eschenmoser 1988). This is shown schematically in Figure 5:2:10.

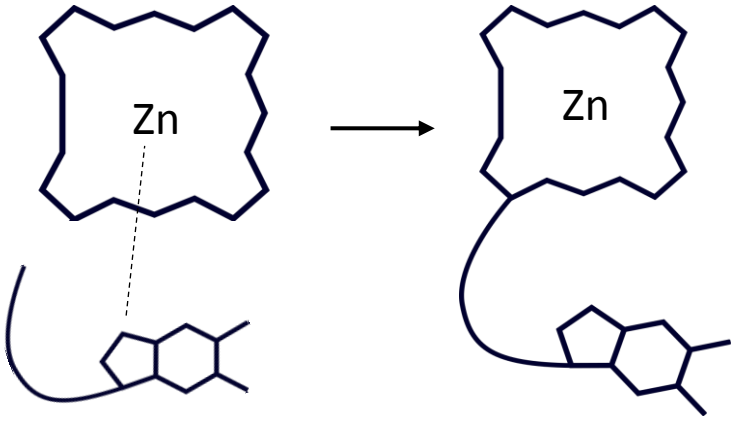

Figure 5:2:10: Schematic representation of the intramolecular positioning of the lower nucleotide loop prior to formation of the amide bond between Zby and the lower nucleotide loop.

The co-ordination of Zby by a nitrogen containing base was investigated spectrophotometrically. N-methyl imidazole was mixed with Zby and a UV-visible absorption spectrum was recorded. N-methyl imidazole was used as a proxy for the dimethylbenzimidazole moiety of the lower nucleotide loop due to its increased solubility in water. The UV-vis spectra recorded on addition of various concentrations of N-methyl imidazole are shown in Figure 5:2:9.

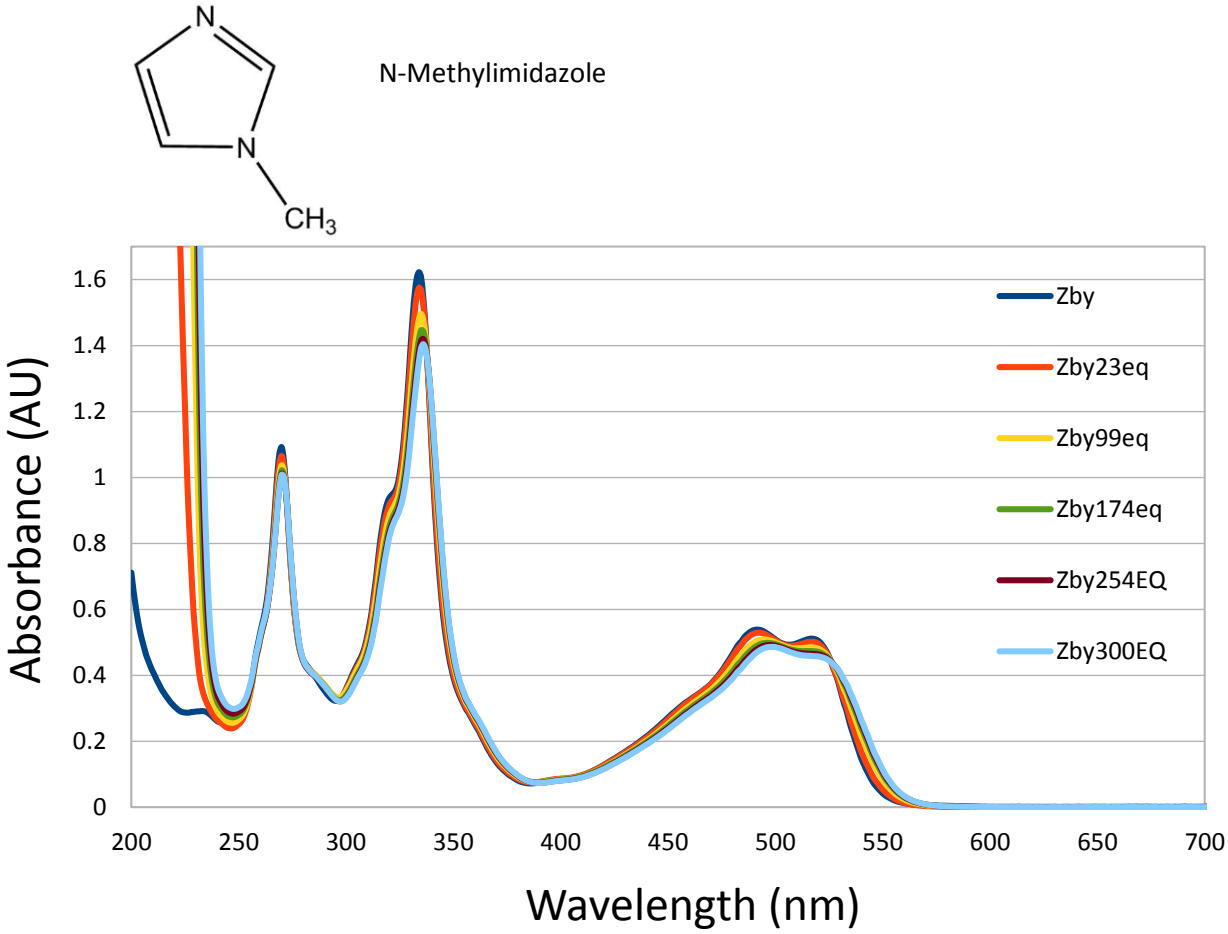

Figure 5:2:11: UV-vis spectra of Zby in 10 mM ammonium acetate pH 7.0 with increasing concentrations of N-methyl imidazole spectra were recorded in a quartz cuvette between 200 nm and 700 nm

The change in spectrum upon addition of N-methyl imidazole indicates a change in the groups acting as ligands for the zinc ion of Zby. The γ band at 335 nm is supressed somewhat at the highest concentration of N-methylimidizole while the α,β bands shift from α 517 nm to 521 nm and β 492 nm to 496 nm. These changes are concentration dependent with lower concentrations of N-methyl imidazole giving rise to mixed spectra.

5:2:7 Nucleotide loop attachment to Zby

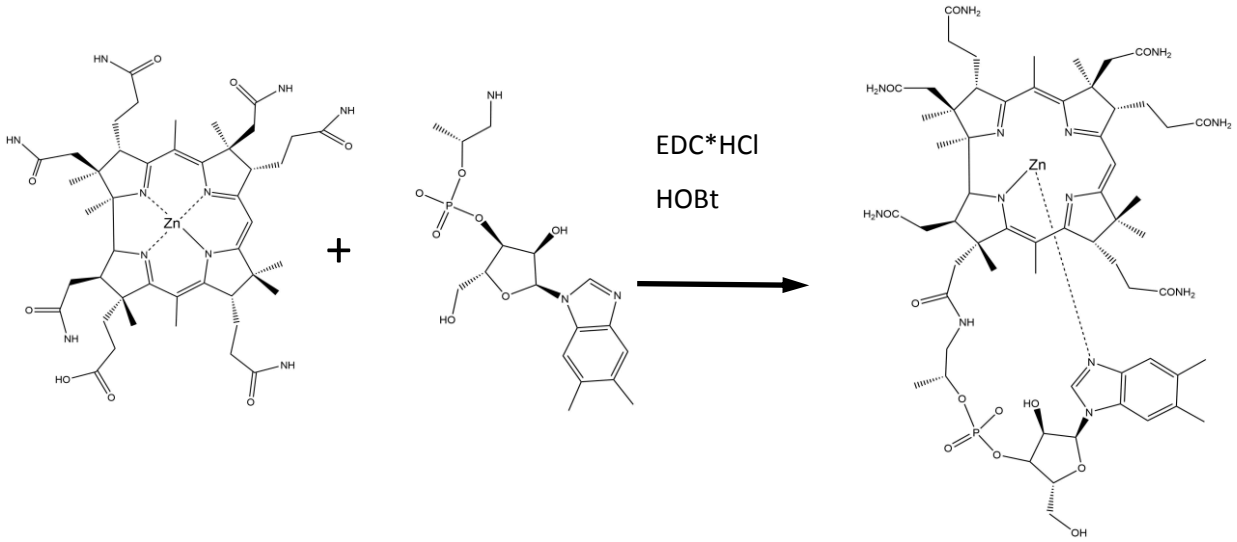

Figure 5:2:12: Reaction scheme for the synthesis of zincobalamin from Zby and free lower nucleotide loop. Carbodiimide coupling was used to attach the lower nucleotide loop to sidechain f.

The final step in the synthesis of zincobalamin is the attachment of the lower nucleotide loop to the *f* sidechain of Zby. Peptide coupling chemistry was used in order to form an amide bond between the amine group of the free nucleotide loop and the propionic acid function of sidechain *f* of Zby. N-(3-Dimethylaminopropyl)-N'-ethylcarbodiimide hydrochloride (EDC*HCl) was used in order to activate the propionic acid of sidechain *f* making it more reactive towards the amine group of the free nucleotide loop it is converted to a more reactive *O*-acylisourea. This highly reactive group was converted to an ester with hydroxybenzotriazole (HOBT) as the reduced reactivity prevents the formation of potential side reactions (König and Geiger 1970).

The free nucleotide loop of B_{12} used in this synthesis was kindly provided by Professor B. Kräutler at the University of Innsbruck as a free amine. However, this molecule could feasibly be generated by selective aminolysis of cobalamin by either enzyme or chemical means (Woodson et al 2006; Zou et al 1995). Alternatively, well documented synthetic schemes specific to the synthesis of the α enantiomers of α ribazole containing nucleotides could be used in order to generate the dimethylbenzimidazole nucleotide as well as analogues on the gram scale (Chandra et al 2005, 2006, 2008).

Zincobyric acid (4.71 mg) was mixed with 2.21 mg (1.1 equivalents) of lower nucleotide loop along with 2.3 mg (2 equivalents) of hydroxybenzotriazol. The reactants were dissolved in 2.5 ml of H_2O and stirred at room temperature under an argon atmosphere. 9.3 mg (9.4 equivalents) of 1-ethyl-3-(3-dimethylaminopropyl) carbodiimide hydrochloride (EDC*HCl) was dissolved in 500 µL H_2O. The two solutions were mixed under an argon atmosphere and allowed to react at room temperature for 4 hours. The reaction was stopped by binding the material to RP-18 resin equilibrated in 10 mM ammonium acetate. The resin was washed with 10% acetonitrile followed by 15% acetonitrile in 10 mM ammonium acetate pH7. Zincobalamin was eluted in 30% acetonitrile. Acetonitrile was removed by rotary evaporation. Zincobalamin (6.62 mg) was produced in this way giving a yield of 96%. The proposed structure of zincobalamin is shown in Figure 5:2:13.

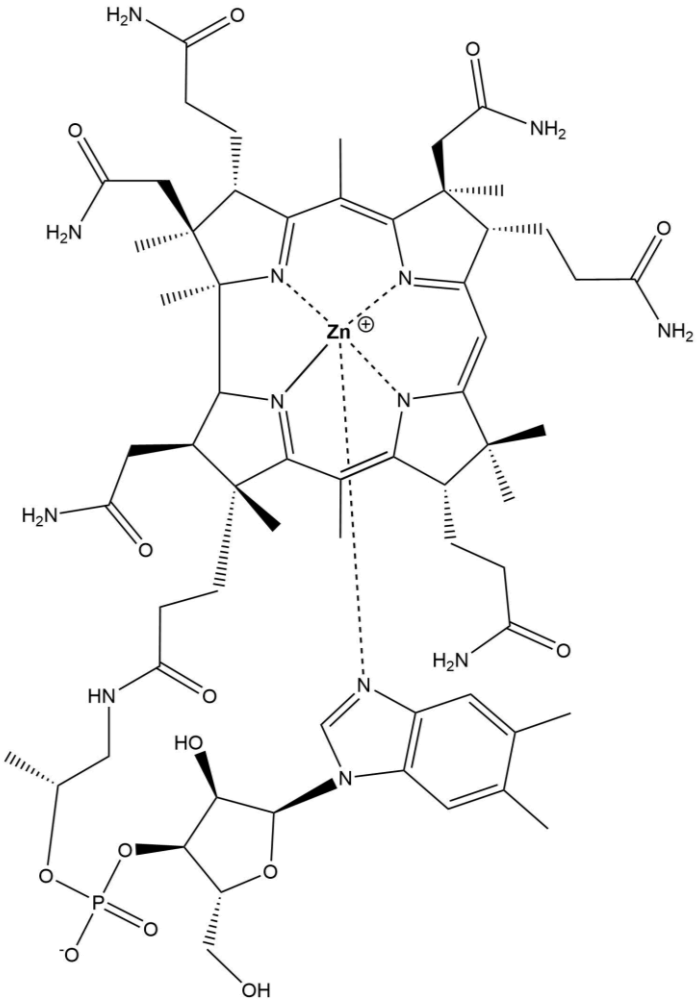

Figure 5:2:13: Proposed structure of zincobalamin along with the chemical formula and molecular mass.

5:2:7 UV-vis mass spec analysis of Zbl

Zincobalamin was analysed by UV-vis spectroscopy (Figure 5:2:14) and mass spectroscopy (Figure 5:2:15).

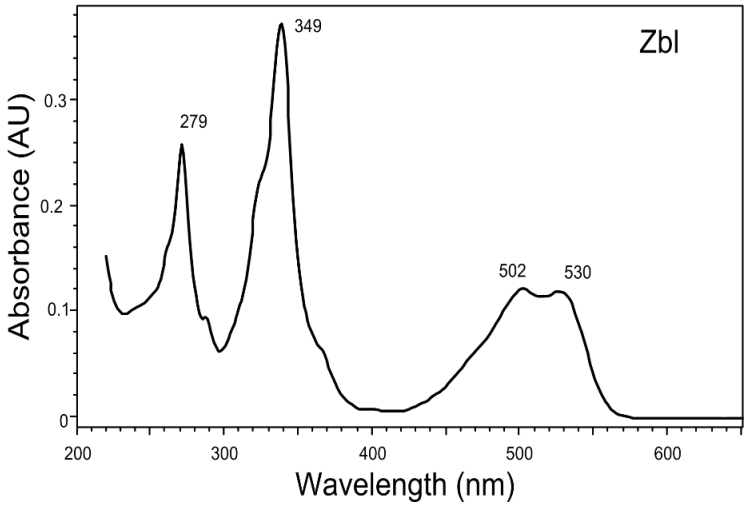

Figure 5:2:14: UV-vis spectrum of zincoabalmin recorded in H_2O and measured in a quartz cuvette.

The UV-vis spectrum of zincobalamin (Figure 5:2:14) retains many of the features of the spectra of Zby and Hby with a large γ band at 349 nm and α, β bands at 530 nm and 502 nm. A comparison of the UV-vis spectrum of Zby (Figure 5:2:2) to Zbl (Figure 5:2:12) reveals that the γ band of Zbl 349 nm has undergone a bathochromic shift when compared to the γ band of Zby 335 nm. The α (502 nm) and β (530 nm) bands of Zbl have undergone a similar shift when compared to the α band (525 nm) and β (493 nm) bands of Zby.

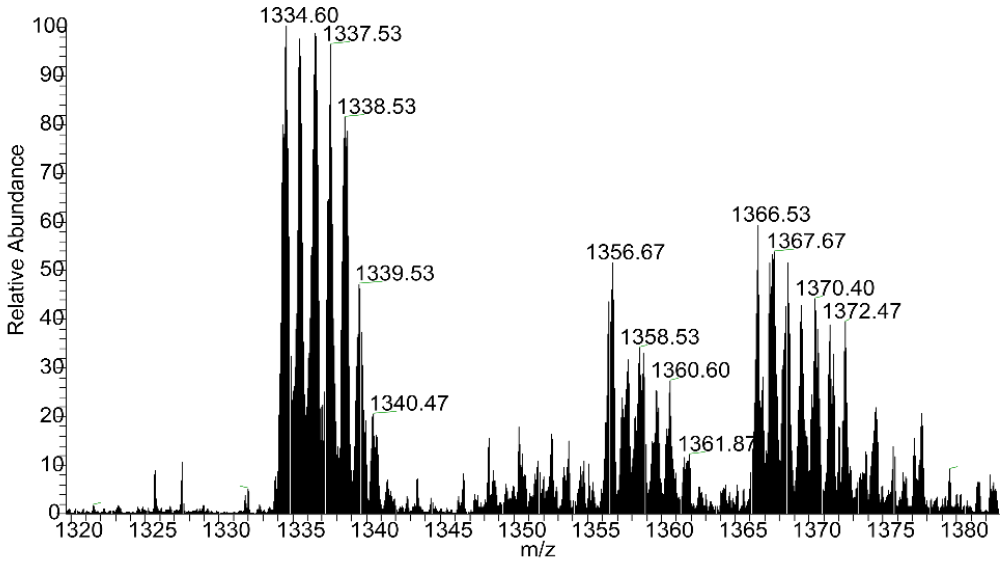

Figure 5:2:15: Mass spectrum of Zbl dissolved in methanol and ionised by electrospray. The pseudomolecular ion can be seen at 1334.6 m/z along with the sodium adduct at 1356.67 m/z and the potassium adduct at 1366.53 m/z. The expected mass for Zbl ($C_{62}H_{88}N_{13}O_{14}PZn$) is 1333.56 Da.

The mass spectrum gives a pseudomolecular ion with a m/z of 1334.6 in keeping with predicted mass of Zbl. The isotopic pattern of zinc can still be seen in the spectrum indicating it is still present. Two higher mass species can also be seen, which correspond to the sodium and potassium adducts of Zbl.

5:2:8 NMR analysis of Zbl

Zbl was analysed by NMR spectroscopy and the 1D spectrum of Zby in D_2O is shown in Figure 5:2:16. A ROESY experiment was used in order to identify ^1H atoms that are spatially close to one another. ^1H atoms on adjacent carbon atoms were identified by COSY. The couplings from these two experiments are depicted in Figure 5:2:17.

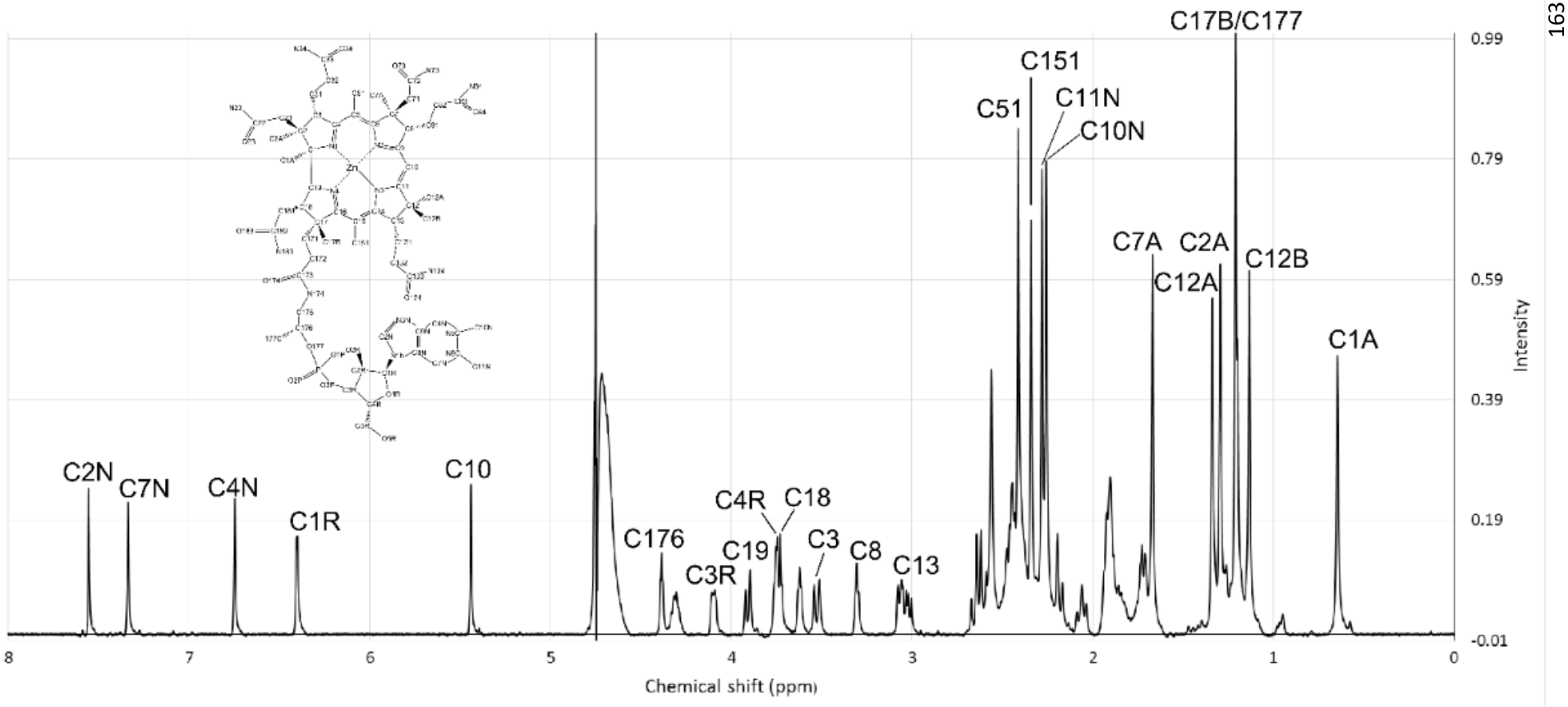

Figure 5:2:16: 1D ^{1}H NMR spectrum of Zbl in D_2O

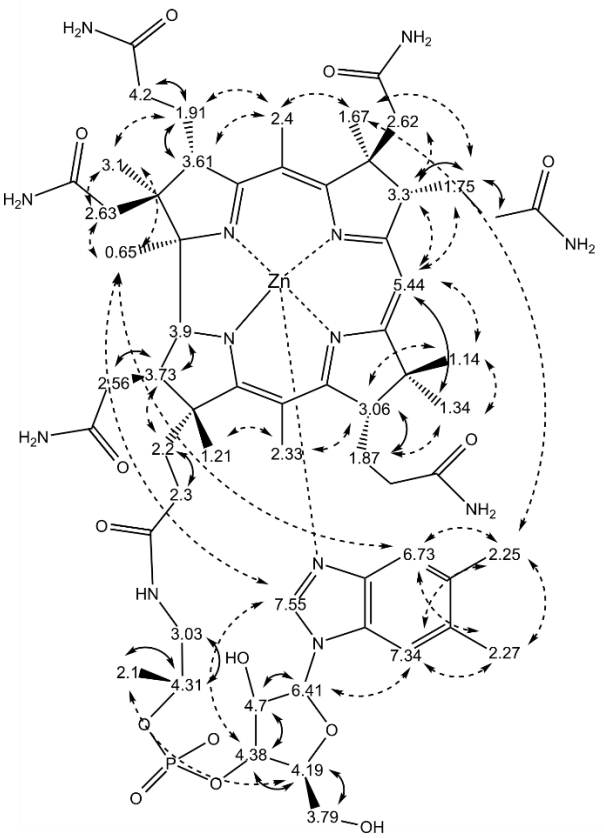

Figure 5:2:17: Through space correlations between ^{1}H atoms as determined by ROESY (dashed arrows). J couplings between adjacent ^{1}H atoms as determined by COSY (solid arrows). Chemical shifts for ^{1}H atoms are expressed in ppm.

The 1D ^{1}H NMR spectrum of Zbl shown in Figure 5:2:16 shares many of the chemical features of the Zby (Figure 5:2:4). Signals corresponding to the methyl groups of Zbl are in the region between 0.5 to 2.9 ppm. Compared to the spectrum of Zby the Zbl spectrum contains signals corresponding to the methyl group that forms part of the amino-propanol linker comprising the lower nucleotide loop. The low field portion of the spectrum 5.5 to 7.8 ppm contains signals corresponding to the methyl groups of dimetylbenzimidazole.

Through space correlations for the ^{1}H atoms of Zbl were generated using a ROESY pulse sequence. Long range coupling between DMB attached ^{1}H atoms and ^{1}H atoms of methyl groups attached to the corrin ring suggest that at least under neutral aqueous conditions the lower nucleotide loop of Zbl adopts a base on conformation.

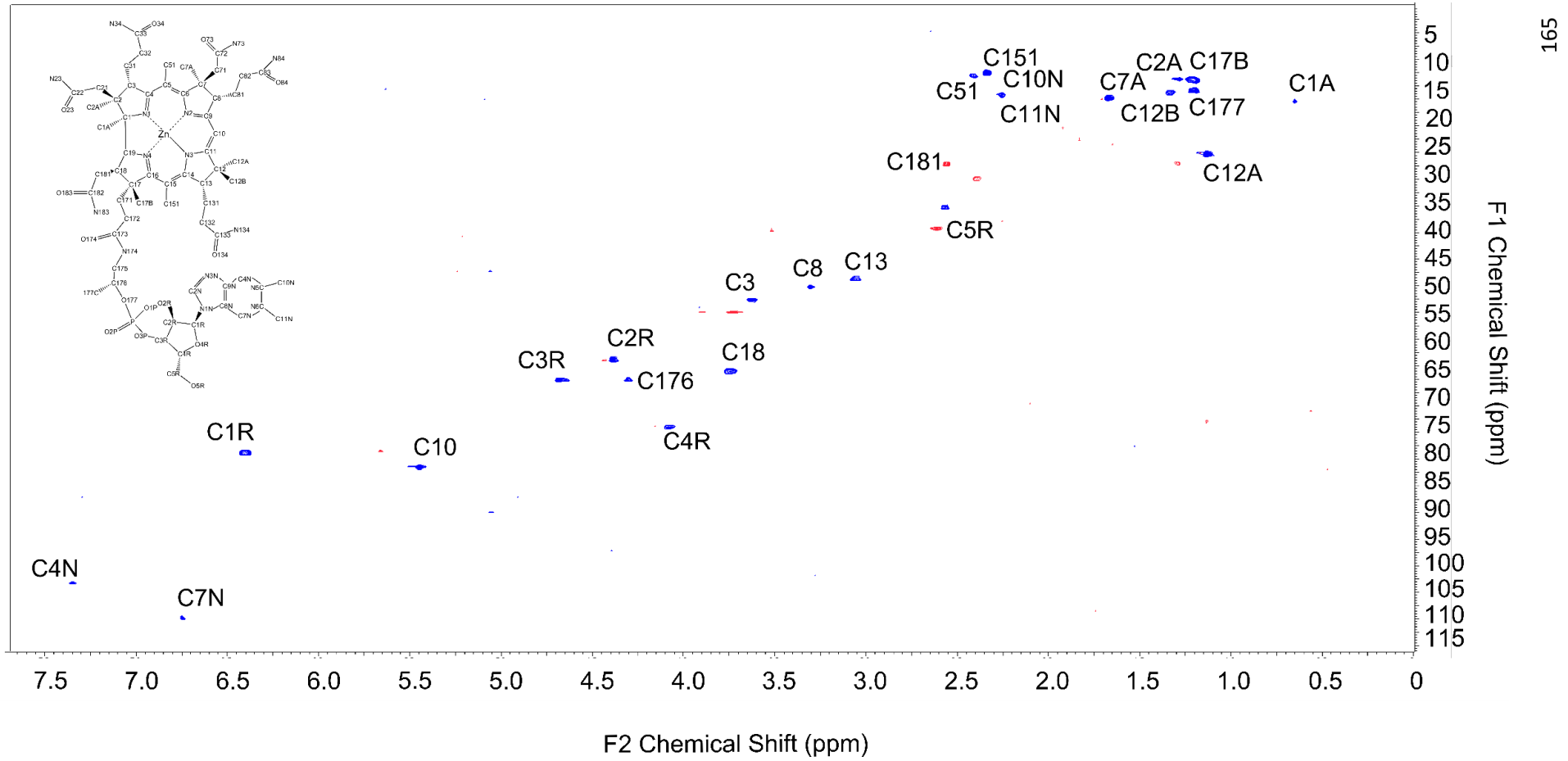

Figure 5:2:18: 2D ^{1}H ^{13}C HSQC allowing the chemical shifts for ^{13}C atoms attached to ^{1}H atoms to be determined.

5:2:9 biological activity of Zbl

The activity of Zbl as a B_{12} antagonist was investigated through the use of the plate bioassay used to investigate the activity of Hby and Zby. Here a reporter strain of *S. enterica* AR2680 *cysG, metE* was embedded in agar as described in Method 2:3:8. Growth of *S. enterica* in this bioassay is dependent on the cofactor activity of methyl cobalamin with the enzyme methionine synthase (MetH). This enzyme requires the methyl transferase activity of methyl cobalamin to generate methionine from homocysteine, as no other sources of methionine are available to *S. enterica* therefore the growth of *S. enterica* is dependent upon exogenous B_{12} or methionine (Raux et al 1996). The activity of B_{12} in methionine synthase is due to the carbon cobalt bond between the central cobalt ion of B_{12} and the attached methyl group (Banerjee et al 1990). As zinc should be unable to form the same metal-carbon bond it is predicted to be inactive as a cofactor for methionine synthase.

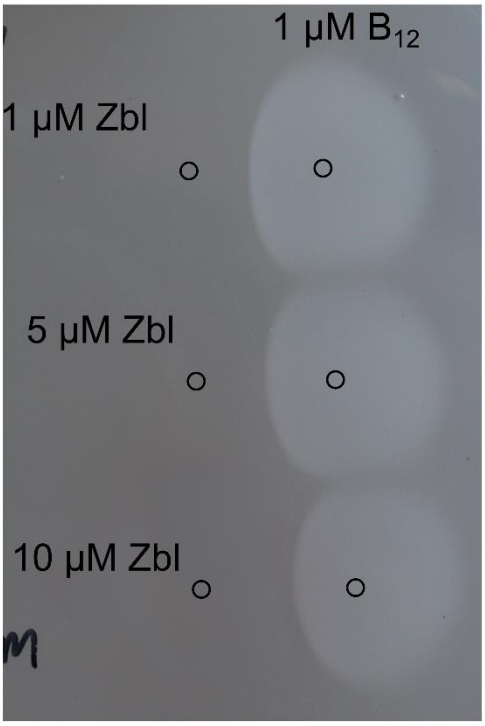

Figure 5:2:19: Bioassay investigating the effect of Zbl on B_{12} dependent S. enterica. Here 5 µL of a 1 µM solution of B_{12} was dropped adjacent to 5 µL of a Zbl solution at 1, 5 and 10 µM. The position of each drop is marked by a black circle.

Additon of Zbl alone shows that this molecule is unable to promote the growth of *S. enterica* dependent on exogenous B_{12}. Therefore, Zbl is unable to fulfil the same role as its cobalt containing counterpart in acting as a cofactor for methionine synthase. As with Zby and Hby, Zbl perturbs the B_{12} stimulated growth of *S. enterica.* The inhibiton is again at the interface of the B_{12} and Zbl drops and is concentration dependent with higher concentrations of Zbl exhibiting a greater inhibitory effect.

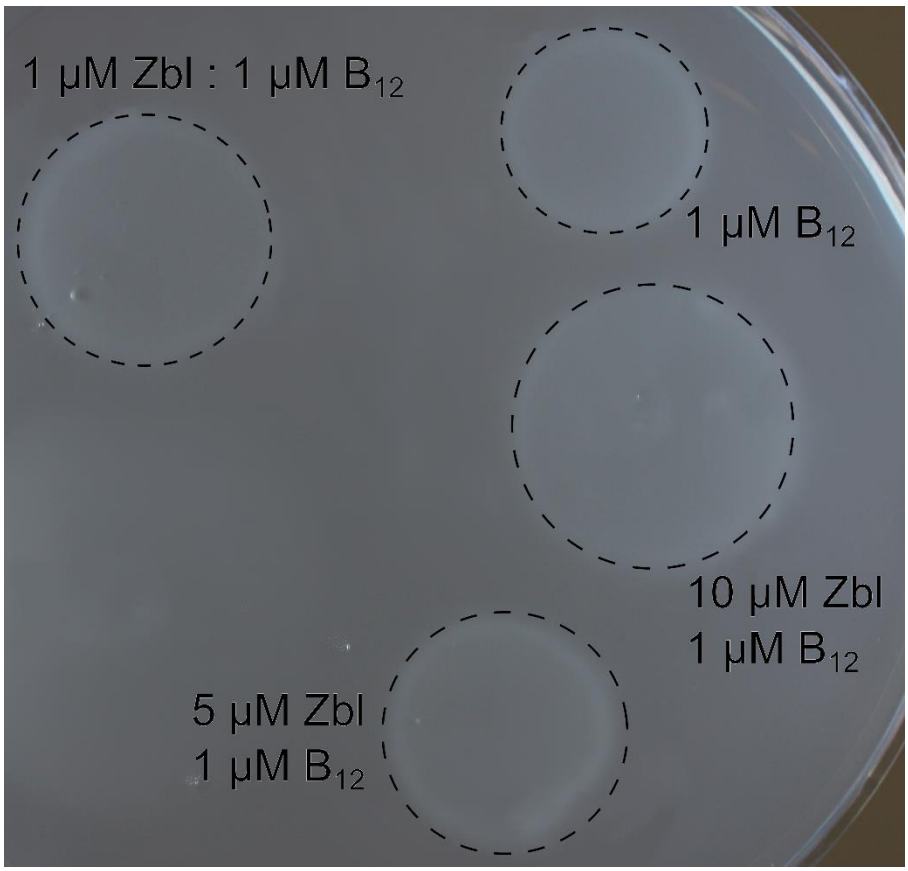

Figure 5:2:20: 5 µL of B_{12} at a concentration of 1 µM was dropped onto a bioassay plate. Adjacent to this 5 µL of Zbl was dropped at a concentration of 1, 5 or 10 µM.

Addition of Zbl in conjunction to a fixed amount of B_{12} results in circles of *S. enterica* growth with a larger diameter than that of the Cbl only control. Despite the larger diameter of growth circle the density of *S. enterica* is reduced comapred to the control spot. Previous work concerning rhodibalamin showed that the rhodium analogue of adenosyl-cobalamin exhibits a similar effect on the growth of *S. enterica* under similar conditions (Widner et al 2016).

5:2:10 synthesis of hydrogenobalamin

Previous work has proposed that sidechain *f* is thermodynamically the preferred positon for nucleotide loop attachment if the loop can coordinate a metal ion at the centre of the corrin ring prior to bond formation at sidechain *f* (Eschenmoser 1988). The role of the metal ion at the centre of Zby in improving the efficiency of the nucleotide loop coupling reaction was investigated by conducting the analogous reaction in a metal free system. In order to test this hypothesis the lower nucleotide loop was joined to sidechain *f* by carbodiimide coupling to form hydrogenobalamin (Figure 5:2:21).

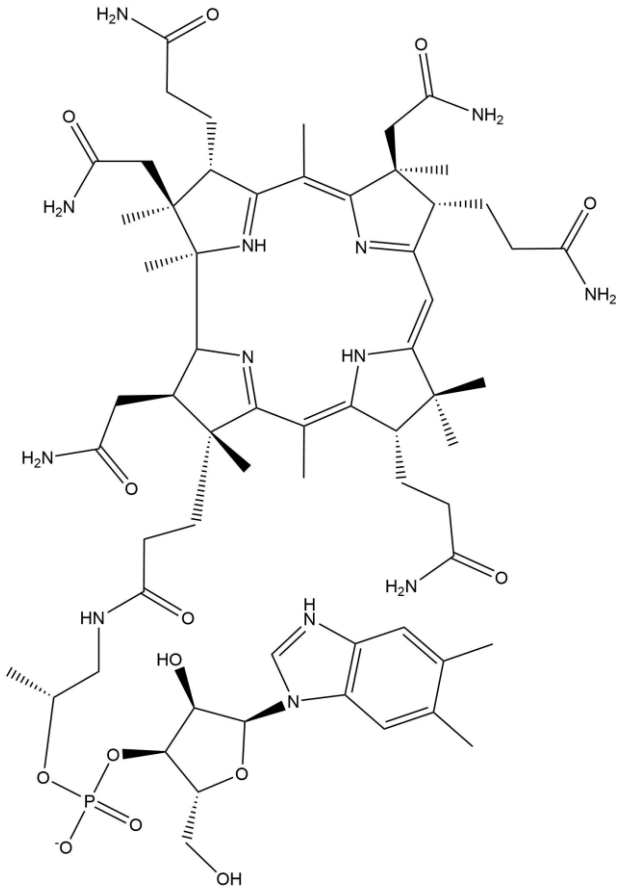

Figure 5:2:21: Proposed structure of hydrogenobalamin along with chemical formula and mass.

Hydrogenobyrinic acid (0.5 mg) was mixed with 0.26 mg (1.1 equivalents) of lower nucleotide loop along with 0.15 mg (2 equivalents) of hydroxybenzotriazol. The reactants were dissolved in 1 ml of H_2O and stirred at room temperature under an argon atmosphere. To this solution 1.03 mg (9.4 equivalents) of 1-ethyl-3-(3-dimethylaminopropyl) carbodiimide hydrochloride (EDC*HCl), dissolved in 500 µL H_2O. The two solutions were mixed under an argon atmosphere and allowed to react at room temperature. After 4 hours a sample of the reaction mixture was analysed by HPLC (Figure 5:2:22).

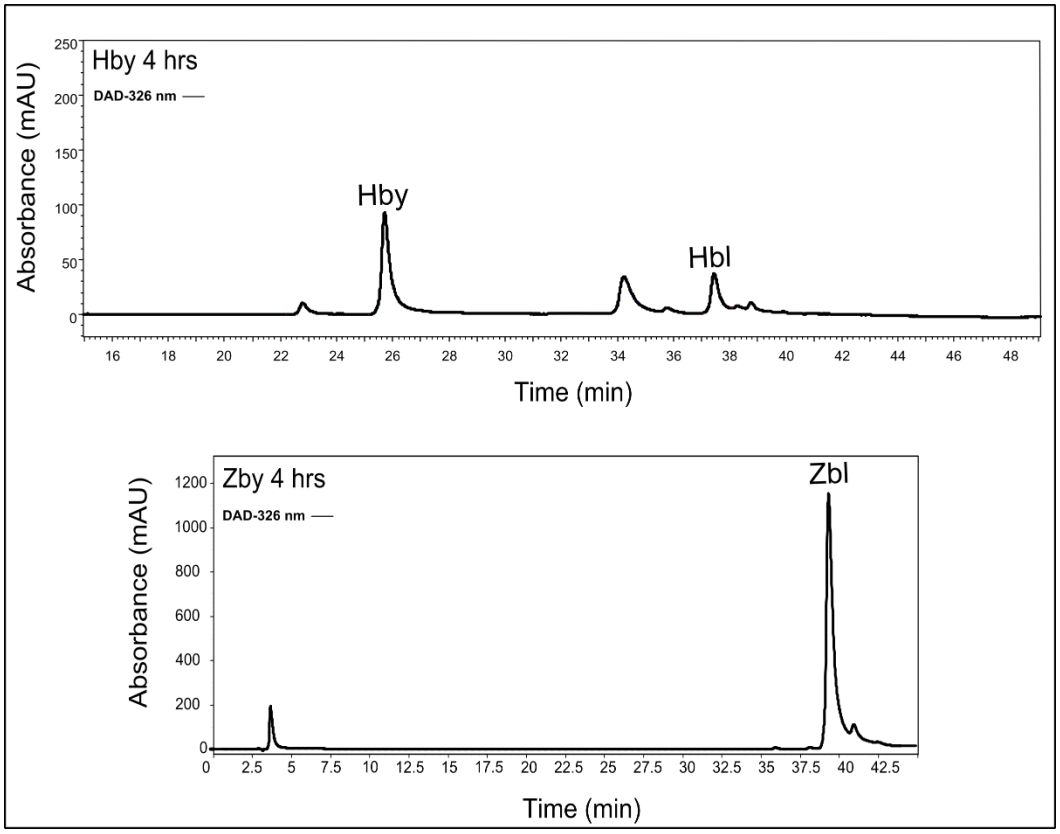

Figure 5:2:22: Comparison of the coupling reactions between Hby and the lower nucleotide loop after 4 hours (top) and coupling the lower nucleotide loop to Zby bottom.

HPLC analysis of the lower loop coupling reaction between Hby and the lower nucleotide loop shows that after 4 hours only 15 % of the material in the reaction mixture is hydrogenobalamin as determined by its retention time. A majority of the Hby present (51 %) remains unreacted. A third peak at 34.4 minutes probably corresponds to an intermediate of the coupling reaction. In contrast to this the analogous coupling reaction between Zby and the lower nucleotide loop is completed by this time as HPLC analysis of the reaction mixture shows a single peak corresponding to Zbl.

5:2:11 UV-vis and mass spectral analysis of Hbl

Hbl was isolated from the lower loop coupling reaction mixture by reverse phase chromatography. Purified Hbl was analysed by UV vis spectroscopy (Figure 5:2:23) and mass spectroscopy (Figure 5:2:24).

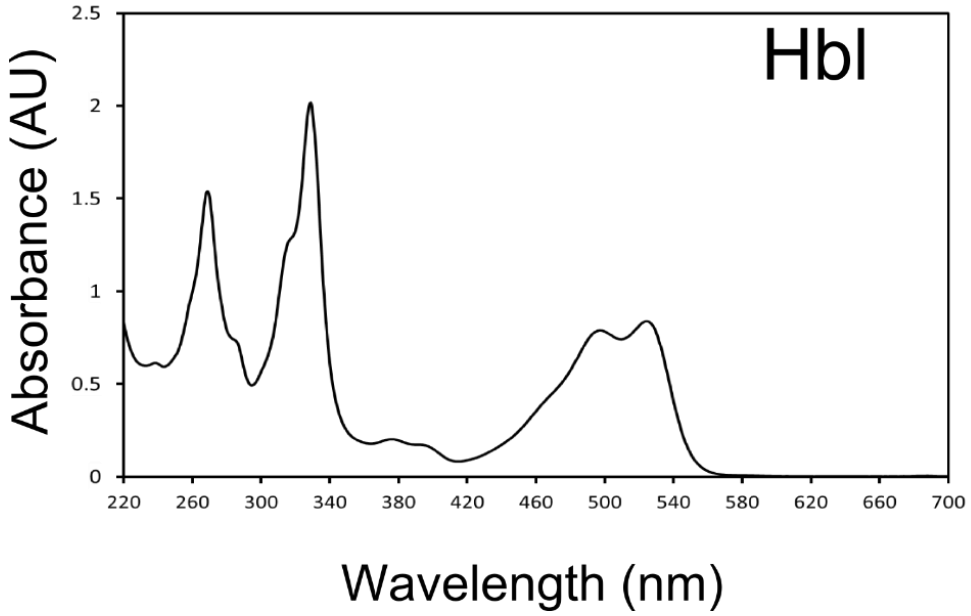

Figure 5:2:23: UV-vis spectrum of Hbl dissolved in H_2O. The spectrum was recorded in a quartz cuvette.

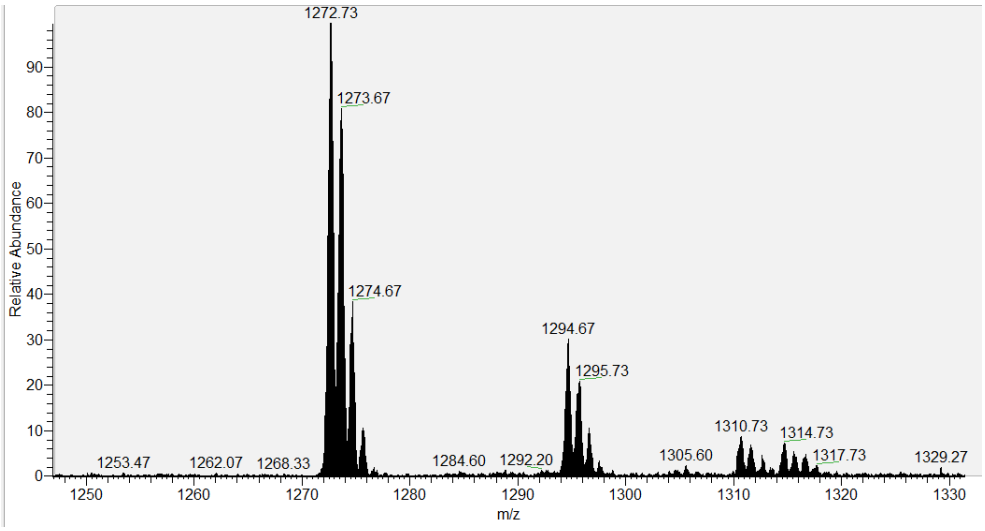

Figure 5:2:24: Mass spectrum of Hbl dissolved in methanol the pseudomolecular ion is present at 1272.73 m/z the sodium adduct at 1294.67 m/z

The UV-visible absorbance spectrum of Hbl shows strong similarity to the equivalent spectrum of Hby (Figure 4:2:16). The γ band of Hbl is at 329 nm whereas it is shifted slightly in Hby being present at 325 nm. The α and β bands of Hbl have maxima at 525 nm and 496 nm respectively. Again these bands are shifted relative to the spectrum of Hby where the α and β bands are present at 517 nm and 493 nm (Figure 4:2:16).

Mass spectral analysis of Hbl gives a pseudo-molecular ion at 1272.73. This mass is in keeping with the mass of the formula for Hbl proposed in Figure 5:2:21. Two higher mass species are also present corresponding to the sodium and potassium adducts of Hbl.

5:3:1 Discussion

Zbl was synthesised from Hby via the zinc containing intermediate Zby. Inserting zinc into the macrocycle of Hby was successful with yields of Zby approaching 95% after purification. Characterisation of Zby by UV-vis spectroscopy revealed that insertion of zinc into the macrocycle of Hby produces a compound with different spectral properties compared to the starting material. Changes in the UV-vis spectra of both Zby and Zbl relative to Hby and Hbl show that the presence of a zinc ion at the centre of the macrocycle of these compounds alters the π electrons that make up the chromophore producing a different spectrum.

NMR analysis of Zby shows that apart from the central zinc ion the other chemical features of this compound remain the same relative to Hby with no change in the amount and position of the ^{1}H atoms making up Zby. The chemical environment of some of these ^{1}H atoms is different resulting in different chemical shifts as detected by NMR spectroscopy. The main changes when comparing the chemical shifts of ^{1}H atoms of Hby and Zby occur at the C10 meso position as well as C19. These ^{1}H atoms are attached directly to the macrocycle and as such, feel acutely any changes in chemical environment as a result of zinc being present at the centre of the macrocycle.

While NMR data gives the position of each ^{1}H atom relative to one another it is unable to give the absolute structure of the molecule. In order to determine the absolute structure of Zby the compound was crystallised and the structure solved by X-ray diffraction. The crystal structure of Zby is shown in Figure 5:3:1 (Christoph Kieninger unpublished data).

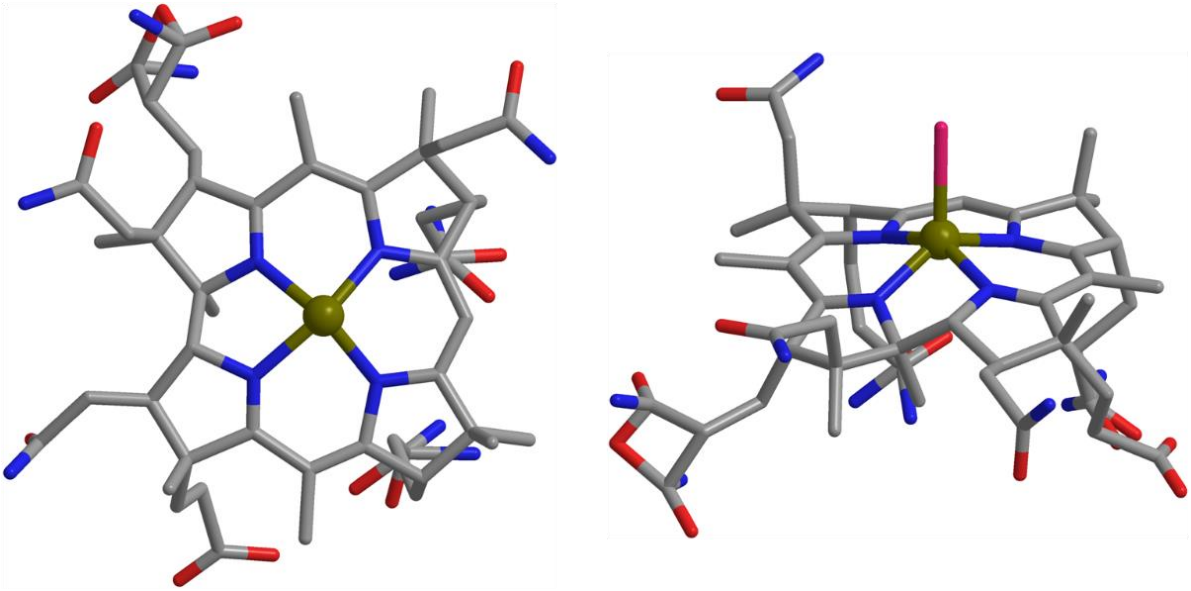

Figure 5:3:1: Crystal structure of Zby. The amide groups of sidechains b,d and e can adopt multiple conformations confusing their absolute positons in the crystal lattice. As the ionic radius of zinc is somewhat small than cobalt the corrin ring is distorted in order to provide the 4 pyrrole nitrogen atoms as ligands to chelate zinc.

The crystal structure of Zby shows a highly distorted corrin ring. The C1 carbon atom is pushed below the plane of the corrin macrocycle in order to position the pyrrole nitrogen atom of ring A in such a way that the zinc ion is co-ordinated. This distortion of the corrin ring is also seen in cobalt containing corrins as both Zn^{2+} and Co^{2+} ions have similar ionic radii. Recent work concerning the crystal structure of rhodibalamin suggests that Rh^{3+} is a better fit for the corrin macrocycle than Co^{3+} due to the larger radius of the rhodium ion. Rh^{3+} has a similar ionic radius to Co^{2+} it is therefore hypothesised that the corrin ring of B_{12} evolved to stabilise the transition between Co^{3+} – Co^{2+} – Co^{1+} ions. This cycling between cobalt species is important for the function of cobalamin as a cofactor (MetH).

In the presence of light Zby degrades to form yellow coloured compounds. The UV-vis spectrum of the yellow product of Zby is shown in Figure 5:2:9. This property of zinc containing corrins has been documented previously (Koppenhagen and Pfiffner 1970). The mechanism by which these molecules degrade remains unclear. The equivalent metal-free compounds Hby and Hbl are more stable in the presence of light, retaining the same UV-vis spectrum over time, although it is also possible for these compounds to form a lactam between C6 and sidechain *c* (Grüning et al 1985). Previous work concerning the yellow products of cobalt containing corrins demonstrated that a C6 lactam can be formed in this set of molecules (Bonnett 1963). The formation of yellow compounds in zinc containing corrins appears to be more rapid than the formation of yellow corrins when the corrin contains either cobalt or is metal free. This observation could implicate the zinc ion in the possible degradation pathway of Zby.

The yellow colour of the degraded product of Zby indicates a change in the conjugation of the macrocycle of Zby. It has been suggested that the acetamide sidechain *c* is the most predisposed to lactam formation at either C6 or C8. Formation of a bond between C8 and the nitrogen atom of sidechain *c* causes no disruption to the conjugated π system and results in no change to the UV-vis spectrum. In contrast formation of a lactam between C6 and sidechain *c* would result in disruption of the double bond predicted to be at this position and by extension alter the UV-vis spectrum of this new molecule. A similar lactam is found as a feature of the nickel containing isobacteriochlorin co-enzyme F430 (Figure 1:1:1), which is also bright yellow (Thauer 1998).

The synthesis of Zbl from Zby and free lower nucleotide loop was achieved with a yield of around 96 % Zbl after purification. The reaction required near stoichiometric amounts of the reagents with a slight excess of lower nucleotide loop (1.1 molar equivalents) being used. A comparison of the lower loop coupling reactions with Hbl and Zbl shows that the presence of zinc at the centre of the corrin macrocycle significantly improves the efficiency of the coupling reaction.

HPLC analysis of the two reaction mixtures after 4 hours shows that attachment of the lower nucleotide loop is complete after this time whereas a majority of the Hby present remains unreacted (Figure 5:2:22). It is predicted that the coupling reaction between Zby and lower nucleotide loop proceeds faster than the analogous reaction with Hby due to the co-ordination of the lower nucleotide loop. The pre-positioning of the loop in such way relative to sidechain *f* that the carbodiimide coupling of the two compounds is enhanced. Adapting this synthetic scheme for the production of additional metal analogues it would be important to select a metal ion that is capable of harbouring at least 5 ligands in solution in order to take advantage of this prepositioning to improve the efficiency of this reaction.

There is some variety in the structures of cobamides synthesised by bacteria and archaea. While the cobalt containing corrin system of these molecules remains the same the nature of the lower loop exhibits some variation between organisms (Stupperich et al 1990; Seth et al 2015). The synthesis of Zbl (Section 5:2:7) used a dimethyl benzimidazole containing lower nucleotide loop to produce the zinc analogue of B_{12}. DMB is the preferred lower nucleotide loop for humans as well as a number of enteric bacteria. The synthetic scheme used to synthesise Zbl could be adapted to allow for the attachment of alternative nucleotide loops. The synthesis of various α-ribonucleotides have been described previously (Chandra et al 2005, 2006, 2008) these synthetic schemes could be adapted to produce a number of naturally occurring and unnatural nucleotide loops. By producing metal analogues of B_{12} that contain the preferred lower nucleotide loop for certain subsets of bacteria (Kräutler et al 1988, Kräutler et al 2003, Stupperich et al 1988). These analogues can be specifically targeted towards certain bacteria selectively delivering a compound capable of disrupting B_{12} dependent metabolism in these organisms.

The central zinc ion of Zbl is expected to be pentacoordinate. Four of these ligands are provided by the pyrrole nitrogen atoms of the macrocycle (Huber et al 2008). The remaining fifth ligand in Zbl is expected to be provided by the DMB group of the lower nucleotide loop. NMR analysis of Zbl, in particular the ROESY

experiment shows, through space correlations between ^{1}H atoms of groups attached to the ring of Zbl interacting with ^{1}H atoms of the lower nucleotide loop. These through space correlations between the ^{1}H atoms of the α-facing methyl groups (C1A and C7A) with C2N and C10N of DMB support a base on conformation for Zbl at neutral pH (Figure 5:2:17).

Both Zby and Zbl inhibit the growth of B_{12} dependent *S. enterica* in solid culture. However, the growth phenotype when each zinc compound is mixed with B_{12} differs between the two. When Zby is mixed with B_{12} and dropped onto a bioassay plate the area of growth of *S. enterica* remains the same but the density of the areas of growth is reduced (Figure 5:2:8). In contrast when Zbl is mixed with B_{12} and dropped onto a bioassay plate the area of *S. enterica* growth increases but the density of the spots is reduced in comparison to a Cbl only control (Figure 5:2:19).

Zby and Zbl exhibit different growth phenotypes when these each of these compounds are mixed with a solution of B_{12} and applied to a *S. enterica* AR2680 *cysG, metE* bioassay plate (Figure 5:2:8, Figure 5:2:20).

When a mixture of B_{12} and Zbl was applied to a *S. enterica* bioassay plate the area of growth in Zbl treated areas was larger than that of the B_{12} only control area but with a reduced cell density. Previous work has shown that the rhodium analogue of $B_{12,}$ adenosyl-rhodibalamin has a similar effect on the growth of *S. enterica* under bioassay conditions (Widner et al 2016). The growth phenotype observed when *S. enterica* was exposed to adenosyl-rhodibalamin in conjunction with B_{12} was areas of growth with a diameter significantly larger than that of the control spots but with a lower density of bacteria. Comparison of the data presented in this paper with experimental data shown in Figure 5:2:20 shows that adenosyl-rhodibalamin has a similar effect on the growth of *S. enterica* as Zbl.

It was hypothesised by Widner et al that adenosyl-rhodibalamin was able to influence the expression of the B_{12} uptake protein BtuB by binding to a riboswitch element present upstream of the gene coding region of the mRNA. Riboswitch elements are found in a number of bacteria and act as a mechanism by which the presence of certain metabolites or other molecules can modulate the expression

of various proteins (Mandal et al 2004). The presence of adenosyl-cobalamin switches off the expression of BtuB once a certain threshold level of B_{12} is acquired by the cell. Therefore, the larger areas of growth with reduced density is due to adenosyl-rhodibalamin being taken up by *S. enterica* and switching off translation of BtuB. In so doing the cells take up less B_{12} resulting lower growth but allowing B_{12} to diffuse further across the plate.

It has been shown that adenosyl-cobalamin has the greatest inhibitory effect on expression of BtuB. While the ring portion is the main determinant for binding to the riboswitch element of BtuB both the lower nucleotide loop and upper adenosyl groups are important recognition elements (Gallo et al 2008). Zbl is lacking an upper adenosyl moiety but the presence of a lower nucleotide loop is probably what allows Zbl to interact with the riboswitch element of BtuB switching off expression as the growth phenotype of Zby and Hby are distinct from Zbl.

When supplemented with Zby the size of the B_{12} induced growth area of *S. enterica* stays somewhat constant but with reduced density (Figure 5:2:8). It is possible that Zby is able to compete with B_{12} for some aspect of the uptake system or is able to bind to the B_{12} dependent methionine synthase that *S. enterica* requires for growth under the bioassay conditions. The reduced growth of *S. enterica* without an increase in diameter of the area of growth may suggest that Zby is inhibiting the growth of *S. enterica* through interaction with MetH. The size of the growth area reflects the amount of B_{12} available to *S. enterica* a set distance away from the point of application of the B_{12} solution.

Therefore, in order to maintain the same area of growth the same amount of B_{12} needs to be sequestered by cells within that area. Sequestering of B_{12} prevents its diffusion further out over the plate. Due to the lower density of cells within the growth area of the Zby treated areas the amount of B_{12} per cell must be higher in order to maintain the same area of growth as the control.

3:11:4 Conclusions

Zby was synthesised by inserting zinc into the macrocycle of Hby, the reaction scheme based upon the previous synthesis of Zbl from Hbl allowed for the efficient conversion of Hby to Zby.

Zbl was synthesised from Zby and free lower nucleotide loop. Attachment of the lower nucleotide loop was enhanced by the presence of a central zinc ion presumably by pre-positioning of the lower nucleotide loop through co-ordination before formation of an amide bond between sidechain *f* and the lower nucleotide loop.

NMR and mass spec characterisation of these compounds confirmed that the structure of each is consistent with the predicted structures presented for each molecule (Figure 5:2:1, Figure 5:2:13).

Both Zby and Zbl failed to stimulate the growth of *S. enterica* under bioassay conditions when added to the plates alone. When these compounds were added to the plates in addition to B_{12} different growth phenotypes were observed. The observation of differing growth phenotypes indicates different modes of inhibition for the two zinc compounds.

It is predicted that Zbl acts as an inhibitor through interaction with the BtuB riboswitch preventing *S. enterica* from taking up sufficient B_{12} for optimal growth. Lower concentrations of B_{12} per cell allows the remaining B_{12} to diffuse further resulting in a larger area of growth with a lower density of bacteria.

Application of Zby in addition to B_{12} as part of the bioassay outlined in Figure 5:2:8, results in a growth phenotype whereby the area of growth is the same as that of a B_{12} only control with lower cell density. This indicates that Zby is having an effect upon the B_{12} metabolism of *S. enterica* independent of B_{12} uptake.

Chapter 6: Discussion

6:1 Conclusion

The biosynthesis of the main corrin component of B_{12} follows one of two well defined routes, typified by early or late cobalt insertion. As is the case with most biosynthetic pathways the intermediates involved are conserved between organisms capable of B_{12} biosynthesis. The conservation of B_{12} biosynthesis does not extend to that of the lower nucleotide loop as variation exists regarding the nature of this group (Kräutler et al 1988, Stupperich et al 1988). Different organisms display different preferences for the analogues of B_{12} that they will make and use. *Allochromatium vinosum* appears to be one of a few organisms that show some variation in the production of the core corrin ring component of B_{12}, specifically the production of a B_{12} analogue lacking a central cobalt atom (Toohey et al 1965).

Annotation of the *A. vinosum* genome shows that this organism harbours the genes required to form both an almost complete aerobic and anaerobic B_{12} biosynthetic pathway. Notably genes associated with cobalt insertion are missing, as are genes associated with adenosylation of the central cobalt ion of B_{12} intermediates. This organism is however, reported to produce Hbl the cobalt free analogue of B_{12}. The lack of crucial biosynthetic genes alongside any annotated B_{12} dependent enzymes therefore calls into question whether *A. vinosum* requires B_{12} and the possible function, if any of Hbl. *A. vinosum* is an anaerobic bacteria dependent upon photosynthesis in order to live (Kampf et al 1980). The presence of a B_{12} dependent enzyme involved in a crucial step of bacteriochlorophyll biosynthesis leads to the conclusion that *A. vinosum* either acquires B_{12} from the environment, calling into question the utility of an almost complete set of B_{12} biosynthetic genes or it is capable of B_{12} biosynthesis. Previous reports regarding the production of Hbl describe culturing *A. vinosum* in a growth media devoid of cobalt in order to stimulate the production of Hbl, these publications do not describe the production of cobalt containing corrins when cobalt is present.

Isolation of CobQ from *A. vinosum* and its subsequent incubation with glutamine, ATP and HBAd results in the generation of Hby, the cobalt free analogue of cobyric acid. The action of *A. vinosum* CobQ on HBAd represents an out of turn step when

compared to the aerobic biosynthesis of B_{12} in other organisms. The pathway in *R. capsulatus* and other organisms that follow the aerobic biosynthetic pathway for B_{12} amidation of sidechains *b, d, e* and *g* follows cobalt insertion and adenosylation. In the case of the *R. capsulatus* CobQ this enzyme will only act upon cobalt containing, adenosylated substrates.

A. vinosum CobQ is undoubtedly a useful tool for the synthesis of metal analogues of B_{12}. The substrate specificity of *A. vinousm* CobQ allows for the production of B_{12} analogues that cannot be stably adenosylated. Specific amidation of sidechains *b, d, e* and *g* while leaving sidechain *f* differentiated is technically one of the more challenging aspects of the synthesis of B_{12} analogues. While it would be possible to amidate these groups chemically the lack of specificity afforded by such an approach would result in a complex mixture of compounds with various patterns of amides requiring a complex chromatographic separation of the products. Instead, enzymatic conversion of HBAd to Hby results in the specific formation of the target compound. The chromatographic behaviour of the lesser amidated species produced as part of the *in vitro* conversion of HBAd to Hby indicates that amide groups are added in a specific order to HBAd. If the action of CobQ was random then it would be expected that a larger number of species could be detected by HPLC (Williams et al 2007).

The chemical properties of Hby make it ideal as a starting point for the synthesis of metal analogues of B_{12}. The production of Hby *in vivo* was explored as part of the effort to develop an efficient workflow for the production of mg amounts of Hby. To this end the plasmid pET3a-Hby was produced, containing all the genes necessary for the production of Hby. Expression of pET3a-Hby in *E. coli* BL21 (DE3)-plysS cells resulted in the formation of Hby. However, the majority of the Hby produced in this way was found in the growth media as opposed to the cell pellet as is the case for HBAd. Interestingly Hby is the only corrin compound found in the growth media of cells expressing pET3a-Hby. The lack of lesser amidated species within the growth media would suggest that Hby is being specifically transported out of the cell as compounds with fewer amide groups can be isolated

form the cell pellets of these cultures. The mechanism by which Hby export occurs is currently unknown as no system for B_{12} export has been described so far for any organism. There is, however, some evidence that B_{12} export exists as some algae and bacterial communities form symbiotic relationships based upon the sharing of a number of compounds including cobalamins (Croft et al 2005, Taga and Walker 2010).

As a proof of concept for the synthesis of a metal analogue of B_{12}, zinc was inserted into the macrocycle of Hby to form Zby. Zinc chelation was achieved in a single step by heating Hby with an excess of zinc acetate in aqueous solution under an argon atmosphere. The resulting compound, Zby, had chemical properties distinct from the starting material, most notably in the nature of the UV-vis spectrum of Zby relative to Hby. The largest changes in the UV-vis spectrum centre on a bathochromic shift of both the α and γ bands of Zby relative to Hby. This is coupled with the disappearance of two small maxima normally present in the UV-vis spectrum of Hby at 396 and 378 nm. Changes to the UV-vis spectrum reflect changes within the corrin macrocycle as the zinc ion influences the delocalised π electrons of the ring. Analysis of Zby by mass spectroscopy confirmed the presence of zinc within the macrocycle of this compound due to the unique distribution of isotopes. Zinc has a number of stable naturally occurring isotopes, the distribution of which is reflected in the isotopic distribution of Zby ions when analysed by mass spectroscopy.

Zby was expected to harbour many of the same physical properties as Hby. However, unexpectedly, the presence of a zinc ion at the centre of Zby results in the formation of a compound that is highly sensitive to visible light. Under conditions of direct illumination solutions of Zby degrade through formation of a yellow compound after a few hours. The same degradation occurs with Hby but over an extended time scale taking days for the same transformation to occur.

The synthetic steps required for the production of Zbl from HBAd can potentially be completed in any order regarding the timing of metal insertion relative to lower loop attachment. While the synthesis of Hbl from Hby shows that it is

possible to attach the lower nucleotide prior to insertion of a central metal ion, this step is far less effective than the analogous reaction with a metal containing corrin. The presence of a metal ion at the centre of the corrin macrocycle enhances the attachment of the lower nucleotide loop through co-ordination of the lower nucleotide loop prior to bond formation with sidechain *f*. Interestingly, nature makes no use of the pre-positioning of the nucleotide and instead relies upon attachment of the lower nucleotide loop in a piecemeal fashion with the components spatially arranged via binding to biosynthetic enzymes (Blanche et al 1995).

In order to support the theory that the presence of a metal ion at the centre of Zby would enhance the nucleotide loop attachment reaction, the co-ordination of the zinc ion of Zby by an analogue of DMB was investigated. Here N-methylimidazole was added to a solution of Zby and changes to the absorption spectrum measured. Changes to the UV-vis spectrum of Zby under increasing concentrations of N-methylimidazole indicates that zinc is co-ordinated by N-methylimidazole. Changes to the UV-vis spectrum of Zby in the presence of N-methylimidazole can be detected due to the intimate relationship between the central zinc ion and delocalised electrons surrounding the corrin ring. Changes in the outer electrons of zinc through co-ordination of a ligand are "reported" back to the π electrons of the corrin ring therefore altering the UV-vis spectrum of the compound (Butler et al 2005).

All of the intermediates produced *en-rotue* to Zbl were analysed by NMR spectroscopy. Initial spectra were collected when Hby was dissolved in D_2O and were sufficient to assign the core structure of the compound. As the ^1H atoms of the amide groups are solvent exchangeable experiments conducted in D_2O could not provide any information about the position of the amide groups. In order to define the positon of these groups further experiments were conducted in 90 % H_2O, 10 % D_2O. These spectra confirmed the presence of amide groups at sidechains *a, b, c, d, e,* and *g*, with no amide group present at sidechain *f*. Assignment of the positions of the amide groups and the position of ^1H atoms attached to the macrocycle, peripheral methyl group and sidechains of Hby

allowed the proposed structure of this compound to be validated. Spectra for Zby and Zbl were collected in D_2O only as the amide sidechains were expected to remain unchanged relative to Hby, apart from sidechain *f* of Zbl which is the site for lower loop attachment. The chemical shifts of some of the ^1H atoms attached directly to the macrocycle of Zby and Zbl are shifted relative to Hby. Incorporation of zinc into the corrin ring of Hby results in a shift for the ^1H atom attached to C3 to a higher field positon (3.49 ppm Hby, 3.56 ppm Zby) this shift indicates that the ^1H atom at C3 of Zby is de-shielded relative to Hby. The remaining macrocycle attached ^1H atoms are shifted to a low field positon in the ^1H spectrum of Zby relative to Hby. These shifts indicate a greater degree of electron density in the vicinity of these atoms as a result of the centrally chelated zinc ion. Attachment of the lower nucleotide loop to Zby results in some additional changes to the chemical shifts of macrocycle attached ^1H atoms. The biggest changes are the high field shift for signals associated with ^1H atoms attached to C3 and C18 relative to Zby. Zbl C3 has a chemical shift of 3.61 ppm whereas the same ^1H atom of Zby has a chemical shift of 3.56 ppm. Zbl C18 has a chemical shift of 3.8 ppm whereas Zby C18 has a chemical shift of 2.73 ppm.

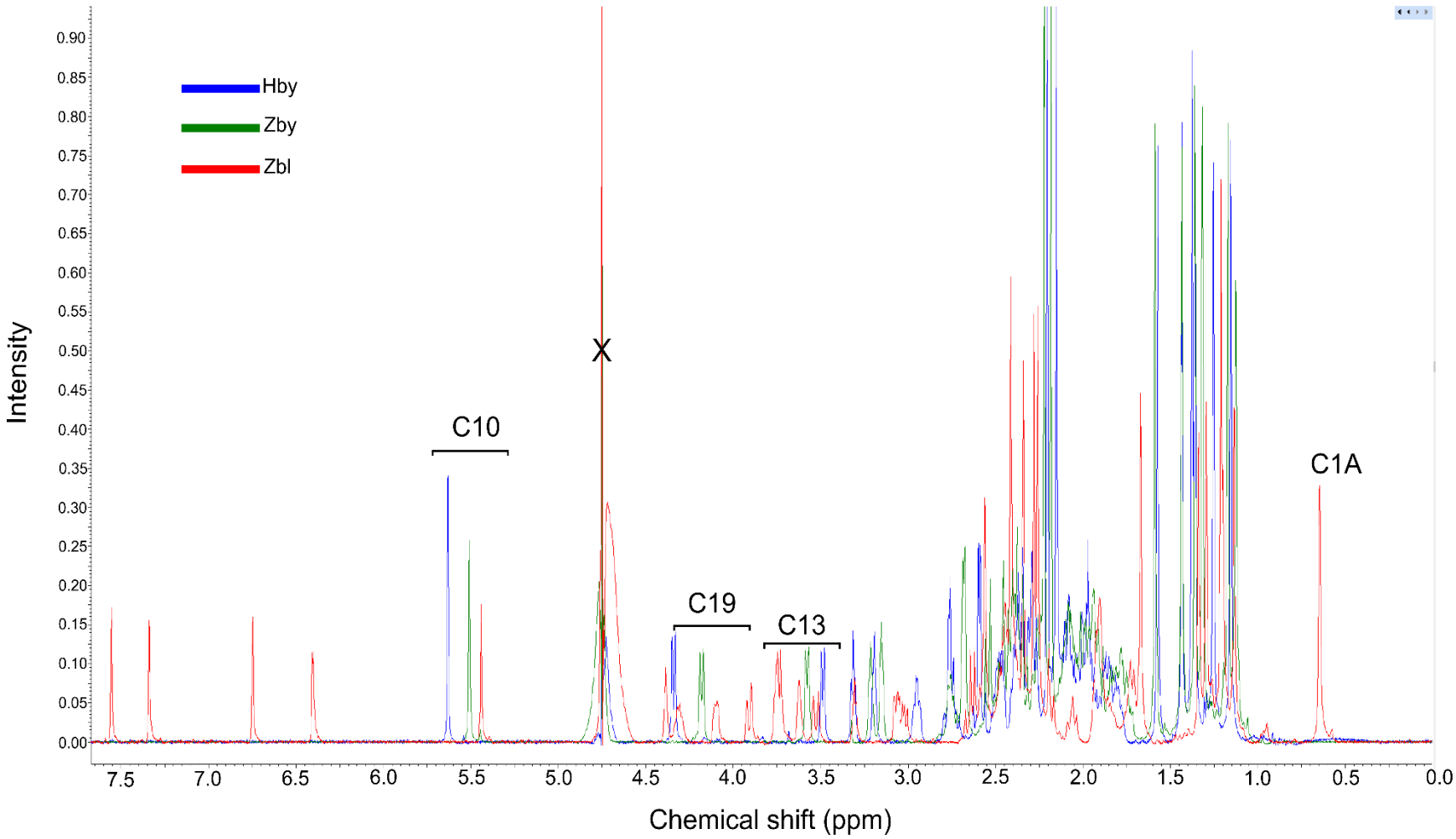

Figure 6:1:1: Overlay of Hby, Zby and Zbl 1D ^{1}H NMR spectra. Generally the signals associated with the corrin attached methyl groups cluster together apart from the C1A methyl group of Zbl. The largest differences in the chemical shifts between compounds can be seen in ^{1}H atoms attached directly to the corrin ring.

The greatest difference in chemical shifts between the ^{1}H spectra of Zby and Zbl is seen at C18 where the signal for the ^{1}H atom at this position is shifted to a low field positon. It has been suggested that the electron withdrawing properties of the lower nucleotide loop is responsible for this shift. The crystal structure of Zby (Figure 5:3:1) shows that C18 is bent down towards the α face of the molecule. This ruffling is expected to remain after attachment of the lower nucleotide loop bringing C18 and its attached ^{1}H group close to the nucleotide portion of the lower loop. The proximity to DMB may therefore be sufficient to explain the shift of the ^{1}H signal at C18 (Bax et al 1987).

Hby, Zby and Zbl were tested for biological activity against a B_{12} dependent strain of *S. enterica*. Due to the metabolic cost of producing cobalamins many organisms import intermediates of B_{12} biosynthesis even if they are capable for its *de-novo* biosynthesis (Woodson and Escalante-Semerena 2003). The earliest intermediate taken up in this way is cobyric acid. As Hby and Zby are the metal free and zinc containing analogues of cobyric acid they would also be expected to be taken up by *S. enterica*. Zbl is the zinc analogue of cobalamin and should therefore be taken up via the same pathway as B_{12}. Supplementation of *S. enterica* with either Zbl, Zby or Hby alone results in no growth of *S. enterica* growth demonstrating that all of these compounds are unable to fulfil the role of methylcobalamin in *S. enterica* MetH or are not converted to a compound that can replace methylcobalamin.

When these compounds are supplied to *S. enterica* in conjunction with B_{12} they perturb the stimulatory effect B_{12} exerts, reducing *S. enterica* growth. Addition of Zbl in conjunction with B_{12} results in the area of *S. enterica* growth increasing relative to a B_{12} only control but having a lower cell density. A similar phenotype has been observed when the same bioassay system was exposed to adenosylrhodibalamin in conjunction with B_{12} (Widner et al 2016). It was postulated that adenosylrhodibalamin is able to interact with the B_{12} dependent riboswitch that controls expression of BtuB, a key component of the B_{12} uptake machinery in a number of organisms. It is possible that Zbl is able to interact and with and ultimately supress the expression of BtuB in a similar fashion to adenosylrhodibalamin as indicated by similarities in the growth phenotype

exerted by these two compounds (Widner et al 2016). Previous work has shown that the BtuB riboswitch from *E. coli* has a preference for adenosylated compounds but is still able to bind non-adenosylated compounds provided the lower nucleotide loop is present (Gallo et al 2008). Neither Zby nor Hby are predicted to interact with the BtuB riboswitch due to the lack of a lower nucleotide loop and would be expected to exhibit a growth phenotype distinct from Zbl and adenosylrhodibalamin if this was the case.

When *S. enterica* is supplemented with either Hby or Zby in addition to B_{12} the growth of the organism is diminished relative to a B_{12} only control. The growth phenotype exhibited by these compounds is distinct from Zbl and adenosylrhodibalamin as the diameter of the area of growth remains then same or is reduced at higher Hby or Zby concentrations. It is likely that the mode of inhibition for these compounds is through competition with B_{12} for MetH binding and not through interaction with the BtuB riboswitch.

The ubiquitous nature of carbodiimide coupling chemistry as a result of its use in peptide synthesis means that functional groups can be attached to either free amino or carboxylic acids containing compounds such as analogues of cobyric acid. These groups could range from fluorescent compounds to analogues of the lower nucleotide loop. Modification of Hby or a metal analogue of Hby through attachment of groups to sidechain *f* could potentially be used as a method to bring compounds into bacterial cells. Previous work has detailed how B_{12} can be used as a "Trojan horse" to smuggle cytotoxic or antibiotic compounds into cells. Previous approaches for the synthesis of this class of compound have focused on attachment of groups to the central cobalt ion, the ribose moiety of the lower nucleotide loop or by direct attachment to the peripheral sidechains (Gruber et al 2011, Kunze et al 2004, Petrus et al 2009). Each of these approaches is potentially hampered by B_{12} uptake as the uptake of B_{12} is tightly controlled through translation level control of the expression of the BtuB, BtuC, BtuD import system. Once a certain threshold level of B_{12} is reached expression of these elements is switched off and further B_{12} uptake is no longer possible. This B_{12} sensor therefore limits how much B_{12} and by extension B_{12} analogue can be taken up by individual

cells. This may be problematic if the threshold for the activity of the attached group is higher than the intracellular concentration of B_{12} it is possible to achieve. Cobyric acid is unable to actuate the BtuB riboswitch of *E. coli* but is still taken up by this organism (Gallo et al 2008). Analogues of cobyric acid prepared form Hby could therefore be used to import compounds of interest into cells at a higher concentration compared to conjugation to B_{12}.

This work has outlined a synthetic scheme for the synthesis of zincobalamin. The modular nature of the steps should allow for the adaptation of this scheme to produce a number of metal analogues of B_{12}. The most important considerations when adapting this synthesis concern the co-ordination chemistry of the metal ion to be inserted. It would be preferable to select a metal ion that is able to co-ordinate at least 5 ligands in order to take advantage of the enhancement of lower loop attachment by pre-positioning nucleotide.

It has been demonstrated in this work and within the literature that metal analogues of B_{12} are able to interfere with B_{12} dependent processes within bacterial cells. Due to the role methylcobalamin plays in the recycling of tetrahydrofolate and the synthesis of purine nucleotides rapidly dividing cells have a high requirement for B_{12}. Metal analogues of B_{12} may therefore disrupt the B_{12} dependent metabolism of these cells. Through production of metal analogues of B_{12} it should be possible to produce a number of compounds and screen for enhanced anti-microbial or anti-cancer activity. Metal analogues of B_{12} may also be used to investigate the B_{12} metabolism of various organisms as they are able to induce a B_{12} deficient state through competitive uptake and binding to B_{12} dependent enzymes *in vivo*. The evolutionary rational behind natures selection of cobalt for the centre of cobalamin may also be investigated through the synthesis and characterisation of a number of metal analogues.

References

Allen, S.H.G., Kellermeyer, R.W., Stjernholm, R.L. and Wood, H.G., 1964. Purification and properties of enzymes involved in the propionic acid fermentation. Journal of Bacteriology, 87(1), pp.171-187.

Allen, R.H., Stabler, S.P., Savage, D.G. and Lindenbaum, J., 1993. Metabolic abnormalities in cobalamin (vitamin B12) and folate deficiency. The FASEB journal, 7(14), pp.1344-1353.

Armstrong, G.A., 1997. Genetics of eubacterial carotenoid biosynthesis: a colorful tale. Annual Reviews in Microbiology, 51(1), pp.629-659.

Bali, S., Palmer, D.J., Schroeder, S., Ferguson, S.J. and Warren, M.J., 2014. Recent advances in the biosynthesis of modified tetrapyrroles: the discovery of an alternative pathway for the formation of heme and heme d1. Cellular and molecular life sciences, 71(15), pp.2837-2863.

Banerjee, R.V. and Matthews, R.G., 1990. Cobalamin-dependent methionine synthase. The FASEB journal, 4(5), pp.1450-1459.

Banerjee, R., 2003. Radical carbon skeleton rearrangements: catalysis by coenzyme B12-dependent mutases. Chemical Reviews, 103(6), pp.2083-2094.

Banerjee, R. and Ragsdale, S.W., 2003. The many faces of vitamin B12: catalysis by cobalamin-dependent enzymes. Annual review of biochemistry, 72(1), pp.209-247.

Bauerle, M.R., Schwalm, E.L. and Booker, S.J., 2015. Mechanistic diversity of radical S-adenosylmethionine (SAM)-dependent methylation. Journal of Biological Chemistry, 290(7), pp.3995-4002.

Battersby, A. R. "Tetrapyrroles: the pigments of life." Natural product reports 17, no. 6 (2000): 507-526.

Bax, A., Marzilli, L.G. and Summers, M.F., 1987. New insights into the solution behavior of cobalamins. Studies of the base-off form of coenzyme B12 using modern two-dimensional NMR methods. Journal of the American Chemical Society, 109(2), pp.566-574.

Battersby, A.R., 1993. Biosynthesis of vitamin B12. Accounts of chemical research, 26(1), pp.15-21.

Beale, S.I., 1970. The biosynthesis of δ-aminolevulinic acid in Chlorella. Plant physiology, 45(4), pp.504-506.

Bieganowski, R. and Friedrich, W., 1979. Preparation and some properties of ferribalamin, the Fe (III)-analogue of vitamin B12. FEBS letters, 97(2), pp.325-326.

1) Blanche, F., Couder, M., Debussche, L., Thibaut, D., Cameron, B. and Crouzet, J., 1991. Biosynthesis of vitamin B12: stepwise amidation of carboxyl groups b, d, e, and g of cobyrinic acid a, c-diamide is catalyzed by one enzyme in Pseudomonas denitrificans. Journal of bacteriology, 173(19), pp.6046-6051.

2) Blanche, F., Debussche, L., Famechon, A., Thibaut, D., Cameron, B. and Crouzet, J., 1991. A bifunctional protein from Pseudomonas denitrificans carries cobinamide kinase and cobinamide phosphate guanylyltransferase activities. Journal of bacteriology, 173(19), pp.6052-6057.

3) Blanche, F., Robin, C., Couder, M., Faucher, D., Cauchois, L., Cameron, B. and Crouzet, J., 1991. Purification, characterization, and molecular cloning of S-adenosyl-L-methionine: uroporphyrinogen III methyltransferase from Methanobacterium ivanovii. Journal of bacteriology, 173(15), pp.4637-4645.

1) Blanche, F., Famechon, A., Thibaut, D., Debussche, L., Cameron, B. and Crouzet, J., 1992. Biosynthesis of vitamin B12 in Pseudomonas denitrificans: the biosynthetic sequence from precorrin-6y to precorrin-8x is catalyzed by the cobL gene product. Journal of bacteriology, 174(3), pp.1050-1052.

2) Blanche, F., Thibaut, D., Famechon, A., Debussche, L., Cameron, B. and Crouzet, J., 1992. Precorrin-6x reductase from Pseudomonas denitrificans: purification and characterization of the enzyme and identification of the structural gene. Journal of bacteriology, 174(3), pp.1036-1042.

Blanche, F., Cameron, B., Crouzet, J., Debussche, L., Thibaut, D., Vuilhorgne, M., Leeper, F.J. and Battersby, A.R., 1995. Vitamin B12: how the problem of its biosynthesis was solved. Angewandte Chemie International Edition, 34(4), pp.383-411.

Blanche, F., Cameron, B., Crouzet, J., Debussche, L., Thibaut, D. and Remy, E., Aventis Pharma SA, 2000. Biosynthesis method enabling the preparation of cobalamins. U.S. Patent 6,156,545.

Bobik, T.A., Ailion, M. and Roth, J.R., 1992. A single regulatory gene integrates control of vitamin B12 synthesis and propanediol degradation. Journal of bacteriology, 174(7), pp.2253-2266.

Bonnett, R., 1963. The Chemistry of the Vitamin B12 Group. Chemical Reviews, 63(6), pp.573-605.

Borths, E.L., Poolman, B., Hvorup, R.N., Locher, K.P. and Rees, D.C., 2005. In vitro functional characterization of BtuCD-F, the Escherichia coli ABC transporter for vitamin B12 uptake. Biochemistry, 44(49), pp.16301-16309.

Brenner, D.J., Krieg, N.R., Staley, J.T. and Garrity, G.M., 2005. The Proteobacteria, Bergey's manual of systematic bacteriology.

Bridwell-Rabb, J., Zhong, A., Sun, H.G., Drennan, C.L. and Liu, H.W., 2017. A B12-dependent radical SAM enzyme involved in oxetanocin A biosynthesis. Nature, 544(7650), pp.322-326.

Brindley, A.A., Raux, E., Leech, H.K., Schubert, H.L. and Warren, M.J., 2003. A story of chelatase evolution identificantion and characterisation of a small 13–15-kDa "ancestral" cobaltochelatase (CbiXS) in the archaea. Journal of Biological Chemistry, 278(25), pp.22388-22395.

Brink, N.G. and Folkers, K., 1949. Vitamin B12. VI. 5, 6-Dimethylbenzimidazole, a degradation product of vitamin B12. Journal of the American Chemical Society, 71(8), pp.2951-2951.

Broderick, J.B., Duffus, B.R., Duschene, K.S. and Shepard, E.M., 2014. Radical S-adenosylmethionine enzymes. Chemical reviews, 114(8), pp.4229-4317.

Burgess, J. and Prince, R. H. 2006. Zinc: Inorganic & Coordination Chemistry. Encyclopedia of Inorganic Chemistry.

Butler, P., Ebert, M.O., Lyskowski, A., Gruber, K., Kratky, C. and Kräutler, B., 2006. Vitamin B12: a methyl group without a job. Angewandte Chemie International Edition, 45(6), pp.989-993.

Cadieux, N., Bradbeer, C., Reeger-Schneider, E., Köster, W., Mohanty, A.K., Wiener, M.C. and Kadner, R.J., 2002. Identification of the periplasmic cobalamin-binding protein BtuF of Escherichia coli. Journal of bacteriology, 184(3), pp.706-717.

Cameron, B., Blanche, F., Rouyez, M.C., Bisch, D., Famechon, A., Couder, M., Cauchois, L., Thibaut, D., Debussche, L. and Crouzet, J., 1991. Genetic analysis, nucleotide sequence, and products of two Pseudomonas denitrificans cob genes encoding nicotinate-nucleotide: dimethylbenzimidazole phosphoribosyltransferase and cobalamin (5'-phosphate) synthase. Journal of bacteriology, 173(19), pp.6066-6073.

Carmel, R. and Koppenhagen, V.B., 1977. The effect of rhodium and copper analogs of cobalamin on human cells in vitro. Archives of biochemistry and biophysics, 184(1), pp.135-140.

Chandra, T. and Brown, K.L., 2005. Direct glycosylation: Synthesis of a-indoline ribonucleosides. Tetrahedron letters, 46(12), pp.2071-2074.

Chandra, T., Zou, X., Valente, E.J. and Brown, K.L., 2006. Regio-and stereoselective glycosylation: synthesis of 5-haloimidazole a-ribonucleosides. The Journal of organic chemistry, 71(13), pp.5000-5003.

Chandra, T. and Brown, K.L., 2008. Vitamin B 12 and a-ribonucleosides. Tetrahedron, 64(1), pp.9-38.

Charlton, J.C. and Hamilton, A.L., GE Healthcare Ltd, 1979. Vitamin B-12 cobalt-57 and process. U.S. Patent 4,133,951.

Cheng, Z., Li, K., Hammad, L.A., Karty, J.A. and Bauer, C.E., 2014. Vitamin B12 regulates photosystem gene expression via the CrtJ antirepressor AerR in Rhodobacter capsulatus. Molecular microbiology, 91(4), pp.649-664.

Croft, M.T., Lawrence, A.D., Raux-Deery, E., Warren, M.J. and Smith, A.G., 2005. Algae acquire vitamin B 12 through a symbiotic relationship with bacteria. Nature, 438(7064), p.90.

Crouzet, J., Cameron, B., Cauchois, L., Rigault, S., Rouyez, M.C., Blanche, F., Thibaut, D. and Debussche, L., 1990. Genetic and sequence analysis of an 8.7-kilobase Pseudomonas denitrificans fragment carrying eight genes involved in transformation of precorrin-2 to cobyrinic acid. Journal of bacteriology, 172(10), pp.5980-5990.

Debussche, L., Thibaut, D., Cameron, B., Crouzet, J. and Blanche, F., 1990. Purification and characterization of cobyrinic acid a, c-diamide synthase from *Pseudomonas denitrificans*. Journal of bacteriology, 172(11), pp.6239-6244.

Debussche, L., Couder, M., Thibaut, D., Cameron, B., Crouzet, J. and Blanche, F., 1991. Purification and partial characterization of Cob (I) alamin adenosyltransferase from *Pseudomonas denitrificans*. Journal of bacteriology, 173(19), pp.6300-6302.

Debussche, L., M. Couder, D. Thibaut, B. Cameron, J. Crouzet, and F. Blanche. "Assay, purification, and characterization of cobaltochelatase, a unique complex enzyme catalyzing cobalt insertion in hydrogenobyrinic acid a, c-diamide during coenzyme B12

biosynthesis in *Pseudomonas denitrificans*." Journal of bacteriology 174, no. 22 (1992): 7445-7451.

Deery, E., Schroeder, S., Lawrence, A.D., Taylor, S.L., Seyedarabi, A., Waterman, J., Wilson, K.S., Brown, D., Geeves, M.A., Howard, M.J. and Pickersgill, R.W., 2012. An enzyme-trap approach allows isolation of intermediates in cobalamin biosynthesis. Nature chemical biology, 8(11), pp.933-940.

Drennan, C.L., Matthews, R.G. and Ludwig, M.L., 1994. Cobalamin-dependent methionine synthase: the structure of a methylcobalamin-binding fragment and implications for other B 12-dependent enzymes. Current opinion in structural biology, 4(6), pp.919-929.

Dresow, B., Schlingmann, G., Ernst, L. and Koppenhagen, V.B., 1980. Extracellular metal-free corrinoids from Rhodopseudomonas spheroides. Journal of Biological Chemistry, 255(16), pp.7637-7644.

Elsenhans, B. and Rosenberg, I.H., 1984. Influence of metal substitution on vitamin B12 binding to human intrinsic factor and transcobalamins I and II. Biochemistry, 23(5), pp.805-808.

Escalante-Semerena, J.C., Suh, S.J. and Roth, J.R., 1990. cobA function is required for both de novo cobalamin biosynthesis and assimilation of exogenous corrinoids in Salmonella typhimurium. Journal of bacteriology, 172(1), pp.273-280.

Escalante-Semerena, J.C., 2007. Conversion of cobinamide into adenosylcobamide in bacteria and archaea. Journal of bacteriology, 189(13), pp.4555-4560.

Eschenmoser, A., 1988. Vitamin B12: experiments concerning the origin of its molecular structure. Angewandte Chemie International Edition, 27(1), pp.5-39.

Eschenmoser, A., 2011. Etiology of potentially primordial biomolecular structures: from vitamin B12 to the nucleic acids and an inquiry into the chemistry of life's origin: a retrospective. Angewandte Chemie International Edition, 50(52), pp.12412-12472.

Fan, C. and Bobik, T.A., 2008. The PduX enzyme of Salmonella enterica is an L-threonine kinase used for coenzyme B12 synthesis. Journal of Biological Chemistry, 283(17), pp.11322-11329.

Fiedor, L., Kania, A., Myśliwa-Kurdziel, B., Orzeł, Ł. and Stochel, G., 2008. Understanding chlorophylls: central magnesium ion and phytyl as structural determinants. Biochimica et Biophysica Acta (BBA)-Bioenergetics, 1777(12), pp.1491-1500.

Finke, R.G. and Hay, B.P., 1984. Thermolysis of adenosylcobalamin: a product, kinetic, and cobalt-carbon (C5') bond dissociation energy study. Inorganic Chemistry, 23(20), pp.3041-3043.

Fischer, H., 1937. Chlorophyll. Chemical Reviews, 20(1), pp.41-68.

Fontecave, M., Mulliez, E. and Logan, D.T., 2002. Deoxyribonucleotide synthesis in anaerobic microorganisms: the class III ribonucleotide reductase. Progress in nucleic acid research and molecular biology, 72, pp.95-127.

Frank, S., Deery, E., Brindley, A.A., Leech, H.K., Lawrence, A., Heathcote, P., Schubert, H.L., Brocklehurst, K., Rigby, S.E., Warren, M.J. and Pickersgill, R.W., 2007. Elucidation of Substrate Specificity in the Cobalamin (Vitamin B12) Biosynthetic Methyltransferases structure and function of the C20 methyltransferase (CbiL) from *Methanothermobacter thermautotrophicus*. Journal of Biological Chemistry, 282(33), pp.23957-23969.

Fresquet, V., Williams, L. and Raushel, F.M., 2004. Mechanism of cobyrinic acid *a, c*-diamide synthetase from *Salmonella typhimurium* LT2. Biochemistry, 43(33), pp.10619-10627.

Frey, P.A., 2001. Radical mechanisms of enzymatic catalysis. Annual review of biochemistry, 70(1), pp.121-148.

Fukuzaki, S., Nishio, N. and Nagai, S., 1989. Isolation of extracellular cobalt-free corrinoid from *Methanosarcina barkeri*. Agricultural and biological chemistry, 53(9), pp.2455-2460.

Gallo, S., Oberhuber, M., Sigel, R.K. and Kräutler, B., 2008. The corrin moiety of coenzyme B12 is the determinant for switching the btuB riboswitch of E. coli. ChemBioChem, 9(9), pp.1408-1414.

Galperin, M.Y. and Grishin, N.V., 2000. The synthetase domains of cobalamin biosynthesis amidotransferases cobB and cobQ belong to a new family of ATP-dependent amidoligases, related to dethiobiotin synthetase. Proteins: Structure, Function, and Bioinformatics, 41(2), pp.238-247.

Gasteiger E., Hoogland C., Gattiker A., Duvaud S., Wilkins M.R., Appel R.D., Bairoch A.; Protein Identification and Analysis Tools on the ExPASy Server; (In) John M. Walker (ed): The Proteomics Protocols Handbook, Humana Press (2005). pp. 571-607

Gopinath, K., Moosa, A., Mizrahi, V. and Warner, D.F., 2013. Vitamin B12 metabolism in Mycobacterium tuberculosis. Future microbiology, 8(11), pp.1405-1418.

Gough, S.P., Petersen, B.O. and Duus, J.Ø., 2000. Anaerobic chlorophyll isocyclic ring formation in Rhodobacter capsulatus requires a cobalamin cofactor. Proceedings of the National Academy of Sciences, 97(12), pp.6908-6913.

Granick, S., 1951. Biosynthesis of chlorophyll and related pigments. Annual Review of Plant Physiology, 2(1), pp.115-144.

Gray, M.J. and Escalante-Semerena, J.C., 2007. Single-enzyme conversion of FMNH2 to 5, 6-dimethylbenzimidazole, the lower ligand of B12. Proceedings of the National Academy of Sciences, 104(8), pp.2921-2926.

Grimm, C., Chari, A., Reuter, K. and Fischer, U., 2010. A crystallization screen based on alternative polymeric precipitants. Acta Crystallographica Section D: Biological Crystallography, 66(6), pp.685-697.

Gruber, K., Puffer, B. and Kräutler, B., 2011. Vitamin B 12-derivatives—enzyme cofactors and ligands of proteins and nucleic acids. Chemical Society Reviews, 40(8), pp.4346-4363.

Grüning, B., Holze, G., Jenny, T.A., Nesvadba, P., Gossauer, A., Ernst, L. and Sheldrick, W.S., 1985. Structure and Reactivity of Xanthocorrinoids. Part II. Influence of the c-acetic-acid chain on the course of the hydroxylation of the corrin chromophore by oxygen in the presence of ascorbic acid. Helvetica chimica acta, 68(6), pp.1754-1770.

Hay, B.P. and Finke, R.G., 1987. Thermolysis of the cobalt-carbon bond in adenosylcorrins. 3. Quantification of the axial base effect in adenosylcobalamin by the synthesis and thermolysis of axial base-free adenosylcobinamide. Insights into the energetics of enzyme-assisted cobalt-carbon bond homolysis. Journal of the American Chemical Society, 109(26), pp.8012-8018.

Hazra, A.B., Tran, J.L., Crofts, T.S. and Taga, M.E., 2013. Analysis of substrate specificity in CobT homologs reveals widespread preference for DMB, the lower axial ligand of vitamin B12. Chemistry & biology, 20(10), pp.1275-1285.

Hazra, A.B., Han, A.W., Mehta, A.P., Mok, K.C., Osadchiy, V., Begley, T.P. and Taga, M.E., 2015. Anaerobic biosynthesis of the lower ligand of vitamin B12. Proceedings of the National Academy of Sciences, 112(34), pp.10792-10797.

Heinemann, I.U., Jahn, M. and Jahn, D., 2008. The biochemistry of heme biosynthesis. Archives of biochemistry and biophysics, 474(2), pp.238-251.

Helliwell, K.E., Lawrence, A.D., Holzer, A., Kudahl, U.J., Sasso, S., Kräutler, B., Scanlan, D.J., Warren, M.J. and Smith, A.G., 2016. Cyanobacteria and eukaryotic algae use different chemical variants of vitamin B12. Current Biology, 26(8), pp.999-1008.

Heyes, Derren J., and C. Neil Hunter. "Biosynthesis of Chlorophyll and Barteriochlorophyll." In *Tetrapyrroles*, pp. 235-249. Springer, New York, NY, 2009.

Hodgkin, D.C., Pickworth, J., Robertson, J.H., Trueblood, K.N., Prosen, R.J. and White, J.G., 1955. The crystal structure of the hexacarboxylic acid derived from B12 and the molecular structure of the vitamin. Nature, 176, pp.325-328.

Hodgkin, D.C., Kamper, J., Mackay, M., Pickworth, J., Trueblood, K.N. and White, J.G., 1956. Structure of vitamin B12. Nature, 178(4524), pp.64-66.

Hogenkamp, H.P.C., 1963. A cyclic nucleoside derived from coenzyme B12. Journal of Biological Chemistry, 238(1), pp.477-480.

Huber, V., Sengupta, S. and Würthner, F., 2008. Structure–Property Relationships for Self-Assembled Zinc Chlorin Light-Harvesting Dye Aggregates. Chemistry-A European Journal, 14(26), pp.7791-7807

Huang, D.D. and Wang, W.Y., 1986. Chlorophyll biosynthesis in Chlamydomonas starts with the formation of glutamyl-tRNA. Journal of Biological Chemistry, 261(29), pp.13451-13455.

Jancarik, J. and Kim, S.H., 1991. Sparse matrix sampling: a screening method for crystallization of proteins. Journal of applied crystallography, 24(4), pp.409-411.

Jost, M., Simpson, J.H. and Drennan, C.L., 2015. The transcription factor CarH safeguards use of adenosylcobalamin as a light sensor by altering the photolysis products. Biochemistry, 54(21), pp.3231-3234.

Kampf, C. and Pfennig, N., 1980. Capacity of Chromatiaceae for chemotrophic growth. Specific respiration rates of Thiocystis violacea and Chromatium vinosum. Archives of Microbiology, 127(2), pp.125-135.

Kanehisa, M. and Goto, S., 2000. KEGG: kyoto encyclopedia of genes and genomes. Nucleic acids research, 28(1), pp.27-30.

Kajiwara, Y., Santander, P.J., Roessner, C.A., Pérez, L.M. and Scott, A.I., 2006. Genetically Engineered Synthesis and Structural Characterization of Cobalt− Precorrin 5A and− 5B, Two New Intermediates on the Anaerobic Pathway to Vitamin B12: Definition of the Roles of the CbiF and CbiG Enzymes. Journal of the American Chemical Society, 128(30), pp.9971-9978.

Karpowich, N.K., Huang, H.H., Smith, P.C. and Hunt, J.F., 2003. Crystal structures of the BtuF periplasmic-binding protein for vitamin B12 suggest a functionally important reduction in protein mobility upon ligand binding. Journal of Biological Chemistry, 278(10), pp.8429-8434.

Kelley, L.A., Mezulis, S., Yates, C.M., Wass, M.N. and Sternberg, M.J., 2015. The Phyre2 web portal for protein modeling, prediction and analysis. Nature protocols, 10(6), p.845.

König, W. and Geiger, R., 1970. Eine neue Methode zur Synthese von Peptiden: Aktivierung der Carboxylgruppe mit Dicyclohexylcarbodiimid unter Zusatz von 1-Hydroxy-benzotriazolen. European Journal of Inorganic Chemistry, 103(3), pp.788-798.

Koppenhagen, V.B. and Pfiffner, J.J., 1970. Currins and zirrins, two new classes of corrin analogues. Journal of Biological Chemistry, 245(21), pp.5865-5867.

Koppenhagen, V.B. and Pfiffner, J.J., 1971. a-(5, 6-Dimethylbenzimidazolyl) hydrogenobamide and its copper and zinc analogues. Journal of Biological Chemistry, 246(9), pp.3075-3077.

Koppenhagen, V.B., Wagner, F. and Pfiffner, J.J., 1973. a-(5, 6-Dimethylbenzimidazolyl) rhodibamide and Rhodibinamide, the Rhodium Analogues of Vitamin B12 and Cobinamide. Journal of Biological Chemistry, 248(23), pp.7999-8002.

Kräutler, B., Moll, J. and Thauer, R.K., 1987. The corrinoid from Methanobacterium thermoautotrophicum (Marburg strain). The FEBS Journal, 162(2), pp.275-278.

Kräutler, B., Kohler, H.P.E. and Stupperich, E., 1988. 5'-Methylbenzimidazolyl-cobamides are the corrinoids from some sulfate-reducing and sulfur-metabolizing bacteria. The FEBS Journal, 176(2), pp.461-469.

Kräutler, B., Fieber, W., Ostermann, S., Fasching, M., Ongania, K.H., Gruber, K., Kratky, C., Mikl, C., Siebert, A. and Diekert, G., 2003. The Cofactor of Tetrachloroethene Reductive Dehalogenase of Dehalospirillum multivorans Is Norpseudo-B12, a New Type of a Natural Corrinoid. Helvetica Chimica Acta, 86(11), pp.3698-3716.

Kräutler, B., 2005. Vitamin B12: chemistry and biochemistry.

Kräutler, B., 2015. Antivitamins B12—A Structure-and Reactivity-Based Concept. Chemistry-A European Journal, 21(32), pp.11280-11287.

Kunze, S., Zobi, F., Kurz, P., Spingler, B. and Alberto, R., 2004. Vitamin B12 as a ligand for technetium and rhenium complexes. Angewandte Chemie, 116(38), pp.5135-5139.

Lauritsen, I., Willemoës, M., Jensen, K.F., Johansson, E. and Harris, P., 2011. Structure of the dimeric form of CTP synthase from Sulfolobus solfataricus. Acta Crystallographica Section F: Structural Biology and Crystallization Communications, 67(2), pp.201-208.

Law, P.Y. and Wood, J.M., 1973. The photolysis of 5’-deoxyadenosylcobalamin under anaerobic conditions. Biochimica et Biophysica Acta (BBA)-Nucleic Acids and Protein Synthesis, 331(3), pp.451-454.

Lawrence, A.D., Deery, E., McLean, K.J., Munro, A.W., Pickersgill, R.W., Rigby, S.E. and Warren, M.J., 2008. Identification, characterization, and structure/function analysis of a corrin reductase involved in adenosylcobalamin biosynthesis. Journal of Biological Chemistry, 283(16), pp.10813-10821.

Liptak, M.D. and Brunold, T.C., 2006. Spectroscopic and computational studies of Co1+ cobalamin: spectral and electronic properties of the “superreduced” B12 cofactor. Journal of the American Chemical Society, 128(28), pp.9144-9156.

Mancia, F., Keep, N.H., Nakagawa, A., Leadlay, P.F., McSweeney, S., Rasmussen, B., Diat, O. and Evans, P.R., 1996. How coenzyme B 12 radicals are generated: the crystal structure of methylmalonyl-coenzyme A mutase at 2 Å resolution. Structure, 4(3), pp.339-350.

Mancia, F. and Evans, P.R., 1998. Conformational changes on substrate binding to methylmalonyl CoA mutase and new insights into the free radical mechanism. Structure, 6(6), pp.711-720.

Mandal, M. and Breaker, R.R., 2004. Gene regulation by riboswitches. Nature Reviews Molecular Cell Biology, 5(6), pp.451-463.

Marsh, E.N.G. and Drennan, C.L., 2001. Adenosylcobalamin-dependent isomerases: new insights into structure and mechanism. Current opinion in chemical biology, 5(5), pp.499-505.

Marsh, E.N.G., Patterson, D.P. and Li, L., 2010. Adenosyl radical: reagent and catalyst in enzyme reactions. ChemBioChem, 11(5), pp.604-621.

Martens, J.H., Barg, H., Warren, M. and Jahn, D., 2002. Microbial production of vitamin B 12. Applied microbiology and biotechnology, 58(3), pp.275-285.

Masuda, J., Shibata, N., Morimoto, Y., Toraya, T. and Yasuoka, N., 2000. How a protein generates a catalytic radical from coenzyme B 12: X-ray structure of a diol-dehydratase–adeninylpentylcobalamin complex. Structure, 8(7), pp.775-788.

Massiere, F. and Badet-Denisot, M.A., 1998. The mechanism of glutamine-dependent amidotransferases. Cellular and Molecular Life Sciences CMLS, 54(3), pp.205-222.

Matthews, R.G., 2009. Cobalamin-and corrinoid-dependent enzymes. Metal ions in life sciences, 6, p.53.

Mendel, R.R., Smith, A.G., Marquet, A. and Warren, M.J., 2007. Metal and cofactor insertion. Natural product reports, 24(5), pp.963-971.

Min, C., Atshaves, B.P., Roessner, C.A., Stolowich, N.J., Spencer, J.B. and Scott, A.I., 1993. Isolation, structure, and genetically engineered synthesis of precorrin-5, the pentamethylated intermediate of vitamin B12 biosynthesis. Journal of the American Chemical Society, 115(22), pp.10380-10381.

Minot, G.R. and Murphy, W.P., 1926. Treatment of pernicious anemia by a special diet. Journal of the American Medical Association, 87(7), pp.470-476.

Moore, S.J., Lawrence, A.D., Biedendieck, R., Deery, E., Frank, S., Howard, M.J., Rigby, S.E. and Warren, M.J., 2013. Elucidation of the anaerobic pathway for the corrin component of cobalamin (vitamin B12). Proceedings of the National Academy of Sciences, 110(37), pp.14906-14911.

Moore, S.J., Sowa, S.T., Schuchardt, C., Deery, E., Lawrence, A.D., Ramos, J.V., Billig, S., Birkemeyer, C., Chivers, P.T., Howard, M.J. and Rigby, S.E., 2017. Elucidation of the biosynthesis of the methane catalyst coenzyme F 430. Nature, 543(7643), p.78.

Muchmore, C.R., Krahn, J.M., Smith, J.L., Kim, J.H. and Zalkin, H., 1998. Crystal structure of glutamine phosphoribosylpyrophosphate amidotransferase from Escherichia coli. Protein Science, 7(1), pp.39-51.

Nandi, D.L. and Shemin, D., 1968. δ-Aminolevulinic acid dehydratase of Rhodopseudomonas spheroides III. Mechanism of porphobilinogen synthesis. Journal of Biological Chemistry, 243(6), pp.1236-1242.

Nordlund, P. and Reichard, P., 2006. Ribonucleotide reductases. Annu. Rev. Biochem., 75, pp.681-706.

Olson, J.M., 1998. Chlorophyll organization and function in green photosynthetic bacteria. Photochemistry and photobiology, 67(1), pp.61-75.

Ortiz-Guerrero, J.M., Polanco, M.C., Murillo, F.J., Padmanabhan, S. and Elías-Arnanz, M., 2011. Light-dependent gene regulation by a coenzyme B12-based photoreceptor. Proceedings of the National Academy of Sciences, 108(18), pp.7565-7570.

Payne, K.A., Quezada, C.P., Fisher, K., Dunstan, M.S., Collins, F.A., Sjuts, H., Levy, C., Hay, S., Rigby, S.E. and Leys, D., 2015. Reductive dehalogenase structure suggests a mechanism for B12-dependent dehalogenation. Nature, 517(7535), pp.513-516.

Petrus, A.K., Fairchild, T.J. and Doyle, R.P., 2009. Traveling the vitamin B12 pathway: oral delivery of protein and peptide drugs. Angewandte Chemie International Edition, 48(6), pp.1022-1028.

Pfennig, N. and Trüper, H.G., 1981. Isolation of members of the families Chromatiaceae and Chlorobiaceae. In The prokaryotes (pp. 279-289). Springer, Berlin, Heidelberg.

Ragsdale, S.W., 2008. Catalysis of methyl group transfers involving tetrahydrofolate and B 12. Vitamins & Hormones, 79, pp.293-324.

Raux, E., Lanois, A., Levillayer, F., Warren, M.J., Brody, E., Rambach, A. and Thermes, C., 1996. Salmonella typhimurium cobalamin (vitamin B12) biosynthetic genes: functional studies in S. typhimurium and Escherichia coli. Journal of bacteriology, 178(3), pp.753-767.

Raux, E., Thermes, C., Heathcote, P., Rambach, A. and Warren, M.J., 1997. A role for Salmonella typhimurium cbiK in cobalamin (vitamin B12) and siroheme biosynthesis. Journal of bacteriology, 179(10), pp.3202-3212.

Reitzer, R., Gruber, K., Jogl, G., Wagner, U.G., Bothe, H., Buckel, W. and Kratky, C., 1999. Glutamate mutase from Clostridium cochlearium: the structure of a coenzyme B 12-dependent enzyme provides new mechanistic insights. Structure, 7(8), pp.891-902.

Richards, N.G., Humkey, R.N., Li, K., Meyer, M.E. and de Sintjago, T.C.C., 2010. Tunnels and Intermediates in the Glutamine-Dependent Amidotransferases.

Rickes, E.L., Brink, N.G., Koniuszy, F.R., Wood, T.R. and Folkers, K., 1948. Crystalline vitamin B12. Science (Washington), 107, pp.396-397.

Roessner, C.A. and Scott, A.I., 2006. Fine-tuning our knowledge of the anaerobic route to cobalamin (vitamin B12). Journal of bacteriology, 188(21), pp.7331-7334.

Roper, J.M., Raux, E., Brindley, A.A., Schubert, H.L., Gharbia, S.E., Shah, H.N. and Warren, M.J., 2000. The Enigma of Cobalamin (Vitamin B12) Biosynthesis in Porphyromonas

gingivalis Identification and characterization of a functional corrin pathway. Journal of Biological Chemistry, 275(51), pp.40316-40323.

Roth, J.R., Lawrence, J.G., Rubenfield, M., Kieffer-Higgins, S. and Church, G.M., 1993. Characterization of the cobalamin (vitamin B12) biosynthetic genes of Salmonella typhimurium. Journal of bacteriology, 175(11), pp.3303-3316.

Russell-Jones, G., McTavish, K., McEwan, J., Rice, J. and Nowotnik, D., 2004. Vitamin-mediated targeting as a potential mechanism to increase drug uptake by tumours. Journal of inorganic biochemistry, 98(10), pp.1625-1633.

Santander, P.J., Roessner, C.A., Stolowich, N.J., Holderman, M.T. and Scott, A.I., 1997. How corrinoids are synthesized without oxygen: nature's first pathway to vitamin B12. Chemistry & biology, 4(9), pp.659-666.

Sattler, I., Roessner, C.A., Stolowich, N.J., Hardin, S.H., Harris-Haller, L.W., Yokubaitis, N.T., Murooka, Y., Hashimoto, Y. and Scott, A.I., 1995. Cloning, sequencing, and expression of the uroporphyrinogen III methyltransferase cobA gene of Propionibacterium freudenreichii (shermanii). Journal of bacteriology, 177(6), pp.1564-1569.

Schlingmann, G., Dresow, B., Koppenhagen, V.B., Becker, W. and Sherldrick, W.S., 1980. Structure of Yellow Metal-Free and Yellow Cobalt-Containing Corrinoids. Angewandte Chemie International Edition, 19(4), pp.321-322.

Schwartz, P.A. and Frey, P.A., 2007. 5 ‘-Peroxyadenosine and 5 ‘-peroxyadenosylcobalamin as intermediates in the aerobic photolysis of adenosylcobalamin. Biochemistry, 46(24), pp.7284-7292.

Schubert, H.L., Wilson, K.S., Raux, E., Woodcock, S.C. and Warren, M.J., 1998. The X-ray structure of a cobalamin biosynthetic enzyme, cobalt-precorrin-4 methyltransferase. Nature Structural and Molecular Biology, 5(7), p.585.

Schubert, H.L., Raux, E., Wilson, K.S. and Warren, M.J., 1999. Common chelatase design in the branched tetrapyrrole pathways of heme and anaerobic cobalamin synthesis. Biochemistry, 38(33), pp.10660-10669.

Scott, A.I., 1993. How Nature Synthesizes Vitamin B_{12} A Survey of the Last Four Billion Years. Angewandte Chemie International Edition, 32(9), pp.1223-1243.

Scott, A.I., Roessner, C.A., Stolowich, N.J., Spencer, J.B., Min, C. and Ozaki, S.I., 1993. Biosynthesis of vitamin B12: discovery of the enzymes for oxidative ring contraction and insertion of the fourth methyl group. FEBS letters, 331(1-2), pp.105-108.

Shemin, D. and Rittenberg, D., 1945. The utilization of glycine for the synthesis of a porphyrin. Journal of Biological Chemistry, 159(2), pp.567-568.

Smith, E.L., 1948. Purification of anti-pernicious anaemia factors from liver. Nature, 161(4095), pp.638-638.

Shipman, L.W., Li, D., Roessner, C.A., Scott, A.I. and Sacchettini, J.C., 2001. Crystal structure of precorrin-8x methyl mutase. Structure, 9(7), pp.587-596.

Shorb, M.S., 1947. Unidentified essential growth factors for Lactobacillus lactis found in refined liver extracts and in certain natural materials. Journal of bacteriology, 53(5), pp.669-669.

Sievers, F., Wilm, A., Dineen, D., Gibson, T.J., Karplus, K., Li, W., Lopez, R., McWilliam, H., Remmert, M., Söding, J. and Thompson, J.D., 2011. Fast, scalable generation of high-quality protein multiple sequence alignments using Clustal Omega. Molecular systems biology, 7(1), p.539.

Spencer, J.B., Stolowich, N.J., Roessner, C.A., Min, C. and Scott, A.I., 1993. Biosynthesis of vitamin B12: ring contraction is preceded by incorporation of molecular oxygen into precorrin-3. Journal of the American Chemical Society, 115(24), pp.11610-11611.

Spencer, J. B., Stolowich, N. J., Roessner, C. A., and Scott, A. I. (1993) FEBS Letts. 335, 57–60.

Stupperich, E., Eisinger, H.J. and Kräutler, B., 1988. Diversity of corrinoids in acetogenic bacteria. The FEBS Journal, 172(2), pp.459-464.

Summers, M.F., Marzilli, L.G. and Bax, A., 1986. Complete proton and carbon-13 assignments of coenzyme B12 through the use of new two-dimensional NMR experiments. Journal of the American Chemical Society, 108(15), pp.4285-4294.

Taga, M.E. and Walker, G.C., 2010. Sinorhizobium meliloti requires a cobalamin-dependent ribonucleotide reductase for symbiosis with its plant host. Molecular plant-microbe interactions, 23(12), pp.1643-1654.

Taga, M.E., Larsen, N.A., Howard-Jones, A.R., Walsh, C.T. and Walker, G.C., 2007. BluB cannibalizes flavin to form the lower ligand of vitamin B 12. Nature, 446(7134), p.449.

Tamiaki, H., 1996. Supramolecular structure in extramembraneous antennae of green photosynthetic bacteria. Coordination chemistry reviews, 148, pp.183-197.

Tanaka, R. and Tanaka, A., 2007. Tetrapyrrole biosynthesis in higher plants. Annu. Rev. Plant Biol., 58, pp.321-346.

Taranto, M.P., Vera, J.L., Hugenholtz, J., De Valdez, G.F. and Sesma, F., 2003. Lactobacillus reuteri CRL1098 produces cobalamin. Journal of bacteriology, 185(18), pp.5643-5647.

Tauer, A. and Benner, S.A., 1997. The B12-dependent ribonucleotide reductase from the archaebacterium Thermoplasma acidophila: an evolutionary solution to the ribonucleotide reductase conundrum. Proceedings of the National Academy of Sciences, 94(1), pp.53-58.

Thauer, R.K., 1998. Biochemistry of methanogenesis: a tribute to Marjory Stephenson: 1998 Marjory Stephenson prize lecture. Microbiology, 144(9), pp.2377-2406.

Thibaut, D., Couder, M., Famechon, A., Debussche, L., Cameron, B., Crouzet, J. and Blanche, F., 1992. The final step in the biosynthesis of hydrogenobyrinic acid is catalyzed by the cobH gene product with precorrin-8x as the substrate. Journal of bacteriology, 174(3), pp.1043-1049.

Thibaut, D., Couder, M., Famechon, A., Debussche, L., Cameron, B., Crouzet, J. and Blanche, F., 1992. The final step in the biosynthesis of hydrogenobyrinic acid is catalyzed by the cobH gene product with precorrin-8x as the substrate. Journal of bacteriology, 174(3), pp.1043-1049.

Thomson, A.J., 1969. Polarized fluorescence spectra of some naturally occurring corrins. Journal of the American Chemical Society, 91(10), pp.2780-2785.

Toohey, J.I., 1965. A vitamin B12 compound containing no cobalt. Proceedings of the National Academy of Sciences, 54(3), pp.934-942.

Toohey, J., 1974. Process for production of corrinoid compounds containing no metal. U.S. Patent 3,846,237.

Van Heyningen, S. and Shemin, D., 1971. Quaternary structure of δ-aminolevulinate dehydratase from Rhodopseudomonas spheroides. Biochemistry, 10(25), pp.4676-4682.

Walker, L.A., Jarrett, J.T., Anderson, N.A., Pullen, S.H., Matthews, R.G. and Sension, R.J., 1998. Time-resolved spectroscopic studies of B12 coenzymes: the identification of a metastable cob (III) alamin photoproduct in the photolysis of methylcobalamin. Journal of the American Chemical Society, 120(15), pp.3597-3603.

Watanabe, F., Katsura, H., Takenaka, S., Fujita, T., Abe, K., Tamura, Y., Nakatsuka, T. and Nakano, Y., 1999. Pseudovitamin B12 is the predominant cobamide of an algal health food, spirulina tablets. Journal of agricultural and food chemistry, 47(11), pp.4736-4741.

Weissgerber, T., Zigann, R., Bruce, D., Chang, Y.J., Detter, J.C., Han, C., Hauser, L., Jeffries, C.D., Land, M., Munk, A.C. and Tapia, R., 2011. Complete genome sequence of Allochromatium vinosum DSM 180 T. Standards in genomic sciences, 5(3), p.311.

Widner, F.J., Lawrence, A.D., Deery, E., Heldt, D., Frank, S., Gruber, K., Wurst, K., Warren, M.J. and Kräutler, B., 2016. Total Synthesis, Structure, and Biological Activity of Adenosylrhodibalamin, the Non-Natural Rhodium Homologue of Coenzyme B12. Angewandte Chemie International Edition, 55(37), pp.11281-11286.

Widner, F.J., Gstrein, F. and Kräutler, B., 2017. Partial Synthesis of Coenzyme B12 from Cobyric Acid. Helvetica Chimica Acta.

Williams, L., Fresquet, V., Santander, P.J. and Raushel, F.M., 2007. The multiple amidation reactions catalyzed by cobyric acid synthetase from Salmonella typhimurium are sequential and dissociative. Journal of the American Chemical Society, 129(2), pp.294-295.

Woodson, J.D. and Escalante-Semerena, J.C., 2004. CbiZ, an amidohydrolase enzyme required for salvaging the coenzyme B12 precursor cobinamide in archaea. Proceedings of the National Academy of Sciences of the United States of America, 101(10), pp.3591-3596.

Wooh, J.W., Kidd, R.D., Martin, J.L. and Kobe, B., 2003. Comparison of three commercial sparse-matrix crystallization screens. *Acta Crystallographica Section D: Biological Crystallography*, *59*(4), pp.769-772.

Zappa, S., Li, K. and Bauer, C.E., 2010. The tetrapyrrole biosynthetic pathway and its regulation in Rhodobacter capsulatus. In Recent Advances in Phototrophic Prokaryotes (pp. 229-250). Springer, New York, NY.

Zhou, S., Alkhalaf, L.M., de los Santos, E.L. and Challis, G.L., 2016. Mechanistic insights into class B radical-S-adenosylmethionine methylases: ubiquitous tailoring enzymes in natural product biosynthesis. Current opinion in chemical biology, 35, pp.73-79.